



7<sup>th</sup> International Symposium on **Exploitation  
of Renewable Energy Sources and Efficiency**

March 19 - 21, 2015

Subotica, Serbia

# ***EXPRES 2015***



**Proceedings**

7<sup>th</sup> Exploitation of Renewable  
Energy Sources and Efficiency

---

**EXPRES 2015**

---

**7<sup>th</sup> International Symposium on Exploitation of Renewable Energy Sources**

March 19-21, 2015

Subotica, Serbia

ISBN 978-86-82621-15-7

---

<http://conf.uni-obuda.hu/expres2015>

---

CIP - Каталогизacija y публикацији  
Библиотека Матице српске, Нови Сад

620.9(082)

INTERNATIONAL Symposium on Exploitation of Renewable Energy  
Sources and Efficiency (7 ; 2015 ; Subotica)

Proceedings / 7th International Symposium on Exploitation  
of Renewable Energy Sources and Efficiency EXPRES 2015,  
Subotica, March 19-21, 2015 ; [proceedings editor József  
Nyers]. - Subotica : Inženjersko-tehničko udruženje  
vojvodanskih Mađara, 2015 (Subotica : Čikoš štampa). - 156  
str. : ilustr. ; 30 cm

Tekst štampan dvostubačno. - Tiraž 65. - Bibliografija uz  
svaki rad.

a) Обновљиви извори енергије - Енергетска ефикасност -  
Зборници  
COBISS.SR-ID 294903815

# EXPRES 2015

7<sup>th</sup> International Symposium on  
Exploitation of Renewable Energy  
Sources and Efficiency

Subotica, Serbia  
March 19-21, 2015

---

# Proceedings

---

---

## Committees

---

### HONORARY COMMITTEE

János Fodor, Óbuda University Budapest, Hungary  
Branislav Todorović, University of Beograd, Serbia  
Imre J. Rudas, Óbuda University Budapest, Hungary

### GENERAL CHAIR

József Nyers, Óbuda University, Subotica Tech

### INTERNATIONAL ADVISORY COMMITTEE

János Beke SzIE, University, Gödöllő-, Budapest, Hungary  
László Kajtár, BME, Budapest, Hungary  
Dušan Petraš, University of Bratislava, Slovakia

### ORGANIZING COMMITTEE CHAIR

Erika Kudlik, Subotica City Government  
Zoltán Pék, László Veréb, V3ME, V3ME, Subotica,

### ORGANIZING COMMITTEE

József Gáti, Óbuda University Budapest, Hungary  
Gyula Kártyás, Óbuda University Budapest, Hungary

### TECHNICAL PROGRAM COMMITTEE CHAIRS

Péter Láng, BME, Budapest  
Péter Kádár, Óbuda University, Budapest  
Péter Odry, Subotica Tech

### TECHNICAL PROGRAM COMMITTEE

Marija Todorović, Univ. Beograd, Serbia  
Milorad Bojić, Univ. Kragujevac, Serbia  
László Garbai, BME, Budapest, Hungary  
Dušan Gvozdenac, Univ. Novi Sad, Serbia  
Jenő Kontra, BME, Budapest, Hungary  
László Tóth, Univ. SzIE, Gödöllő, Hungary  
István Farkas Univ. SzIE, Gödöllő, Hungary  
Stevan Firstner, SuboticaTech, Serbia  
Kornél Kovács, Univ. Szeged, Hungary  
Djordje Kozić, Univ. Beograd, Serbia  
Felix Stachowicz, Univ. Rzesov, Poland  
László Sikolya, Nyíregyháza College, Hungary  
Dusan Golubovic, Univ. East Sarajevo, Bosnia and Herzegovina.

### SECRETARY GENERAL

Anikó Szakál, Óbuda University  
[szakal@uni-obuda.hu](mailto:szakal@uni-obuda.hu); [nyers@uni-obuda.hu](mailto:nyers@uni-obuda.hu)

### PROCEEDINGS EDITOR

József Nyers, Óbuda University  
[nyers@uni-obuda.hu](mailto:nyers@uni-obuda.hu)

---

<http://conf.uni-obuda.hu/expres2015>

---



# Table of Contents

<b>Investigation of unbalancing problems in central heating systems</b> .....	<b>7</b>
<b>Ferenc Kalmár*, Sándor Hámori*</b>	
* University of Debrecen / Department of Building Services and Building Engineering Faculty of Engineering Department, Debrecen, Hungary	
<b>Optimum of external wall thermal insulation thickness using total cost method</b> .....	<b>13</b>
<b>Jozsef Nyers*, Peter Komuves**</b>	
*Obuda University Budapest, Becsi ut 96, 1034 Budapest, Hungary **V3ME, Subotica-Szabadka, M.Corvin 6	
<b>Direct numerical simulation of Navier-Stokes equation for the forced rayleigh-be nard convection of temperature variation at the lower wall</b> .....	<b>18</b>
<b>Sadoon Ayed*, Gradomir Ilic**, Predrag Živković**, MladenTomic**, Amir Rashid**</b>	
*University of Technology/ Department of Mechanical Engineering, Baghdad, Iraq **University of Nis/Faculty of Mechanical Engineering, Nis, Serbia	
<b>Solar thermal energy use in Hungary: potentials and new opportunities</b> .....	<b>23</b>
<b>B. Bokor*, L. Kajtár*, L. Herczeg*</b>	
*Budapest University of Technology and Economics (BME) / Department of Building Service and Process Engineering, Budapest, Hungary	
<b>Some questions of utilizing heat generated in waste dumps</b> .....	<b>30</b>
<b>Kontra Jenő, Várfalvi János</b>	
Budapest University of Technology and Economics H-1111 Budapest, Műgyetem rkp. 3.	
<b>Ray tracing study to determine the characteristics of the solar image in the receiver for a thermal solar concentration system</b> .....	<b>35</b>
<b>Saša R. Pavlovic*, Velimir P. Stefanović*, Predrag Rajković**, Emina P. Petrovic,*** Sadoon Ayed****</b>	
*Nis. Serbia, Faculty of Mechanical Engineering, Department for Energetics and Process technique, University in Niš, Serbia ** Nis. Serbia, Faculty of Mechanical Engineering, Department for Mathematics and Natural Sciences University in Niš, Serbia *** Nis. Serbia, Faculty of Mechanical Engineering, Mechatronic and Control Systems, University in Niš, Serbia ****University of Technology, Department of Mechanical Engineering, Baghdad ,Iraq,	
<b>Comfort analyzing based on probability theory in office building</b> .....	<b>40</b>
<b>László Kajtár*, János Szabó*</b>	
* Budapest University of Technology and Economics, Department of Building Service and Process Engineering, Hungary	
<b>Enhance of the efficiency of exploitation of geothermal energy</b> .....	<b>46</b>
<b>Ján Takács</b>	
Department of Building Services, Faculty of Civil Engineering, Slovak University of Technology in Bratislava, Slovakia, Radlinského 11, 813 68 Bratislava, Slovak Republic	
<b>Central ventilation of industrial building with wood working operation</b> .....	<b>50</b>
<b>Zuzana Straková</b>	
Slovak University of Technology in Bratislava, Faculty of Civil Engineering, Department of Building Services, Bratislava, Slovak Republic	
<b>Comparison of various ACH test results of rooms</b> .....	<b>55</b>
<b>László Fülöp*, György Polics*</b>	
* Faculty of Engineering and Information Technology, University of Pécs,Hungary	

<b>Maximal and Optimal DHW Production with Solar Collectors for Single Family Houses</b> .....	<b>59</b>
<b>Miklós Horváth*, Tamás Csoknyai *</b>	
* Budapest University of Technology and Economics/Department of Building Services and Process Engineering, Budapest, Hungary	
<b>Sizing methods of domestic hot water recirculation systems</b> .....	<b>65</b>
<b>Kristóf Hargita*, Zoltán Szánthó*</b>	
*Department of Building Service and Process Engineering, Budapest University of Technology and Economics, Hungary	
<b>Numerical investigation of offset jet attaching to a wall</b> .....	<b>70</b>
<b>Balázs Both*, Zoltán Szánthó*, Róbert Goda*</b>	
* Budapest University of Technology and Economics/Department of Building Service Engineering and Process Engineering, Budapest, Hungary	
<b>Determination of optimal pipe diameters for radial fixed-track district heating networks</b> .....	<b>74</b>
<b>László Garbai, Andor Jasper,</b>	
Department of Building Service and Process Engineering, Budapest University of Technology and Economics, Hungary	
<b>Building energy performance improvement from the aspect of envelope upgrading</b> .....	<b>79</b>
<b>N. Harmati*, R. Folić* and Z. Magyar**</b>	
* University of Novi Sad, Faculty of Technical Sciences/Department of Civil Engineering, Novi Sad, Serbia	
** Budapest University of Technology and Economics/Department of Building Energetics and Building Services, Budapest, Hungary	
<b>Distributed mathematical model of the heat pump's evaporator with boundary condition</b> .....	<b>83</b>
<b>Jozsef Nyers Dr. Sci *, **, Jozsef Tick Dr. habil*, Zoltan Pek PhD student*</b>	
* University Obuda Budapest, Hungary	
**VTŠ Subotica, Department of Energy, Subotica, Serbia	
<b>The effect of thermal insulation of an apartment house on thermo-hydraulic stability of the space heating system</b> .....	<b>88</b>
<b>Mária Kurčová*</b>	
* Slovak University of Technology in Bratislava, Faculty of Civil Engineering, Department of Building Services, Slovakia	
<b>Experimental investigations of indoor climate parameters a swimming pool during summer operation period</b> .....	<b>92</b>
<b>R. Ruzza, Belo B. Furi*</b>	
* Department of Building Services, Faculty of Civil Engineering STU in Bratislava, Bratislava, Slovakia	
<b>Revealing the costs of air pollution caused by coal-based electricity generation in serbia</b> .....	<b>96</b>
<b>F.E. Kiss* and Đ.P. Petković**</b>	
* University of Novi Sad/Faculty of Technology, Novi Sad, Serbia	
** University of Novi Sad/Faculty of Economics, Subotica, Serbia	
<b>Detailed analytical method for ventilation energy consumption investigation</b> .....	<b>102</b>
<b>Miklos Kassai*, Laszlo Kajtar*</b>	
* Budapest University of Technology and Economics/Department of Building Service Engineering and Process Engineering, Budapest, Hungary	

<b>Expansion of the photovoltaic solar power plants in the Romanian electric energy industry</b> .....	<b>106</b>
<b>István Vallasek</b>	
MTA-KAB: Renewable Energetics Work-team CLUJ - Romania	
<b>Green and more green information technology</b> .....	<b>109</b>
<b>Imre Petkovics* and Ármin Petkovics **</b>	
*Assistant professor, The Faculty of Economics Subotica, Department of Business Informatics and Quantitative Methods, Subotica, Serbia	
*Professor for Applied Studies, Subotica Tech - College of Applied Sciences, Department of Informatics, Subotica	
** PhD student, Department of Networked Systems and Services, Budapest University of Technology and Economics	
<b>Tribological characteristics of bio lubricants</b> .....	<b>113</b>
<b>M. Stojilković*, D. Golubović**, D. Ješić**</b>	
* NIS Gaspromneft, Novi Sad, Serbia, e-mail: miles.ns@gmail.com	
** Faculty of Mechanical Engineering in East Sarajevo, Republic of Srpska	
<b>Experimental and investigating of different engineering materials</b> .....	<b>116</b>
<b>A. Nagy, B. Dudinszky</b>	
*Budapest University of Technology and Economics, Department of Building Service and ProcessEngineering, H-1111 Budapest, Műegyetem rkp.3-9.	
<b>COP of refrigerants in heat pumps</b> .....	<b>121</b>
<b>Jozsef Nyers*, Daniel Stuparic**, Arpad Nyers***</b>	
*Obuda University Budapest, Becsi ut 96, 1034 Budapest, Hungary	
***Budapest University of Technology & Economics, Budapest, Muegyetem rkp. 3-5	
**VTS Subotica, M. Oreskovica 16, Serbia	
<b>Simulation of the nuclear power plant cooling using the TEG</b> .....	<b>125</b>
<b>A. Szente*, I. Farkas** and P. Odry***</b>	
* Paks Nuklear Power Plant, Paks, Hungary	
** College of Dunaújváros/Computer Engineering, Dunaújváros, Hungary	
***Polytechnic of Subotica/Electrical Engineering, Szabadka, Serbia	
<b>Technological features of biogas plants using mixed materials</b> .....	<b>129</b>
<b>L. Tóth*, J.Beke*, Z. Bártfai**, I. Szabó**, G. Hartdégen, I. Oldal**, Z. Blahunka**</b>	
Szent István University, Hungary, 2100 Gödöllő, Páter K. u. 1.	
* Institute of Process Engineering, ** Institute of Mechanics and Machinery	
<b>Energy efficiency as a precondition of sustainable tourism</b> .....	<b>134</b>
<b>Slavica Tomić *, Aleksandra Stoilković **</b>	
* University of Novi Sad, Faculty of Economics in Subotica, Serbia	
** University of Novi Sad, Faculty of Economics in Subotica, Serbia	
<b>Fluidized bed drying of granules</b> .....	<b>140</b>
<b>T. Poós* and V. Szabó*</b>	
*Department of Building Services and Process Engineering, Faculty of Mechanical Engineering, Budapest University of Technology and Economics, Budapest, Hungary	
<b>The status and history of the Hungarian district heating</b> .....	<b>145</b>
<b>László Garbai Dr.*, Gergely Pacza</b>	
*Budapest University of Technology and Economics, Hungary	
<b>Approach to the Concurrent Programming in the Microsystems</b> .....	<b>149</b>
<b>Anita Sabo*, Bojan Kuljić**, Tibor Szakáll***, Andor Sagi****</b>	
Subotica Tech, Subotica, Serbia	
<b>Energy sources for heating/cooling and lowexergy systems</b> .....	<b>154</b>
<b>Dušan Petráš</b>	
Department of Building Services, Faculty of Civil Engineering, Slovak University of Technology in Bratislava, Slovakia Radlinského 11, 813 68 Bratislava, Slovak Republic	

<b>The present state of district heating in Hungary .....</b>	<b>157</b>
<b>György 'Sigmond</b>	
MaTáSzSz (Association of Hungarian District Heating Enterprises)	

# Investigation of unbalancing problems in central heating systems

Ferenc Kalmár\*, Sándor Hámori\*

\* University of Debrecen / Department of Building Services and Building Engineering  
Faculty of Engineering Department, Debrecen, Hungary

fkalmar@eng.unideb.hu, sandor.hamori@eng.unideb.hu

**Abstract**— In countries with temperate climate heating represents about 60% from the total energy consumption of a building with average thermal characteristics of the envelope. Energy saving and reduction of greenhouse gas emissions are strongly supported research directions in European countries. Different national programs were started in order to refurbish the existing building stock. Heating systems have to be refurbished simultaneously with the building envelope; otherwise the expected energy savings will not be obtained. In this paper different aspects of hydraulic balancing and control of central heating systems are analyzed, from energy point of view. The interrelation between mass flow deviation and supplementary energy consumption was developed, and the influences of supply temperature and temperature drop on the energy consumption were identified. Furthermore the effects of heat storage capacity of building elements on the supplementary energy demand were analyzed. It was found that unbalancing can lead to 2%-10% supplementary energy consumption.

## I. INTRODUCTION

The main goal of the central heating design process is to obtain appropriate thermal comfort in buildings minimising the investment and operational costs. This could be theoretical realised with the available modern control techniques. However practice has shown that, if the preconditions are not fulfilled the correct operation of the heating system could not be assured even by the most sophisticated control equipment [1, 2].

In central heating systems the warm water supply temperature could have different values. In the past the most used value for supply temperature was 90 °C, while the temperature drop usually was 20 °C. Nowadays the supply temperature usually is lower. Through boiler control important energy savings can be obtained [3].

If the warm water flow differs from the designed value, the control elements could not fulfil their function (to increase or decrease of the mass flow). This situation could often appear in practice because of the lack of the proper balance equipment on one hand and differences between the constructed and designed system on the other hand. Therefore the thermal comfort is not realised unless with higher energy consumption [4].

The above mentioned problems could appear even at heating systems equipped with thermostatic valves, [5]. In this case the valve opens totally in vain if the required

flow is not assured at the radiator, the flow will not increase.

Rhee et al. investigated the effect of hydronic balancing on individual room control of radiant floor heating systems, [6]. Rhee et al. suggested an evaluation strategy of balancing valve performance for radiant floor heating systems. In their strategy, adjustment range and accuracy are evaluated by using the  $K_v$  value, in order to evaluate the balancing performance for practical applications of balancing valves, [7]. Hydronic balancing plays an important role in case of performance analysis, modelling and economic optimization of heating systems, [8], [9], [10]. Central heating systems are operating more than 80% of the heating season under 50% of the nominal capacity. The hydronic balancing ensure the proper warm water flow at the heating elements under dynamic variation of operational conditions, [11]. Building energy management system has to be utilized in fault detection and diagnosis, practical explanations of faults and their related effects are important to building caretakers. Without hydronic balancing of central heating systems the energy management systems cannot detect the faults properly. Djuric et al. presented an overview of the real causes of the faults and their effects both on the energy consumption and on the indoor air temperature, [12]. Different simulators were developed in order to help the optimization of the design of hydronic network, [13]

In the followings the effects of unbalancing is analysed in case of central heating systems and the obtained thermal comfort and the energy consumption is analysed.

## II. INTERNAL TEMPERATURE

In a room the thermal comfort is appropriate if the comfort parameters are kept at the prescribed values correspondingly to the building/room function. One of the most important comfort parameter is the operative temperature, which can be defined as the average of the mean radiant and ambient air temperatures weighted by their respective heat transfer coefficients. The heat demand of rooms and the radiator outputs are calculated taking into account the internal air set-point temperature.

Based on the specific degree-day curve the design value of the external temperature occurs 2...5 times in a heating season, hence the heating system output have to be

controlled. In the case of a qualitative control system the warm water supply temperature theoretical follows the chosen control curve, where in function of the design values of the supply temperature and temperature drop, the required values of the supply temperatures could be determined depending on the outdoor temperature. In practice the characteristic curve of the control valves is linear, so thus two parallel lines give the supply and return temperatures.

The theoretical control curve could be determined as follows. If the “0” index characterize the design situation, then for any other case the followed equation can be written:

$$\frac{m}{m_0} \frac{t_f - t_r}{t_{f0} - t_{r0}} = \frac{t_i - t_e}{t_{i0} - t_{e0}} \quad (1)$$

where:  $m$  is the warm water flow;  $t_i$  – internal temperature;  $t_e$  – outdoor temperature;  $t_f$  – supply (forward) temperature;  $t_r$  – return temperature.

At the same time:

$$T_R = T_{R0} \left( \frac{t_i - t_e}{t_{i0} - t_{e0}} \right)^{\frac{1}{n}} \quad (2)$$

where:  $T_R$  is the average logarithmic temperature difference;  $n$  – radiator exponent.

In the case of a qualitative control system the ratio of the mass flows is constant and equal to 1 at any value of the outdoor temperature. Consequently, using (1) and (2) a general relation can be written:

$$F(t_f) = T_{R0} \left( \frac{t_i - t_e}{t_{i0} - t_{e0}} \right)^{\frac{1}{n}} \ln \frac{t_f - t_i}{t_f - t_i - \frac{t_i - t_e}{t_{i0} - t_{e0}} (t_{f0} - t_{r0})} - \frac{t_i - t_e}{t_{i0} - t_{e0}} (t_{f0} - t_{r0}) = 0 \quad (3)$$

In this equation if the internal temperature is constant and equal to set-point value, at different external temperature values the required supply temperature could be calculated.

However, if the warm water flow at radiators differs from the designed value, the return temperatures will not follow the theoretical curve as it could be seen in Figure 1.

In this case the internal temperature will differ from the designed value. Assuming steady state processes, the internal temperature values could be determined from the following equation:

$$F(t_i) = T_{R0} \left( \frac{t_i - t_e}{t_{i0} - t_{e0}} \right)^{\frac{1}{n}} \ln \frac{t_f - t_i}{t_f - t_i - \frac{t_i - t_e}{t_{i0} - t_{e0}} (t_{f0} - t_{r0}) \frac{m_0}{m}} - \frac{t_i - t_e}{t_{i0} - t_{e0}} (t_{f0} - t_{r0}) \frac{m_0}{m} = 0 \quad (4)$$

In this relation the values of the supply temperatures are introduced based on the control curve.

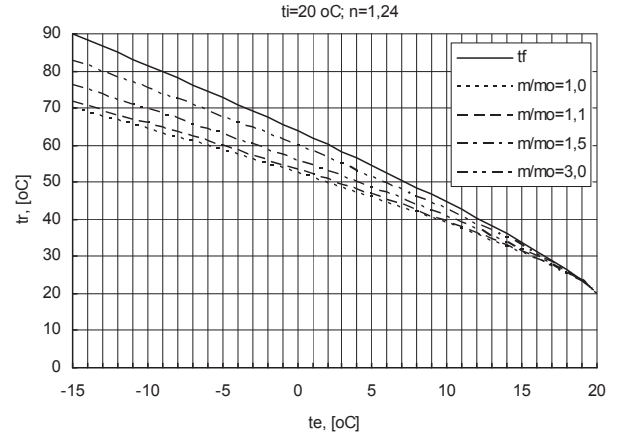


Figure 1. Return temperature values at different flow ratio (90/70 °C)

At different mass flow ratios the obtained internal temperature values are presented in Figure 2. It could be seen that in case of steady state processes the variation is linear. Therefore at given supply temperature and temperature drop and given internal set-point temperature the variation of internal temperature could be written as:

$$t_i = t_{i0} + (t_{i0} - t_e) \text{grad} t_i \quad (5)$$

where the gradient of the internal temperature is given by:

$$\text{grad} t_i = \frac{t_{i(t_{e0})} - t_{i0}}{t_{i0} - t_{e0}} \quad (6)$$

where  $t_{e0}$  is the design value of the external temperature.

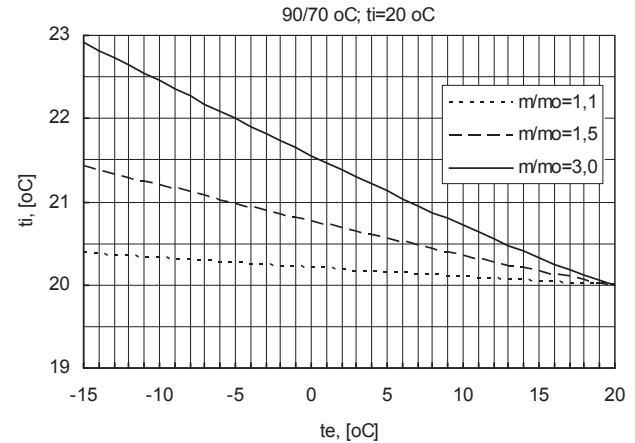


Figure 2. Internal temperature in steady state conditions

Accordingly, it is enough to determine the internal temperature value at a single value of the outdoor temperature (e.g. design value) at any other outdoor temperatures the internal temperatures could be determined using equation (5). In Figure 3 the internal temperature values at design value of the external temperature are presented in function of the mass flow ratio taking into account different values of the set point temperature. The variation of the internal temperature at different values of the forward temperature and temperature drop are presented in Figure 4.



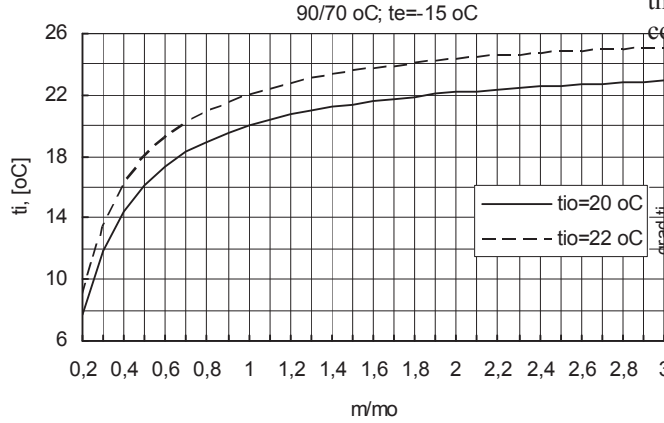


Figure 3. Internal temperature at 90/70 °C temperature drop

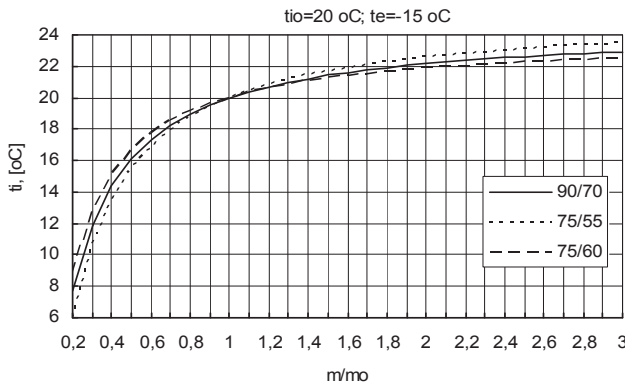


Figure 4. Internal temperature in different design conditions of the heating system

At different values of the set point temperatures, if the mass flow exceeds the design value, the difference between the resulted values of the internal temperature hardly varies. Nevertheless, at mass flow ratio values lower than 1, the difference between the obtained internal temperatures decrease. So that, at higher values of the set point temperatures the differences between the set point and the obtained internal temperature are higher, if the warm water flow is lower than the designed one. At the same time, the design value of the supply temperature and the design value of the temperature drop influence as well the obtained internal temperature. At the same value of the temperature drop, the lower supply temperature will lead to higher absolute values of the differences between the obtained internal temperature and the set-point values, if the mass flow differs from the design value. At the same value of the supply temperature the lower temperature drop will lead to a higher stability of the internal temperature.

In Figure 5 the variation of the internal temperature gradient is presented at different design conditions of the central heating system.

It could be observed that at the same value of the temperature drop, higher value of the supply temperature results in more stable internal temperature. The stability of

the heating system operating at lower supply temperature could be increased decreasing the temperature drop.

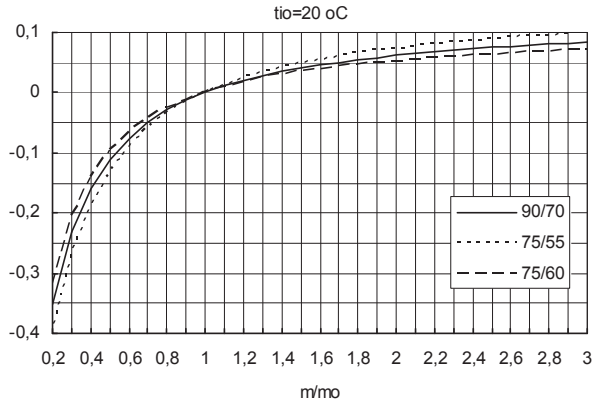


Figure 5. Gradient of the internal temperature variation

### III. MASS FLOW

As it could be seen from previous chapters if a central heating system is unbalanced in some of rooms/buildings either extra energy consumption appears or the thermal comfort level will decrease. The next questions which should be analyzed are: which mass flow differences may appear and what the effects on the system appropriate operation are. In most cases if in a room the set-point temperature is not reached the operation is “corrected” increasing the total flow. Therefore the total energy consumption of the system will increase. In the followings the operation of an unbalanced column would be analysed. At this column  $n$  radiators are connected (Fig. 6). On the radiators the pressure drop is  $\Delta p$  the warm water flow is  $m$ , on the column pipe sections the pressure drop is  $\Delta p'$ , the mass flow is  $m'$ .

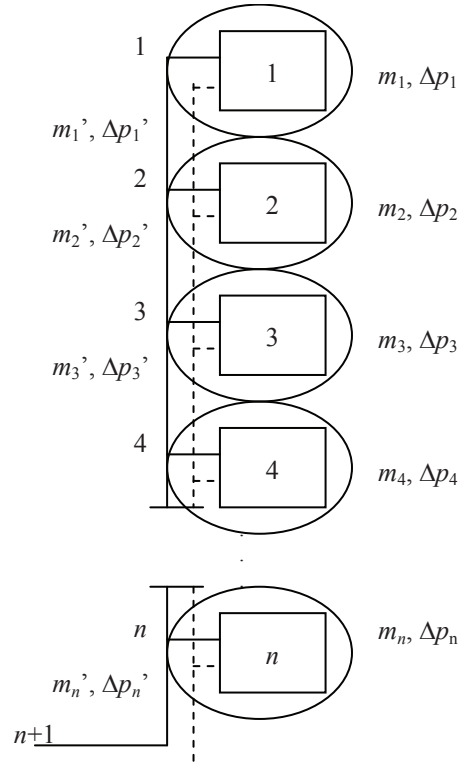


Figure 6. Column of a central heating system

If the system is unbalanced in the connection points the pressure balance is established based on the distributed warm water flow. Therefore in the intersection point no. 2 it can be written that:

$$\Delta p_2 = \Delta p_1 + \Delta p_1' \quad (7)$$

The pressure drop on the radiator  $i$  is:

$$\Delta p_i = \Psi \frac{16m_i^2}{\pi^2 \rho d^4} \quad (8)$$

where:

$$\Psi = \lambda \frac{l}{d} + \sum \zeta \quad (9)$$

On the column pipe sections the local pressure drop is assumed to be  $\beta\%$  from linear one:

$$\Delta p_i' = (1 + \beta) \Delta p_i' \quad (10)$$

If we use the following notations:

$$\chi_i = \frac{\chi_{i-1}}{\varepsilon_{i-1}^2} + (1 + \beta) \frac{\lambda l_i}{\Psi d_i} \quad (11)$$

and

$$\varepsilon_i = 1 + \sqrt{\chi_i} \quad (12)$$

on the subsequent column pipe sections, the relation between warm water flow will be:

$$m_i' = \frac{m_{i+1}'}{\varepsilon_i} \quad (13)$$

where:  $i = \overline{1, n}$  and  $\chi_0 = 1; \varepsilon_0 = 1$ .

Using the developed recursive equation group the flow ratio on the subsequent column pipe section could be calculated and if the column total flow is known the radiator flows could be determined. If the system is unbalanced, usually warm water flow is lowest at the topmost radiator. The mass flow might be lower than required at the bottom radiator either. Nevertheless at the radiators from the intermediate floors the water flow could exceed the design value. If this system could not be balanced the necessary flow at the most unfavourable radiator may be obtained increasing the column total flow, although this solution will lead to higher flows also at the other radiators and at higher energy consumption of the system.

Considering every column as a radiator the recursive equation group could be used also to analyse the column flows, if the distribution is not balanced.

#### IV. CASE STUDY

In the following let's assume a building  $54 \times 11 \times 14$  m (41 flats), built from medium size monolithic panels. The external walls are 30 cm slag concrete with  $U_{wall}=1.5$  W/(m<sup>2</sup>·K), the flat roof is reinforced concrete with air cavities, where the slope is provided with slag in variable thickness,  $U_{roof}=1.1$  W/(m<sup>2</sup>·K).

Let us analyze a column of the central heating system, assuming at a radiator connection  $l=1$  m;  $d=15$  mm;

$\lambda=0.002$  and  $\Sigma\zeta=10.5$ . In these conditions using (9) results that  $\Psi=11$ . The radiator outputs are:  $R_1=2265$  W;  $R_2=R_3=R_4=1759$  W;  $R_5=2295$  W. The ratio between linear and local pressure losses is considered  $\beta=0.2$ .

If the columns of the heating system are balanced but the radiators are not, the column will get the necessary total flow (0.1175 kg/s) but at the radiators the real flow will differ from the required one. The flow ratio values (real/design) at the radiators are presented in table 1.

Table 1

Flow ratio at the radiators

R1	R2	R3	R4	R5
0.75	0.98	1.06	1.18	1.07

If we would like to obtain the required flow at the topmost radiator the column total flow have to be increased. The flow ratio values at the radiators when the topmost radiator gets the necessary flow are presented in table 2.

Table 2

Flow ratio at the radiators

R1	R2	R3	R4	R5
1.00	1.31	1.41	1.58	1.42

In this case the column flow exceeds with 33.3% the designed value ( $m_t$ ). In Figure 7 the flow ratio values at the radiator could be seen depending on the total column flow ratio.

After a complex energy and economy analysis the "optimal" thickness of the additional insulation layer could be determined [6]. In this case the thickness of the additional expanded polystyrene layer is 12 cm. For the studied rooms the necessary output values will decrease to:  $R_1=1528$  W;  $R_2=R_3=R_4=1022$  W;  $R_5=1558$  W. If the radiator outputs are not adjusted after thermal rehabilitation of the building to the new heat demand the warm water flow ratio at the radiators, due to the lower design values, will increase (Table 3).

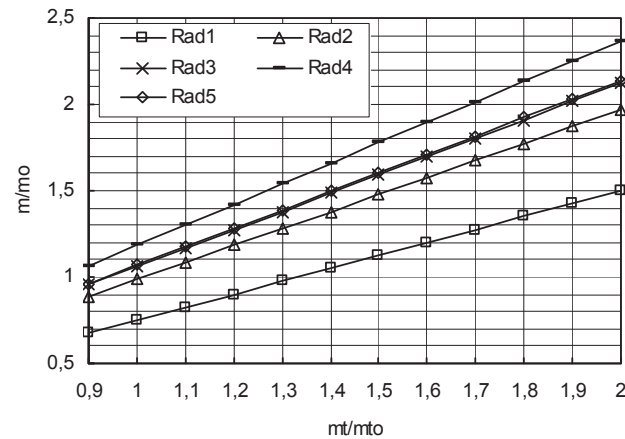


Figure 7. Flow ratio variation at the radiators

Table 3  
Flow ratio at the radiators

R1	R2	R3	R4	R5
1.11	1.69	1.82	2.04	1.57

In lots of cases after building thermal rehabilitation the radiators are equipped with thermostatic valves. It could be seen that if the supply temperature is not changed it is impossible to realize a proper control with thermostatic valves in this case, [15]. Depending on the rehabilitation level of the building the “optimal” supply temperature could be determined [16].

If the radiator outputs after thermal rehabilitation are equal to the rooms heat demand and the column total flow is equal to the design value (0.0735 kg/s), but the radiators are not balanced, the flow ratio values at the radiators are contained in Table 4.

Table 4  
Flow ratio at the radiators

R1	R2	R3	R4	R5
0.69	1.06	1.14	1.27	0.98

Comparing that values with those from table 1 it could be stated that after thermal rehabilitation of the building the flow distribution at the radiators is more disproportionate. To obtain the necessary flow at the radiator 1 the total flow is increased. From this reason at the other radiators the flow will increase either. In this situation the flow ratio values are presented in Table 5.

Table 5  
Flow ratio at the radiators

R1	R2	R3	R4	R5
1.00	1.52	1.64	1.83	1.41

In this case the column total flow will exceed with 43.8% the design flow. After building thermal retrofit the flow ratio variation at the radiators depending on the column total flow is presented in Figure 8.

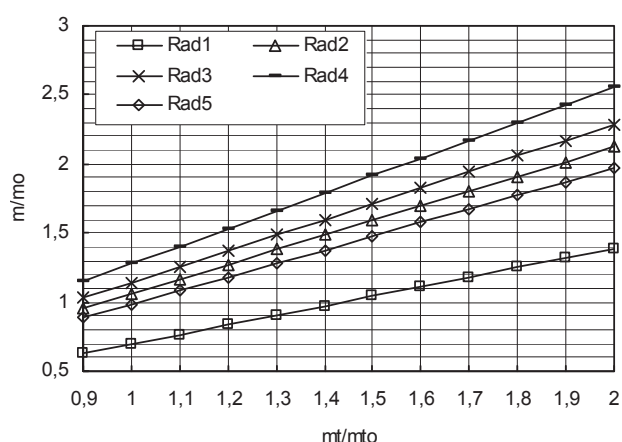


Figure 8. Flow ratio variation at the radiators

If the design temperature drop of the system is lower (e.g. 15 °C), the flow ratio values are the same as in the above studied case (20 °C).

Using the developed diagrams, based on the flow ratio values the expected internal temperature values could be determined and also the energy use can be calculated before building refurbishment (case 1). For heating systems with different operational parameters these values are presented in table 6.

Table 6  
Internal temperature and supplementary energy use  
(case 1)

(case 1)

Room		90/70 °C			
		Before insulation		After insulation	
Indoor air temperature	4th floor	20		20	
	3rd floor	20.85		21.12	
	2nd floor	21.05		21.26	
	1st floor	21.33		21.5	
	ground fl.	21.07		20.95	
(real energy used)/ (expected energy use)	4th floor	0		0	
	3rd floor	102.43		103.20	
	2nd floor	103.00		103.66	
	1st floor	103.81		104.27	
	ground fl.	103.05		102.70	
Room		75/55 °C		75/60 °C	
		Before insul.	After insul.	Before insul.	After insul.
Indoor air temperature	4th fl.	20	20	20	20
	3rd fl.	21.02	21.36	20.74	20.98
	2nd fl.	21.26	21.57	20.92	21.12
	1st fl.	21.61	21.95	21.03	21.31
	ground fl.	21.29	21.15	20.94	20.83
(real energy used)/ (expected energy use)	4th fl.	0	0	0	0
	3rd fl.	102.93	103.89	102.11	102.80
	2nd fl.	103.62	104.45	102.61	103.20
	1st fl.	104.60	104.83	103.31	103.75
	ground fl.	103.68	103.28	102.65	102.37

As it could be seen the unbalancing in this case could lead to 2...5% supplementary energy use in the rooms.

If the heating system was balanced before the thermal rehabilitation of the building but after that the system was

not balanced again and adjusted to the new heat demand values (case 2), the internal temperature will be higher than the set-point value. At design value of the external temperature the expected internal temperature values and the yearly extra energy use of the rooms are presented in table 8.

Table 8  
Indoor air temperature and supplementary energy use (case 2)

Floor		90/70 °C	75/55 °C	75/60 °C
4	Indoor air temperature	21.06	21.28	20.93
3		21.38	21.68	21.21
2		21.38	21.68	21.21
1		21.38	21.68	21.21
0		21.05	21.26	20.90
4	(real energy used)/(expected energy use)	103.02	103.88	102.65
3		103.93	104.81	103.45
2		103.93	104.81	103.45
1		103.93	104.81	103.45
0		102.98	103.82	102.61

It could be seen, if the heating system is not adjusted to the new energy demand values of the retrofitted building the yearly energy consumption may exceed the design value with 3...5%.

It should be kept in mind that reducing the operational temperature of the heating system the exergy consumption will decrease [17], [18], [19]. Unbalancing of the central heating system will lead to higher exergy consumption for heating. Furthermore, in case of energy use analysis or exergy consumption analysis to obtain better results the variable degree day method have to be used [20].

## V. CONCLUSIONS

In case of central heating systems, the unbalancing will lead supplementary energy consumption and deterioration of indoor thermal comfort. When the real flow is lower than the required value, the higher the set-point temperature is, the higher the decrease of the expected internal temperature will be. At the same time, the internal temperature is influenced by the design value of the supply temperature and temperature drop. At the same value of the temperature drop, the difference between the obtained internal temperature and the set point value is higher at lower values of the design supply temperature. The stability of the low temperature heating system could be improved decreasing the temperature drop. The gradient of the internal temperature variation will give the difference between the real yearly energy consumption of a room and the design value. The gradient variation is independent by the internal set-point temperature value.

## REFERENCES

- [1] Peeters, L., Van der Veken, J., Hens, H., Helsens, L., D'haeseleer, W., Control of heating systems in residential buildings: Current practice., *Energy and Buildings* 40 (2008) 1446–1455.
- [2] Petitjean, R. Total hydronic balancing, Ljung: Tour&Andersson AB, 1997.
- [3] Liao, Z., Dexter, A.L. The potential for energy saving in heating systems through improving boiler controls, *Energy and Buildings* 36 (2004) 261–271.
- [4] Paris, B., Eynard, J., Grieu, S., Talbert, T., Polit, M., Heating control schemes for energy management in buildings, *Energy and Buildings* 42 (2010) 1908–1917.
- [5] Liao, Z., Swainson, M., Dexter, A.L., On the control of heating systems in the UK, *Building and Environment* 40 (2005) 343–351.
- [6] Rhee, K.N., Ryu, S.R., Yeo, M.S., Kim, K.W., Simulation study on hydronic balancing to improve individual room control for radiant floor heating system, *Building Services Engineering Research and Technology*, 31(1), (2010), 57-73.
- [7] Rhee, KN, Shin, MS, Yeo, MS, Kim, KW, Development of an evaluation strategy of hydronic balancing valves for radiant floor heating systems *Building Service Engineering Research and Technology* 35 (6), (2014), doi: 10.1177/0143624414557838
- [8] Sanaye, S., Mahmoudimehr, J., Aynechi, M., Modelling and economic optimisation of under-floor heating system *Building Service Engineering Research and Technology*, 33(3), (2012), 191-202.
- [9] Rhee, K.N., Yeo, M.S., Kim, K.W., Development of an emulation method for the performance evaluation of radiant floor heating systems *Building Service Engineering Research and Technology* 35(5), (2014), 488-506.
- [10] Olesen, B.W., De Carli, M., Calculation of the yearly energy performance of heating systems based on the European Building Energy Directive and related CEN standards, *Energy and Buildings*, 43(5), (2011), 1040–1050.
- [11] Taylor, S.T., Stein, J., Balancing Variable Flow Hydronic Systems, *ASHRAE Journal*, October 2002, 17-24.
- [12] Djuric, N., Novakovic, V., Frydenlund, F., Heating system performance estimation using optimization tool and BEMS data, *Energy and Buildings*, 40 (8), (2008), 1367–1376.
- [13] Couillaud, N., Riederer, P., Jandon, M., Diab, Y., Balancing Operation for the Optimization of Hydronic Networks, *Proceedings of the 5th International Conference for Enhanced Building Operations*, Pittsburgh, Pennsylvania, October 11-13, 2005, ESL-IC-05-10-23.
- [14] Kalmár, F. Energy analysis of building thermal insulation, *Proc. 11<sup>th</sup> Symposium for Building Physics*, Dresden, Germany, September 26-30, 2002, 103-112.
- [15] Kalmár, F., Optimal forward temperature in retrofitted buildings, *Proc. 2nd International Conference in Building Physics*, Leuven, Belgium, 14-18 September, 2003, p. 649-656.
- [16] Kalmár, F., Heat Gains influence on Balance Point Temperature and Thermal Comfort, 7th Nordic Building Physics Symposium, 13-15 June 2005, Reykjavik, Iceland. vol. II. p. 953-960
- [17] Kalmár, F., Exergy quality of buildings, *Advanced Materials Research* 899 (2014) 30-35.
- [18] Zmeureanu, R., Wu, X.Y., Energy and exergy performance of residential heating systems with separate mechanical ventilation, *Energy*, 32 (3), (2007), 187–195.
- [19] Schmidt, D., Ala-Juusela, M., Low Exergy Systems for Heating and Cooling of Buildings, *Plea2004 - The 21st Conference on Passive and Low Energy Architecture*. Eindhoven, The Netherlands, 19 – 22, September 2004.
- [20] Verbai, Z., Lakatos, A., Kalmár, F., Prediction of energy demand for heating of residential buildings using variable degree day, *Energy* 76 (2014) 780-787.

# Optimum of external wall thermal insulation thickness using total cost method

Jozsef Nyers\*, Peter Komuves\*\*

\*Obuda University Budapest, Becsi ut 96, 1034 Budapest, Hungary

\*\*V3ME, Subotica-Szabadka, M. Corvin 6

E-mail: [nyers@uni-obuda.hu](mailto:nyers@uni-obuda.hu); [nyarp@yahoo.com](mailto:nyarp@yahoo.com); [south@yunord.net](mailto:south@yunord.net);

EXPRES 2015

March 19-21. 2015

**Abstract** - This article investigates the energy-economic optimum of thermal insulation thickness for external wall. The investigation was performed by applying the method 'total cost'. An appropriate steady-state mathematical model was developed. The mathematical model consists of energy and economic part. The economic part of the model contains algebraic equations for investment and exploitation. The considered wall was made of brick and covered with polystyrene as thermal insulation material. The energy-economic optimum was obtained by applying an analytical-numerical and graph-numerical method. The optimization criterion was the minimum of total cost. The numerical results obtained by the simulation are presented graphically. The optimum thickness of the thermal insulation layer is shown in the diagrams. In addition, by applying the developed mathematical model and mathematical methods the optimum thickness of thermal insulation layer was obtained for energy-economic conditions in Serbia in 2015.

---

**Keywords**- total cost method, energy-economic optimum, mathematical model, thermal insulation, objective function

---

## Nomenclature

$q$	Heat flux per unit area [ $W/m^2$ ]
$Q$	Heat per unit area per year [ $Wh/m^2/year$ ]
$\alpha$	Convective heat transfer coefficient [ $W/m^2/K$ ]
$\lambda$	Conductive heat transfer coefficient [ $W/m/K$ ]
$k$	Overall heat transfer coefficient [ $W/m^2/K$ ]
$t$	Temperature [ $^{\circ}C$ ], [ $K$ ]
$\Delta t$	Temperature difference [ $^{\circ}C$ ], [ $K$ ]
$T$	Time period per year [ $h/year$ ]
$\tau$	Time period [ $h$ ]
$\delta$	Thickness of thermal insulation layer [ $m$ ]
$\Delta$	Difference [-]
$C$	Price [ $\epsilon$ ]
$f$	Function
$n$	Number

## Subscripts and superscripts

i	input, investment
s	savings
o	output
m	middle/mean
w	wall
is	isolation
sc	anchor screw

ne fiberglass network

gl cement-based adhesive. Glue

## I. INTRODUCTION

From the economic-energy efficiency point of view of the buildings, it is essential to use a thermal insulation layer to cover all external surfaces. The thermal insulation layer significantly reduces building heat loss. The reduction of losses depends mainly on the thickness of the thermal insulation layer.

Increasing the thermal insulation layer increases investment costs, but reduces the costs of exploitation. The costs for investment and exploitation have opposite tendencies. Thus, there is a technical-economic optimum of thermal insulation thickness.

The optimum can be found by applying appropriate mathematical model and an efficient mathematical method of optimization. From the stand point of analysis, the important issue is to apply the appropriate method for displaying the results. The graphic display one of the convenient forms of representation is. The advantage of graphics is that it visually shows the solutions and the trends of solutions.

This paper analyses the energy-economic optimum thickness of thermal insulation layer for external brick wall. An appropriate mathematical model is required for the analysis. The model is composed of correlations to describe the cost of investment and exploitation. In the functions, the values are expressed in Euros. The independent variables are the thickness of thermal insulation layers ( $\delta$ ) and the payback period of the investment ( $T$ ).

In order to solve the model's equations system a graph-numerical and an analytical-numerical method were applied. The pure analytical method is much more complex than numerical. The numerical solutions are presented in the graphs of the total cost as a function of the thickness. The graphs show the optimum thickness of the thermal insulation layer.

In addition by applying the total cost optimization principle and the developed mathematical model, determined the optimum thickness of the thermal insulation layer and adequate payback period. For technical-economic conditions in Serbia, 2015 the obtained results are:



1. If payback period 1 year the thickness is 5.25 cm
  2. If payback period 2 year the thickness is 9.02 cm
  3. If payback period 2.2 year the thickness is 9.7 cm
- The obtained results valid if the price of electric energy is 0.08 [€/kWh].

## II. THE PHYSICAL MODEL

The considered physical system for techno-economic optimization consisted of an external wall with thermal insulation. The static part of the wall was made of 25 cm brick while thermal insulation was of polystyrene.

From the aspect of thermal calculation of building, only transmission heat losses were taken into account. Both layers generated heat resistance the brick and the thermal insulation layer, too.

The ventilation heat losses were not taken into account since they do not affect the energy-economic optimum of the thermal insulation layer thickness.

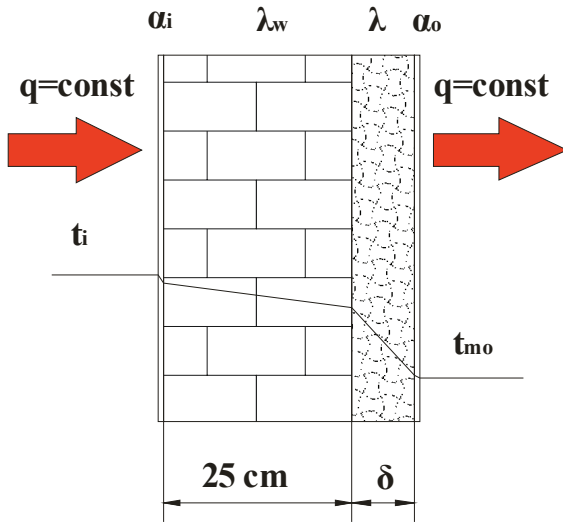


Figure 1. The cross section of the external walls, made of 25 cm brick and thermal insulation layer of polystyrene

## III. ENERGY PART OF THE MATHEMATICAL MODEL

In energy part of the mathematical model the energy losses through external wall was defined.

### A. Transmission heat losses through the external wall

Only transmission thermal losses depend on of the thermal insulation layer thickness, ventilation losses do not.

#### a. Mean heat flux through the external wall

The mean heat flux through the external wall per unit area is defined by the mean temperature difference of the heating season and overall heat transfer coefficient.

$$q_m = k(\delta) \cdot \Delta t_m \quad (1)$$

$$q_m = \frac{1}{\frac{1}{\alpha_i} + \frac{\delta}{\lambda_w} + \frac{1}{\alpha_o}} \cdot (t_i - t_{mo}) \quad (2)$$

Where:

- overall heat transfer coefficient is.

$$k(\delta) = \frac{1}{\frac{1}{\alpha_i} + \frac{\delta}{\lambda_w} + \frac{1}{\alpha_o}} \quad (3)$$

- mean temperature difference between the temperature of the internal  $t_i$  and the mean outside air temperature  $t_{mo}$  for the heating season is.

$$\Delta t_m = t_i - t_{mo} \quad (4)$$

### b. Heat demand of the heating season

Heat demand per unit area of the heating season per year equal to product of the mean heat flux and the time period per year.

$$Q = q_m \cdot T = k(\delta) \cdot \Delta t_m \cdot T \quad (5)$$

$$Q = \frac{1}{\frac{1}{\alpha_i} + \frac{\delta}{\lambda_w} + \frac{1}{\alpha_o}} \cdot (t_i - t_{mo}) \cdot T \quad (6)$$

## IV. ECONOMIC PART OF THE MATHEMATICAL MODEL

In economic part of the mathematical model the total cost was defined. Total cost comprises the investment and exploitation cost.

### A. Investment function

Investment is the sum of wage-pay and material cost.

The investment function is:

$$f_i = C_{is}(\delta) + C_{sc}(\delta) + C_{ne} + C_{gl} + C_{pay} \quad (7)$$

The price of thermal insulation material and the screw anchors depend on of the thermal insulating layer thickness, while other terms can be considered as a constant.

#### a. Constant part of the investment function

Constant part of the investment function makes fiber glass net price, price of glue for polystyrene and labour price, per  $m^2$ .

$$C = C_{ne} + C_{gl} + C_{pay} \quad (8)$$

### B. Final form of the investment function

The investment function is the sum of independent and dependent terms of thickness.

$$f_i = C_{isol}(\delta) + C_{screw}(\delta) + C \quad (9)$$

### C. Exploitation cost function

Exploitation cost is product of the heat losses throu the thermal insulation external wall per unit area and price of the energy source.

$$f_e = Q \cdot T \cdot e(\tau) \quad (10)$$

$$f_e = k(\delta) \cdot \Delta t_m(T) \cdot T \cdot e(T) \quad (11)$$



## V. SIMULATION

### A. About the simulation

A simulation to determine the optimum thickness of thermal insulating layer was done based on the technical-economic situation in Serbia in 2015.

### B. Data of the simulation

- Brick wall thickness  $\delta = 0.25$  m.
- Coefficient of heat conduction for the brick wall  $\lambda = 0.5$  W/m/K.
- Coefficient of heat conduction of polystyrene  $\lambda_w = 0.05$  [W/m/K].
- Convection heat transfer coefficient of the indoor air  $\alpha_i = 8$  [W/m<sup>2</sup>/K].
- Convection heat transfer coefficient of the outside air  $\alpha_o = 20$  [W/m<sup>2</sup>/K].
- Internal mean temperature  $t_i = 20$  [°C].
- Mean outdoor temperature of the heating season  $t_{mo} = 4$  [°C].
- Polystyrene price  $C_{in,m} = 40$  [€/m<sup>2</sup>m].
- Glue price  $C_{gl} = 3\text{€}/25 \text{ kg} \cdot 7\text{kg}/\text{m}^2 = 0.84$  [€/kg].
- Consumption of glue  $7$  [kg/m<sup>2</sup>].
- Price of the screw anchors for 5cm thickness  $C_{s5} = 0.03$  [€/piece].
- Price of the screw anchors for 10cm thickness  $C_{s10} = 0.043$  [€/piece].
- Number of the screw anchors per m<sup>2</sup>  $n_s = 6$ .
- Labour price for the installation of thermal insulating layer  $6$  [€/m<sup>2</sup>].
- Mean unit price of electric energy in Serbia 2015  $e = 0.08$  [€/kWh]  $= 0.08 \cdot 10^{-3}$  [€/Wh].

### C. Functions of simulation

#### a. Exploitation cost function with data

$$f_e = k(\delta) \cdot \Delta t_m \cdot T \cdot e \quad (12)$$

$$f_e = \frac{0.05}{0.03375 + \delta} \cdot 16 \cdot T \cdot 0.08 \cdot 10^{-3} \quad (13)$$

Where:

The overall coefficient difference of the heat transfer through the wall.

$$k(\delta) = \frac{1}{\frac{1}{20} + \frac{0.25}{0.5} + \frac{\delta}{0.05} + \frac{1}{8}} = \frac{0.05}{0.03375 + \delta} \text{ [Wh/m}^2\text{K]} \quad (14)$$

#### b. Investment function with data

$$f_i = C_{is}(\delta) + C_{sc}(\delta) + C_{ne} + C_{gl} + C_{pay} \quad (28)$$

$$f_i = 40 \cdot \delta + 0 + 2 + 1.4 + 6 \text{ [€/m}^2\text{]} \quad (29)$$

$$f_i = 40 \cdot \delta + 9.4 \text{ [€/m}^2\text{]} \quad (29)$$

#### c. Objectiv function with data

$$f_o = f_i + f_e$$

$$f_o = 40 \cdot \delta + 9.4 + \frac{0.05}{0.03375 + \delta} \cdot 16 \cdot T \cdot 0.08 \cdot 10^{-3}$$

## VI. TOTAL COST OPTIMIZATION METHOD

The goal of optimizations is to find the optimum thickness of the thermal insulation layer according to minimum cost.

### A. Objectiv function of total cost method

The implicit objectiv function of total cost method is equal to sum of the investment and exploitation cost.

$$f_o = f_i + f_e \quad (15)$$

The investment and exploitation cost functions.

$$f_i = C_{is}(\delta) + C_{sc}(\delta) + C \quad (16)$$

$$f_e = k(\delta) \cdot \Delta t_m \cdot T \cdot e \quad (17)$$

The implicit objectiv function.

$$f_o = C_{is}(\delta) + C_{sc}(\delta) + C + k(\delta) \cdot \Delta t_m \cdot T \cdot e \quad (18)$$

Equation (36) contains four independent variables: the insulating layer thickness, the payback period, the mean temperature difference and energy unit price. The equation can be solved by each of the four independent variables.

### B. Analytical optimization method

The mathematical optimum condition is the first derivative of objective function with respect to thickness equal zero.

$$\frac{\partial f_o}{\partial \delta} = 0 \quad (19)$$

$$\frac{\partial}{\partial \delta} (C_{is}(\delta) + C_{sc}(\delta) + C + k(\delta) \cdot \Delta t_m \cdot T \cdot e) = 0 \quad (20)$$

After derivation

$$\left( \frac{\partial C_{is}(\delta)}{\partial \delta} + \frac{\partial C_{sc}(\delta)}{\partial \delta} \right) + \frac{\partial k(\delta)}{\partial \delta} \cdot \Delta t_m \cdot T \cdot e = 0 \quad (21)$$

The first derivative of the thermal insulation price with respect to thickness

$$C_{is}(\delta) = C_{is,m} \cdot \delta \quad (22)$$

$$\frac{\partial C_{is}(\delta)}{\partial \delta} = \frac{\partial (C_{is,m} \cdot \delta)}{\partial \delta} = C_{is,m} \quad (23)$$

The first derivative of the screw price with respect to thickness is.

$$C_{sc}(\delta) = \left( C_{s5} + \frac{C_{s10} - C_{s5}}{\delta_{10} - \delta_5} \cdot (\delta - \delta_5) \right) \cdot n_s \quad (24)$$

$$\frac{\partial C_{sc}(\delta)}{\partial \delta} = \frac{C_{s10} - C_{s5}}{\delta_{10} - \delta_5} \cdot n_s \quad (25)$$

The first derivative of the overall coefficient with respect to thickness is.

$$k(\delta) = \frac{1}{\frac{1}{\alpha_i} + \frac{\delta_w}{\lambda_w} + \frac{\delta}{\lambda} + \frac{1}{\alpha_o}} \quad (26)$$

$$\frac{\partial k(\delta)}{\partial \delta} = \frac{\partial}{\partial \delta} \left( \frac{1}{\frac{1}{\alpha i} + \frac{\delta_w}{\lambda_w} + \frac{\delta}{\lambda} + \frac{1}{\alpha o}} \right) \quad (27)$$

$$\frac{\partial k(\delta)}{\partial \delta} = \frac{-\frac{1}{\lambda}}{\left( \frac{1}{\alpha i} + \frac{\delta_w}{\lambda_w} + \frac{\delta}{\lambda} + \frac{1}{\alpha o} \right)^2} \quad (28)$$

Objective function for determining the optimum thickness of the thermal insulation layer

$$C_{is,m} + \frac{C_{s10} - C_{s5}}{\delta_{10} - \delta_5} \cdot n_s + \frac{-\frac{1}{\lambda}}{\left( \frac{1}{\alpha i} + \frac{\delta_w}{\lambda_w} + \frac{\delta}{\lambda} + \frac{1}{\alpha o} \right)^2} \cdot \Delta t_m \cdot T \cdot e = 0 \quad (29)$$

Objective function in ather form

$$\left( C_{is,m} + \frac{C_{s10} - C_{s5}}{\delta_{10} - \delta_5} \cdot n_s \right) \cdot \left( \frac{1}{\alpha i} + \frac{\delta_w}{\lambda_w} + \frac{\delta}{\lambda} + \frac{1}{\alpha o} \right)^2 - \frac{1}{\lambda} \cdot \Delta t_m \cdot T \cdot e = 0 \quad (30)$$

The obtained optimum equation with respect to thickness can be solved analytically as second-degree algebraic equation.

For example

$$(40 + 0) \cdot \left( \frac{1}{8} + \frac{0.25}{0.5} + \frac{\delta}{0.05} + \frac{1}{20} \right)^2 - \frac{1}{0.05} \cdot 16 \cdot 2 \cdot 4800 \cdot 0.08 \cdot 10^{-3} = 0 \quad (31)$$

The optimum thermal insulation thickness is 0.09018 [m] for 2 years i.e. 2 · 4800 h payback period.

### C. The numerical - graphical optimization method

The numerical - graphical optimization method is easier performable than the analytical method but not so accurate. The solutions obtained solving the optimum equation are numerically and results are displayed graphically in the coordinate system. The analysis is visual, the graph shows the tendency of total cost variation depend on the thermal insulating layer's thickness.

In addition the total cost chart shows the optimum thickness of the thermal insulating layer and the payback period of the investment.

The simulation algorithm of optimum function (30) was implemented in the Matlab mathematical package.

## VII. THE RESULTS

### A. Analytical resultats

Analytical resultats obtained by solving analytically the algebraic objective function. For example:

The optimum thermal insulation thickness is 0.09018 [m] for 2 years i.e. 2 · 4800 h payback period. The total cost 18 [€/m<sup>2</sup>].

### B. Numerical results

The numerical results obtained by simulation are presented graphically in Figures 2.

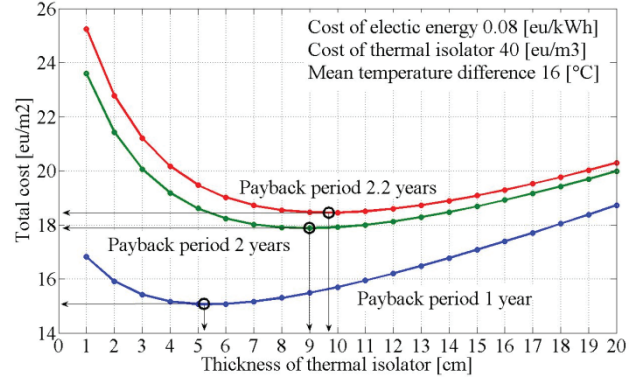


Figure 2. The total cost functions with optimum thermal insulation thickness for different payback periods in Serbia 2015.

## VIII. CONCLUSIONS

The aim of this study was to find the optimum thickness of thermal insulation layer for external wall by using the total cost method.

The total cost method is based on the condition, minimum total cost.

The mathematical model consists of energy and economic part. The energy part includes the equation of heat demand with thermal insulation. The economic part comprises the equation of investment and exploitation.

The optimization procedure were analytical-numerical and graphic-numerical.

Comparison results obtained applying the analytical-numerical or graphical-numerical methods, are exactly the same.

The graph shows, the optimum polystyrene thickness is:

- 5.25 [cm] for 1 years, total cost 15.1 [€/m<sup>2</sup>]
- 9.018 [cm] for 2 years, total cost 18 [€/m<sup>2</sup>]
- 9.8 [cm] for 2.2 year, total cost 18.5 [€/m<sup>2</sup>] Figure 2.

All the above data are valid for Subotica-Serbia, for the year 2015.

## REFERENCES

- [1] Ray Galvin: Thermal upgrades of existing homes in Germany: The building code, subsidies, and economic efficiency. *Energy and Buildings*, Volume 42, Issue 6, June 2010, Pages 834–844.
- [2] Meral Ozel: Cost analysis for optimum thicknesses and environmental impacts of different insulation materials. *Energy and Buildings*, Volume 49, June 2012, Pages 552–559.
- [3] Surapong Chiraratananon, Vu Duc Hien: Thermal performance and cost effectiveness of massive walls under thai climate, *Energy and Buildings*, Volume 43, Issue 7, July 2011, Pages 1655–1666.
- [4] Imrich Bartal, Hc László Bánhidi, László Garbai: Analysis of the static thermal comfort equation. *Energy and Buildings* Vol. 49 (2012), pp. 188-191.
- [5] Nyers J., Tomic S., Nyers A.: “Economic Optimum of Thermal Insulating Layer for External Wall of Brick ”. *International J. Acta Polytechnica Hungarica* Vol. 11, No. 7, pp. 209-222, 2014.
- [6] Nagy Károly, Divéki Szabolcs, Odry Péter, Sokola Matija, Vujicic Vladimir: "A Stochastic Approach to Fuzzy Control", *I.J. Acta Polytechnica Hungarica*, Vol. 9, No 6, 2012, pp. 29-48. (ISSN: 1785-8860).
- [7] László Garbai, Róbert Sánta: Flow pattern map for in tube evaporation and condensation, 4th International Symposium on Exploitation of Renewable Energy Sources, EXPRESS 2012, ISBN: 978-86-85409-70-7, pp. 125-130, 9-10 March, Subotica, Serbia.
- [8] Kajtár L., Hrustinszky T.: Investigation and influence of indoor air quality on energy demand of office buildings. *WSEAS Transactions on Heat and Mass Transfer*, Issue 4, Volume 3, October 2008. 219-228 p.
- [9] László Kajtár, Miklós Kassai, László Bánhidi: Computerised simulation of the energy consumption of air handling units. 2011. *Energy and Buildings*, ISSN: 0378-7788, (45) pp. 54-59.
- [10] László Kajtár, Levente Herczeg: Influence of carbon-dioxide concentration on human wellbeing and intensity of mental work. Bp. 2012. *Időjárás, Quarterly Journal of the Hungarian Meteorological Service*, Vol. 116 No.2 april-june 2012. p. 145 – 169. ISSN 0324-6329.
- [11] K Dabis, Z Szánthó: Control of Domestic Hot Water production is instantaneous heating system with a speed controlled pump, 6<sup>th</sup> International symposium “EXPRES 2014 VTS.” Subotica. Serbia, 2014. pp. 101-106. ISBN 978-86-85409-96-7.

# Direct numerical simulation of Navier-Stokes equation for the forced rayleigh-be nard convection of temperature variation at the lower wall

Sadoon Ayed<sup>\*</sup>, Gradomir Ilic<sup>\*\*</sup>, Predrag Živković<sup>\*\*</sup>, MladenTomic<sup>\*\*</sup>, Amir Rashid<sup>\*\*</sup>

<sup>\*</sup>University of Technology/ Department of Mechanical Engineering, Baghdad, Iraq

<sup>\*\*</sup>University of Nis/Faculty of Mechanical Engineering, Nis, Serbia

[sadun\\_kad@yahoo.com](mailto:sadun_kad@yahoo.com); [pzivkoc@masfak.ni.ac.rs](mailto:pzivkoc@masfak.ni.ac.rs); [tomicmladen@yahoo.com](mailto:tomicmladen@yahoo.com);

[amircraft.2011@yahoo.com](mailto:amircraft.2011@yahoo.com)

**Abstract—** Numerical study of the effect variation temperature viscous fluid between two parallel plates is gradually increased during a certain time period ,the temperature distribution on the lower plate is not constant at x direction and there is longitudinal sinusoidal temperature variation imposed on the mean temperature .We investigate the amplitude and wavenumber influence of this variation on the stability of Rayleigh-Be nard convection cells by direct numerical simulation of 2-D Navier-Stokes and energy equation although the architecture of the hot plate makes it possible to know the distribution of the convection coefficient exchanges with the vortices and stream function of fluid, we have used pseudo spectral numerical code, where we have used Fourer - Galarkin method for homogeneous direction. For time discretization, we have used Adem\_ Bashworth two-steps, second order accurate, and method.

## I. INTRODUCTION

The Rayleigh–Benard convection is the flow between two walls heated at the bottom and cooled at the top. Due to the importance of this flow in industrial and environmental applications, summarized most of the previous experimental and numerical works .The Rayleigh–Be nard convection is characterized by a large cellular motion. When the Rayleigh number is relatively small, this cellular motion is clearly observed from experiments or numerical calculations, however, when the Rayleigh number is large, very little is known from the experiment and numerical solutions. One can obtain a detailed thermal–hydraulic information from a numerical simulation.

Rayleigh solved the problem of stability of the conducting state when a fluid in a gravitational field is bound from above and below with spatially constant but unequal wall temperatures. Rayleigh number and it is the ratio between the driving buoyancy and the damping viscosity forces. Another parameter, that measures the relative strength of the non-linearity in the momentum equations v. s. that of heat equation, is the Prandtl

number as the ratio of kinematic viscosity to thermal diffusivity are defined in the following way:

$$Ra = \frac{\beta g (\theta_1 - \theta_2) d^3}{\nu \alpha}, \quad Pr = \frac{\nu}{\alpha}.$$

Here  $g$  is the gravitational acceleration,  $\beta$  is the thermal expansion coefficient,  $\theta_1$  is the temperature of lower plate and  $\theta_2$  is the temperature of upper plate,  $d=2H$  is the distance between the plates,  $\nu$  is the kinematic viscosity and  $\alpha$  is the thermal diffusivity. In the above definition of the Rayleigh number, the fluid properties are calculated at mean temperature  $\theta_m = (\theta_1 + \theta_2)/2$ , because this is the best reference temperature. In our calculation,  $\theta_1$  is a temporal and x-direction variable function, and so is the Ra number, which is a non-dimensional parameter for the measure of the ratio of buoyancy and diffusive forces.

*Navier- Stokes, continuity and energy equation.*

Navier-Stokes and energy equation for incompressible isothermal flow in vorticity-streamfunction formulation for two-dimensional flow in no dimensional form read

$$\frac{\partial \omega}{\partial t} + \frac{\partial \psi}{\partial y} \frac{\partial \omega}{\partial x} - \frac{\partial \psi}{\partial x} \frac{\partial \omega}{\partial y} = Pr Ra \frac{\partial T}{\partial x} + Pr \left( \frac{\partial^2 \omega}{\partial x^2} + \frac{\partial^2 \omega}{\partial y^2} \right), \quad (1)$$

$$\omega + \frac{\partial^2 \psi}{\partial x^2} + \frac{\partial^2 \psi}{\partial y^2} = 0, \quad (2)$$

$$\frac{\partial T}{\partial t} + \frac{\partial \psi}{\partial y} \frac{\partial T}{\partial x} - \frac{\partial \psi}{\partial x} \frac{\partial T}{\partial y} = \frac{\partial^2 T}{\partial x^2} + \frac{\partial^2 T}{\partial y^2}, \quad (3)$$

Boudary conditions is

$$T = 0, \quad \psi = 0, \quad \partial \psi / \partial y = 0, \quad \text{at } y = 1, \quad (4)$$

$$T = 1, \quad \psi = 0, \quad \partial \psi / \partial y = 0, \quad \text{at } y = -1, \quad (5)$$

And Intial conditions

$$\psi(x, y, 0) = \psi_0(x, y), \quad T(x, y, 0) = T_0(x, y) \quad \text{on } \Omega. \quad (6)$$

Here  $\omega$  - is dimensionless vorticity of fluid,  $\psi$  - dimensionless streamfunction,  $T$ -dimensionless temperature, which are functions of coordinate  $x$ ,  $y$  and time  $t$ . The dimensionless temperature is defined in the following way

$$T = \frac{\theta - \theta_2}{\theta_1 - \theta_2},$$

where  $\theta$  is the fluid temperature. The domain  $\Omega$  is defined as  $\Omega = \{(x, y) \in \mathbb{R}^2 | 0 \leq x \leq 2\pi \wedge -1 < y < 1\}$ . We have designated the upper domain boundary  $\Gamma_u = \{(x, y) \in \mathbb{R}^2 | 0 \leq x \leq 2\pi \wedge y = 1\}$  and the lower domain boundary  $\Gamma_l = \{(x, y) \in \mathbb{R}^2 | 0 \leq x \leq 2\pi \wedge y = -1\}$ . The time domain is defined as  $\tau = \{t \in \mathbb{R} | 0 \leq t \leq \tau_e\}$ , where  $\tau_e$  is the end of the simulation. We have anticipated the periodic boundary conditions in streamwise direction ( $x$ -axis), which are in accordance with the periodic perturbations obtained by periodic temperature modulation on both plates.

## II. NUMERICAL TREATMENT OF THE GOVERNING EQUATIONS

For the problem stated in the previous section, for the basis function in  $x$ -direction we have taken trigonometric polynomials, and for  $y$ -direction we have taken Chebyshev polynomials. The domain in  $x$ -direction is equally discretized  $\Delta x = 2\pi/N$ , and domain in  $y$ -direction is discretized by Gauss-Lobatto-Chebyshev points defined as  $y_j = \cos(\pi j/N)$  for  $0 \leq j \leq N$ , where is  $N$ -number of discretization points in  $x$ - and  $y$ -direction. For stream wise direction, we have used Fourier-Galerkin method, and for stream normal direction Chebyshev-collocation method. The truncated Fourier series for vorticity, streamfunction and temperature read:

$$\omega_N(x, y, t) = \sum_{k=-N/2}^{k=N/2} \hat{\omega}_k(y, t) e^{I k x}, \quad (7)$$

$$\psi_N(x, y, t) = \sum_{k=-N/2}^{k=N/2} \hat{\psi}_k(y, t) e^{I k x}. \quad (8)$$

$$T_N(x, y, t) = \sum_{k=-N/2}^{k=N/2} \hat{T}_k(y, t) e^{I k x}. \quad (9)$$

In the above expressions  $I = \sqrt{-1} = (-1)^{1/2}$  is imaginary unit,  $k$ -wave number,  $\hat{\omega}_k(y, t)$ ,  $\hat{\psi}_k(y, t)$  and  $\hat{T}_k(y, t)$  are Fourier coefficients for vorticity, stream function and temperature respectively. In order to have  $2\pi$ -periodicity in the flow domain, we have chosen that wave number must be from the set of integers,  $k \in \mathbb{Z}$ . We apply Fourier-Galerkin method in  $x$ -direction and then Chebyshev collocation method in  $y$ -direction to the system of equation (1), (2) and (3), with boundary (4) and (5) and initial conditions (6).

We approximate nonlinear convective terms on left hand side, in the following manner:

$$N_1 = \left( \frac{\partial \psi}{\partial y} \frac{\partial \omega}{\partial x} \right)_N(x, y, t) = \sum_{k=-N/2}^{N/2} \left[ \frac{\partial \psi}{\partial y} \frac{\partial \omega}{\partial x} \right]_k(y, t) e^{I k x},$$

$$N_2 = \left( \frac{\partial \psi}{\partial x} \frac{\partial \omega}{\partial y} \right)_N(x, y, t) = \sum_{k=-N/2}^{N/2} \left[ \frac{\partial \psi}{\partial x} \frac{\partial \omega}{\partial y} \right]_k(y, t) e^{I k x}. \quad (10)$$

$$N_3 = \left( \frac{\partial \psi}{\partial y} \frac{\partial T}{\partial x} \right)_N(x, y, t) = \sum_{k=-N/2}^{N/2} \left[ \frac{\partial \psi}{\partial y} \frac{\partial T}{\partial x} \right]_k(y, t) e^{I k x}, \quad (11)$$

$$N_4 = \left( \frac{\partial \psi}{\partial x} \frac{\partial T}{\partial y} \right)_N(x, y, t) = \sum_{k=-N/2}^{N/2} \left[ \frac{\partial \psi}{\partial x} \frac{\partial T}{\partial y} \right]_k(y, t) e^{I k x}, \quad (12)$$

Substituting, (7), (8) and (9) in (1), (2) and (3) we obtain the following residuals equations:

$$\frac{\partial}{\partial t} \sum_{k=-K}^K \hat{\omega}_k(y, t) e^{I k x} + \sum_{k=-K}^K \left[ \frac{\partial \psi}{\partial y} \frac{\partial \omega}{\partial x} \right]_k(y, t) e^{I k x} - \sum_{k=-K}^K \left[ \frac{\partial \psi}{\partial x} \frac{\partial \omega}{\partial y} \right]_k(y, t) e^{I k x} - \text{Pr Ra} \frac{\partial}{\partial x} \sum_{k=-K}^K \hat{T}_k(y, t) e^{I k x} \quad (13)$$

$$- \text{Pr} \left( \frac{\partial^2}{\partial x^2} + \frac{\partial^2}{\partial y^2} \right) \sum_{k=-K}^K \hat{\omega}_k(y, t) e^{I k x} \neq 0,$$

$$\sum_{k=-K}^K \hat{\omega}_k(y, t) e^{I k x} + \left( \frac{\partial^2}{\partial x^2} + \frac{\partial^2}{\partial y^2} \right) \sum_{k=-K}^K \hat{\psi}_k(y, t) e^{I k x} \neq 0. \quad (14)$$

$$\frac{\partial}{\partial t} \sum_{k=-K}^K \hat{T}_k(y, t) e^{I k x} + \sum_{k=-K}^K \left[ \frac{\partial \psi}{\partial y} \frac{\partial T}{\partial x} \right]_k(y, t) e^{I k x} - \sum_{k=-K}^K \left[ \frac{\partial \psi}{\partial x} \frac{\partial T}{\partial y} \right]_k(y, t) e^{I k x} = \left( \frac{\partial^2}{\partial x^2} + \frac{\partial^2}{\partial y^2} \right) \sum_{k=-K}^K \hat{T}_k e^{I k x}, \quad (15)$$

If we apply Galerkin method to the equations (13)(14) and (15), i.e. we take for the weight functions the same as the basis functions, we obtain:

$$\frac{\partial \hat{\omega}_k(y, t)}{\partial t} + \left[ \frac{\partial \psi}{\partial y} \frac{\partial \omega}{\partial x} \right]_k(y, t) - \left[ \frac{\partial \psi}{\partial x} \frac{\partial \omega}{\partial y} \right]_k(y, t) - \text{Pr Ra} I k \hat{T}_k(y, t) = \text{Pr} \left( -k^2 + \frac{\partial^2}{\partial y^2} \right) \hat{\omega}_k(y, t) \quad (16)$$

$$l = k = 0, 1, \dots, N/2.$$

$$\hat{\omega}_k(y, t) + \left( -k^2 + \frac{\partial^2}{\partial y^2} \right) \hat{\psi}_k(y, t) = 0,$$

$$l = k = 0, 1, \dots, N/2.$$

(17)



$$\begin{aligned} \frac{\partial \hat{T}_k}{\partial t}(y, t) + \left[ \frac{\partial \psi}{\partial y} \frac{\partial T}{\partial x} \right]_{kN}(y, t) - \left[ \frac{\partial \psi}{\partial x} \frac{\partial T}{\partial y} \right]_{kN}(y, t) = \\ = (Ik)^2 \hat{T}_k(y, t) + \frac{\partial^2 \hat{T}_k}{\partial y^2}(y, t), \end{aligned} \quad (18)$$

Applying now the Chebyshev-collocation method in inhomogeneous direction ( $y$ -axis) to the above system of equations, we get the

$$\begin{aligned} \frac{\partial \hat{\omega}_{kN}}{\partial t}(y_j, t) + \left[ \frac{\partial \psi}{\partial y} \frac{\partial \omega}{\partial x} \right]_{kN}(y_j) - \left[ \frac{\partial \psi}{\partial x} \frac{\partial \omega}{\partial y} \right]_{kN}(y_j) - \\ - \text{Pr Ra } Ik \hat{T}_{kN}(y_j, t) = \text{Pr} \left( -k^2 + \sum_{l=0}^N d_{j,l}^{(2)} \right) \hat{\omega}_{kN}(y_j, t), \end{aligned} \quad (19)$$

$$k = 0, 1, \dots, N/2, \quad j = 1, \dots, N-1,$$

$$\hat{\omega}_{kN}(y_j, t) + \left( -k^2 + \sum_{l=0}^N d_{j,l}^{(2)} \right) \hat{\psi}_{kN}(y_j, t) = 0, \quad (20)$$

$$k = 0, 1, \dots, N/2, \quad j = 1, \dots, N-1.$$

$$\begin{aligned} \frac{\partial \hat{T}_{kN}}{\partial t}(y_j, t) + \left[ \frac{\partial \psi}{\partial y} \frac{\partial T}{\partial x} \right]_{kN}(y_j, t) - \left[ \frac{\partial \psi}{\partial x} \frac{\partial T}{\partial y} \right]_{kN}(y_j, t) = \\ = \left( -k^2 + \sum_{l=0}^N d_{j,l}^{(2)} \right) \hat{T}_{kN}(y_j, t), \end{aligned} \quad (21)$$

$d_{j,l}^{(2)}$  are elements of second order Chebyshev differentiation matrix [2]. This system of equations is discretized in time by using Adams-Bashworth semi-implicit finite difference scheme with second order accuracy. This system of equations (19), (20) and (21) together with boundary (4), (5) and initial conditions (6) should be solved numerically. The system is represented by  $2(N+1) \times 2(N+1)$  three time levels matrix equation. The nonlinear advective terms have been computed by pseudo spectral technique [3], so that full Navier-Stokes equation in vorticity-stream function formulation and energy equation can be simulated for the case of 2D-plane channel flow. The problem of two boundary conditions for stream function and none for vorticity has been successfully resolved by applying the influence matrix method [4].

### III. TEMPERATURE MODULATION ON PLATES

In order to simulate the process of forced Rayleigh-Bernard convection we have to specify the initial and boundary conditions on both plates. The initial condition and boundary conditions. The temperature at the lower and upper wall is not constant in  $x$ -direction, it depends on  $q_m$ -modulation wavenumber, amplitude  $\delta_m$  and  $\omega$ -frequency.

$$\begin{aligned} \omega(x, y, t=0) = 0, \quad \psi(x, y, 0) = 0, \quad T(x, y, 0) = 0, \\ \text{for } \forall (x, y) \in D = \{(x, y) \in \mathbb{R} \mid 0 \leq x \leq 2\pi, -1 \leq y \leq 1\}. \end{aligned} \quad (22)$$

Rayleigh number  $Ra$  measures the average temperature gradient, while the additional spatial modulation is characterized by small amplitude  $\delta_m$  and wavenumber  $q_m$ . In the absence of forcing ( $\delta_m=0$ ), convection rolls with wavenumber  $q_c$ , bifurcate only for  $Ra$  above the critical Rayleigh number  $Ra_c$ .

$$\begin{aligned} T(x, y = -1, t) &= (1 + \delta_m \sin q_m x + \delta_m \cos q_m x) \sin \omega t, \\ T(x, y = 1, t) &= (\delta_m \sin q_m x + \delta_m \cos q_m x) \sin \omega t \\ 0 \leq t &\leq \pi/2\omega \\ T(x, y = -1, t) &= (1 + \delta_m \sin q_m x + \delta_m \cos q_m x), \\ T(x, y = 1, t) &= (\delta_m \sin q_m x + \delta_m \cos q_m x). \\ \pi/2\omega &< t. \end{aligned} \quad (23)$$

The onset of convection is characterized by a parabolic linear stability curve (neutral curve) in parameter space with  $Ra$  as the abscissa and  $q$  on the ordinate axis. The neutral curve has its minimum at the critical wavenumber  $q_c=3.117$ , with the critical Rayleigh number  $Ra_c=1707.8$ . To our best knowledge, the first experiments on steadily forced RBC ( $\delta_m=0$ ) with  $q_m \approx q_c$ , where  $q_c$  is critical wavenumber, have been performed only recently [5], [6], [7] and [8]. Here, the distance  $d$  between the horizontal plates confining the convection cell has been periodically modulated by gluing an array of equidistant polymer stripes of height  $h_d$  on the inner surface of the lower plate. The average layer height  $d$  can be varied to some extent and thus  $q_c \sim d^{-1}$  as well, which allows exploration of forced rolls with wavenumbers  $q_m$  in a finite interval about  $q_c$ . The experiments present a wealth of new phenomena, whose detailed analysis has just started. There are good theoretical arguments [7], [9] that the geometrical boundary modulation in the RBC experiments can be satisfactorily mapped onto a pure temperature modulation at the lower plate with a small amplitude  $\delta_m \sim O(0.03)$ . We have thus restricted ourselves in this paper to a temperature modulation model, which is much easier to analyze than the geometrical modulations. In our previous paper, we have taken into account [10] the temperature modulation on lower plate, but in this one on the both plates with same amplitude and wavenumber.

### IV. THE RESULTS OF FLOW SIMULATION

In this section, we show the results of direct numerical simulation for the forced Rayleigh-Bernard convection flow. The results are shown in the fig.1 and we can see the vorticity evolution for four different instant of time, we can notice. The instability of convection rolls in this time, where the result of simulation for  $t=3\pi$  show the stable flow pattern, where concentration of vorticity lifts up from lower plate to the upper one. The concentration of vortices at the upper plate is lower than on the lower plate, although the amplitude  $\delta_m=0.3$  and wavenumber  $q_m=10$  are identical for both plates. The vorticity gradients on the hotter plate are much higher than on the colder one. The lower plate serves as the source of vorticity in this case and the convection of vorticity is



upwards. The maximal and minimal (extreme) values of vorticity are on the lower plate. At the next instant of time  $t=3\pi$  we can see that vorticity distribution has been altered significantly. The concentration of vorticity attains higher values in the area  $y=-0.5$ , than they were in the previous instant of time. The vorticity distribution and its intensity on lower plate is unaltered, which can be easily seen on the color bar on the right-hand side for both instant of time  $t=3\pi$  and  $t=4\pi$  and  $t=5\pi$ . In the next instant of time  $t=6\pi$  the situation has been changed dramatically. We can see that the vorticity distribution alters its structure, which is completely disturbed, and has jump in its intensity. The extreme values of vorticity attain the value  $\omega_{max}>25$  and  $\omega_{min}<-15$ . They are located on the upper plate ( $y=1$ ) and in the middle of the channel ( $y=0$ ) at  $x=1.7$  and  $x=4.9$ . The regular pattern, ten vortex pair on upper and lower plate with clockwise (blue) and counterclockwise rotation (red), collapses and now quite different vortex distribution establishes on lower (hot) and upper (cold) plate and also in the space between them. Vorticity gradients are much higher in the region close to lower plate for all four instants of time in fig.1

Figure 2 shows the stream function evolution for the problem described, for the corresponding instants of time. At the moment  $t=3\pi$  we can see fairly regular pattern for stream function distribution which corresponds to the modulation wavenumber  $q_m=10$ . The gradients in  $x$ -direction correspond to the velocity in negative  $y$ -direction ( $v=-\partial\psi/\partial x$ ) and gradients in  $y$ -direction correspond to the velocity in  $x$ -direction ( $u=\partial\psi/\partial y$ ). 2D channel viscous. Fluid flow for  $t=3\pi, 4\pi, 5\pi, 6\pi$ .

## V. CONCLUSIONS

In this simulation we can notice that the gross of vorticity perturbation is concentrated in the region close to the lower wall of channel. The qualitative change in vorticity and stream function distribution takes place in time period  $3\pi \leq t \leq 6\pi$ , where the instability of forced Rayleigh-Benard convection is noticeable. We can see the transition from regular pattern (laminar fluid flow) to irregular pattern (turbulent fluid flow). The forced RBC has been immediately established and its stability disturbed in time period shown in fig.1 and fig.2.

We can notice that the distribution of stream function and its intensity alters between the instants of time shown in the fig.2. The regular pattern is disturbed in  $t=4\pi$  and changed completely at  $t=6\pi$ , where instead of two pairs of positive and negative stream function area in regular form, we two pairs with irregular form. The values for this simulation we have chosen subcritical values  $Ra=1000$ , modulation wavenumber  $q_m=10$ , frequency  $\omega=1$ , which are far away from neutral stability curve according to linear stability analysis. We have taken  $Pr=7$ ,  $\Delta t=\pi/100$ ,  $\delta_m=0.03$ , number of Fourier modes  $K=20$ , number of nodes  $N_x=512$ , number of Chebyshev collocation points  $N_y=256$ .

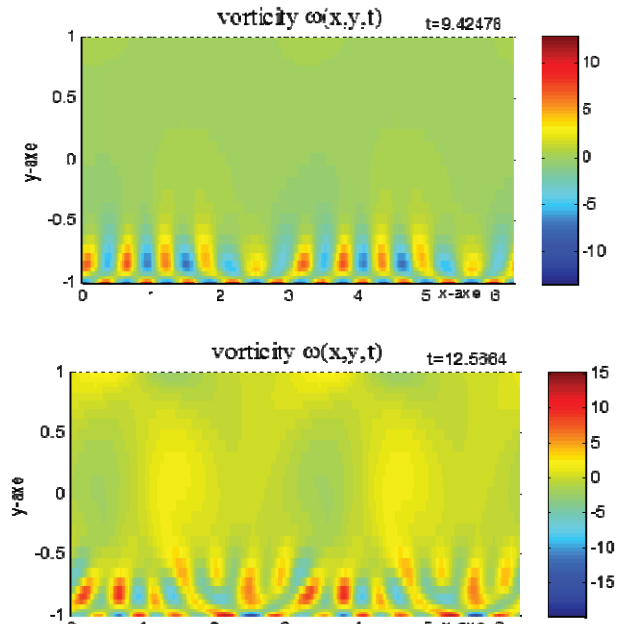


Figure1.vorticity distribution  $\omega(x,y,t)$  in 2D channel viscous fluid flow for  $t=3\pi, 4\pi, 5\pi$ ,

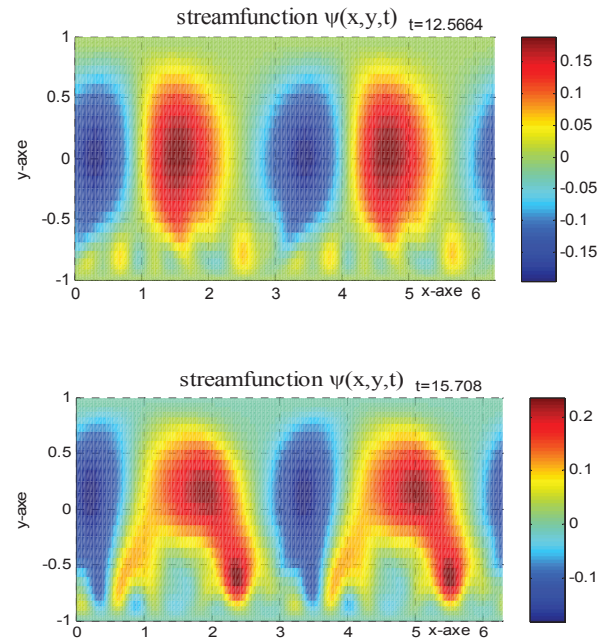


Figure 2.stream function distribution  $\psi(x,y,t)$  in 2D channel viscous Fluid flow for  $t=3\pi, 4\pi, 5\pi, 6\pi$

## REFERENCES

- Jovanović M.(2009), Simulation of temporal hydrodynamic stability for the plane channel viscous flow, 2<sup>nd</sup> international congress of Serbian society of mechanics (IConSSM), Palić, Subotica, Serbia, 1-5<sup>th</sup> June 2009, B09-B23.
- Parviz M. (2001), Fundamentals of Engineering Numerical Analysis, CUP.
- Fornberg B (2005), Pseudospectral methods, Cambridge University Press.
- Kleiser L., Schumann U.,(1980): Treatment of incompressibility and boundary conditions in 3D numerical spectral simulation of

plane channel flows. Hirschel E.H.(ed.): Third GAMM Conference  
 rical Methods in Fluid Dynamics,Vieweg, pp.165-173.

- [5] McCoy, J. (2008), Pattern formation due to spatially periodic forcing. PhD thesis, Cornell University.
- [6] McCoy, J. H., Brunner, W., Pesch, W., Bodenschatz, E. (2008), Self-organization of topological defects due to applied constraints. *Phys. Rev. Lett.* 101, 254102.
- [7] Seiden, G., Weiss, S., McCoy, J. H., Pesch, W. and Bodenschatz, E. (2008), Pattern forming system in the presence of different symmetry-breaking mechanisms. *Phys. Rev. Lett.* 101, 214503.
- [8] Weiss, S. (2009), On forcing in thermal convection experiments. PhD thesis, Universität Göttingen.
- [9] Kelly, R. E. & Pal, D. 1978 Thermal convection with spatially periodic boundary conditions: resonant wavelength excitation. *J. Fluid Mech.* 86, 433–456.
- [10] Jovanović M., Živković D., Nikodijević J., Rayleigh-Bénard convective instability in the presence of temperature variation on the lower wall, *Thermal Science*, year(2012).vol.16,suppl.2 pp.pp, s281-s184.
- [11] Nyers J., Nyers A.: “Hydraulic Analysis of Heat Pump's Heating Circuit using Mathematical Model”. 9rd IEEE ICC International Conference” Proceedings-USB, pp 349-353, Tihany, Hungary. 04-08. 07. 2013. ISBN 978-1-4799-0061-9

# Solar thermal energy use in Hungary: potentials and new opportunities

B. Bokor\*, L. Kajtár\*, L. Herczeg\*

\*Budapest University of Technology and Economics (BME) / Department of Building Service and Process Engineering, Budapest, Hungary

[bokor@epgep.bme.hu](mailto:bokor@epgep.bme.hu) and [kajtar@epgep.bme.hu](mailto:kajtar@epgep.bme.hu)

**Abstract** - Energy efficiency has become one of the key targets of building service design over the past years, as the building sector's enormous savings potential have been revealed. Solar radiation is a stable and predictable source of energy, and for its exploitation countless companies offer a wide range of technical equipment. Hungary's geographical and climate properties make it possible to reach considerable amount of energy out of solar radiation, yet meteorological conditions can influence the part of the year we should concentrate on. Based on the type of the heat consumer, different build-ups of solar collectors are to be chosen. Their construction defines the optimal application field; this connection is explained with the collector's efficiency curves. Yet not widely known products of the solar thermal industry are solar air heaters. Their simple structure makes them a reliable element of a heating system, suitable not only for building services, but also for agricultural use. Many system alternatives are provided to make use of the warm air produced by the collectors. Some of these, and the heat transfer process itself are being examined at the Department of Building Services and Process Engineering of the BME in Budapest.

## I. INTRODUCTION

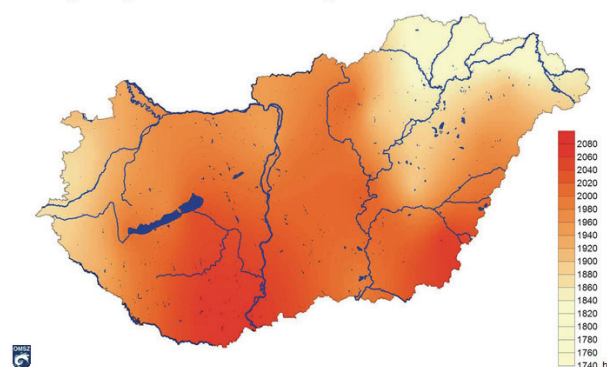
In the 21<sup>st</sup> century the optimal use of energy is a key factor in the planning, construction and maintenance of buildings. The European Union has committed itself to the 20/20/20 targets in its Energy Efficiency Plan of 2011. According to this, the key objectives for 2020 are to reduce the EU's greenhouse gas emission by 20 % from 1990 levels, to increase the share of renewable energies to 20 % in the energy consumption, and the improvement of the EU's energy efficiency by 20 %. [18] The Energy Efficiency Plan points out that the building sector represents a remarkable savings potential.

Therefore, not only passive and low energy houses, but also renovated buildings are being equipped with a wide range of heat generators using renewable sources of energy. Solar collectors produce heat from solar radiation without burning fossil fuels. Most frequently systems are designed for domestic hot water heating, building heating and for industrial purposes, using a liquid as heat transfer medium. However, on the American continent many efficiently operating installations show that even ventilation systems can be directly supplied with solar energy, when the heat transfer medium is air. To see the opportunities this technology can offer for Central European countries, an overview is given on Hungary's solar energy exploitation.

## II. METEOROLOGICAL ASPECTS OF SOLAR ENERGY USE IN HUNGARY [1] [5]

The amount of solar radiation available on a given surface of the Earth depends on geographical location. Most of Hungary's area is to be found between the 46° and the 48.5° of North Latitude. The solar radiation's angle of incidence and the length of daytime essentially influence the amount of heat a solar collector can produce. The maximal position of the Sun varies between 66.5° and 19.5° in Hungary during the year, whereas daytime is 8 hours long at winter solstice, and 16 hours at summer solstice.

### The yearly amount of sunny hours



### The yearly sum of global radiation

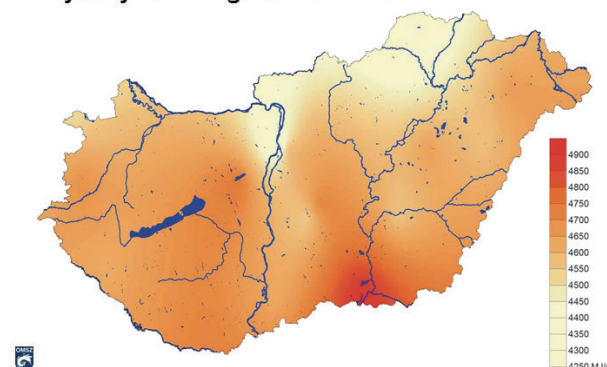


Figure 1. Solar radiation properties in Hungary [16]

Considering the yearly amount of sunny hours and the yearly sum of global solar radiation seen in Figure 1, Hungary's most suitable territories for solar energy exploitation are in the South and the South-East.

Global radiation varies from October to March between 250-600 W/m<sup>2</sup> in the midday hours, whereas from April to September it is to be expected between 600-1000 W/m<sup>2</sup>. Disadvantageous weather conditions in winter months such as snowfall and rime along with the higher heat loss of collectors can worsen the efficiency of the system further on. Therefore, we can say that the expenses of a solar system's installation may recover faster if its main purpose is not only to provide complementary heating in winter, but also heat for consumers all year long.

As the sunlight passes the atmosphere, particles of the air (dust, aerosols) stray it into different components. One part of solar radiation reaches the surface of the Earth directly (direct radiation), another part gets diverted in its direction, resulting in diffuse radiation. Global radiation is the sum of direct and diffuse solar radiation. Figure 2 shows the ratio of diffuse to global solar radiation reaching a horizontal surface.

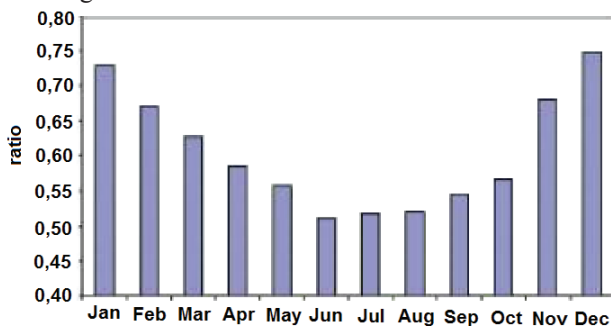


Figure 2. The ratio of diffuse to global solar radiation [5]

In Hungary, even in summer months, the proportion of diffuse to global solar radiation is higher than 50 %, which can reach 70-75 % in winter. This means that in favour of high system efficiency, the collectors selected must be able to exploit diffuse solar radiation as well.

The suitable facing of the collector targets the optimal utilization of direct solar radiation. As diffuse radiation is isotropic, a mechanical repositioning system of the collector area would not result in remarkable extra energy.

### III. SOLAR THERMAL COLLECTORS WITH LIQUID HEAT TRANSFER MEDIUM

Offering an option for heating costs savings as well as energy independence, solar thermal technology has become more and more wide-spread over the past decades in Europe. Techniques have been developed for transferring the sunlight's energy into valuable heat used for a wide range of purposes. Depending on the temperature level required, different collector constructions are used. The appropriate choice of device defines the efficiency of the system, underlining the importance of reliable design. To see how very much a collector's efficiency depends on its construction under various operational properties, Figure 3 shows the efficiency characteristics.

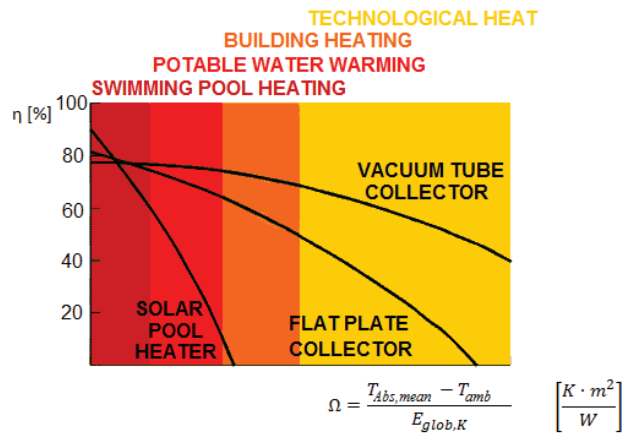


Figure 3. Efficiency characteristics of three different types of solar collectors [19]

As seen in Figure 3, collector efficiency is a function of the temperature difference between the absorber's mean temperature ( $T_{Abs,mean}$ ) and the ambient air temperature ( $T_{amb}$ ). The higher temperature is required at constant ambient air temperature, the bigger the difference will be between the collector's mean temperature and the ambient air temperature. During operation, a solar collector's efficiency is reduced by optical and thermal losses. Due to absorption, reflection and transmission processes inside a collector, not the entire solar radiation arriving onto the collector surface will be transformed into heat we can directly use. The radiation is partially absorbed and reflected by transparent glazing. Yet most of the radiation reaches the absorber, where it is absorbed and transformed into heat. A part of the radiation reaching the absorber is reflected. As there is a difference in temperature between the absorber and the ambience, the absorber will cool down. To minimise this effect, insulation is applied in the collector's structure. The higher temperature a collector is expected to produce, the better insulation is required. To reduce the heat loss through the collector's glazing often two panes of glass are used. It is easy to see that although more sheets provide better insulation, they increase the optical loss at the same time. Therefore, heating systems with solar collectors must be purpose-built with the suitable type of collector selected for the specific use.

As seen in Figure 3, the highest values of collector efficiency can be reached by solar pool heaters. They completely lack of transparent glazing which results in minimal optical loss. Metal or plastic pipelines of matt black colour forming the collector surface are exposed to direct sunlight. The water of a swimming pool can circulate in this pipeline directly. As no high temperatures are necessary, the thermal loss remains still low in lack of insulation. With rising temperature difference between collector and ambience the collector's efficiency will drop significantly, as Figure 3 shows.

Flat plate collectors are very widespread throughout Europe. They offer a solution for many applications in building service engineering. Their structures are insulated and transparent glazing is built in to minimise the absorber's front face heat losses. These provide a higher optical loss compared to solar pool heaters, but the decrease in its efficiency with rising temperature difference between collector and ambience is less intense. Flat plate collectors can produce high enough temperatures to supply heat for domestic hot water



warming and also for building heating systems. Yet the lower temperature is required, the higher the collector's efficiency will remain, as Figure 3 shows. Designing low temperature floor heating systems instead of a system with radiators will enable the collectors to reach higher efficiency.

Yet there are many cases when especially high temperatures are to be provided by a solar heating system. Besides residential applications, hot water is necessary for numerous industrial purposes. For example, some German breweries produce their beer using solar energy for the brewing process. In order to ensure higher temperature produced by solar collector, cutting edge insulation is required to keep the collector's operational temperature high. In vacuum tube collectors the absorbers are insulated with evacuated space around. This makes them the most efficient of all when there is a big difference between the collector's operational temperature and the ambient temperature. The two most common collector types using evacuated tubes are heat pipe and Sydney pipe collectors.

Figure 4 shows the build-up of a vacuum tube collector based on the heat pipe principle. It uses the phase change of an evaporating and condensing process medium in order to transfer heat at very low temperature differences. At one end of the heat pipe the heat of the absorber plate evaporates the process medium which gains the heat of vaporization. The vapour rises to the colder end of the heat pipe where it condenses, transferring its heat of condensation to the heating system. The condensate flows back to the other end, and the process can repeat itself.

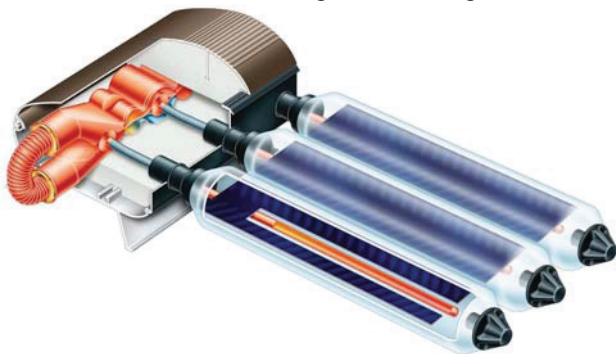


Figure 4. Vacuum tube solar collector based on the heat pipe principle [20]

In direct flow vacuum tube solar collectors (Figure 5) the heat transfer medium circulates directly in the coaxial absorber pipes inside evacuated tubes.

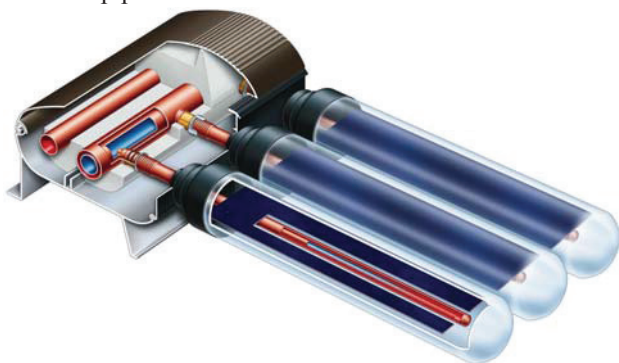


Figure 5. Direct flow vacuum tube solar collector [21]

The Sydney tube, which was developed based on the idea of a Thermos bottle, is a double-walled tube evacuated between the two walls. The inner glass wall of the tube is coated with the absorber layer, which can be heated up to 350 °C [6]. As seen in Figure 5, a so-called Compound Parabolic Concentrator (CPC) reflector directs the radiation onto the absorber surface, making use of the solar radiation falling in between two tubes.



Figure 6. Vacuum tube solar collector with Sydney pipes and CPC reflectors [22]

Knowing that a solar thermal system always produces heat when the sun shines, regardless of the actual needs, it is crucial to know our system's behaviour during the periods with solar radiation but without heat demand. In this case the temperature in the collector will rise up to the highest value, when the gain in energy and the heat loss find balance. This operating condition is called stagnation. On a collector's efficiency curve (Figure 3) this is the intersection point with the horizontal axis. As all the heat gain leaves the collector as heat loss, the efficiency is 0 % and the temperature difference on the horizontal axis defines the maximum a collector can reach over ambient temperature. Endurance of longer stagnation periods and a trouble-free setback to normal operation are requirements of a well-designed system. For this reason stagnation periods must be taken into consideration during system design. Simulation programs can help us find out the approximate length of stagnation periods in certain conditions. The temperature a collector reaches in stagnation is usually above the boiling temperature of the heat transfer liquid, so safety devices i.e. expansion vessels and overpressure valves must be dimensioned for these conditions.

Not only extremely high, but also extremely low temperatures can lead to the malfunction of a system. In winter time the lack of sunshine and low ambient temperature can pose the threat of freezing inside the solar primary circuit. That is why a frost protection agent, usually Propylene-glycol is added to the liquid. This non-toxic, biodegradable organic material of low flammability builds approximately a 40 % part of the heat transfer medium's volume. Due to efficient insulation applied on collectors, solar thermal systems can reach very high temperatures in stagnation periods. The molecules of glycol crack over temperatures of 170 °C, resulting in solid sediments, which can seriously damage the system. This is why a yearly inspection of the heat transfer medium is recommended for installations with longer stagnation periods calculated. Another way to prevent stagnation-related damages is doing without frost protection agent. This can be realised only in systems with vacuum tube collectors which ensure adequate heat

insulation. In this case only external joints and pipeline sections are in danger of frost. To avoid frost in these sections, temperature is monitored at critical points. When it reaches a defined minimum value, which is still over 0 °C, warm water flows back from the heating system into the collectors to prevent damage. Uninterruptible power supply guarantees this function even in the case of an eventual electricity cut. Water heat transfer medium without glycol ensures no damage of heat transfer medium in longer stagnation periods which can be favourable for systems predominantly used for building heating.

In general, we can see that the differences in collector construction are various ways of absorber design, as well as insulation techniques against ambience. The physical process remains the same in all cases: solar radiation warms up the absorber which transfers its heat to the heat consumers via the heat transfer medium.

#### IV. SOLAR AIR HEATERS

The previously outlined overview of solar thermal equipment would not be complete without solar air heaters. These devices are wide-spread in North America and are getting more and more popular on the European continent as well. Having seen the advantages of water as heat transfer medium, it might sound rather unusual to use air for the same purpose. Although air's lower specific heat capacity can cause some initial doubts, numerous advantages show the justification of solar air heaters.

Considering the aforementioned methods to avoid damage in solar collectors with liquid heat transfer medium caused by too high or too low temperature, we can say that these problems do not even exist with solar air heaters. Air does not freeze in winter, neither does it cause any malfunction during stagnation. The following paragraphs show that the simple construction of solar air heaters makes them a reliable source of renewable energy, suitable not only for ventilation systems, but also for special applications.

The construction of solar air heaters is manufacturer-specific. Basically, two categories can be defined: modular collectors and unglazed collectors with perforated absorber.

##### A. Modular Solar Air Heaters

Figure 7 shows the build-up of a modular solar air heater equipped with a solar-powered fan. They are available as ready units which can be connected to each other to ensure the power required.

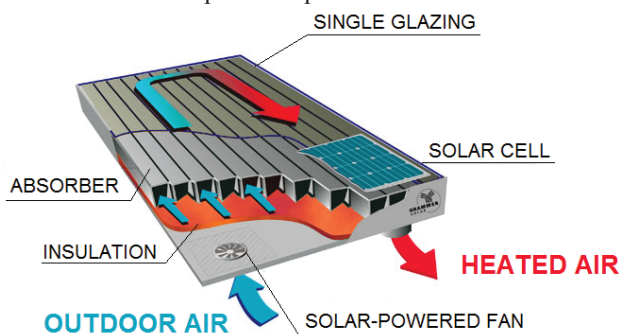


Figure 7. Modular solar air heater with integrated solar powered fan [23]

The construction of the absorber might vary by manufacturer. In order to provide optimal heat transfer, its surface can be plain, equipped with fins, or even porous. The air can flow on one or both sides of the absorber, or even in absorber canals, as seen in Figure 7. Considering that the fan's power demand is also included in the efficiency of the solar air heating system, it is important to keep the collector's pressure drop low.

Many modular solar air heaters (like the one in Figure 7) are equipped with a solar-powered fan, providing an independent operation from public power services. Owners of summer houses can make a good use of this function, as the building structure can be kept dry, tempered over the winter, even when electricity has been switched off. Figure 8 shows an installation on a wooden cottage near Lake Balaton, Hungary.



Figure 8. Hungarian summer cottage with solar air heater on its facade

Based on the system's assembly, modular solar air heaters can warm up both fresh outdoor air and indoor air. Heating outside air includes the problem of rising heat demand of the space with rising volume flow. When circulating indoor air through the collector instead, this problem can be eliminated, as in this case the space's heat demand remains independent from the air's volume flow.

##### B. Unglazed, Transpired Solar Air Heaters

Unglazed, transpired solar air heaters are of simpler construction, compared to modular solar air heaters. As Figure 9 shows, a dark, perforated metal shield is fixed onto a building's façade in a given distance. This metal shield is the absorber.

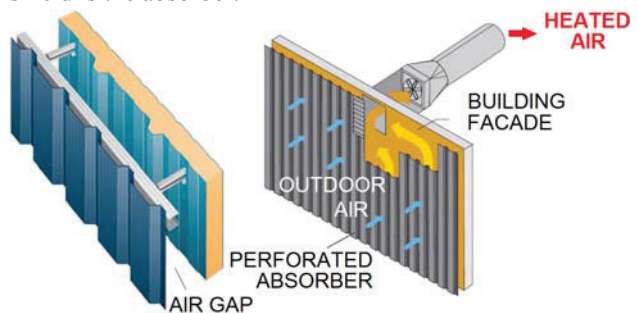


Figure 9. Build-up and operational principle of unglazed solar air heaters with perforated absorber [24][25]



Fresh outdoor air transpires the absorber, rises in the gap and finally a fan forwards it to the building's ventilation system. As seen before, a solar collector's efficiency is limited by optical and thermal losses. Unglazed solar air heaters have the advantage of having minimal optical losses due to the lack of transparent cover, just as previously described for solar pool heaters. They also reach high efficiency at lower operational temperatures, as the temperature difference is little, resulting in low thermal losses, too.

Based on the construction of unglazed, transpired solar air heaters, they can only warm up outdoor air. A thin layer of warm air develops at the outside of the absorber, which is being sucked in through the perforations. While rising up in the gap between absorber and building façade, the air gets heated further. This means, that both sides of the absorber takes an active part in the heat transfer process. Furthermore, the convectional losses of the building envelope can be regained on the surfaces where the air heaters are installed.

### C. PVT Hybrid Collectors

The PV-modules nowadays wide-spread both in private households and in industry transform only 15 % of the solar radiation reaching their surface into electricity. [23] The rest warms up the module and diminishes its electric performance. As seen in Figure 10, a 10 Kelvin drop in the PV module's temperature increases its performance by 3 % [23].

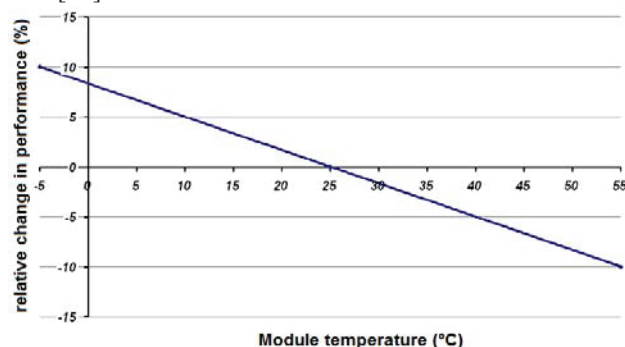


Figure 10. Relative change in a PV cell's performance depending on the module's temperature [23]

The valorisation of the waste heat increases the efficiency and the operational reliability of the PV module and offers an alternative support for the heating system.



Figure 11. PVT hybrid collectors installed on the roof of a German swimming pool [27]

This can be realised with installing PVT hybrid collectors, presented in Figure 11. Air streams in the canals behind the PV modules and receives the waste heat from them. PV modules can be combined with unglazed, transpired absorbers, too.

### D. Suitability of Solar Air Heaters to Different Building Types

The efficiency of a solar air heating system depends very much on the type and use of the building in which it is installed. Influencing factors are internal heat loads, passive solar gain, as well as heat and fresh air demand. Low internal heat load and solar gain are advantageous with a possible high fresh air demand, so that the benefits of the solar air heating system can be realized within a short time.

In residential buildings, especially in low-energy ones, mechanical ventilation supplies the necessary amount of fresh air. The ventilation system can be supplemented with solar air heaters, in order to reduce the heating costs, first of all, if no heat recovery unit was previously installed.

In office buildings both the internal heat load, as well as the solar gain can be high, due to the heat emission of the employees and the high glazing rate of the facades. This is why office buildings do not ensure optimal conditions for solar air heaters. Systems heating fresh outside air can directly reach high efficiency due to the high fresh air demand of employees.

Industrial buildings ensure optimal conditions for the operation of solar air heaters. The high spaces usually have a low glazing rate, resulting in low heat gains. Production processes often demand a high rate of fresh air in ventilation, providing good use of a solar air heater system.

### E. System Solutions for Solar Air Heaters in Building Services

Warm air produced with solar air heaters can not only be directly led into an occupied space, but it can be combined with various system elements, making use of the heat for different applications. In fact, in many cases it is strictly necessary to insert a thermal storage unit into the system, in order to balance the time shift between solar radiation and heat demand. In this paragraph an overview is given about possible system solutions.

Radiant heating dates back to the time of the Roman Empire, when a so-called hypocaust was used in thermal baths and some public homes. A hollowed space was built underneath the rooms, in which a woodstove's exhaust fumes streamed. The fumes rose up inside a double wall and left the building structure through a chimney. It lasted long to reach the adequate surface temperature after the start of combustion, and the ancient heating system was not easy to control. Yet this technology did not disappear without trace, modern-age hypocaust structures can be combined with solar air heating systems. In cooperation with an architect, a special building structure must be designed, in which the solar heated air streams in a hollowed structure under the floor or even in the walls.

The solar-heated air can either circulate closed loop, as shown in Figure 12, but it can also be led into the room as supply air after its way in the hollowed structure. In the latter case the cleanliness of the flow passage is of high

importance. The structure must be designed in the way that the air flow can develop across the whole profile without any blind areas. As the surfaces get slightly warmed up, hypocaust heating provides a high comfort inside. Moreover, the building structure behaves as a heat storage mass, which is very advantageous for solar thermal systems.

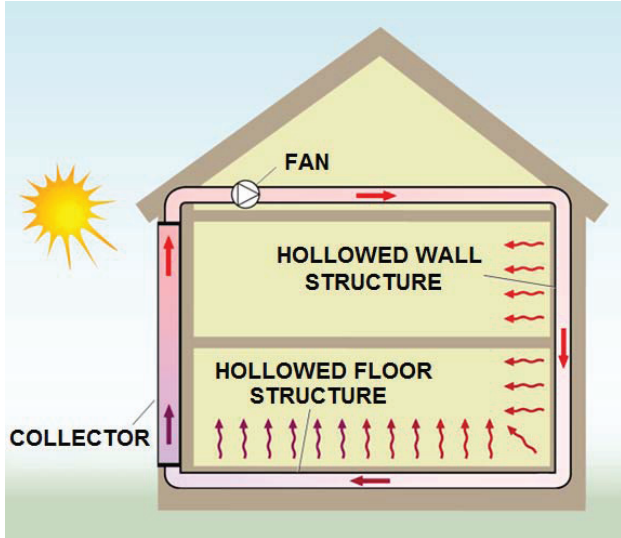


Figure 12. Hypocaust heating scheme in a modern building [28]

In case no hypocaust heating can be built, thermal energy storage can be realised by using a pebble bed thermal energy storage unit. When the air is directed to stream through the pebble bed, it can be charged with surplus heat, or discharged when necessary. For its integration into a building, see Figure 13.

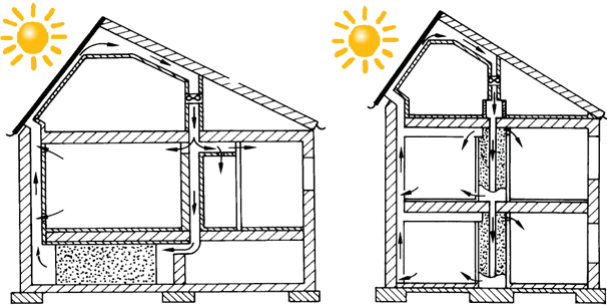


Figure 13. Two optional integration examples of a pebble bed thermal energy storage system into a building's structure [3]

It is important to remark that the specific heat capacity of pebble is lower than that of water. That is why 2.5-3 times of the volume is needed to store the same amount of energy with pebble than with water. [3]

Surplus heat produced with solar air heaters can be also used for domestic hot water heating, when an air-to-water heat exchanger is installed into the air duct. Based on the actual demand on hot air and water an electronic system decides about the air rate between ventilation and water heating.

Unglazed, transpired solar air heaters can be used for a free cooling system when installed onto low slope roofs. Based on the principle of nocturnal radiation, the absorber plates can cool by 10 °C below ambient temperature on a clear night. [17] From then on the whole process is the same as when heating in winter, just the direction of the

heat transfer is the opposite. Warm air transpires the colder collectors and transfers its heat to the surface. Finally, the cool air is led into the building, lowering or even displacing conventional air conditioning from sunset to sunrise. Moreover, the collector surface provides shading for the roof, reducing daytime heat gains normally received through the roof.

## V. SOLAR THERMAL ENERGY IN AGRICULTURE

Besides the aforementioned wide variety of solar air heaters' application in building services, they open up new frontiers for energy conscious-process engineering. Numerous processes require hot air in agriculture, including greenhouse heating and crop drying. The energy amount used for drying processes represents 20 % of Hungary's agricultural energy consumption, including 10 % of electricity, 30-50 % of gas and 10-15 % of oil. [1] Before installing a solar drying system, factors like the highest possible air temperature, the effect of solar drying on the product and the return of investment costs must be taken into consideration.

During sunny hours, outdoor air can be heated up to 55 °C, whereas when the weather is cloudy, the solar air heating system can act as a preheater. This shows that even disperse radiation can be utilised by the system, which is an important factor, having seen the yearly proportion of disperse radiation in Hungary.

Solar air heaters are easily integrated into existing systems, and having a simple construction, they require only basic maintenance. Many efficiently working installations show the option of energy saving in drying fruit, spices, herbs, rice, corn, nuts, or even biomass. As the wellbeing of farmyard animals also demands warm air, this sector carries a possible application field for solar air heaters, too. They have been used in ventilation systems of many poultry and hog stalls to ensure indoor comfort.

## VI. SOLAR AIR HEATING RESEARCH AT BME

Unglazed, transpired solar air heaters offer a wide range of phenomena to be researched. In the lack of transparent glazing, the actual power is a function of the weather. Blowing wind makes the heat transfer coefficient rise on the outer surface of the absorber, resulting in its quicker cooling down. Evaporating raindrops can especially cause this effect, and as mentioned before, certain heat production is also required in cloudy weather conditions. Thermal energy storage units can be inserted into existing systems, in order to make use of the surplus heat arising in sunny periods.

The Department of Building Service and Process Engineering cooperates with Auchan Ltd., which operates solar air heating systems in some of its hypermarkets. In the course of this year, we will start examining one of the systems based on a series of measurements, in order to support a mathematical model of heat transfer between absorber and air. Our research also targets system solutions regarding both building services and agricultural applications.

## REFERENCES

- [1] I. Farkas, „Napenergia a mezőgazdaságban” Mezőgazda Kiadó, Budapest, Hungary, 2003
- [2] J. Ósz, „Energetika”, BME Department of Energy Engineering, Budapest, Hungary, 2013
- [3] H. Drück, Dr.-Ing. – H. Müller-Steinhagen, Prof. Dr.-Ing., „Solartechnik I”, Institut für Thermodynamik und Wärmetechnik, Universität Stuttgart, Germany, 2009
- [4] Viessmann „Planungshandbuch Solarthermie“ Viessmann Werke, Allendorf (Eder), Germany, 2008
- [5] Z. Nagy, „A napenergia-hasznosítás meteorológiai vonatkozásai”, Épületgépész, a Magyar Épületgépészek Szövetségének szaklapja I. évf, 1. szám, pages 24-25
- [6] R. Meissner, Dr., „Heizen mit der Sonne – Sicherheit gegen thermischen Stillstand sorgt für Effizienz“, Sanitär + Heizungstechnik 4/2013 pages 50-54
- [7] J. Morhenne, „Solare Luftsysteme“ BINE Informationsdienst Themen Info II/01. Fachinformationszentrum Karlsruhe, Gesellschaft für wissenschaftlich-technische Information m.b.H., Eggenstein-Leopoldshafen, Germany, 2002
- [8] P. Varga, Napkollektoros rendszerek kivitelezése 2: a napkollektorok elhelyezése, Épületgépész, a Magyar Épületgépészek Szövetségének szaklapja I. évf, 3. szám, pages 36-38.
- [9] J. Takács: „Energetický management v odovzdávacích staniciach tepla.” Facility management 2004: Zborník prednášok z 2. konferencie so zahraničnou účasťou, 10.-11.11.2004, Bratislava. - Bratislava: Slovenská spoločnosť pre techniku prostredia, 2004. ISBN 80-969030-7-1. - s. 75-78
- [10] D. Petráš – O. Lulkovičová – J. Takács – B. Fűri: „Obnoviteľné zdroje energie pre nízkoenergetické systémy.” Bratislava: Jaga Group, s.r.o., 2009. 221 s. ISBN 978-80-8076-075-5
- [11] J. Takács – O. Lulkovičová – B. Fűri: „Helyzetkép a megújuló energiaforrások hasznosítási lehetőségeiről Szlovákiában.” Magyar Épületgépészet. - ISSN 1215-9913. - Roč. 57, č. 12 (2008), s. 24-27
- [12] J. Takács: „Alternatívne energetické zdroje.” In: Technické zariadenia budov. - Základné dielo, stav - október 2006 (2006), nestr. ISSN 1336-9938.
- [13] I. Bartal, Hc L. Bánhidi, L. Garbai: „Analysis of the Static Thermal Comfort Equation” Energy and Buildings Vol. 49 (2012) pp. 188-191
- [14] J. Nyers, S. Tomic, Á. Nyers: „Economic Optimum of Thermal Insulating Layer for External Wall of Brick”, ACTA POLYTECHNICA HUNGARICA 11: (7) pp. 209-222.
- [15] J. Nyers Dr.Sci., .S. Tomić Dr. Ec, „Financial Optimum of Thermal Insulating Layer for the Buildings of Brick” Conference: 5th International Symposium on Exploitation of Renewable Energy Sources "EXPRES 2013", At Subotica-Szabadka, Serbia
- [16] <http://www.met.hu>
- [17] <http://www.solarwall.com>
- [18] [http://ec.europa.eu/clima/policies/package/index\\_en.htm](http://ec.europa.eu/clima/policies/package/index_en.htm)
- [19] <http://www.fys-online.de/>
- [20] [http://www.ductless.ca/images/viessmann\\_vitosol/vitosol\\_300t\\_cu\\_taway.gif](http://www.ductless.ca/images/viessmann_vitosol/vitosol_300t_cu_taway.gif)
- [21] [http://www.ductless.ca/images/viessmann\\_vitosol/vitosol\\_200t\\_cu\\_taway.gif](http://www.ductless.ca/images/viessmann_vitosol/vitosol_200t_cu_taway.gif)
- [22] <http://www.ritter-gruppe.com/>
- [23] <http://www.grammer-solar.com/cms/de.html>
- [24] <http://www.tatasteelconstruction.com>
- [25] <http://www.logixicf.com>
- [26] <http://www.matrixairheating.com>
- [27] <http://www.ee-news.ch>
- [28] <http://www.energiesparen-im-haushalt.de>



# Some questions of utilizing heat generated in waste dumps

Kontra Jenő, Várfalvi János

Budapest University of Technology and Economics  
H-1111 Budapest, Műgyetem rkp. 3.

**Abstract-** There are many clear-out technologies to use gas generated in waste dumps. In waste dumps and recycling centers, energy is present not only in form of burnable gas but also in form of thermal capacity that can be characterized by temperatures of 40 to 60°C. This thermal capacity assures energy recuperation for 15 to 20 years. However, direct presence of thermal energy does not mean that heat mining can be performed in a simple way. There are a lot of thermal problems to be solved.

**Keywords-** Waste dump, heat generation, heat mining, heat utilization.

## I. INTRODUCTION

It is a well-known fact that an increasing quantity of waste develops. A part of this waste is stored in dumps where large depots are formed. Although depots are seemingly at rest observing them from outside, bacteria start complex processes inside the dump converting structure of wastes, and thus, biogas is generated.

Figures 1, 2 and 3 show such gas generating depots in Hungary, in Gyál. Project KMR 12-1-2012-0128 launched within New Széchenyi Plan aims at utilization of heat generated in this depot.

It can be seen in figures that such waste dumps are very large. Their typical connected technological system comprises a gas recuperation system built within the dump and a power plant utilizing this gas. In our case, it means gas engines of 1 MW output. Considering the fact that gas production can be expected during 15 to 20 years, energy production of this waste dump can be valued as considerable.

## II. HEAT GENERATION IN DEPOT

Measurements carried out confirm that inside the depot, the temperature is 40 to 60 °C. This means that optimal life circumstances of bacteria decomposing dump materials may require essentially higher temperatures than human life in general.

In our case, inside the depot, we can count with three groups of bacteria with the following estimated temperatures for their vital functions:

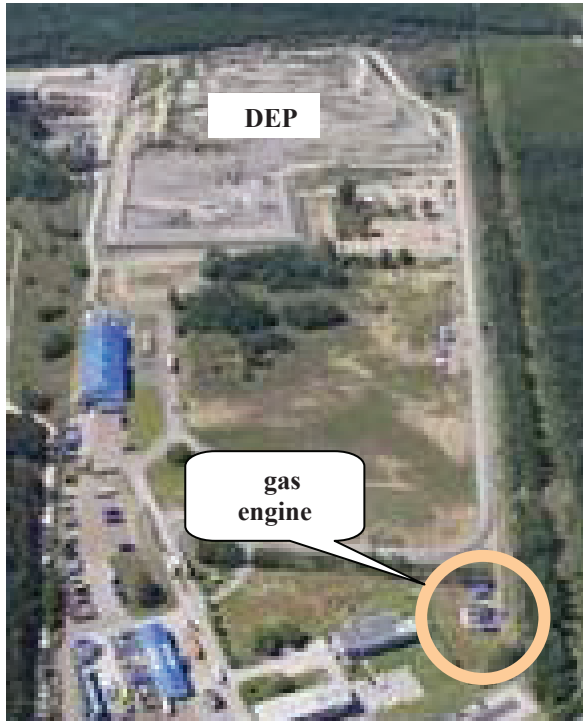
- mesophilic bacteria: 30 to 60°C
- thermophilic bacteria: 50 to 60°C
- hyper-thermophilic bacteria: 60 to 90°C.



Fig. 1: Depot in a satellite picture



Fig. 2: Height dimensions of the depot



**Fig. 3:** Power plant with gas engines at the edge of the waste dump

Obviously, these higher temperatures can be related to the internal heat generation. Calculating with dimensions of the waste depot in Gyál having a ground space of 500x500m and height of 25m, the result is a depot volume of 6,250,000m<sup>3</sup>. Calculating with an average heat generation of 1W a m<sup>3</sup>, heat output of the waste dump is 6.25MW.

During an operation period of 10 years, energy released from waste depot is

$$E = 6.25 \text{ MW} \cdot 8760 \cdot 10 \text{ years} = 547,500 \text{ MWh/10 years}$$

Although no precise data concerning heat quantity are available yet, this simple example above shows that considerable heat energy is produced.

### III. THEORETICAL HEAT UTILIZATION OPTIONS

Taking into account that it is a warm medium with temperatures of 30 to 80°C, there are multiple utilization options to be reviewed. Some of them are here outlined.

#### A. Electricity production

The electricity production is based on the Seebeck effect. Its theoretical circuit diagram is shown in Fig. 4.

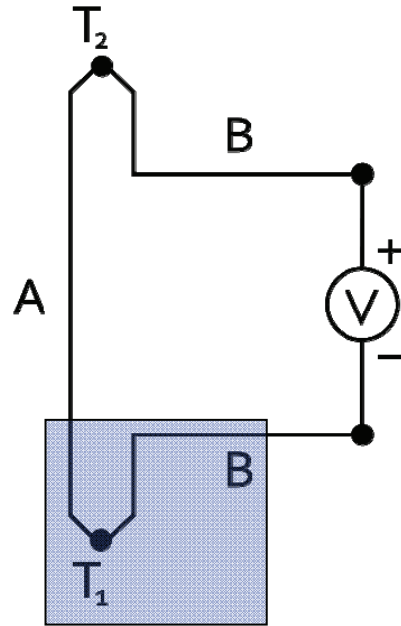


**Fig. 4:** Circuit diagram of Seebeck effect

One soldering point of two soldered metals is in the (warmer) space of temperature  $T_2$  and the other soldering point is located in the (colder) space with temperature  $T_1$ . Volt meter „V” shows a thermovoltage difference of  $\Delta U$ .

As a possible realization is a solid state electric system based on a designed structure of semiconductors. Quality factor (CoP) of thermo-electric systems is low, about 5% at present.

#### B. Mechanical work generation

Obviously, depot heat can be utilized by an external combustion engine. The most efficient principle of such an engine can be realized when operating a Stirling engine. A possible system structure of this engine is depicted in Fig. 5. The engine is composed of two different pistons:

- *Power piston* by which mechanical output is generated in a power machine.
- *Guiding piston* moving power gas between cooling and heating units.

Theoretical efficiency of a Stirling engine can be approximated by the efficiency of the Carnot cycle. Taking 0°C as lower temperature, efficiency can be calculated in function of the higher temperature, and efficiency of about 15% can be expected. Due to the low efficiency, use of Stirling engine is not likely. Even more, the following factors also decrease efficiency:

- Under real circumstances, we shall account with additional diminishing of the efficiency.
- If we take the lower temperature being equal to zero, efficiency continues to drop in summer.



- Obviously, heating energy can be brought to "surface" from the dump by a heat exchanger. Heat exchange goes with decrease of the higher temperature, resulting again in efficiency worsening.

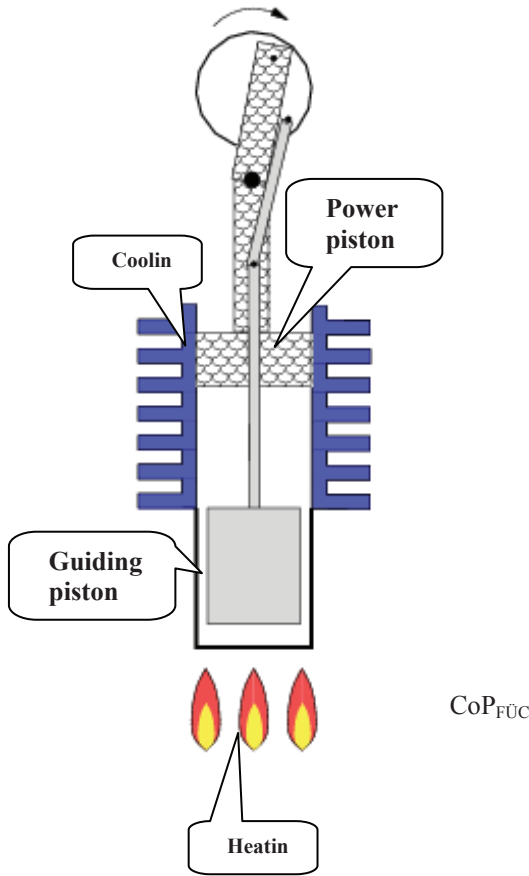


**Fig. 5:** Theoretical scheme of a possible Stirling engine system

### C. Thermal energy utilization by heat exchanger

Changes of state occurring in the heat exchanger are illustrated in Fig. 6. In entropy-temperature chart, theoretical changes of state can be studied. In point **A**, compressor sucks saturated steam. It is compressed in point **B**, where steam becomes overheated. Between points **B-C**, cooling medium cools down until saturated state. Between points **C-D**, steam is condensed. Between points **D-E**, liquid cools farther. Between points **E-G**, gas cutting occurs between pressure and suction spaces of the system.

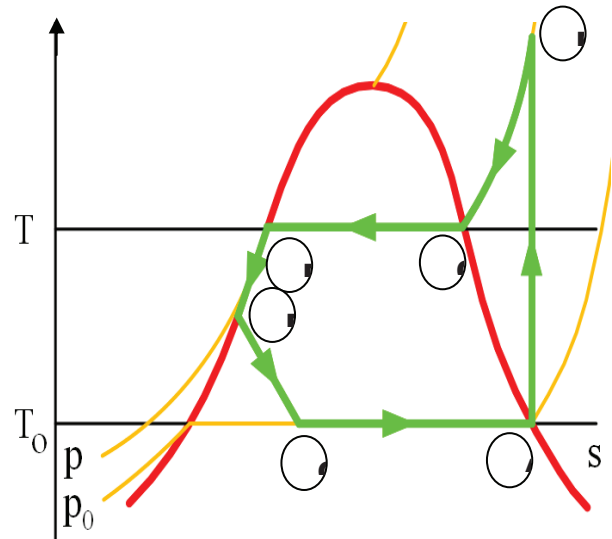


**Fig. 6:** Chaos of state in heat exchanger on T-S charting

Imaging the heat exchanger' operation as an idealized Carnot cycle in reversed operation, specific heating power can be calculated as follows:

$$CoP_{FUC} = \frac{T_F}{T_F - T_A} = \frac{1}{\eta_C}$$

where:

$T_F$  higher temperature

$T_A$  lower temperature

specific heating power in an ideal Carnot cycle in reversed operation

$\eta_C$  efficiency of the heat engine with Carnot cycle

It follows from the above relation that efficiency of a heat engine operating according to Carnot cycle can be qualified as good until the lower and higher temperatures are far from each other; however, in the case of a heat exchanger, efficiency is reversed, i.e. operational circumstances are favourable if the lower and upper temperatures are near to each other.

This effect can be observed in Fig. 7: increasing the lower temperature, efficiency of heat exchanger improves. As we took the higher temperature constant, in our case 50°C, raising the lower temperature implies the difference reduction between these two temperatures, and this favourably affects CoP value. Temperatures in the dump allow increase of the lower temperature.

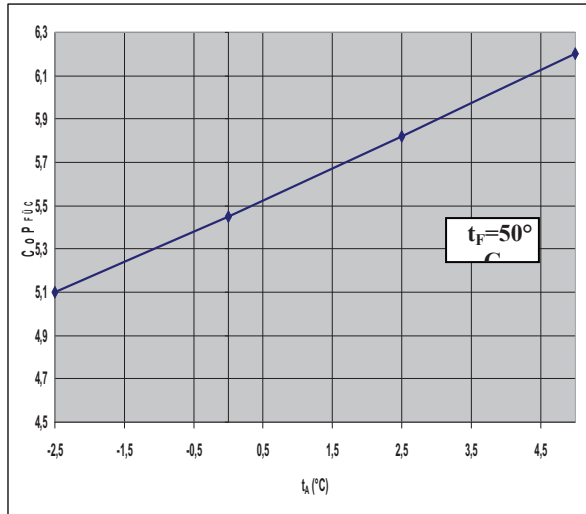


**Fig. 7:** COP characteristic in function of the lower temperature

If anywhere in the dump, temperatures identical with or higher than the upper temperature of the heat exchanger develop, use of a heat exchanger is not justifiable in that specific zone. It may not be excluded that in the case of higher temperatures, energy extracted from the dump – applying absorption systems – can be used for cooling.

#### IV. PRACTICAL ISSUES OF HEAT UTILIZATION

Although the energy extracted is available, theoretically, free-of-charge, the profitability of the "energetic system" to be installed in the depot depends on extraction efficiency fundamentally. Extraction efficiency is mainly related to the following practical issues.

1. Heat mining in a general location.
2. Decrease of losses on the boundary surfaces of dump as a thermal system built in space and time.
3. Exploitation of operational features originating from dynamic adjustment of demands and heat generation.

##### A. Heat mining in a general location:

General location means a place in the dump sufficiently far from edges. In technological realization of heat mining, heat pump operation with soil probes shall be considered, too. Studying this system, the arrangement sketched in Fig. 8 can be proposed for testing.

The heat exchanger depicted in this figure shall operate so that the temperature of the entering medium is essentially lower than depot's temperature and the outlet temperature is near to the depot's temperature. As a result, between the pipe as heat exchanger unit and its environment, a growing temperature distribution develops and this generates heat flows. While in the case of a heat pump system with soil probe, soil temperatures shall not be practically considered,

temperatures of a waste dump may be determinant. This is illustrated in Fig. 9. Temperatures developing close to the pipe may drop below the value necessary for vital functions of the bacteria, and consequently, biogas generation stops.

Therefore, it is advisable to thermodynamically dimension the heat exchanger of heat mining. When designing, differential equation of heat conduction (Fourier–Biot equation) may serve as starting point.

$$\frac{\partial t}{\partial \tau} = a \nabla^2 t + \frac{\dot{q}_V}{\rho \cdot c_p} = a \left( \frac{\partial^2 t}{\partial x^2} + \frac{\partial^2 t}{\partial y^2} + \frac{\partial^2 t}{\partial z^2} \right) + \frac{\dot{q}_V}{\rho \cdot c_p}$$

Considering the fact that processes in a waste dump are slow, quasi-stationary states develop in particular periods, therefore, thermal processes can be described also by the Poisson's equation.

$$0 = a \nabla^2 t + \frac{\dot{q}_V}{\rho \cdot c_p} = a \left( \frac{\partial^2 t}{\partial x^2} + \frac{\partial^2 t}{\partial y^2} + \frac{\partial^2 t}{\partial z^2} \right) + \frac{\dot{q}_V}{\rho \cdot c_p}$$

Value of „ $\dot{q}_V$ ” in the equation may be determinant in our case. This factor quantifies heat generated in  $1\text{m}^3$  of material. In our case, its role is important because, theoretically, only heat amount identical to the internally generated heat quantity is allowed to be removed from the system. Unfortunately, no data for the value of this factor are available. In principle, the method is as follows:

1. Measure coefficient of thermal conduction of the "material" in waste dump.
2. Determine vertical temperature distribution in waste dump.
3. By a computer-aided simulation software, define that value of internal heat generation that can be linked to the measured coefficient of thermal conduction and temperature distribution.

However, investigations of the coefficient of thermal conduction do not supply reliable result because interpretation of the coefficient of thermal conduction is very complex. In order to demonstrate this, we give some approximations here:

- 0.5-1 W/mK based on waste composition
- 1-2 W/mK based on sampling and measurements
- 10-20 W/mK when considering convection processes, possibly vapour condensation processes developing in the depot as equivalent factor.

In addition, the depot is essentially affected by so-called escaped water, and this has also its thermal consequences.

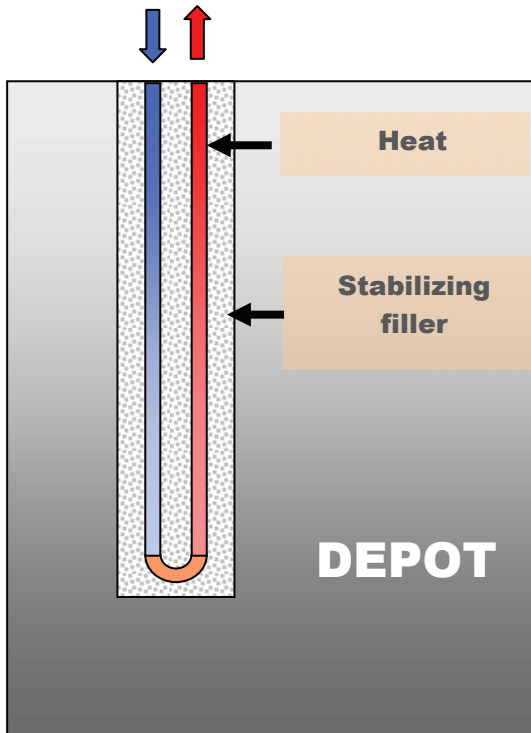


Fig. 8: Heat exchanger in depot

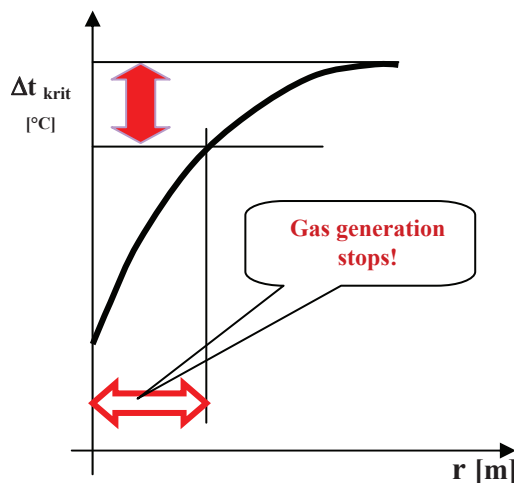


Fig. 9: Temperatures and gas generation

Summarizing what described above, we can state that heat mining tests with on-site measurements are extremely needed in order to define internal heat generation. Determination of the necessary thermal characteristic is only possible by simultaneous and interactive application both of the obtained results and computer-aided simulation. Within the project mentioned above, preparations for on-site tests for investigating heat generation and temperatures related to heat mining are carried out at present. During the tests, multiple probes have been built, and the heat obtained this way heats a greenhouse close to the depot and, in summer, escape water is cooled back in a reservoir in order to organize heat mining into a thermal

cycle. In adequately selected points of the arranged system, temperature and flow sensors are placed enabling monitoring of the tested system.

#### B. Decrease of losses on boundary surfaces:

Usually, waste dumps have huge dimensions; consequently, they have considerable boundary surfaces. Each such boundary surface has its particular features.

*Horizontal surfaces of the dump* are, typically, agricultural fields; they can only be used when agricultural production terminates.

*Supporting side surfaces of the dump* are considerable due to their large heights. The developing temperatures are lower, but loss flows may be considerable because of the large sizes.

*Soil as boundary surface* can be characterized by considerable heat flows. Importance of heat flows towards the soil is increased by the fact that due to the depot technology, dominant part of loss heat flows can be expected on this surface.

Thermal solutions for reducing losses on the boundaries can only be developed after clarification of crucial issues of heat mining in the general location.

#### C. Dynamic adjustment of demands and heat generation

From the aspect of thermal engineering, a depot is such a "boiler" that cannot be stopped until fuel has not been burnt. Consequently, if no heat energy is required on the demand side, storage of heat energy shall be solved. Soil under the depot may offer an option, however, these circumstances can be clarified in a later phase of the research.

## REFERENCES

- [1] Depónia-hő-hasznosítási technológia kidolgozása (Development of technology for heat utilization of depots) – Project KMR 12-1-20212-0128, January–June 2013, BME, Department of Building Energetics and Building Services
- [2] Depónia-hő-hasznosítási technológia kidolgozása (Development of technology for heat utilization of depots) – Project KMR 12-1-20212-0128, July–December 2013, BME, Department of Building Energetics and Building Services
- [3] J. Kontra, J. Várfalvi and G. Köllő: Waste Dump Heat-Mining in Gyál /International Conference in Subotica, 2014
- [4] Nyers J., Nyers A.: "Hydraulic Analysis of Heat Pump's Heating Circuit using Mathematical Model". 9rd IEEE ICCI International Conference" Proceedings-USB, pp 349-353, Tihany, Hungary. 04-08. 07. 2013. ISBN 978-1-4799-0061-9
- [5] Poós, T.; Örvös, M.: Heat- and mass transfer in agitated, co-, or countercurrent, conductive-convective heated drum dryer. Drying Technology 30 (13), 2012, 1457-1468.
- [6] László Kajtár, Miklós Kassai, László Bánhidi: Computerised simulation of the energy consumption of air handling units. 2011. Energy and Buildings, ISSN: 0378-7788, (45) pp. 54-59.

# Ray tracing study to determine the characteristics of the solar image in the receiver for a thermal solar concentration system

Saša R. Pavlovic<sup>\*</sup>, Velimir P. Stefanović<sup>\*</sup>, Predrag Rajković<sup>\*\*</sup>, Emina P. Petrovic<sup>\*\*\*</sup>, Sadoon Ayed<sup>\*\*\*\*</sup>

<sup>\*</sup>Nis. Serbia, Faculty of Mechanical Engineering, Department for Energetics and Process technique, University in Niš, Serbia

<sup>\*\*</sup> Nis. Serbia, Faculty of Mechanical Engineering, Department for Mathematics and Natural Sciences University in Niš, Serbia

<sup>\*\*\*</sup> Nis. Serbia, Faculty of Mechanical Engineering, Mechatronics and Control Systems, University in Niš, Serbia

<sup>\*\*\*\*</sup> University of Technology, Department of Mechanical Engineering, Baghdad ,Iraq,

e-mail : [sasap208@yahoo.com](mailto:sasap208@yahoo.com), [veljas@masfak.ni.ac.rs](mailto:veljas@masfak.ni.ac.rs), [pedja.rajk@masfak.ni.ac.rs](mailto:pedja.rajk@masfak.ni.ac.rs), [smijoc@yahoo.com](mailto:smijoc@yahoo.com), [sadun\\_kad@yahoo.com](mailto:sadun_kad@yahoo.com)

**Abstract--** This study presents the geometric aspects of the focal image for a solar parabolic concentrator (SPC) using the ray tracing technique to establish parameters that allow the designation of the most suitable geometry for coupling the SPC to absorber – receiver. The efficient conversion of solar radiation in heat at these temperature levels requires a use of concentrating solar collectors. In this paper detailed optical design of the solar parabolic dish concentrator is presented. The system has diameter  $D = 3800$  mm and focal distance  $f = 2260$  mm. The parabolic dish of the solar system consists from 11 curvilinear trapezoidal reflective petals. For the construction of the solar collectors, mild steel- sheet and square pipe were used as the shell support for the reflecting surfaces. This paper presents optical simulations of the parabolic solar concentrator unit using the ray-tracing software TracePro. The total flux on receiver and the distribution of irradiance for absorbed flux on centre and periphery receiver are given. The goal of this paper is to present optical design of a low-tech solar concentrator that can be used as a potentially low-cost tool for laboratory-scale research on the medium-temperature thermal processes, cooling, industrial processes, poly generation systems etc.

**Keywords:** ray tracing analysis, optical modelling, thermal solar concentration technology, corrugated Archimedean spiral pipe solar absorber

## I. INTRODUCTION AND SURVEY OF LITERATURE

This paper presents the numerical results of the optimization of the solar image in a receiver for a fixed absorber in a solar parabolic concentrator, which was a project supported by the Ministry of Education, Science and Technological Development of Republic of Serbia. The device which is used to transform solar energy to heat is referred to a solar collector. Solar thermal collectors have been widely used to concentrate solar radiation and convert it into medium-high temperature thermal processes. In addition, the list of possible alternative applications of this technology is growing, due to the problems of oil dependency and global warming. They can be designed as various devices including solar cooker [1], solar hydrogen production [2,3] and Dish Stirling system of harvest electricity [4,5]. The main types

of concentrating collectors are: parabolic dish, parabolic trough, power tower, Fresnel collector with mirror or lens and stationary concentrating collectors. The ideal optical configuration for the solar parabolic thermal concentrator is a parabolic mirror. The parabolic mirror is very expensive to fabricate and its cost escalating rapidly with increase of aperture area. The parabolic mirror can be designed with large number of elementary components known as reflecting petals or facets. Usually reflecting petals are made from glass and their thickness is from 0.7 to 1.0 mm. Traditionally, the optical analysis of radiation concentrators has been carried out by means of computer ray-trace programs. Recently, an interesting analytical solution for the optical performance of parabolic dish reflectors with flat receivers was presented by O'Neill and Hudson [6]. Their method for calculating the optical performance is fast and accurate but assumes that the radiation source is a uniform disk. Imhamed M. Saleh Ali et al. [7] have presented study that aims to develop a 3-D static solar concentrator that can be used as low cost and low energy substitute. Their goal was to design solar concentrator for production of portable hot water in rural India. They used ray tracing software for evaluation of the optical performance of a static 3-D Elliptical Hyperboloid Concentrator (EHC). Optimization of the concentrator profile and geometry is carried out to improve the overall performance of system. Kaushika and Reddy [8] used satellite dish of 2.405 m in diameter with aluminum frame as a reflector to reduce the weight of the structure and cost of the solar system. In their solar system the average temperature of water vapor was 300°C, when the absorber was placed at the focal point. Cost of their system was US\$ 950. El Ouederni et al. [9] was testing parabolic concentrator of 2.2 m in diameter with reflecting coefficient 0.85. Average temperature in their system was 380°C. Y. Rafeeu and M.Z.Z. AbKadir [10] have presented simple exercise in designing, building and testing small laboratory scale parabolic concentrators. They made two dishes from acrylonitrile butadiene styrene and one from stainless steel. Three experimental models with various geometrical sizes and diameters were used to analyze the effect of geometry on a solar irradiation. Zhiqiang Liu et al. [11] presented a procedure to design a facet



concentrator for a laboratory-scale research on medium – temperature thermal processes. The facet concentrator approximates a parabolic surface with a number of flat square facets supported by a parabolic frame and having two edges perpendicular to the concentrator axis.

The decision to make solar parabolic concentrator with 11 petals is based on large number of design concepts that are realized in the world. This concept already proved useful in solar techniques, especially in production of heat and electrical energy as well as in tri generation and poly generation systems.

The basic idea behind this research is to start with primary concept of solar parabolic concentrator which will generate from 10 to 25 kW in poly generation systems. Only with employment of parabolic concentrating systems it is possible to obtain high temperatures in range from 200°C to 800°C and high optical and thermal efficiency of concentrating solar collectors.

## II. GEOMETRICAL MODEL OF THE SOLAR PARABOLIC CONCENTRATOR AND RECEIVER

The design of the solar parabolic thermal concentrator and operation are presented. Optical design is based on parabolic dish with 11 curvilinear trapezoidal petals. Solar dish concentrators are generally concentrators that concentrate solar energy in a small area known as focal point. Dimensions of reflecting surfaces in solar dish concentrator are determined by desired power at maximum levels of insulation and efficiency of collector conversion.

The ray tracing technique is implemented in a software tool that allows the modeling of the propagation of light in objects of different media. This modeling requires the creation of solid models, either by the same software or by any computer aided design (CAD) software. Once in the optical modeling software, portions of the rays of the light source propagate in the flow of light, in accordance with the properties assigned to the relevant objects, which may be absorption, reflection, transmission, fluorescence, and diffusion. The sources and components of the light rays, adhering to various performance criteria involving the system parameters, result in simulation of the spatial and angular distribution, uniformity, intensity, and spectral characteristics of the system. Mathematical representation of parabolic concentrator is parabolic that can be represented as a surface obtained by rotating parabola around axis. Mathematical equations for the parabolic dish solar concentrator in Cartesian and cylindrical coordinate systems are defined as:

$$x^2 + y^2 = 4fz \quad z = r^2/4f \quad (1)$$

where  $x$  and  $y$  are coordinates in aperture plane and  $z$  is distance from vertex measured along the line parallel with the paraboloid axis of symmetry;  $f$  is focal length of paraboloid i.e. distance from the vertex to the focus along the paraboloid axis of symmetry. The relationship between the focal length and the diameter of parabolic dish is known as the relative aperture and it defines shape of the paraboloid and position of focal point. The shape of paraboloid can be also defined by rim angle  $\psi_{rim}$ . Usually paraboloids that are used in solar collectors have rim

angles from 10 degrees up to 90 degrees. The relationship between the relative aperture and the rim angle is given by:

$$f/D = \frac{1}{4 \tan(\psi_{rim}/2)} \quad (2)$$

The paraboloid with small rim angles have the focal point and receiver at large distance from the surface of concentrator. The paraboloid with rim angle smaller than  $50^\circ$  ( $\psi_{rim} = 45,6$ ) is used for cavity receivers while paraboloids with large rim angles are most appropriate for the external volumetric receivers (central receiver solar systems).  $f/D = 0.59$

The geometric concentration ratio can be defined as the area of the collector aperture  $A_{app}$  divided by the surface area of the receiver  $A_{rec}$  and can be calculated by eq.3.

$$CR_g = (\sin^2 \theta_a)^{-1} = A_c A_r^{-1} = A_{app} / A_{rec} \quad (3)$$

The designed solar parabolic concentrator has geometric concentration ratio  $CR_g = 100$ .

### A. Parameters Design of Solar Parabolic Concentrator

Mechanical design of the solar parabolic concentrator is done in 3D design software CATIA, Dassault Systems, USA. Parabolic shape of solar concentrator is obtained by entering  $x$  and  $y$  coordinates for selected points. For calculation of necessary points that define parabola public domain software Parabola Calculator 2.0 [11] is used. The calculated coordinates ( $x$  and  $y$ ) for designed parabola are shown in Table I. The calculated values is performed for 22 point in the parabola curve. The equation for parabola is:

$$y = a(x)^2 + b(x) + c \quad (4)$$

The coefficients describing this parabola are:

$$a = 1.10526 \times 10^{-4}$$

$$b = 0$$

$$c = -2.428275 \times 10^{-14}$$

$$y = 1.10526 \cdot 10^{-4} - 2.428275 \cdot 10^{-14} \quad (5)$$

TABLE I COORDINATES OF DESIGNED PARABOLA

X(cm)	-190.0	-158.3	-126.6	-95.00	-63.33	-31.67	0.0
Y(cm)	39.9	27.7	17.78	9.97	4.43	1.12	0.0
X(cm)	31.67	63.33	95.00	126.6	158.3	190.0	-
Y(cm)	1.12	4.43	9.97	17.78	27.7	39.9	-

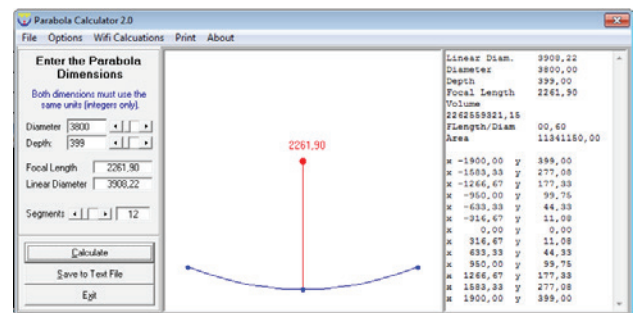


Fig.1. Parabola Calculator 2.0 [11]

Geometrical model of solar parabolic concentrator is parametrically designed from calculated coordinates and it is shown on Fig. 1. Selected model of solar dish concentrator with 11 petals requires very precise definition of parameters during geometrical modelling of



system. Results obtained by optical analysis of solar concentration system are very much dependent on the selected method of the CAD model generation.

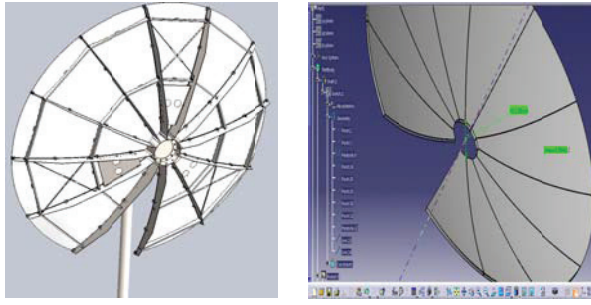


Fig.2 CAD model of solar parabolic concentrator with dimensions and rear view of solar concentration system

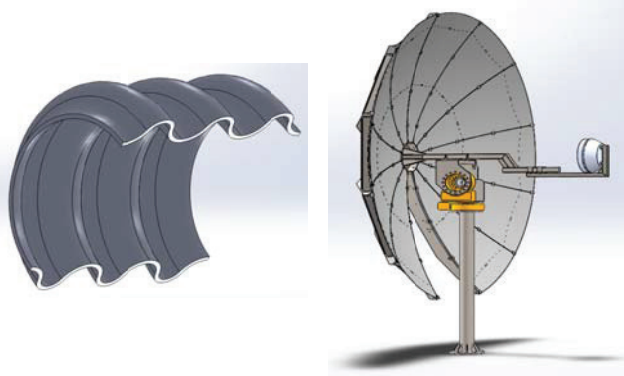


Fig.3 3D CAD model of thermal solar concentration system and sinusoidal profile of corrugated pipe of spiral absorber

A truncated paraboloid of revolution (circular paraboloid) is obtained by rotating the parabola segment about its axis [Fig.4]. Consider a concentrator consisting of 11 trapezoidal reflective petals of identical non-overlapping trapezoidal segments. 3D model of trapezoidal reflective petal of solar parabolic concentrator is presented on Fig. 4. The outer diameter of corrugated pipe is  $D_e = 12.2$  mm, inner diameter  $D_i = 9.3$  mm and thickness of wall pipes is  $s = 0.25$  mm.

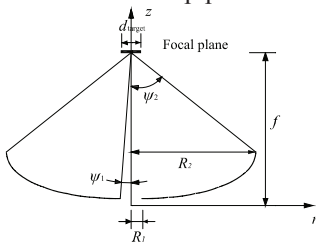


Fig.4 Schematic of truncated parabola



Fig.5 Trapezoidal reflective petal of solar parabolic concentrator

Detailed design parameters of solar parabolic concentrator is given in Table II.

TABLE II DESIGN PARAMETERS OF SOLAR PARABOLIC CONCENTRATOR

Parameters	Numerical value	Unit
Aperture radius $R_1$	0.2	[m]
Radius of smaller hole $R_2$	1.9	[m]
Gross collector area $A_{gross}$	11.82	[m <sup>2</sup> ]
The cross section of the opening parabola $A_{proj}$	9.89	[m <sup>2</sup> ]
A sheltered area of the concentrator $A_{shadow}$	0.126	[m <sup>2</sup> ]

The effective area of the concentrator $A_{ef}=A_{proj}-A_{shadow}$	9,764	[m <sup>2</sup> ]
Receiver diameter	0.40	[m]
Shape of receiver	Corrugated spiral pipe – circular disc	-
Depth of the concentrator	0.399	[m]
Focal length	2.26	[m]
$\psi_1$	6	[°]
$\psi_2$	45,6	[°]

Receiver - absorber is placed in focal area where reflected radiation from solar concentrator is collected. In the process of designing parabolic solar concentrators one always seek for the minimum size of the receiver. With small receiver size one can reduce heat losses as well as cost of whole system. Also small receiver size provide increase of absorbed flux on the surface of receiver. This is the way of obtaining greater efficiency in conversion of solar radiation to heat. In our system receiver - absorber is Archimedean spiral corrugated pipe type with diameter of 400 mm. It is shown on Fig. 6.

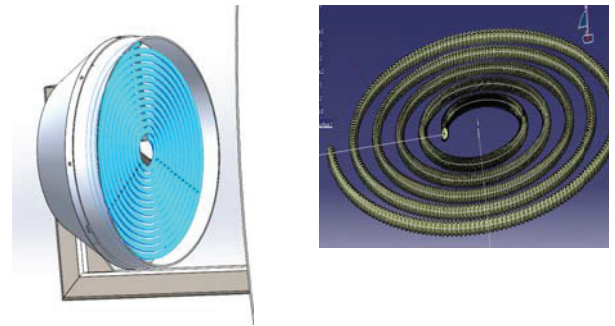


Fig.6 Solar cavity receiver – spiral corrugated pipe type of solar absorber

In this paper only optical properties of receiver are analysed. In our further research we plan to model all necessary details of receiver's geometry which are important for conversion of solar energy into heat of fluid that is used for transfer energy.

### III. NUMERICAL SIMULATIONS AND RAY TRACING STUDIES TO DETERMINE THE OPTICAL CHARACTERISTICS OF THE SOLAR IMAGE

For optical ray tracing analysis of solar parabolic thermal concentrator software Trace Pro, Lamda Research Corporation, USA is used. Simulations have been performed using the technique of ray tracing to describe the behaviour of parabolic dish solar concentrators and such simulations have been used to study the behaviour of such concentrators in non – imaging optics; however, there is no such study or simulation of ray-tracing type to describe parabolic solar concentrators. In TracePro all material properties are assigned. 11 trapezoidal reflective petals are defined as standard mirrors with reflective coating. Reflection coefficient was 95%. Receiver was cylinder with diameter 400 mm placed on 2075 mm from vertex of parabolic dish (optimal focal distance from vertex of parabolic solar concentrator). Absorbing surface was defined as perfect absorber. After definition of geometry of solar parabolic concentrator radiation source was defined. Radiation source was circular with diameter

same as diameter of parabolic dish (3800 mm). Radiation source was placed 2000 mm from vertex of parabolic dish and had circular grid pattern for generating 119401 rays for Monte Carlo ray tracing. Spatial profile of generated rays was uniform and angular profile was solar radiation. Input parameter for optical analysis is solar irradiance 800 W/m<sup>2</sup>. Experiential value for solar irradiation for town of Niš in Serbia is between 750 W/m<sup>2</sup> and 900 W/m<sup>2</sup>. Optical system for solar parabolic concentrator with traced rays is given in Fig. 7.

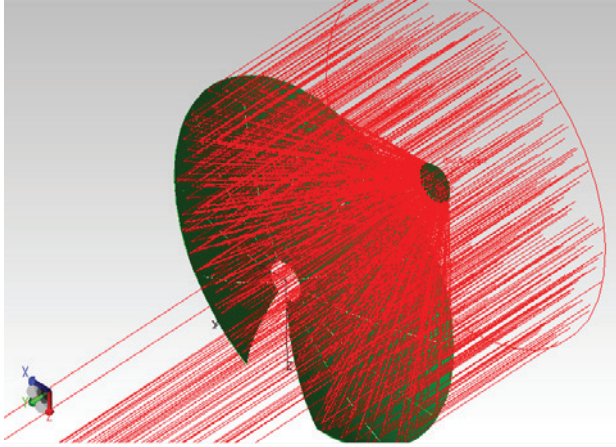


Fig.7. Optical system of solar parabolic concentrator with traced rays

Optical analysis is done by generating and calculating Monte Carlo ray trace for 119401 ray. From all emitted rays only 103029 rays reached absorber surface which is 82% rays of emitted rays are absorbed on receiver. Calculated irradiance for absorbed rays on receiver is from  $1.74 \cdot 10^{-8}$  W/m<sup>2</sup> to 62100 W/m<sup>2</sup>. Total calculated flux on receiver was 7800W. On Fig. 8 is shown total irradiance map for absorbed flux on receiver. When the sunlight shines on the solar collector including the direct and scattered radiation, there are three conditions affecting on the absorption properties of the solar collector: (1) direct solar radiation absorbed directly by the solar collector and the light energy after the specular reflection; (2) the light energy of the scatter solar radiation after the diffuse and specular reflection; (3) the light energy of the direct solar radiation after the diffuse reflection. The slope of incident light is different in different latitude and time, so we deal it with integral processing in the range of incident angle.

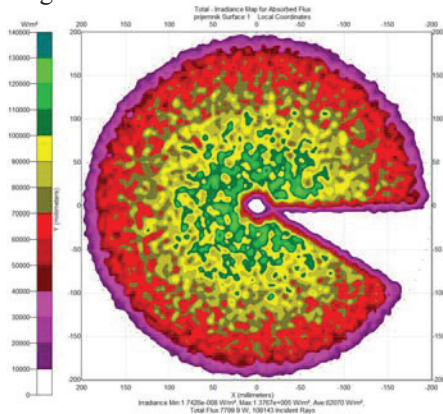


Fig.8. Irradiance map for absorbed flux on spiral receiver (solar focal image)

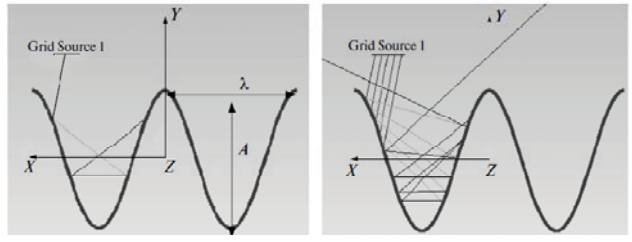


Fig.9. Irradiance diagram at the center of receiver

We take city of Nis (Laboratory for Solar Thermal Engineering) as an example. Nis is located in southeast Serbia longitude 43.30° North latitude and 21.90 east longitude. According to the declination angle  $\delta$  ( $-23.45^\circ$  on winter solstice), sunset hour angle  $\omega$ , altitude of the sun  $h$ , the installation angle of  $45^\circ$  and the North – south placement of solar parabolic collector. In order to calculate the angle of incidence, the sun angle is defined as follows:

$$\delta = 23.45 \sin \epsilon, \epsilon = 2\pi d / 365, \phi = 21.90^\circ, \omega = 15t$$

$$\sin h = \sin \phi \sin \delta + \cos \phi \cos \delta \cos \omega$$

$$\sin \mu = \frac{\sin \omega \cos \delta}{\cosh}, \cos i = \cos \theta \sin h + \sin \theta \cosh \cos \mu,$$

where  $d$  is the number day of 365,  $t$  is the time in hours.

TABLE III DESIGN PARAMETERS OF SOLAR PARABOLIC CONCENTRATOR

Time	Sunset hour angle $[\omega]$	Altitude of the sun $h$	Angle of incident $i$
9:00	$-45^\circ$	$18^\circ$	$55^\circ$
10:00	$-30^\circ$	$25^\circ$	$45^\circ$
11:00	$-15^\circ$	$30^\circ$	$37^\circ$
12:00	$0^\circ$	$32^\circ$	$34^\circ$
13:00	$15^\circ$	$30^\circ$	$37^\circ$
14:00	$30^\circ$	$25^\circ$	$45^\circ$
15:00	$45^\circ$	$18^\circ$	$55^\circ$

The influences of absorption rate for the sinusoidal corrugates absorber plate by aspect ratio and the slope of incident light are plotted in Fig. 10. From the optical point of view, the times of light reflection absorption increases with the aspect ratio, which causes the absorption rate of the absorber plate increasing. Specially, the absorption rate is close to 1, when the aspect ratio tends to infinity.

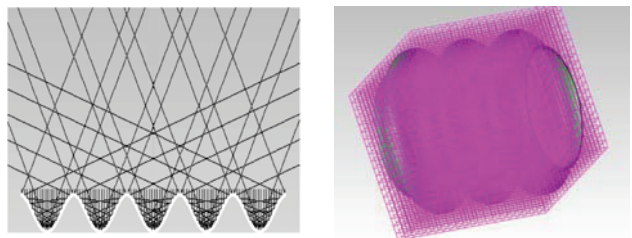


Fig.10. Ray tracing and radiation control volume grid (1000 elements) for part of corrugated pipe

According to the boundary conditions, the optical properties can be obtained after many simulation calculations, which are called the ray tracing method [11].

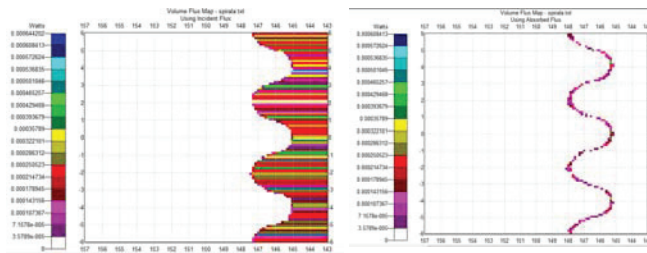


Fig. 11. Volume radiation flux distribution (incident and absorbed flux)

Figure 12. shows scattered model for reflection of incidence angle for solar parabolic dish concentrator with 11 curvilinear trapezoidal reflective petals. In general, the reflectance of a surface increases with angle of incidence. But for a mirror, the reflectance is already very high when the AOI = 0 deg. It can't increase much more. This is why the peak BRDF doesn't change with AOI. However, the reflectance of a black surface increases with AOI, no matter how black the surface.

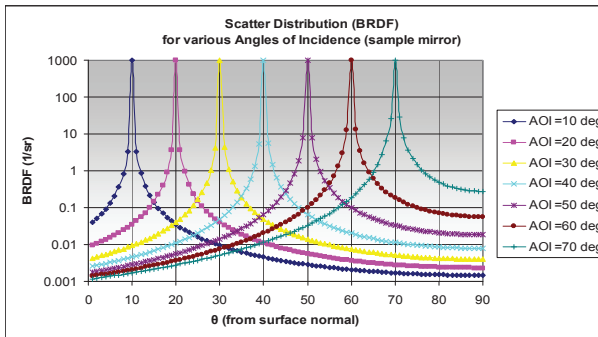


Fig. 12. ABg giving the BRDF as a function of incidence angle

## CONCLUSIONS

This paper presents optical analysis of the solar parabolic concentrator using the ray - tracing software TracePro. One can see that results obtained from optical design of solar parabolic concentrator are satisfactory. Total flux in focal area is good. Irradiance distribution for absorbed flux is relatively uniform for small area for absorber. A detailed simulation and analysis was conducted to evaluate the absorption rate of sinusoidal corrugated absorber pipe. Lights with arbitrary incident angle shinning on the sinusoidal corrugates absorber plate can occur second times of reflection, part of the light have third times and more reflection. In future development of optimization method is planned. This optimization method will make it possible to find optimal geometrical and optical parameters of the various types of solar parabolic dish concentrators as well as geometrical, optical and thermal parameters of different types of solar cavity receivers - absorbers.

## ACKNOWLEDGMENT

This paper is done within the research framework of research projects: III42006 – Research and development of energy and environmentally highly effective poly generation systems based on renewable energy resources. Project is financed by Ministry of Education, Science and Technological Development of Republic of Serbia. Authors acknowledge to Lambda Research Corporation for allowing using software TracePro for PhD Thesis research of Saša Pavlović.

## REFERENCES

- [1] Badran, A.A.Yousef,I.A.,et al.,“Portable solar cooker and water heater”, *Energy Conversion and Management* 51 (8), 1605–1609, 2010.
- [2] Joshi,A.S.,Dincer,I.,Reddy, B.V., “Solar hydrogen production: a comparative performance assessment”, *International Journal of Hydrogen Energy* 36(17),11246–11257, 2011.
- [3] Furler, P.,Scheffe,J.R.,Steinfeld,A., “Syngas production by simultaneous splitting of H<sub>2</sub>O and CO<sub>2</sub> via ceria redox reactions in ahigh-temperature solar reactor”, *Energy & Environmental Science* 5(3),6098–6103,2012.
- [4] Mancini,T.,Heller,P.,Butler,B.,Osborn,B.,Schiel,W.,Goldberg,V., Buck,R.,Diver,R.,Andraka,C.,Moreno,J..“Dish–Stirling systems:an over view of development and status“, *Journal of Solar Energy Engineering-Transactions of the ASME* 125(2),135–151, 2003.
- [5] Mills,D. “Advances in solar thermal electricity technology”, *Solar Energy* 76 (1–3),19–31, 2004.
- [6] O'Neill, M. J. and Hudson, S. L. “Optical Analysis of Paraboloidal Solar Concentrators.” *Proceedings 1978 Annual Meeting, U.S. Section of Int. Solar Energy Society*, August 1978; Denver, CO. Vol. 2.1: p.855
- [7] Imhamed M. Saleh Ali, Tadhg S. O'Donovan , K.S. Reddy, Tapas K. Mallick, “An optical analysis of a static 3-D solar concentrator,” *Solar Energy* 88, 57-70, 2013.
- [8] N.D.Kaushika, K.S.Reddy,“Performance of low cost solar paraboloidal dish steam generating,” *Energy Conversion & Management* 41, 713-726, 2000.
- [9] A.R.El. Ouederni, M. Ben Salah, F.Askri and F. Aloui, “Experimental study of a parabolic solar concentrator, *Revue des Renouvelables*, Vol. 12, 395-404, 2009.
- [10] Rafeeu, M.Z.A.AbKadir, “Thermal performance of parabolic concentrators under Malaysian environment,”: A case study, *Renewable and Sustainable Energy Reviews*, 16, pp. 3826-3835, 2012.
- [11] Zhiqiang Liu, Justin Lapp, Wojciech Lipinski, “Optical design of a flat solar concentrator, *Solar Energy* 86, pp. 1962-1966, 2012.
- [12] <http://mscir.tripod.com/parabola/>
- [13] Lubos Mitás, Quantum Monte Carlo, J. Current Opinion Solid State Mater. Sci., 1997, Vol. 6, no. 2, pp. 696–700.
- [14] Nyers J., Nyers A.: “Hydraulic Analysis of Heat Pump's Heating Circuit using Mathematical Model”. 9rd IEEE ICCI International Conference” Proceedings-USB, pp 349-353, Tihany, Hungary. 04-08. 07. 2013. ISBN 978-1-4799-0061-9



# Comfort analyzing based on probability theory in office building

László Kajtár\*, János Szabó\*

\* Budapest University of Technology and Economics, Department of Building Service and Process Engineering, Hungary

[kajtar@epgep.bme.hu](mailto:kajtar@epgep.bme.hu)

[szaboj@epgep.bme.hu](mailto:szaboj@epgep.bme.hu)

**Abstract**— It is our main priority in the case of office buildings to ensure a suitable comfort level. In addition, the comfort directly influences the productivity of office employees. Poor thermal comfort and poor indoor air quality deteriorates the intensity and quality of human work. On-site measurements were made in summer in such an office building. We evaluated the thermal comfort under *PMV* (Predicted Mean Vote), *PPD* (Predicted Percentage of Dissatisfied) and air quality based on carbon dioxide concentration. The comfort evaluations were based on the requirements of CR 1752. We also evaluated the comfort levels with the comfort questionnaires. The comfort evaluation could be done with continuous on-site measuring and data logging. For the data processing and evaluation we developed a new measuring system assembly and a personally developed computational program. The evaluation could be possible only by the base ground of the probability theory and for that reason we determined the standard deviation and the 95% confidential range of the measuring results. The results of measurements gave assistance to the planning as well as this, measurement results helped improve the regulation of *HVAC* (Heating, Ventilating and Air-Conditioning) systems. The measurements were evaluated with scientific research methods; the results were presented in this article.

**keywords:** carbon dioxide concentration, draft rate, on-site measurement, probability theory, thermal comfort

## I. INTRODUCTION

In office buildings the thermal comfort and indoor air quality determines the comfort sensation and productivity of people. To be efficient at work it is essential to ensure suitable thermal sensation and indoor air quality. It could be possible to evaluate only on an objective measurement method. The best indicators of the thermal sensation are the *PMV*, *PPD* and these values can definitely be measured in an operating office building [1]. The requirements of CR 1752 [2] were based on the evaluation of comfort.

The results of the measurements were evaluated based on the probability theory. The assumption was that the distribution of measurement results did not followed the typically defined probability distribution. The reason of that is the automatically working *HVAC* regulation system. The daily office work period was interpreted between 7 a.m. and 7 p.m. In each office we determined the mean value, standard deviation and 95% confidential range of measured data based on the daily measurements. The CR 1752 comfort categories were determined based on the 95% confidential range.



Figure 1. The arrangement of the instruments at measurements site

Apart from the objective measuring procedures the subjective thermal sensation of the people occupying the area is also important. That is why we carried out the thermal comfort assessment based on a questionnaire.

## II. METHODS

The office building contained six floors, two of which were located below ground level. Offices and meeting rooms are all found above ground level. Some of these were single but most were landscaped offices. The building consisted of two typical sides: west and south facing. The south side was overshadowed by the neighboring buildings. On the western side external glass shade was fixed. In front of the windows a 30cm thick natural ventilating air hole was created. The garage and technical rooms were below ground level. The internal environment assessment was carried out according to CR 1752. We evaluated the temperatures, thermal sensation, draft rates and the carbon dioxide concentration. In each compartment the measurement result determined the comfort categories and their distribution. Offices were air-conditioned by cabinet fan-coils which were fixed on the floor below the windows. The fan-coils were controlled by a 3-phase ventilator and the rooms were regulated based on set-point control default setting. The planned cooling water temperature was 7/13°C. In the offices the planned specific fresh air volume was 36 m<sup>3</sup>/h per person.

We show the comfort measurement results with the analysis of a landscape office. The landscape office consisted west and south oriented external walls. The glazing rate was ~80% in case of west side and ~50% in case of south side. The area of the large office was 280 m<sup>2</sup>, where 45 people worked. On the other 39 m<sup>2</sup> three single offices could be found. The fresh air utilizing air handling unit (AHU) was used for cooling and heating. The AHU's operated from 7 a.m. to 8 p.m. We selected 10 typically oriented points of room to evaluate the comfort in offices. The continuous measures were carried out in June 2011. The measured parameters and sampling frequencies are included in Table 1.

TABLE I.  
COMFORT PARAMETERS

Measured parameter	Sign	Sampling frequency
Air temperature	$t_i$	5 min
Mean radiant temperature	$t_r$	5 min
Relative humidity	$f$	5 min
Mean air velocity	$w$	5 sec
Carbon dioxide concentration	$c_{CO_2}$	5 min

The instruments to measure the temperatures and the thermal parameters were *Testo* instruments. For the carbon dioxide concentration *Horiba* equipment was used. The number of daily measured data was 43 200 which

were processed with a personally developed computing program. The instruments can be seen on Fig. 1.

## III. RESULTS AND DISCUSSION

The results were registered continuously by data loggers. The data were processed with a personally developed computational program and the following parameters were calculated from the data: Predicted Mean Vote (*PMV*), Predicted Percentage of Dissatisfied (*PPD*), local mean air velocity ( $w_a$ ), Turbulence intensity ( $Tu$ ), Draft rating (*DR*). The mean value, standard deviation and 95% confidential range of the calculated and measured values were processed daily and we determined the characteristic of the distribution.

We prepared the local measurements characteristics for the comfort daily diagram. Within the article the typical measuring data can be seen from three chosen places:

- landscape office, in the vicinity of the fan-coil instrument (l=1,5m) [No.1],
- landscape office, in the vicinity of the fresh air grill (r=2,8m) [No.2],
- single office, in the vicinity of the fan-coil instrument (l=0,9m) [No.3].

### A. Air temperature

It can be seen on Fig. 2. the change of air temperature in the measuring areas on the same day. The areas - where the fresh air grill measured - the temperature rose in the room during the operation of the AHU [No.2]. In the vicinity of the fan coil unit the measured areas showed a rise in air temperature of about 1°C due to the southern orientation [No.1]. Within the single office [No.3] the fan coil device, due to the two way regulation of the air temperature periodically fluctuated. The strong fluctuations are the reason for the small air temperature set for the rooms, as well as the high ventilation revolution. The statistical analysis for the measured results is shown by Table 2.

TABLE II.  
AIR TEMPERATURE MEASUREMENT STATISTICAL RESULTS

	t [°C]		
	[No.1]	[No.2]	[No.3]
<b>Mean value</b>	25.61	25.79	21.36
<b>St. deviation</b>	0.25	0.32	1.25
<b>Min.</b>	25.3	25.3	19.7
<b>Max.</b>	26.1	26.3	24.6
<b>95% conf. range</b>	[25.3; 26.0]	[25.3; 26.3]	[19.8; 24.5]



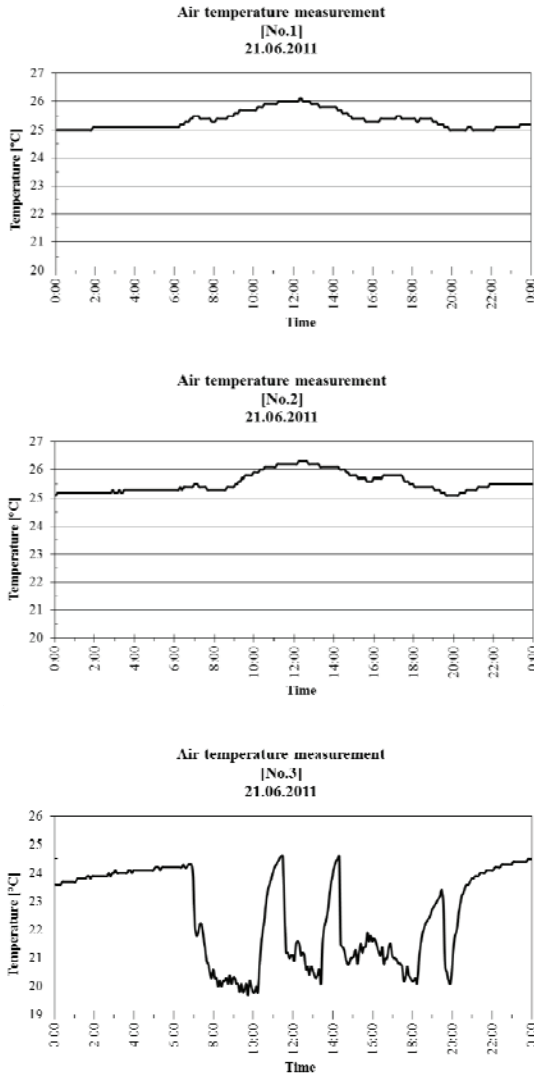


Figure 2. Daily change of air temperature

### B. Thermal sensation

Fig. 3 shows the daily change of  $PMV$  values in the case of three points of office rooms. Fig. 4. shows  $PPD$  values for chosen days of these significant rooms. In the close vicinity of the air grills the measured areas showed pleasant heat comfort levels during the operation of the  $AHU$ 's. In the measuring area No.1 the  $PMV$  change followed the change in air temperature. The  $PMV$  daily fluctuation extent was  $\Delta PMV \approx 0,28$ . At the measuring area No.3 the temperatures large fluctuation was followed by the  $PMV$  fluctuation  $\Delta PMV \approx 1,05$ . The evaluation of the  $PMV$  results measurement can be found in Table 3., the  $PPD$  in the Table 4. [3], [4].

TABLE III.  
PMV EVALUATION STATISTICAL RESULTS

	PMV [1]		
	[No.1]	[No.2]	[No.3]
<b>Mean value</b>	0.63	0.06	-0.29
<b>St. deviation</b>	0.09	0.06	0.27
<b>Min.</b>	0.52	-0.03	-0.69
<b>Max.</b>	0.80	0.25	0.36
<b>95% conf. range</b>	[0.52; 0.79]	[-0.02; 0.18]	[-0.67; 0.30]

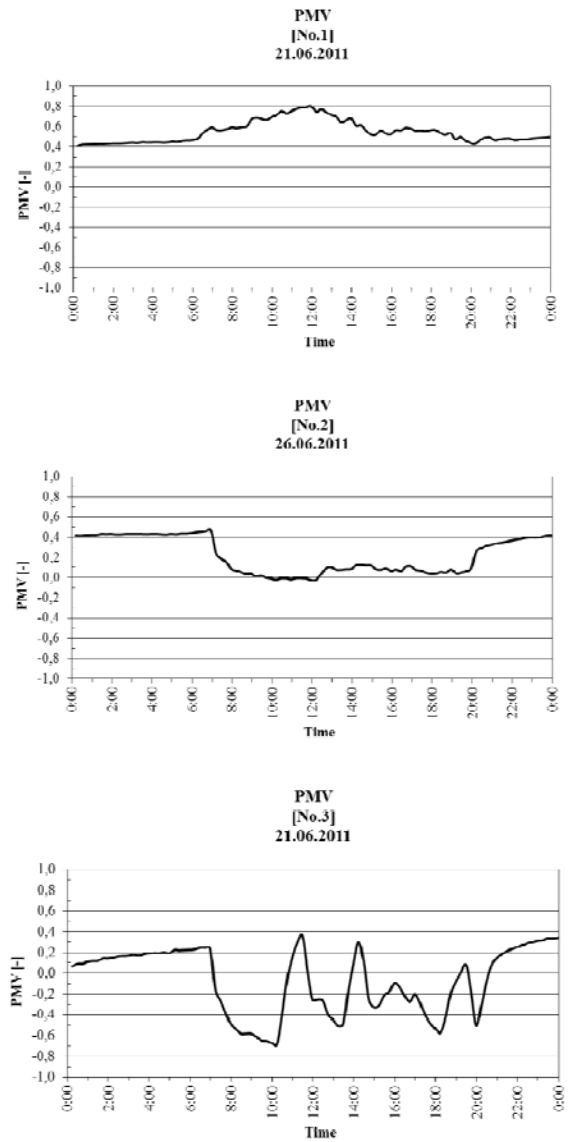


Figure 3. Calculated  $PMV$  values

TABLE IV.  
PPD EVALUATION STATISTICAL RESULTS

	PPD [%]		
	[No.1]	[No.2]	[No.3]
<b>Mean value</b>	13.6	5.1	8.2
<b>St. deviation</b>	2.4	0.2	3.0
<b>Min.</b>	10.7	5.0	5.0
<b>Max.</b>	18.5	6.3	15.0
<b>95% conf. range</b>	[10.7; 18.3]	[5.0; 5.7]	[5.1; 14.5]

### C. Draft

The characteristic of the draft was favorable irrespective of the orientation in the case of the office building by the supply air. The change of the  $w_a$ ,  $Tu$ ,  $DR$  values can be seen in Fig. 5, 6, 7 for the same chosen day

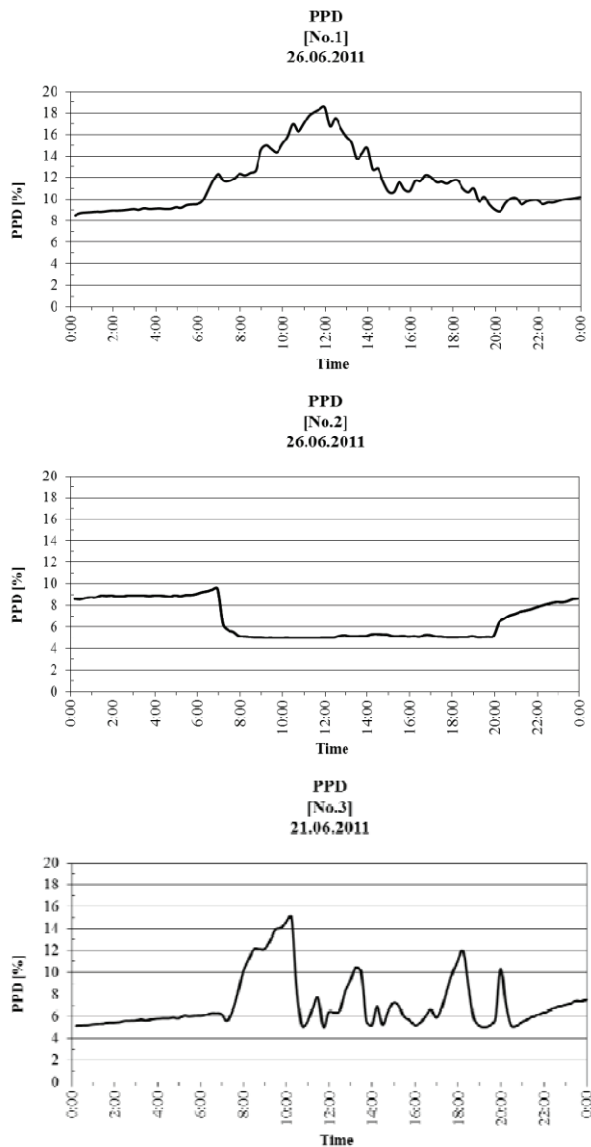


Figure 4. Calculated PPD values

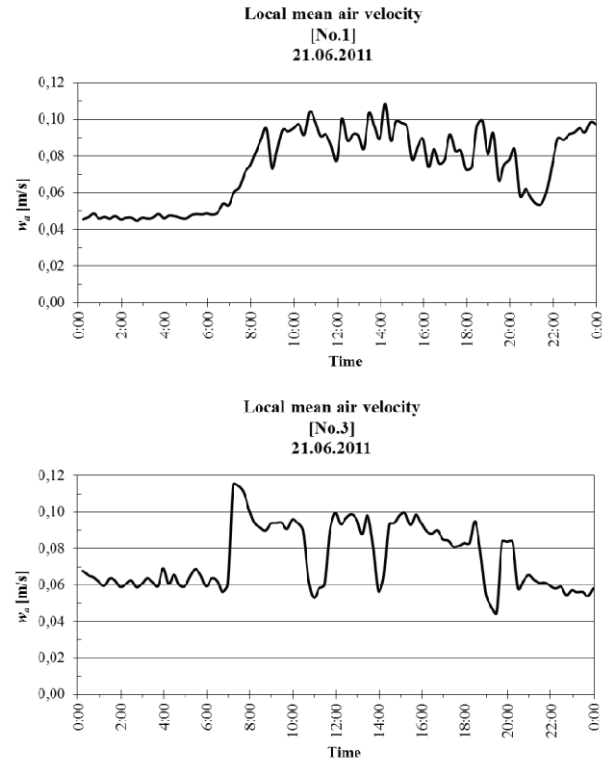


Figure 5. Local mean air velocity

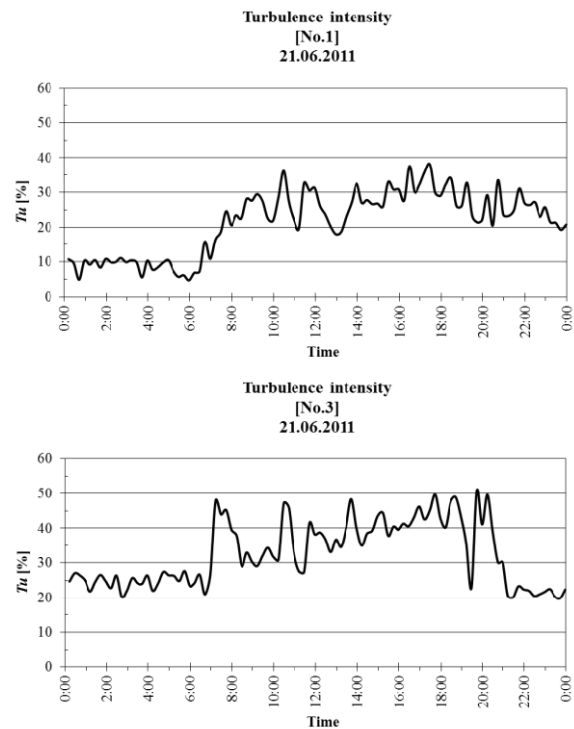


Figure 6. Turbulence intensity

seen on the previous Figures. The individual measured areas show a broad range of result. Due to the regulated automation, the characteristics fluctuated in both measured areas, in almost all cases meeting the “A”

category requirements ( $DR < 15\%$ ). The fluctuation characteristics however differed; this is shown by Fig. 7.

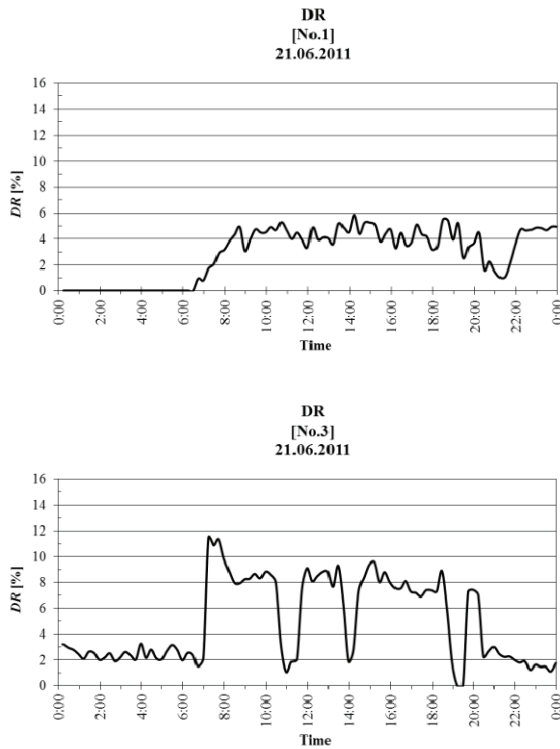


Figure 7. Draft rating

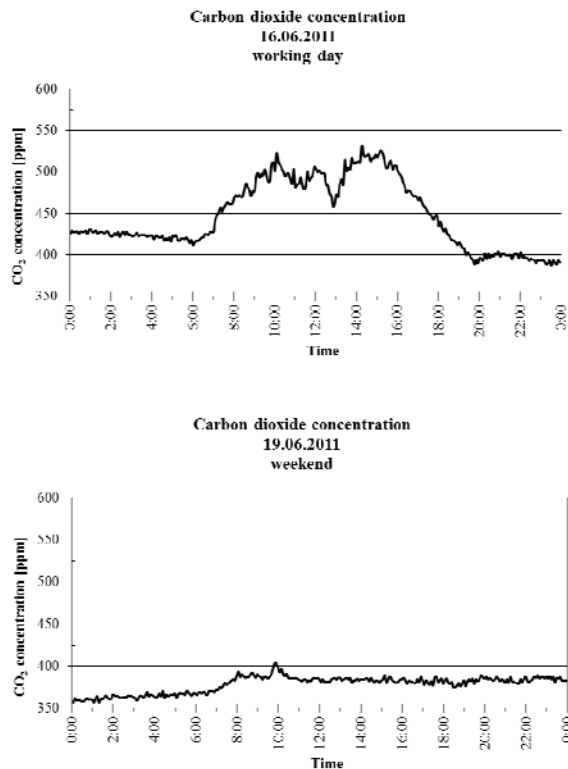


Figure 8. Carbon dioxide concentration

#### D. Indoor air quality

Fig. 8. shows the daily change of the carbon dioxide concentration in the comfort zone on a typical working day and weekend. After commencing the work, the carbon dioxide concentration in the comfort zone increased significantly due to CO<sub>2</sub> exhaling of people. The reduction of carbon dioxide concentration can be seen during the lunchtime period [5], [6], [7].

#### E. Thermal questionnaire

We evaluated the office workers at a subjective 7-grade ASHARE heat comfort scale. The questionnaire was filled out in the morning and in the afternoon in 22 June 2011. The histogram of these evaluations can be seen in Fig. 9. It can be determined that the employee majority valued it as warm and slightly warm [8].

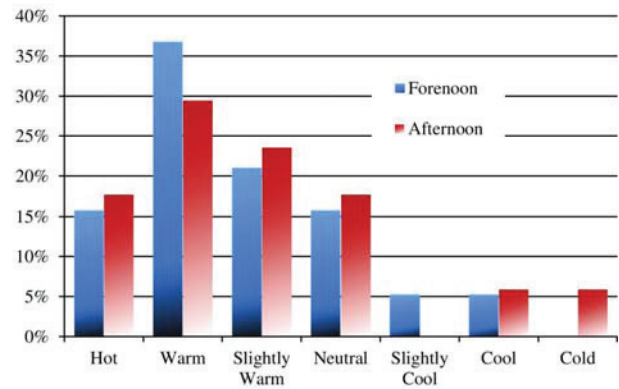


Figure 9. Histogram of thermal comfort questionnaire

#### IV. CONCLUSIONS

During the evaluation we made the distribution of the comfort parameters by comfort categories. Fig. 10. shows the significant difference between the distributions of the thermal comfort, air temperature, draft sensation and carbon dioxide concentration. The distribution of measuring results contains all of measured and evaluated parameters between 7 a.m. and 7 p.m. The examined rooms filled the category „A” requirements in the case of the draft sensation of 80.6%, carbon dioxide concentration of 94%, and air temperature 13.7%.

The measured results show that from the point of view of air quality and draft criteria an “A” category can easily be given. For this to be implemented a 36 m<sup>3</sup>/h per person fresh air supply is satisfactory. The heat comfort requirements cannot be ensured by the cabinet fan coil apparatus on the majority of the comfort zone. The high standard “A” category requires a more complicated and expensive air conditioning system: horizontal fan-coil with air ducts and supply air grill, chilled beam, and cooled ceiling.

The results of thermal questionnaire and instrumental measurements are in accordance with each other. The thermal sensation was the least favorable case from all results of instrumental measurements. According to thermal comfort there was no result for category “A”. The

55.6% of the evaluated results dropped out of the category „A”, „B” and „C”. The 29% (forenoon) and 30% (afternoon) of the thermal questionnaire respondents evaluated the thermal comfort warm, which achievement was the dominant. Another 16% (forenoon) and 18% (afternoon) of respondents hot had been assessed. The analyses of the data also have indicated that the results of 7-grade ASHARE heat comfort scale questionnaire correspond well with the results of the objective instrumental measuring method [1].

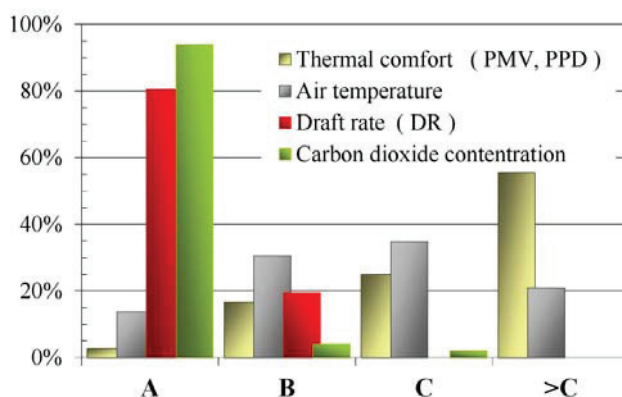


Figure 10. The distribution of measured results by category

#### REFERENCES

- [1] ISO 7730:2005(E), Ergonomics of the thermal environment — Analytical determination and interpretation of thermal comfort using calculation of the PMV and PPD indices and local thermal comfort criteria. Geneva: International Standards Organization; 2005.
- [2] CR 1752, Ventilation for Buildings: Design Criteria for the Indoor Environment. CEN ANSI/ASHRAE Standard 55-2004 Thermal Environmental Conditions for Human Occupancy, Approved by the ASHRAE Standards Committee on January 24, 2004; by the ASHRAE Board of Directors on January 29, 2004; and by the American National Standards Institute on April 16, 2004., ISSN 1041-2336
- [3] Kajtár L., Szabó J., (2010) Effect of window surface on building energy demand (Az üvegfelület hatása az épület energiaigényére) I. Magyar Installateur 2010/5, Budapest, pp. 20-21.
- [4] Kajtár L., Szabó J., (2010) Effect of window surface on building energy demand (Az üvegfelület hatása az épület energiaigényére) II. Magyar Installateur 2010/6-7, Budapest, pp. 46-47.
- [5] Kajtár L., Herczeg L., (2003) Examination of influence of CO2 concentration by scientific methods in the laboratory. 7th International Conference Healthy Buildings 2003, Singapore, Vol. 3, pp. 176-181.
- [6] Kajtár L., Bánhidi L., (2006) Influence of Carbon-Dioxide Pollutant on Human Well-Being and Work Intensity. Proceedings, Healthy Buildings 2006, Lisboa, Vol. 1, pp. 85-90. CD 6p.
- [7] Kajtár L., Hrustinszky T., (2009) Indoor air quality and energy demand of buildings. 9th International Conference Healthy Buildings 2009, Syracuse, 4 p.
- [8] Kajtár L., Leitner A., (2007) High Quality Thermal Environment by Chilled Ceiling in Office Building. 9th REHVA World Congress Clima "Well-Being Indoors" 2007, Helsinki, 6 p.
- [9] Nyers J., Tomic S., Nyers A. : " Economic Optimum of Thermal Insulating Layer for External Wall of Brick ". I J Acta Polytechnica Hungarica Vol. 11, No. 7, pp. 209-222. 2014.
- [10] Nyers J., Nyers A.: "COP of Heating-Cooling System with Heat Pump" 3 IEEE International Symposium "EXPRES 2011." Proceedings ISBN 978-1-4577-0095-8, pp.17-21,
- [11] K Dabis, Z Szánthó: Control of Domestic Hot Water production is instantaneous heating system with a speed controlled pump, 6<sup>th</sup> International symposium "EXPRES 2014 VTS." Subotica. Serbia, 2014. pp. 101-106. ISBN 978-86-85409-96-7.



# Enhance of the efficiency of exploitation of geothermal energy

Ján Takács

Department of Building Services, Faculty of Civil Engineering,  
Slovak University of Technology in Bratislava, Slovakia  
Radlinského 11, 813 68 Bratislava, Slovak Republic  
e-mail: [jan.takacs@stuba.sk](mailto:jan.takacs@stuba.sk)

**Abstract**— Utilization of the renewable energy gains more and more at importance nowadays. Geothermal energy is one of the clean energy sources, however limited only to certain places on the Earth. So, emphasis should be given on efficient utilization of those resources. One way to elevated efficiency is application of sophisticated control systems in geothermal energy plants [1].

The control of utilization of a geothermal well can be quantitative, qualitative or combined. This article compares two situations [3]. First, when the geothermal well has no regulation on the geothermal well head.

The second situation is when the geothermal water is regulated on the head, with quantitative regulation of geothermal water considered. The regulation on the geothermal well head is beneficial to the head because of is consuming only so much geothermal water as it is needed; thus, the lifetime of well is prolonged. In this case of regulation, the efficiency of utilization is increased and remains nearly constant even in winter months.

## I. INTRODUCTION

Slovak republic is a small country, though with lot of geothermal water sources. On the area of 49000 km<sup>2</sup> are round 160 geothermal wells, with temperatures spanning from 15.7°C to 126 °C [2].

The geothermal energy in Slovak republic is used for: recreation (thermal swimming pools), balneology, production of hot water, building heating or heating of greenhouses [3].

Although we have quite high energetic potential in geothermic, the effectiveness of utilization of this valuable energy is low.

The main problem of low effectiveness in utilization of geothermal energy in Slovakia is that usually only one-stage conversion, and not multi-stage cascaded systems, is applied. Next to multi-stage systems, further increasing in effectiveness can be achieved by harmonization of the relation between heat demand and energy supply.

The heat demand depends on the one crucial factor - and this is the weather, or seasons, respectively. On the other hand, geothermal energy supply is practically constant, because the temperature of geothermal water on the well head does not fluctuate much over the year.

The production of well depends on application of a pump. Most geothermal wells in Slovakia have no pump, or a constant flow rate pump.

## II. METHODS

The main emphasis of utilization will be given on relation between heat demand and energy supply. The relation will be demonstrated at particular geothermal well FGT-1, which is situated in a small village – Topoľníky (Fig. 1). The characteristic values of the geothermal well are:

- temperature of geothermal water on the well head -  $\theta_0 = 74\text{ }^{\circ}\text{C}$ ,
- flow rate of geothermal water on the well head -  $m_0 = 23.0\text{ l/s}$ .



Fig. 1 Head of geothermal well FGT-1

Characteristic parameters of utilization of geothermal waters are [3]:

1. available energy potential  $Q$  (kW)

$$Q = m_0 \cdot c_v \cdot \rho \cdot (\theta_0 - \theta_r) \quad (\text{kW}) \quad (1)$$

2. available energy quantity  $E$  (MWh),

$$E = 24 \cdot Q \cdot n \cdot 10^{-3} \quad (\text{kW}) \quad (2)$$

3. available volume of geothermal water  $M$  (m<sup>3</sup>).

$$M = m_0 \cdot n \cdot 24 \cdot 3600 \cdot 10^{-3} \quad (\text{m}^3) \quad (3)$$

Where:

- $m_0$  is flow rate of geothermal water on well head in (l/s),
- $c_v$  is the specific heat of water in (J/kg.K),
- $\rho$  is the specific gravity of water in (kg/m<sup>3</sup>),
- $\theta_0$  is the temperature of geothermal well head in (°C),
- $\theta_r$  is the reference temperature of down cooling in (°C),
- $n$  is the number of days of utilization (day).

The reference temperature means minimal considered temperature of utilized geothermal water – wastewater from geothermal energy system. Usually we consider reference temperature round  $\theta_r = 15$  °C in the winter, while in the summer the reference temperature lies in a range from 20 °C to 26 °C [4].

TABLE I  
CHARACTERISTIC PARAMETERS OF GEOTHERMAL WELL FGT-1

Period	n	Q	E	E	M
	(day)	(kW)	(MWh)	(GJ)	(m <sup>3</sup> )
Day	1	5 682	136	489	1 987
Week	7	5 682	955	3 438	13 910
Month	30	5 682	4 091	14 728	59 616
Summer season	62	5 682	8 455	30 438	123 206
<b>Winter season</b>	<b>202</b>	<b>5 682</b>	<b>27 546</b>	<b>99 166</b>	<b>401 414</b>
Transition period	101	5 682	13 773	49 583	200 707

From Table I. it is evident that in the winter season, we are able to utilize 401 414 m<sup>3</sup> geothermal water, which carries 27 546 MWh of energy.

The geothermal water from the geothermal well FGT-1 supplies heat to 7 equally shaped greenhouses (Fig. 2). In Topoľníky is an open geothermal energy system with direct use and without pump on geothermal well head (Fig. 3). There is not the regulation of geothermal system.

One greenhouse is 93.1 m long and 24.7 m wide. The headroom of the side of the greenhouse is 2.4 m, and its maximum height is 4 m. The heat requirement of one greenhouse is approximately 550 kW, so the total heat requirement of extraction site is 7 x 550 = 3 850 kW.



Fig. 2 Greenhouses in Topoľníky

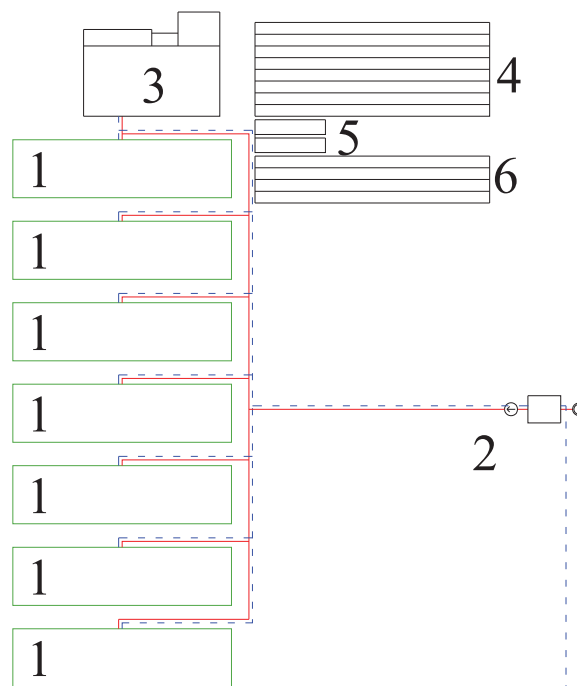


Fig. 3 System wiring diagram of geothermal energy system in Topoľníky

1 – greenhouse LUR 4/93, 2 – geothermal well, 3 – technological building, storage, 4 – heatless industrial hall, 5 – floriculture – heatless, 6 – heatless industrial hall

TABLE II.  
PRESENT IS HEAT REQUIREMENT OF THE GREENHOUSES IN DEPENDENCE ON SEASON WITHOUT REGULATION

Name	Month						
	10	11	12	1	2	3	4
Average exterior temperature (°C)	11,0	5,1	1,1	-1,0	0,9	6,0	11,1
Proportional load (empirical) (-)	0,33	0,75	1,0	1,0	1,0	0,75	0,33
Heat demand of one's greenhouse (kW)	182	413	550	550	550	413	182
Heat demand of all greenhouses (kW)	1271	2888	3850	3850	3850	2888	1271
Temperature difference between input and output from one's greenhouse system (K)	1,9	4,3	5,7	5,7	5,7	4,3	1,9
Temperature difference between input and output from all greenhouse system (K)	13,2	29,9	39,9	39,9	39,9	29,9	13,2
Temperature after utilization in one greenhouse (°C)	70,1	67,7	66,3	66,3	66,3	67,7	70,1
Temperature after utilization all greenhouses (°C)	58,8	42,1	32,1	32,1	32,1	42,1	58,8
Unexploited energy in percentage (%)	75	42	23	23	23	42	75

TABLE III  
HEAT REQUIREMENT OF GREENHOUSES IN DEPENDENCE ON SEASON WITH WELL REGULATION

Name	Month						
	10	11	12	1	2	3	4
Average exterior temperature (°C)	11,0	5,1	1,1	-1,0	0,9	6,0	11,1
Proportional load (empirical) (-)	0,33	0,75	1,0	1,0	1,0	0,75	0,33
Heat demand of one's greenhouse (kW)	1271	2888	3850	3850	3850	2888	1271
Heat demand of all greenhouses (kW)	6,4	14,6	19,5	19,5	19,5	14,6	6,4
Temperature difference between input and output from one's greenhouse system (K)	47,4	47,2	47,2	47,2	47,2	47,2	47,4
Temperature difference between input and output from all greenhouse system (K)	24,6	24,8	24,8	24,8	24,8	24,8	24,6
Temperature after utilization in one greenhouse (°C)	1393	3179	4246	4246	4246	3179	1393
Temperature after utilization all greenhouses (°C)	9	9	9	9	9	9	9

### III. RESULTS

The energy quantity of geothermal well FGT-1 for winter is calculated for reference temperature  $\theta_r = +20^\circ\text{C}$ . This reference temperature is more relevant as the abovementioned temperature  $\theta_r = +15^\circ\text{C}$ . Table 2 presents heat requirement of greenhouses in dependence on season without regulation on the geothermal water inlet.

The Table 2 shows that the geothermal well FGT-1 is utilized below 90% (supposing 10% reserve of geothermal energy) even in the coldest months in the year like December, January and February. Although the utilization in the coldest months in the year is 77% the utilization in those months is satisfactory. However, the utilization in the months March and November is comparatively low, and in October and April is insufficient.

geothermal well head, according to the immediate heat demand of greenhouses.

Figure 4 is a mapping graph of utilization of geothermal water for greenhouses heating without regulation on the geothermal well head.

Table II. Present is heat requirement of the greenhouses in dependence on season without regulation

As can be seen in the Figure 4, the utilization of geothermal water without regulation of flow rate is not effective. In this system, only round 50% from the maximum available energy is utilized (Utilized geothermal energy). So, large part of energetic potential is leaving the system as waste (Unutilized geothermal energy).

If we use regulation of flow rate on geothermal well head, the utilization of geothermal water will become more effective. Table 3 presents heat requirement of greenhouses in dependence on season with regulation on the geothermal well head.

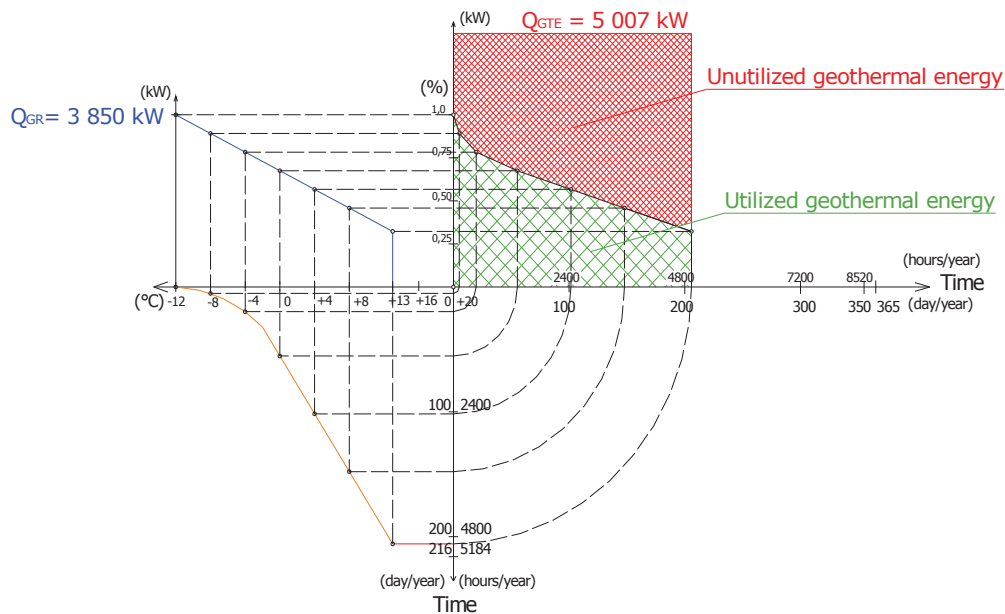


Fig. 4. The mapping graph of heating without regulation on the geothermal well head

The Table III. shows that the geothermal well FGT-1 is utilized approximately 91% and the rest of energy is

like the reserve of geothermal energy. The flow rate of geothermal well is in the coldest months in the year

reduced to the value  $m_1 = 19.5$  l/s, in March and November is it reduced to the value  $m_2 = 14.6$  l/s and in October and April to the value  $m_3 = 6.4$  l/s. This approach to the utilization of geothermal energy safeguards the reserve approximately 10 % in each

month. So, in this case the degree of utilization of geothermal water is constant.

Figure 5 is a mapping graph of utilization of geothermal water for greenhouses heating with regulation on the geothermal well head.

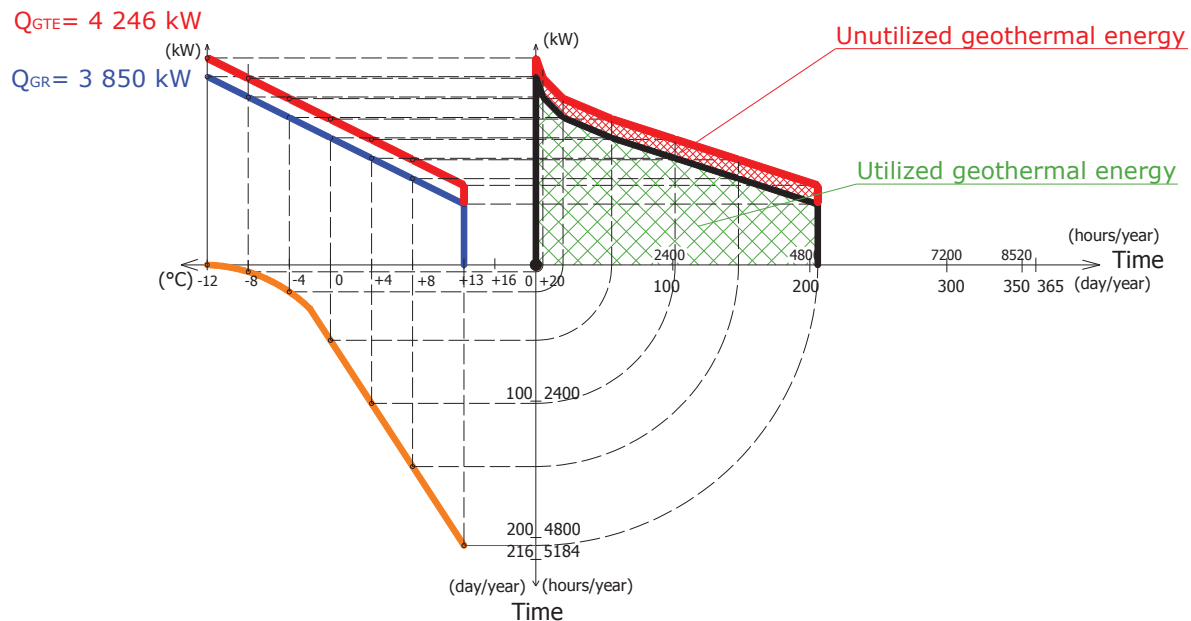


Fig. 5 The mapping graph of heat demand for greenhouses with the regulation on the geothermal

As can be seen in the Figure 5 the utilization of geothermal water with regulation of flow rate is more effective than first case. In this system round 90% from the maximum available energy is utilized (Utilized geothermal energy). So, much smaller part of energetic is leaving as waste from system (Unutilized geothermal energy).

System adapts on exterior conditions therefore utilization of geothermal water is more effective.

#### IV. DISCUSSION

The hugest advantage of geothermal energy is the absence of control systems based on weather conditions as the sun or wind. Nowadays a typical solution is the utilization of geothermal energy for heating of greenhouses without regulation on the geothermal well head [4]. In the coldest months the control of flow rate on the geothermal well head is in the example only 85% in compare with the measured

value on the well head. This shows fact that in the area of the village Topoľníky could be supply more than seven greenhouses. If the flow rate of geothermal water would be 23.0 l/s, we could heat together ten greenhouses. The control on the well head safeguards preferable mapping curve for greenhouses and the reserve in each month is constant

Another approach is that in the coldness months could be pump more geothermal water as is calculated for these months, but the accounting quantity of geothermal water for winter season should not be exceeded. Therefore more than seven or ten greenhouses could be supply because for control on the well head. In the coldest months (December, January and February) in the year the flow rate would be increase and would have higher value as measured value on the well head. But in other months the flow rate would be reduced less or more in according to the season.

#### REFERENCES

- [1] Fendek, M., Bím, M., Fendeková, M. 2005. *Hodnotenie energetického potenciálu geothermal-nych vôd na Slovensku*, Enviromagazin č. 4/2005, ročník 10, p. 12-14
- [2] Petraš, D. a kol.: *Nízkoenergetické vykurovanie a obnoviteľné zdroje energie*. Jaga, Bratislava 2000, 271 strán
- [3] Kontra J.: *Hévízhasznosítás*. Műegyetemi könyvkiadó, Budapest 2004
- [4] Popovski, K. *Geothermally Heated Green-houses in the World, Guideline and Proc. International Workshop on Heating Greenhouses with Geothermal Energy*, Ponta Delgada, Azores, 1998. 42 - 48s.
- [5] Takács, J.: *Využívání geotermální energie v areáloch rekreačných zariadení*. Konferencia s medzinárodnou účasťou
- Geotermálne vody ich využitie a zneškodnenie. Aqua Park Tatralandia Liptovský Mikuláš, 5.-7.11.2007, str.125 - 130,
- [6] Petraš, D. a kol.: *Obnoviteľné zdroje energie pre nízkoenergetické systémy*. Jaga, Bratislava 2009
- [7] Lulkovičová, O. – Takács, J.: *Netradičné zdroje energie*, Bratislava: Slovenská technická univerzita v Bratislave, Stavebná fakulta, 2003
- [8] Popovski, K., Popovska-Vasilevska, *Heating Greenhouses with Geothermal*, S. 1993
- [9] Nyers J, Nyers L.: "Monitoring of heat pumps" 'Studies in Computational Intelligence', Springer's book series, ISBN 978-3-642-15220-7 Vol. p. 243, 573-581, Heidelberg, Germany. 2009.
- [10] Nyers J., Nyers A.: "COP of Heating-Cooling System with Heat Pump" 3 IEEE International Symposium "EXPRES 2011." Proceedings ISBN 978-1-4577-0095-8, pp.17-21,



# Central ventilation of industrial building with wood working operation

**Zuzana Straková**

Slovak University of Technology in Bratislava, Faculty of Civil Engineering,  
Department of Building Services, Bratislava, Slovak Republic  
zuzana.strakova@stuba.sk

**Abstract** - The development of wood industry and legislative requirements on the quality of the working environment results in increased demands on HVAC equipment, which should be definitely a part of every newly constructed premise. Greater emphasis is put on the clean working environment, energy savings and heat recovery, but maximum attention must be paid to safety requirements, economic efficiency, operational reliability and service life of machinery.

Based on above mentioned requirements, HVAC have become an integral part of technology equipment, particularly in relation to the nature of wood processing operations. A large production of wood waste is typical for this type of operation, beginning from very fine dust to chips and fragments with a size of a few cm. Waste exhaust facilities are designed to capture the waste at the place of production, thus avoiding the unwanted spread and deposition in the area of operation. Afterwards, the waste is transported to the separation and equipment, where it is sorted and stored for further use. That is why the air-conditioning equipment plays a crucial role in the protection and creation of a better working environment. [1], [7]

## I. INTRODUCTION

The aim of the HVAC designer's work is to design functional and energy efficient ventilation and exhaust systems with the help of a suitable HVAC configuration. The following example shows one of the appropriate technical solutions of central ventilation and local extraction in a carpentry workshop where final wood works intended for the window frames are carried out. From the layout point of view, it is a one-nave hall building with some office and warehouse space [6]. Work progress of the designer could be briefly summarized in the following points:

- Defining the requirements for the parameters of the indoor environment in a human's working area - a dusty industrial hall type of operation.
  - Calculation of emerging pollutants in wood working process.
  - Proposal of distribution network of the central ventilation.
  - Design of local extraction, filtering and separating equipment of exhaust air.
  - HVAC heat recovery system design.
  - Implementation of the drawing part of the project documentation.
  - Technical report and specifications of piping elements and their components.
- [4], [5]



Figure 1. Wood industrial facility hall [12]

## II. INDOOR ENVIRONMENT REQUIREMENTS

The parameters of the indoor environment in wood industrial facilities (see Figure 1.) are defined according to the requirements and values defined in Decree no. 259/2008 Coll [8]. To relevant qualitative indicators of indoor environment suitable for humans belong: heat-humidity microclimate, complex heat, humidity and air flow activity and determination of the amount of solids suspended in the air.

### A. Thermal-hygrometry microclimate

People's clothing and total body heat production (according to the classes of actions listed in Table I.) are the main factors in determining the optimal and acceptable conditions of thermal-hygrometry microclimate.

TABLE I.  
CLASS ACTIVITIES

Class	Total energy expenditure		Examples of activities
	$q_M$ (W/m <sup>2</sup> )	$q_M$ (met)	
1c	106 - 130	1,82 - 2,23	Standing activity with permanent involvement of both hands, arms and legs together with carrying loads up to 10 kg (shop assistant's work at high frequency of customers, painting, welding, drilling machine, lathes and milling machines operators, light trucks pulling or pushing). Slow walking on the flat ground.

Thermal production of the body is equal to its energy expenditure. In terms of activity type, the operation in a wood processing industry belongs - within the meaning of the decree - to the class 1c.

In the areas intended for long-term stay, the optimum conditions of thermal-hygrometry microclimate are to be secured during the warm as well as the cold season of the year. The structural design of the building is a prerequisite for optimal climatic conditions. Where the structural design does not enable it, these conditions must be secured by technical equipment. The optimal and allowable operational temperature for specific clothing or activity may be more accurately determined (see Table II., Table III.). [11]

TABLE II.  
CONDITIONS OF THERMAL-HYGROMETRY MICROCLIMATE  
FOR WARM SEASON

Class	Operation temperature $\theta_o$ (°C)		Allowable airflow speed $v_a$ (m/s)	Allowable air humidity $\varphi$ (%)
	optimal	allowable		
1c	20 - 24	17 - 26	$\leq 0,3$	30 - 70

TABLE III.  
CONDITIONS OF THERMAL-HYGROMETRY MICROCLIMATE  
FOR COLD SEASON

Class	Operation temperature $\theta_o$ (°C)		Allowable airflow speed $v_a$ (m/s)	Allowable air humidity $\varphi$ (%)
	optimal	allowable		
1c	15 - 20	12 - 22	$\leq 0,3$	30 - 70

#### B. Air-change rate

All areas of long-term and short-term stay must be ventilated. Ventilation of buildings is either natural or forced. Ventilation capacity is determined by the number of persons, type of activity (see Table IV.), the thermal load and the extent of air pollution in order to meet the requirements for the amount of air to breathe and the indoor air cleanliness. Natural ventilation is used for air exchange in areas without sources of pollutants and heat. The method of ventilation, the position and size of air intake and exhaust openings will be determined by calculation. In other cases, the exchange must be secured by forced mechanical ventilation. When replacing the air - the principle of air drop pressure must be respected. In our case, we choose the pressure equalized system because the air exchange between the ventilated space and other spaces is not taken into account. The quality of supply and exhaust air will be considered acceptable if its composition neither endanger nor worsen the living conditions of people in the areas of the building or its surroundings. [2]

TABLE IV.  
MINIMUM AMOUNT OF OUTDOOR AIR SUPPLY

Class	Type of human activity	Minimum amount $V_e$ (m³/h)
1c	work predominantly in sitting position	50
	work mostly standing and walking	70
	heavy physical work	90

Note: At the warm air ventilation and air conditioning may not fall the proportion of outdoor air below 15 % of the total supply air into the room; at the same time must be observed a requirement for the supply of outdoor air per person.

#### C. Limit values of noxious factors in the indoor air

These values are determined as limit values of selected chemical, microbiological and biological pollutants and solids. The limit values of chemical substances and solids are shown in Table V. According to the type of dust premise only values for the production of solids in the air are worth mentioning. [9]

TABLE V.  
LIMIT VALUES OF CHEMICAL SUBSTANCES AND SOLIDS  
IN INDOOR AIR AREAS

Art. №.	Pollutant	Index	Max. allowable value (µg/m³)	Time (h)	Note
2.	solids	PM <sub>10</sub>	50	24	Dust elements whose predominant size is of a diameter of 10 µm and which can pass a special selective filter with a 50 % efficiency.

#### D. Wood waste

A significant production dust solid elements occur during the wood working process. This may be considered harmful when exhausted freely in the air either of indoor or outdoor environment. As for the wood waste, local exhaust is designed and this from every working station, where the production is intended. This waste is exhausted from its place of origin through the exhaust system into the filter system where it is captured, stored and shifted for further processing.

The amount of wood waste is directly proportional to the intensity of production, performance and character of machines. This amount is highly variable because the production is not continuous and even machine manufacturers do not specify this information. [3], [8]

Depending on the type of wood and the nature of the wood working process, we can define the properties of the solid waste and the method of filtration. A few examples are listed in Table VI. [9]

TABLE VI.  
BASIC WOOD WORKING OPERATIONS

Operations	Tool	Waste	Separation
Cutting	Frame saw	coarse	separation chamber
	Band saw		
	Circular saw		
	Cutting saw	coarse - medium	separation chamber cyclone separator
	CNC saw		
Chipping	Wood chip flaker	coarse	separation chamber
Milling	Milling machine	coarse - medium	separation chamber cyclone separator

Operations	Tool	Waste	Separation
Drilling	Wood drill	coarse - fine	cyclone separator buckle filter
Planning	Planning machine	coarse	buckle filter
Grinding	Grinding machine	fine – very fine	buckle filter

### E. Chemicals

Exposure to chemical substances in the premises of the project that can be exhausted into the atmosphere and cause pollution are not taken into account. Therefore it is not necessary to apply additional measurements.

### F. Heat production

During the warm season the heat production is considered to be a thermal load, so measurements are to be taken in order to sustain the acceptable temperature. During winter, the production helps lower the energy demands for space heating to the desired temperature. In accordance with STN EN 15243:2008, the calculated total heat load  $\Phi$  was of value 66,469 W.

## III. DESIGN OF CENTRAL VENTILATION SYSTEM OF INDUSTRIAL BUILDING WITH WOODWORKING OPERATION

The hall building is located in a city Zuberec, Slovak Republic.

Parameters of outdoor and indoor air:

- Outdoor calculation temperature of air in the winter

$$\theta_e = -17^\circ \text{C}$$

- Indoor calculation temperature of air in the winter

$$\theta_i = +16^\circ \text{C}$$

- Outdoor calculation temperature of air in the summer

$$\theta_e = +30^\circ \text{C}$$

- Indoor calculation temperature of air in the summer

$$\theta_i = +26^\circ \text{C}$$

Calculating volumetric airflow [10]:

- Central ventilation system 4 176 m<sup>3</sup>/h
- System of destratification units 12 000 m<sup>3</sup>/h
- Local exhaust system 16 980 m<sup>3</sup>/h

### Equipment No. 1

#### Central ventilation of production area

The central ventilation system (see Figure 2.) is secured by central modular HVAC, composed of two filter and fan chambers, heater and heat recovery exchanger. The unit is in the HVAC engine room. The exhaust is situated on the north-western facade. The outdoor air supply is located on the north-eastern wall of a building provided with a louvre against the rain. The exhaust pipe is situated on the north-western facade.

The air supply into the hall will be secured by large-scale industrial diffusers of cylindrical shape with thermal regulation of the air flow. The exhaust air is secured by the efferent grids set directly into the cut out of a circular pipe.

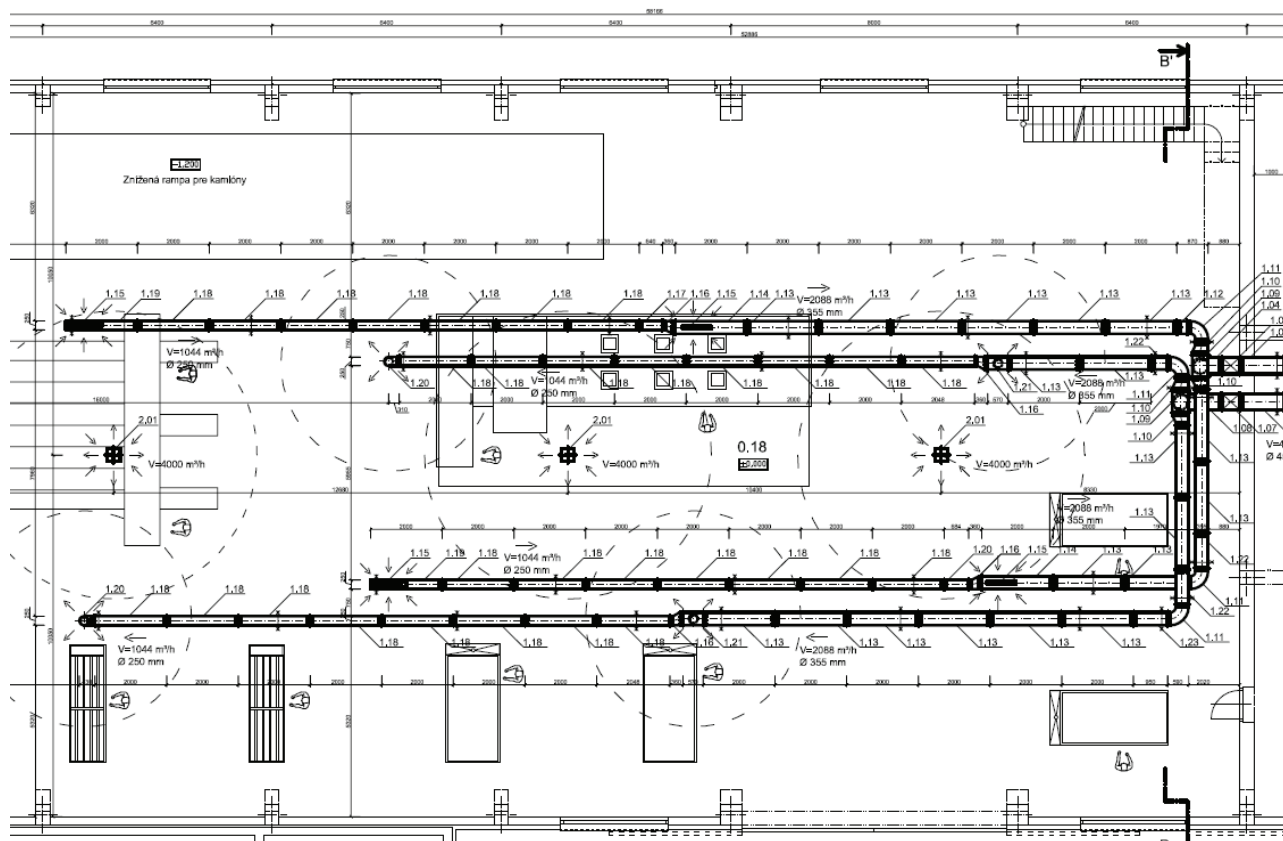


Figure 2. Central ventilation equipment – Plan of industrial building with woodworking operation [13]

*Equipment No. 2 - Destratification units*

The system of destratification units is situated on the roof in the roof lights (see Figure 3.). Its role is to ensure the exhaust of the overheated air in the summer in order to avoid the excessive overheating of the space. In winter, these units help improve the heating system by transporting the warmer air from the roof space into the working area.

*Equipment No. 3*

Equipment producing wood waste and its local exhaustion

The exhaust system (see Figure 3) ensure the transport of waste particles produced during the woodwork process. The pipe network consists of two parts. Each one can work independently and simultaneously as well. 100%

interaction of all devices is considered within one branch. The system consists of a suction pipe network made of a circular pipe, transport radial fans, a filter and separator unit, and a piping network to return the filtered air back into the production space through large-scale textile diffusers. The exhausted devices are connected to the exhaust system using a flexible hosepipe designed especially for the wood industry. Filtration equipment and transport ventilators are located outdoors and are equipped with anti-explosion and fire system.

The pipes transferring the returned filtered air into the production area are equipped with the mixing chamber in the exterior space. Its role is to exhaust the air directly into the exterior during summer and into the interior in winter.

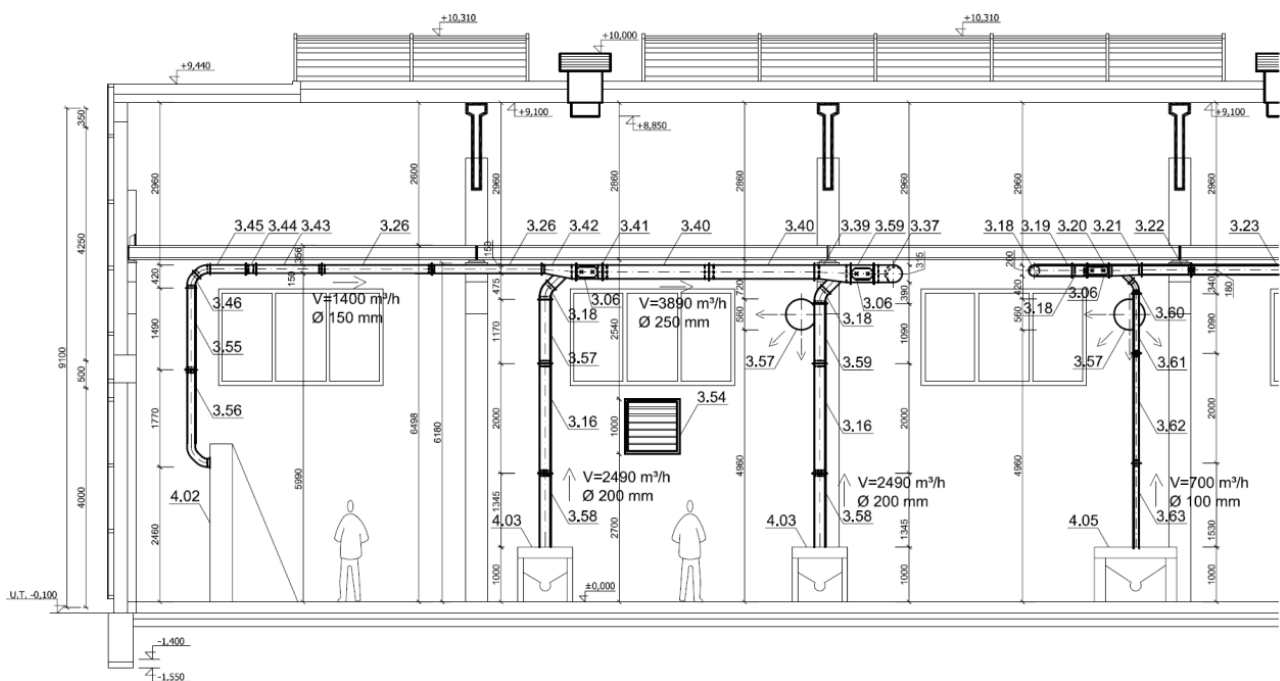


Figure 3. Local exhaust equipment – Cross section of industrial building with woodworking operation [13]

## IV. DISCUSSION

Hygienically optimal thermal-hygrometry condition of the indoor environment is created all year round only in rare cases. Mostly (for economic reasons) are in the interior ventilated and air conditioned buildings maintained satisfactory conditions (acceptable, admissible). Requirements on air quality are always limits.

The only way to achieve these limits in the wood industrial facilities is to apply all three systems of ventilation and air conditioning, which in our example are listed as equipment No. 1, 2 and 3. To propose only some of these systems would lead to under-ventilated space solution and thus also a threat to human health.

## V. CONCLUSION

The role of the central ventilation system is to ensure the hygienic air exchange in the area of production, whereby the air is evenly distributed in the workshop. Energy requirements for air treatment are minimized and aimed only to reheat the air from exterior using a water heater. Placing a plate regenerative heat exchanger in HVAC unit can reduce the demand for heating air by up to 40 %.

All systems are designed to ensure their seamless interaction with respect to the health conditions in the working environment, energy efficiency and to minimize the ecological burden on the environment.



# ACKNOWLEDGMENT

This article is supported by the Scientific Grant Agency of the Ministry of Education of the Slovak Republic and the Presidency of the Slovak Academy of Sciences (VEGA No. 1/0725/15).

# REFERENCES

- [1] Hajzok, L. *Vzduchotechnické zariadenia drevopriemyslu*. (HVAC equipment in wood industry). Bratislava : ALFA, 1986. 181 p. ISBN 80-05-00188-6.
- [2] Kotrbatý, M. – Hojer, O. – Kovářová, Z. *Hospodaření teplem v průmyslu, Nejlevnější energie je energie ušetřena*. (The heat management in industry. The cheapest energy is energy spared). Praha : ČSTZ, 2009. 266 p. ISBN 978-80-86028-41-5.
- [3] Kotrbatý, M. – Seidl, J. *Průmyslové otopné soustavy*. (The industry heating systems). Praha : STP, 2000. 64 p. ISBN 80-02-01693-9
- [4] Kotrbatý, M. – Kovářová, Z. *Intelligentní průmyslové haly. Část 1*. (The intelligent industry halls. Part No. 1). 2009. [www.tzb-info.cz](http://www.tzb-info.cz)
- [5] Kotrbatý, M. *Intelligentní průmyslové haly. Část 2*. (The intelligent industry halls. Part No. 2). 2010. [www.tzb-info.cz](http://www.tzb-info.cz)
- [6] Oppl, L. *Větrání v průmyslu*. (The industry ventilation). Praha : SNTL, 1957. 250 p. ISBN – not specified.
- [7] Petráš, D. a kol. *Vytápění velkoprostorových a halových objektů*. (The heating of large-area and hall objects). Bratislava : Jaga, 2006. 205 p. ISBN 80-8076-040-3.
- [8] Wagnerová, E. - Uriček, D. *Priemyselná vzduchotechnika*. (The industry airing). Prešov : Vydavateľstvo Michala Vaška, 2003. 166 p. ISBN 80-7165-370-5.
- [9] Vyhláška MZ SR č. 259/2008 Z.z. *o podrobnostiach o požiadavkách na vnútorné prostredie budov*. (Decree no. 259/2008 Coll. about the details and requirements for indoor climate environment).
- [10] STN EN 15243:2008 *Vetranie budov. Výpočet vnútorných teplôt, záťaže a energie pre budovy so systémami klimatizácie*. (Ventilation for buildings. Calculation of room temperatures and of load and energy for buildings with room conditioning systems).
- [11] STN EN 15251:2012 *Vstupné údaje o vnútornom prostredí budov na navrhovanie a hodnotenie energetickej hospodárnosti budov - kvalita vzduchu, tepelný stav prostredia, osvetlenie a akustika*. (Indoor environmental input parameters for design and assessment of energy performance of buildings addressing indoor air quality, thermal environment, lighting and acoustics)
- [12] Wood industrial facility hall – photo from [www.dimechanik.sk](http://www.dimechanik.sk)
- [13] The implementation project: Heating and ventilation of wood industrial facilities hall. Viconcal s.r.o. Bratislava 2014.
- [14] Nyers J., Garbai L., Nyers A. : “*Analysis of Heat Pump's Condenser Performance by means of Mathematical Model*”. International J. Acta Polytechnica Hungarica Vol. 11, No. 3, pp. 139-152, 2014.

# Comparison of various ACH test results of rooms

László Fülöp\*, György Polics\*

\* Faculty of Engineering and Information Technology, University of Pécs, Hungary  
fulop@pmmik.pte.hu gyorgy.polics@pmmik.pte.hu

**Abstract** - Results of air tightness and ACH tests in Hungary within an IPA cooperation project are presented. The aim of this work is to find correlation between the natural ACH and Blower Door type “A” 50 Pa ACH test results as well as between the results of Blower Door type “A” and Blower Door type “B” 50 Pa tests. Tracer gas concentration decay test is applied to specify the natural ACH as a reference without influencing the tested phenomena. Calculated natural ACH values derived from Blower Door tests are compared to the results of tracer gas tests. Blower Door tests cannot be replaced by tracer gas tests since it is especially sensitive to the changes of the external conditions and it is not suitable to test multiple room sets.

## I. INTRODUCTION

Referring the article published at the 6th International Symposium on Exploitation of Renewable Energy Sources (EXPRES 2014) titled: Air Change Rate Test Results in the Croatian and Hungarian Border Region, Blower Door type A test results were presented.

Blower Door tests valid at 50 Pa pressure difference, which shall not provide information about actual spontaneous ACH. An interesting field of research is to examine how we can derive the natural ACH rate of the building from 50 Pa ACH, which can be derived for Hungary as 4 Pa for annual average pressure difference.

Another possible testing method for measuring spontaneous ACH is using tracer gas, which has an advantage as compared to Blower Door is that this test method does not influence the test results to the least extent. During the research tracer gas tests were executed in Baranya County, Hungary. The selected tracer gas for this purpose is SF<sub>6</sub>.

Supplementary instrument set applied: KIMO KH 250 for measuring temperature and relative humidity and KIMO AQ200 non-directional air velocity meter.

Types of Blower-Door tests:

### A. Air Change Rate (ACH) test

Type A test: for testing the building ACH as is during normal use.

### B. Air Tightness test

Type B test: testing the air tightness of the building envelope. All purposely made openings of the envelope (e.g. vents, chimneys) had to be closed or sealed.

Magnitude of ACH

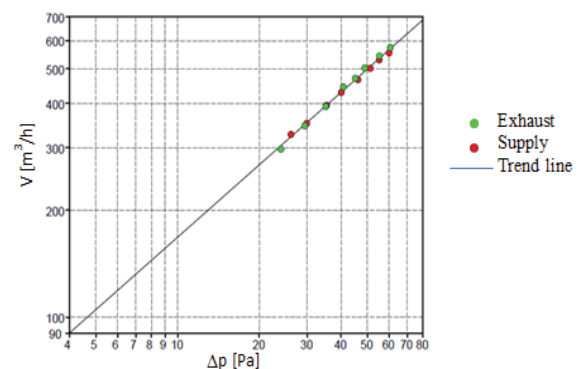
Table 1. Magnitude of n<sub>50</sub> ACH [6]

Magnitude of n <sub>50</sub> ACH	n <sub>50</sub> [1/h]
old building	7...
today's new buildings HU	5...10
today's new buildings DE	2...6
low energy consumption house	0,17...5
passive house	0,17...0,6

## II. DETERMINING SPONTANEOUS ACH BY TYPE “A” 50 PA BLOWER DOOR TEST

Blower Door tests are evaluated by the Tectite 3.6 software, according to the example of Figure 1. (The results are presented in an article of EXPRES 2014 Page 41, Table 3.– 7.6 )

The procedure includes a series of tests at various pressure differences, both exhaust and supply.



Averages:								
Δp [Pa]	60	55	50	45	40	35	30	25
Δp [Pa]	60,6	55,3	51	44,7	39,9	35,4	30,2	25,3
V [m³/h]	760.8	722.3	685.5	634.5	587.0	542.4	484.1	430.7

Figure 1. BlowerDoor test results presented by Tectite 3.6 software

Tectite software provides both the multiplying factor and the exponent of the describing equation belonging to the trend lines created for both pressurization and depressurization. They can be even derived exporting the software results (measured pressure difference and the related air flow) by an Excel spreadsheet, such as seen in Figure 2.

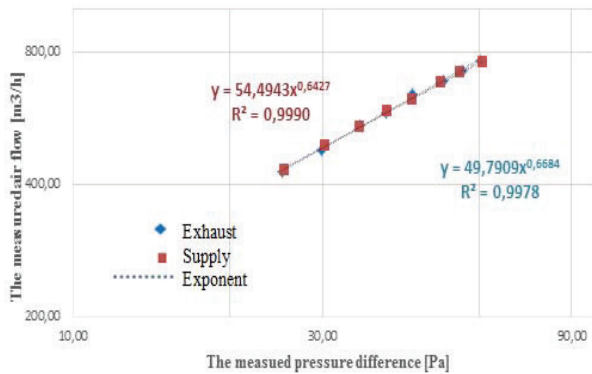


Figure 2. BlowerDoor test results exported and evaluated in Excel spreadsheet

Next, the values of air change rate value characteristic for the building can be calculated. The following results were yielded for the detached house tested:

- In case of overpressure (supply):

The exponent of the descriptive equation:  $n=0,6427$

The multiplying factor of the describing equation:  $C=54,4943$

ACH for 50 Pa pressure difference:  $n_{50}=1,85$  1/h

- In case of depression (exhaust):

The exponent of the descriptive equation:  $n=0,6684$

The multiplying factor of the describing equation:  $C=49,7909$

ACH for 50 Pa pressure difference:  $n_{50}=1,87$  1/h

- In case of the mean value of depression (exhaust) and overpressure (supply):

The exponent of the descriptive equation:  $n=0,6501$

The multiplying factor of the describing equation:  $C=53,1409$

The equation describing the results:

$$\dot{V} = C \cdot \Delta p^n \quad [m^3/h] [1]$$

Where:

$\dot{V}$  - the measured air flow by the Blower Door

$C$  - the multiplying factor of the describing equation

$\Delta p$  - pressure difference at the point of testing

$n$  - the exponent of the descriptive equation

Following the 50 Pa type “A” Blower Door test, knowing the multiplication factor and the exponent of the describing equation depending on the characteristics of the buildings, ACH can be calculated of any pressure difference. A good approximation by statistic methods found despite the fact that some leaks can behave quite differently in case of diverse pressure differences. The most important factors are: turbulent or laminar flow or opening pressure difference.

For testing natural ACH the annual natural pressure difference should be known which is dependent on the weather conditions, such as actual indoor and outdoor temperature difference and the prevailing wind force. In Hungary, the average pressure difference is 4 Pa in the heating season. Substituting this value into the equation [1] the natural ACH rate can be specified.

Assuming 4 Pa pressure difference, the natural filtration air flow is:

$$\dot{V}_{4Pa} = C_L \cdot \Delta p^n = 53,14 \cdot 4^{0,65} = 130,8 \quad [m^3/h]$$

With 4 Pa spontaneous pressure difference, the ACH found as:

$$n_4 = \frac{\dot{V}_4}{V} = \frac{130,8}{363,2} = 0,36 \quad [1/h]$$

In Table 2 ACH test results are introduced in 17 tested homes in traditional brickwork houses.

TABLE 2.  
MEASURED  $n_{50}$  AND CALCULATED  $n_4$  ACH RATES IN THE TESTED APARTMENTS

No.	Year of construction	Type of object tested	C	n	$n_{50}$	$n_4$
			-	-	[1/h]	[1/h]
1	1900	House	96,9	0,563	7,75	1,87
2	1979	House	150,4	0,569	11,42	2,71
3	1979	House	243,9	0,595	7,23	1,61
4	1980	Room	6,0	0,632	1,10	0,23
5	1984	House	135,9	0,590	6,08	1,37
6	1985	Flat	87,5	0,649	4,85	0,94
7	1989	House	471,7	0,596	10,00	2,22
8	2002	House	24,5	0,596	2,41	0,54
9	2003	House	192,5	0,609	5,02	1,08
10	2004	House	64,1	0,664	2,48	0,46
11	2006	House	89,1	0,566	6,25	1,49
12	2008	House	162,9	0,601	8,10	1,52
13	2010	House	75,3	0,591	2,89	0,65
14	2011	House	57,7	0,636	3,19	0,64
15	2011	House	171,7	0,689	8,28	1,45
16	2011	House	53,1	0,650	1,86	0,36
17	2012	Room	15,0	0,628	3,49	0,72

It could be important to know that the expected 4 Pa spontaneous ACH can be determined quite precisely from the result of type “A” 50 Pa Blower Door ACH test results without forming any functions. For this purpose a comparison graph created to find out whether is there a good correlation between the tested  $n_{50}$  and calculated  $n_4$  values (see Figure 3.) using the results of Table 2.

The measured  $n_{50}$  and calculated  $n_4$  pairs of values plotted against each other, whereby a trend line is fitted indicating the equation describing the function concerned. Using this equation, any of  $n_4$  spontaneous ACH can be determined from the relevant  $n_{50}$  ACH test result. The high correlation coefficient  $R^2=0,9819$  suggests that the results can be considered quite reliable except some pieces of data points. These points out of a required narrow range also indicate that a more sophisticated test method is required to achieve more reliable values. However in case there are no other values available than  $ACH_{50}$  this method suggest better correlation than the equation specified in Standard EN ISO 13789, see below. (Please note, that this very simple method was specified by Sherman (1987) attributes to Kronvall and Persily as a rule of thumb.)

$$ACH \approx \frac{ACH_{50}}{20} [7]$$

The quite obvious advantage of this method is that the seasonal average over pressure is taken into account.

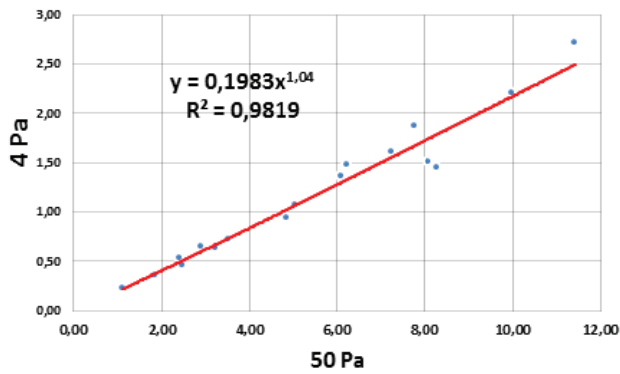


Figure 3.  $ACH_4$  values as a function of  $ACH_{50}$  ones

Results of the  $ACH_4$  values from tests compared to the calculated ones are shown in Figure 4. The highest differences between the calculated and measured values are 19% and -12%. The average of the absolute values of the differences is 7.4%

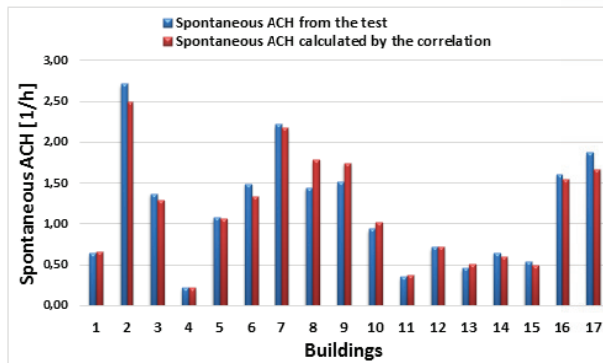


Figure 4. Comparison of spontaneous ACH and the calculated ACH rates

### III. DETERMINING SPONTANEOUS ACH BY TRACER GAS

Tracer gas tests were executed by an INNOVA 1412i Photoacoustic Gas Monitor of LumaSense Technologies. The gas chosen for the tests is Sulphur-hexafluorid ( $SF_6$ ). A specific characteristic of the test is that it is difficult to apply for measuring the ACH of multi-space buildings due to the lack of appropriate mixture of air. However, it is perfectly suitable for measuring the spontaneous ACH of a single space.  $SF_6$  gas is approximately 5 times heavier than air. Therefore during the test the appropriate mixing fan should be applied. The test cycles as a function of time and the evaluation is presented in Figure 5.

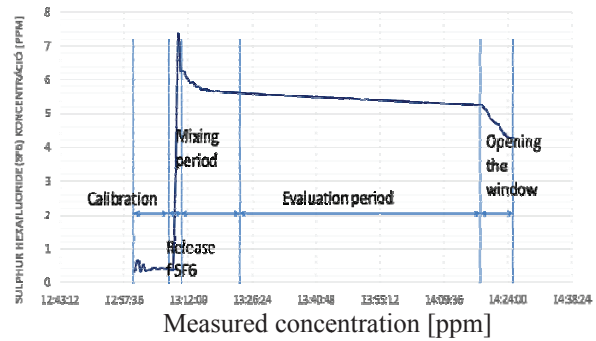


Figure 5. Procedure of a tracer gas test

The evaluable period of the change of gas concentration is shown in Figure 6.

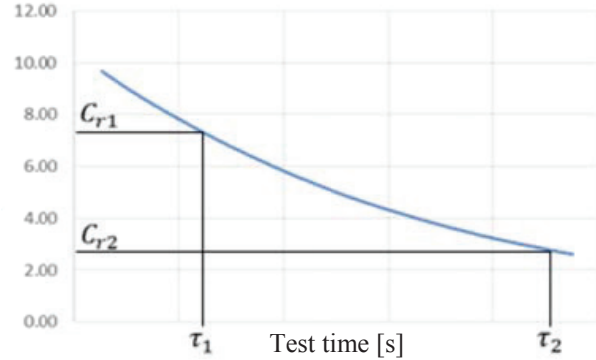


Figure 6. Evaluation method of tracer gas test

The spontaneous ACH can be calculated if concentration decline is divided by the time elapsed:

$$n = \frac{\ln(C_{r1}) - \ln(C_{r2})}{\Delta\tau} \left[ \frac{1}{h} \right] [2]$$

Where:

$C_{r1}$ : is the concentration at the beginning of the phase suitable for evaluation

$C_{r2}$ : is the concentration at the end of the phase suitable for evaluation

$\Delta\tau$ : is the time elapsed in between the two concentration values



#### IV. CORELATION BETWEEN BLOWER DOOR TYPE "A" AND TYPE "B" TEST RESULTS AT 50 PA

Blower Door Tests of both type "A" and "B" have been completed and the results compared. The summarized results are included in Table 3 and Figure 7.

Table 3. Blower Door Type "A" and Type "B" test results

no	Year of Construction	Type of object tested	A-type Blower Door $n_{50}$ ACH [1/h]	B-type Blower Door $n_{50}$ Air tightness [1/h]
1	1900	room	9,28	9,28
2	1979	house	11,42	10,11
3	1979	room	5,5	5,5
4	1979	room	6,0	6,0
5	1979	room	6,96	6,96
6	1980	room	1,1	1,1
7	1984	house	6,08	5,31
8	1984	flat	8,91	7,14
9	1989	house	10,0	10,0
10	2002	house	2,41	1,45
11	2004	house	2,48	2,4
12	2006	house	6,25	5,25
13	2008	house	8,1	6,92
14	2011	house	3,19	2,75
15	2011	house	1,86	1,38
16	2011	room	3,45	3,45
17	2012	room	3,49	3,49

Evaluating the results of the above table, it can be seen that if air tightness or ACH measures were completed only for one room, generally the results reveal no difference. The reason for this fact is that in traditional rooms usually there are not further vents of fans, not even a chimney. The only opening is the window. See the results in bar chart in Figure 7.

Traditional rooms usually have a chimney causing difference between the results of Type A and Type B tests, but there are exceptions in cases where there is a central heating installed from the beginning. There are very few cases where there is no chimney in the whole house since the boiler is outside of the heated area.

Concentrating to the cases where there are differences between types "A" and "B" test results a quasi-correlation is found. (See Figure 8.) The correlation coefficient is very high  $R^2=0.9893$  indicating good correlation between Type A and Type B test results.

However, it is important to point out that there are several factors influencing the test results e.g. the shape and size of the openings that can result in significant differences compared to the determined equation. The number of samples is too small for a high confidence.

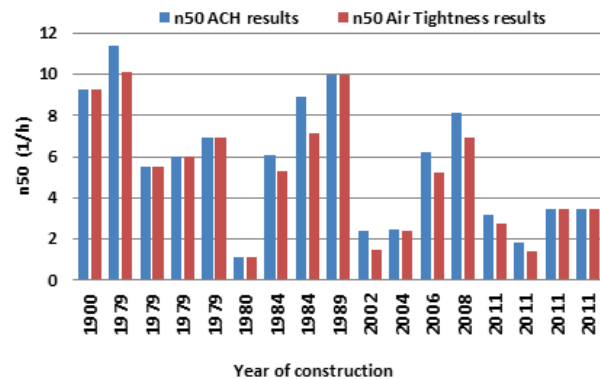


Figure 7. Blower Door Type "A" (ACH) and Type "B" (Air Tightness) test results

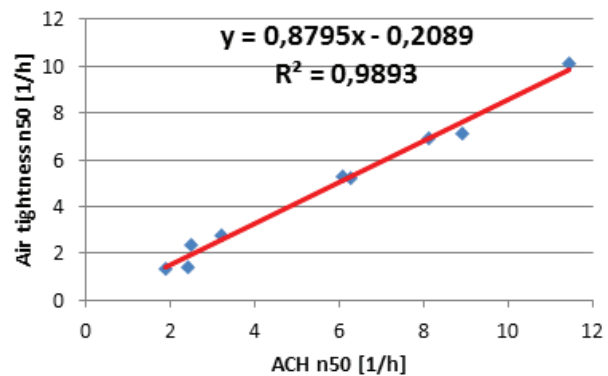


Figure 8. Comparison of Blower Door Type "A" (ACH) and Type "B" (Air Tightness) test results

#### V. ACKNOWLEDGMENT

Acknowledgement for EU Hungary-Croatia IPA (Instrument for Pre-Accession Assistance) Cross-border Co-operation Programme for funding the project including the equipment procurements and man power.

#### VI. REFERENCES

- [1] Fülöp László, Željko Koški, Irena Ištoka Otković, Hrvoje Krstić, Magyar Zoltán, Martina Španić: Helyiségek légtömörség vizsgálata energetikai és komfort szempontból. Air Tightness, HUHR/1001/2.1.3/0009 projekt kiadvány, 2013.
- [2] Polics György PTE-PMMIK ÉG Tanszék, A mérési eredmények összefoglalása és összehasonlítása. Air Tightness, HUHR/1001/2.1.3/0009 projektzáró konferencia előadása. 2013.06.27-28.
- [3] United Nations Development Programme - UNDP, Handbook for Energy Certification in Buildings, Zagreb, 2010
- [4] Age distribution of housing stock, Housing Statistics in the European Union 2010
- [5] Lenkovics László PTE-PMMIK ÉG Tanszék, A blower door légtömörség mérési eredményei Magyarországon. Air Tightness, HUHR/1001/2.1.3/0009 projektzáró konferencia előadása. 2013.06.27-28.
- [6] Luftdichte Projektierung von Passivhausen, CEPHEUS, Passivhaus Institut, 2002.
- [7] Standard EN ISO 13789
- [8] Nyers J., Kajtar L., Tomic S., Nyers A.: "Investment-savings method for energy-economic optimization of external wall thermal insulation thickness". International J. Energy and Buildings. Vol. 86, pp. 268–274, 2015.  
DOI.org/10.1016/j.enbuild.2014.10.023

# Maximal and Optimal DHW Production with Solar Collectors for Single Family Houses

Miklós Horváth\*, Tamás Csoknyai \*

\* Budapest University of Technology and Economics/Department of Building Services and Process Engineering,  
Budapest, Hungary  
[horvath@epgep.bme.hu](mailto:horvath@epgep.bme.hu)  
[csoknyaitamas@gmail.com](mailto:csoknyaitamas@gmail.com)

**Abstract** — The energy performance of newly erected buildings has radically improved in the last decade in Europe. The process will continue in the following years. It is partly induced by the 2010/31/EC directive [1] on the energy performance of buildings. The directive prescribes that all new communal buildings erected after 2019 and all communal and residential buildings after 2021 have to be built as nearly zero energy buildings (NZEB). The directive also requires that the energy demand of NZEB buildings have to be covered to a very significant extent by on-site or nearby renewable energy sources. Thus, the better knowledge on low and nearly zero energy buildings and integration of renewable energies are key issues nowadays. These buildings have some special characteristics compared to traditional buildings, therefore they require a special, more detailed modeling approach.

## I. INTRODUCTION

The utilization of solar energy in low energy buildings is fundamental due to the strict energy regulations, which favor the use of on-site or nearby produced renewable energy. Our paper focuses on solar energy utilization, which is a technically achievable option in most of the cases. There are two main ways to utilize solar energy. The first way is the passive use, which means that incoming energy is passively used for space heating. The second way is the active utilization, which means that an energy collecting device such as solar collector or PV panel is used. During the design process of a building it is important to accurately estimate the available solar energy, thus the energy demand for heating and cooling can be minimized and the energy produced on site could be maximized considering economical aspects. In this paper the solar energy potential of active solar thermal systems are examined in case of a single family house. Not only the solar yield, but also heat demands and system losses are analyzed.

## II. MODELED BUILDING, METEOROLOGY AND CALCULATION METHOD

### A. Parameters of the modeled building

For this paper a typical, newly erected single family house was examined with three different orientations. The house fulfills the requirements of the Hungarian building code and also the energy requirements for NZEB buildings. The overall dimensions of the building are 18.75 x 8.5 m. The house is one storey high and has basement, where all HVAC appliances are placed. The basement is not heated, thus temperature varies

throughout the year. The building has a pitched roof which has a 40° slope. The layout of the building and the maximal possible solar collector arrays for different orientations are shown in Figure 1.

The building has three bedrooms, two bathrooms, a utility room and a combined kitchen with living room along with a small entrance hall and an office room. The domestic hot water (DHW) system was planned for the building. The internal dimension of the DHW pipes is 20 mm and the total length is 57.6 m. For family houses the usual DHW storage tank size was considered, thus a widely used DINOXD USW-2 300 l tank was selected, covered with 10 cm heat insulation. The schematic illustration of the solar collector system is shown in Figure 2.

In the paper the maximal possible solar collector area was determined for the building, although this is economically not a viable solution. However in order to indicate the maximal possible energy production for single family houses this option should also be examined. For this case not only DHW demand and losses were taken into account as demand, but also the heating energy demand was considered. In case of NZEB buildings the usual values in Central-Europe for heating energy demand are 15 – 30 kWh/(m<sup>2</sup>year). Although in Hungary the national regulation (based on the 2010/31/EC directive [1]) gives a definition for the NZEB building, in our paper a broader approach was applied. For the performed calculations heat demand of 15 and 30 kWh/(m<sup>2</sup>year) were taken into account.

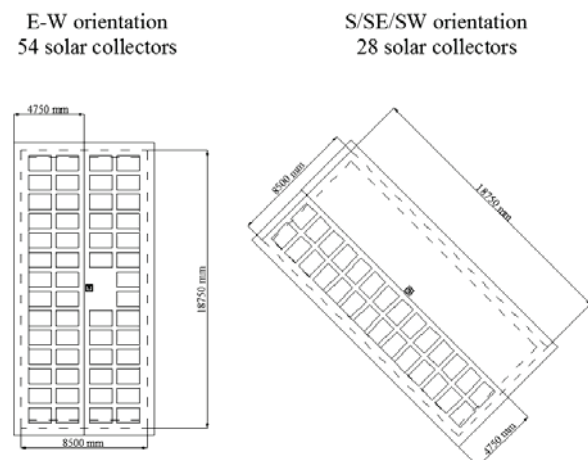


Figure 1. Layout of the building and the collector arrays for different orientations

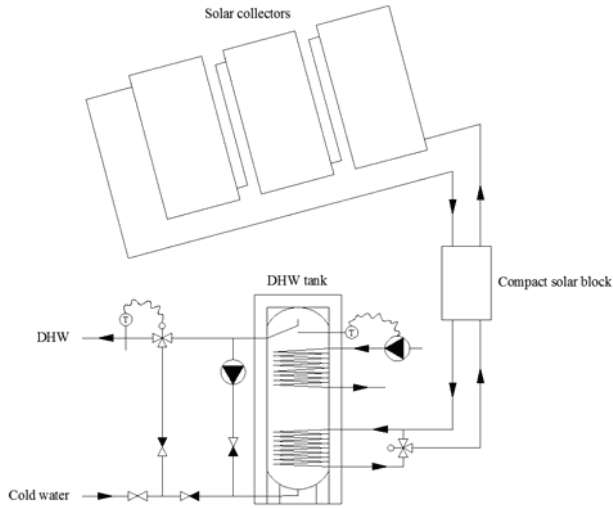


Figure 2. Schematic illustration of the solar collector system

### B. Meteorological parameters building site, estimation of available solar radiation

The meteorological parameters for buildings basically depend on the building site. In this paper, the building was placed in the suburbs of Budapest. For the calculations two basic meteorological parameters, the monthly average of external temperature and the sum of global solar radiation are required. The average external temperature was calculated for the time period between 1981 and 2000, which data were taken from the Hungarian Meteorological Service database [2]. The incoming solar radiation was calculated based on sunny hours measurement data which was taken from the CarpatClim database, and the considered time period was from 1981 to 2010 [3]. There are several models to calculate solar radiation, from which 11 were compared in [4]. In the paper the models were examined for South orientation with 40° tilt angle. The models were compared at 4 different sky condition and the “relative performance of the individual models was determined by a combination of both statistical and graphical analysis.” In the paper it was concluded, that the Hay model was performing “best under all sky, clear and partially cloudy conditions”. According to the conclusions of model comparison in [4] the radiation calculations were performed with the Reindl et al. model [5], which is the improved version of the Hay model. In this model the global radiation is calculated as the sum of direct, diffuse and reflected radiation. In the model diffuse radiation consist of three parts:

- diffuse radiation from the sky dome
- circumsolar diffuse radiation
- diffuse radiation from the horizon.

The incoming radiation calculations were performed for every 15 minutes and the results were summed for each month of the year. The calculated monthly global radiation and average temperature for the building site is presented in Table 1. In the Reindl et al. model for monthly global solar radiation there is no difference between the calculated values for East and West and values for Southeast and Southwest oriented surfaces, due to the fact that the model is symmetric to the middle of the day. Thus, in case of east and west orientation the only

difference in the global radiation is just in the time when it occurs during the day. For this reason, for the further calculations these orientation differences were not examined.

Table 1. Monthly values of monthly global radiation and average temperature

	$Q_{sol}$ [kWh/(m <sup>2</sup> month)]			$T_{i,e}$ [°C]
Orientation	E/W	SE/SW	S	-
Jan.	35.8	53.5	62.5	0.6
Feb.	52.7	73.6	83.6	2.2
Mar.	89.8	111.7	119.9	6.6
Apr.	126.0	142.3	144.5	11.9
May	160.6	167.3	163.5	17.0
June	167.1	167.1	160.7	19.8
July	175.4	178.9	172.8	22.1
Aug.	157.7	174.6	174.3	21.8
Sept.	111.7	137.7	145.7	17.1
Oct.	74.4	103.5	116.9	11.7
Nov.	39.7	58.6	68.0	5.4
Dec.	28.5	42.7	49.8	1.7

### C. Calculation of energy demand and losses of the DHW system, and the estimated heating demand

DHW demand for the building was calculated based on the number of inhabitants: four inhabitants were considered which represent an average family. The energy demand calculations were based on the idea in [6]. The temperature of the DHW for the calculations was 50 °C, the cold water temperature was 11.6 °C, which is the yearly average temperature of the building site. The considered daily DHW consumption was 50 l/person, which is the standard value for Hungary. The DHW demand was calculated as in (1).

$$Q_{DHW} = c_w \cdot \rho_w \cdot (n_{pers} \cdot V_{DHW}) \cdot (T_{DHW} + T_{cw}) / 3600 \quad (1)$$

where:

- $Q_{DHW}$  – is the DHW demand [kWh/month]
- $c_w$  – is the specific heat of the water [kJ/(kgK)]
- $\rho_w$  – is the density of water [kg/m<sup>3</sup>]
- $n_{pers}$  – is the number of inhabitants [-]
- $V_{DHW}$  – is the monthly DHW demand [m<sup>3</sup>/person]
- $T_{DHW}$  – is the temperature of the DHW [°C]
- $T_{cw}$  – is the temperature of the cold water [°C]

For the DHW distribution the pipes were planned inside the floor in a protective tube without any insulation. The heat loss of pipes were calculated for different pipe depth and floor types and also for different temperature differences. As an average result 7 W/m was obtained as a specific heat loss for the distribution pipes. This result is applied for the whole building, regardless of the depth of the pipe and the floor type. In the building no circulation was planned, thus it was assumed that only in one fourth

of the day has distribution heat losses. This assumption was made due to the fact that in the rest of the day there is no DHW use. The distribution losses were calculated according to (2).

$$Q_{DIST} = l_{pipes} \cdot q_{pipes} \cdot \tau_m \cdot / 4 / 1000 \quad (2)$$

where:

- $Q_{DIST}$  – is the distribution loss [kWh/month]
- $l_{pipes}$  – is the total length of the pipes [m]
- $q_{pipes}$  – is the specific loss of the pipes [W/m]
- $\tau_m$  – is the number of hours in the month [h/month]

The specific heat loss of the storage tank was determined for the chosen DHW tank, the calculated value was 1.5 W/K. In order to determine the storage losses the monthly average temperature of the unheated basement had to be determined. The inner temperature of the basement was calculated for -13 °C and 36 °C external temperatures. Between the calculated values relationship is linear. The temperature of the basement was calculated for every month according to the average external temperature. The storage loss was calculated monthly according to (3).

$$Q_{STOR} = q_{storage} \cdot (T_{DHW} - T_{basement}) \cdot \tau_m / 1000 \quad (3)$$

where:

- $Q_{STOR}$  – is the storage loss [kWh/month]
- $q_{storage}$  – is the specific loss of the pipes [W/m]
- $T_{DHW}$  – is the temperature of the DHW [°C]
- $T_{basement}$  – is the temperature of the basement [°C]

The total energy demand was calculated as the sum of the DHW demand and the distribution and the storage losses. The monthly heating demands were also calculated. The degree days for each month were calculated and the yearly demand was distributed accordingly. The calculated DHW demand and losses, along with the heating demand are presented in Table 2.

Table 2. Calculated energy demand of the DHW system and heating per building area [kWh/(m<sup>2</sup>year)]

	$Q_{DHW}$	$Q_{DIST}$	$Q_{STOR}$	$Q_{DEMAND}$	$Q_{H15}$	$Q_{H30}$
Jan.	1.739	0.235	0.275	2.250	3.021	6.041
Feb.	1.571	0.213	0.245	2.028	2.506	5.011
Mar.	1.739	0.235	0.259	2.234	2.088	4.175
Apr.	1.683	0.228	0.236	2.147	0.607	1.214
May	1.739	0.235	0.230	2.205	0	0
June	1.683	0.228	0.215	2.127	0	0
July	1.739	0.235	0.217	2.191	0	0
Aug.	1.739	0.235	0.217	2.192	0	0
Sept.	1.683	0.228	0.223	2.134	0.443	0.886
Oct.	1.739	0.235	0.245	2.220	1.298	2.595
Nov.	1.683	0.228	0.254	2.165	2.199	4.398
Dec.	1.739	0.235	0.272	2.247	2.839	5.679
Year	20.5	2.8	2.9	26.1	15.0	30.0

#### D. Monthly energy yield of solar collectors, maximal and optimal case

To calculate the energy yield of solar collectors the previously described meteorological data and calculated DHW system parameters and monthly heat demand were used. For the calculation a widely used solar collector type, a Thermosolar TS 300 was considered. The energy yield of the solar collectors was calculated according to [7], however some additional data from [8] was also used. For the calculations the following collector and system parameters were used (Table 3):

Table 3. Solar collector and system parameters

Parameter	Value
$\eta_0$	0.8177
$k_1$	3.65
$k_2$	0.009
$K_{dir}(50^\circ)$	0.95
FR	0.95
FR'/FR	0.8
$T_{ref}$	100 °C

With the previously described input parameters the energy yield of solar collectors were calculated. In (4) the temperature correction, in (5) the storage capacity correction was calculated.

$$\frac{X_{c1}}{X} = \frac{(11.6 + 1.18 \cdot T_{DHW} + 3.86 \cdot T_{cw} - 2.32 \cdot T_{i,e})}{(T_{ref} - T_{i,e})} \quad (4)$$

where:

- $X_{c1}/X$  – is the temperature correction factor [-]
- $T_{i,e}$  – is the monthly average temperature [°C]
- $T_{ref}$  – is the reference temperature [°C]

$$\frac{X_{c2}}{X} = \left( \frac{V_{t,a}}{V_{t,opt}} \right)^{-0.25} = \left( \frac{0.7 \cdot V_t}{0.075 \cdot A_{coll}} \right)^{-0.25} \quad (5)$$

where:

- $X_{c2}/X$  – is the storage size correction factor [-]
- $V_{t,a}$  – is the active storage capacity [m<sup>3</sup>]
- $V_{t,opt}$  – is the optimal storage capacity [m<sup>3</sup>]
- $V_t$  – is the total storage capacity [m<sup>3</sup>]
- $A_{coll}$  – is the total collector area [m<sup>2</sup>]

The monthly solar fraction was calculated according to (6) with the use of (7), (8) and (9).

$$f_i = MIN \left( \frac{1.029 \cdot Y - 0.065 \cdot X_c - 0.245 \cdot Y^2 +}{+ 0.0018 \cdot X_c^2 + 0.0215 \cdot Y^3; 1} \right) \quad (6)$$

$$Y = \eta_0 \cdot Q_{sol} \cdot FR' / FR \cdot K_{dir}(50^\circ) \cdot A_{coll} / Q_{DEMAND} \quad (7)$$

$$X_c = X \cdot (X_{c1} / X) \cdot (X_{c2} / X) \quad (8)$$



$$X = \left( \frac{(FR \cdot k_1 + FR \cdot k_2 \cdot (T_{DHW} - T_{i,e})) \cdot FR' / FR \cdot (T_{ref} - T_{i,e}) \cdot \tau_m \cdot A_{coll} / Q_{DEMAND}}{1000} \right) \quad (9)$$

where:

- $f_i$  – is the monthly solar fraction [-]
- $\eta_0, k_1, k_2, K_{dir}(50^\circ)$  – are collector parameters [-]
- $FR, FR', T_{ref}$  – are solar system parameters [-]
- $Q_{DEMAND}$  – is the total energy demand of the DHW system [kWh/month]

The energy produced by solar collectors are calculated for every month as in (10)

$$Q_{coll} = f_i \cdot Q_{DEMAND} \quad (10)$$

The calculations were performed for three separate cases. In the first case the total roof area was covered with solar collectors as shown in Figure 1. In this case the produced thermal energy was calculated for three options. In the first option only the DHW demand was supplied by the solar collector system, in the second and third options both DHW and heating demand was supplied. The only difference between these options was the heating demand, as in one case it was 15 (H15) and in the other it was 30 (H30) kWh/(m<sup>2</sup>year).

For the second case only the DHW system's demand was taken into consideration. In this option the number of collectors were reduced to the amount which is necessary to still achieve the value of 1 for the yearly solar fraction with maximal system efficiency. In this case only the DHW system's demand was considered as thermal energy demand.

The third case was an optimized case, for which the system was designed for an economically feasible solution: acceptable solar fraction at affordable cost. The following boundary conditions were made:

- the number of collectors has to be an integer
- the annual system efficiency ( $\eta_{system}$ ) is maximal
- the monthly solar share has to be greater than 0.9 and less than 0.95 in June, July and August.

In this option only the DHW demand was supplied by the solar collector system, and the optimization was made for only this option.

### III. RESULTS OF THE CALCULATIONS

The results of performed calculations for separate cases are presented in Table 4. In the first case for South and Southeast/Southwest orientations there are 28 collectors placed on the building, in case of the East/West orientation 54 ( $A_{coll}=1.78$  m<sup>2</sup> per piece). From the table it is clearly visible, that in the first case the total DHW demand of the house can be supplied, however with just a really low system efficiency. If solar collectors are used for space heating as well, it can be stated, that in case of South and Southeast/Southwest orientations the energy demand cannot be supplied only by solar collectors throughout the year. In case of the East/West oriented

building enough solar collectors can be placed on the roof to supply the DHW and heating energy demand of the building. This is due to the fact that in case of East/West oriented building the maximal number of placed collectors is nearly the double of what can be placed in the other examined orientations.

In the second case, when the number of collectors were reduced, it can be seen that without reducing solar fraction the number of collectors can be reduced by at least 42.9%, and the system efficiency can be increased from 3.92-7.55% to 10.44-13.9%.

In the third case the rational optimization of solar collectors is done. By this optimization process, optimal number of collectors were determined for all three orientations. In every case the optimal number of collectors were 3. This means that the number of collectors were reduced from the first case by 89.3% and 94.4% and compared to the second case by 81.3% and 85.7%. System efficiency is the highest in this case due to the fact that this case has the lowest collector area, thus the smallest amount of incoming solar energy but the DHW system's demand is the same in all cases. The number of collectors for each case are presented in Figure 3.

For the optimal case the monthly results for different calculations are presented in Figure 4, Figure 5 and Figure 6. From these diagrams it is clearly visible that in summer, regardless of the orientation, 90% of the DHW system's demand is covered. The orientation differences are significant in winter, when the East/West oriented collectors barely operate, while in case of the other orientations still at least 10% of the DHW demand can be supplied.

Table 4. Calculated results for the different cases ( $A_{coll}=1.78$  m<sup>2</sup>)

Case	Collector array, supplied system(s)	Orientation	Nr. of coll.	$f_i$	$\eta_{sys}$
I.	Maximal, DHW	S	28	1	7.55
		SE/SW	28	1	7.55
		E/W	54	1	3.92
	Maximal, DHW+H15	S	28	0.992	12.69
		SE/SW	28	0.976	12.20
		E/W	54	1	6.72
	Maximal, DHW+H30	S	28	0.846	11.89
		SE/SW	28	0.814	10.63
		E/W	54	1	9.53
II.	Maximal optimized, DHW	S	16	1	13.90
		SE/SW	16	1	13.22
		E/W	21	1	10.44
III.	Optimal, DHW	S	3	0.624	35.17
		SE/SW	3	0.596	32.41
		E/W	3	0.503	24.98

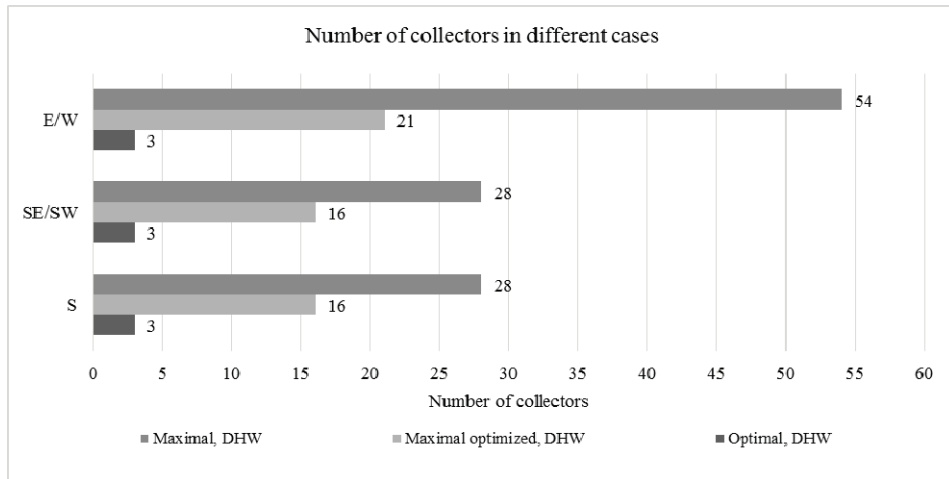


Figure 3. The number of collectors in different cases

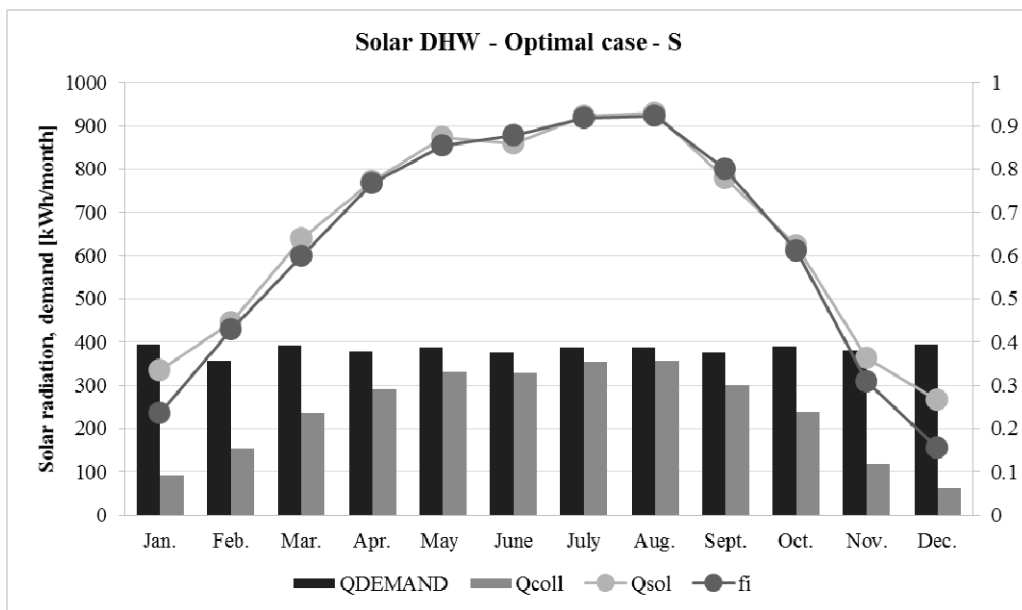


Figure 4. Monthly results for South oriented building with optimized number of collectors

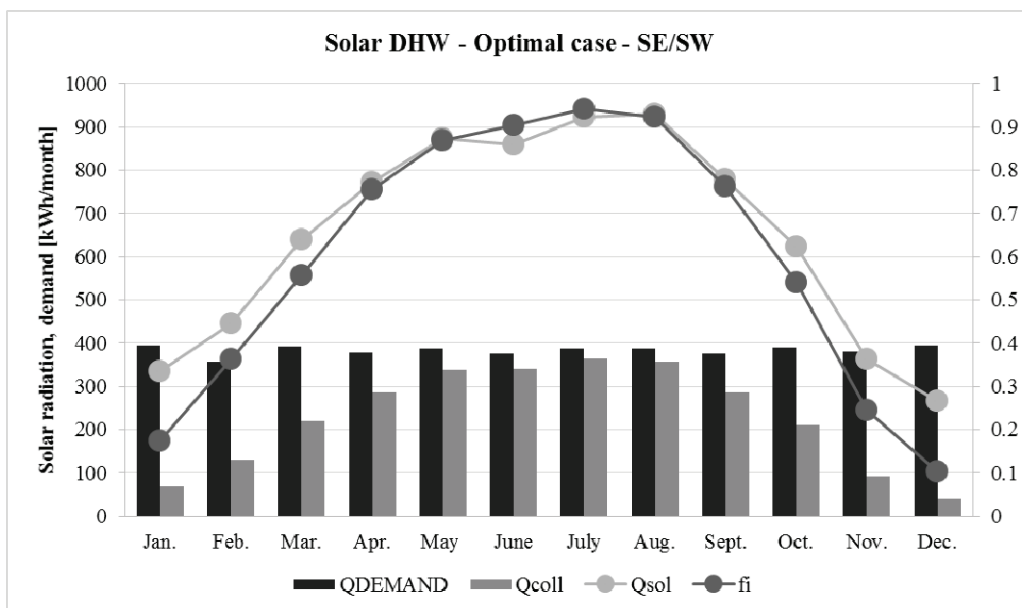


Figure 5. Monthly results for Southeast/Southwest oriented building with optimized number of collectors

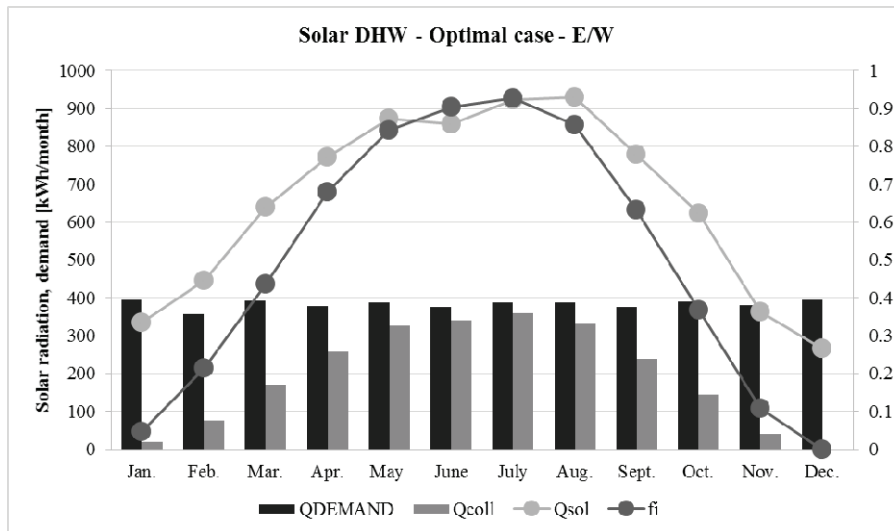


Figure 6. Monthly results for East/West oriented building with optimized number of collectors

#### IV. CONCLUSION

In the paper three different solar collector arrays were examined for a single family house. In the first case the total roof area was covered with collectors and the produced thermal energy was calculated for three different demands. In the second case the number of solar collectors were determined which are able to fulfill the DHW demand throughout the year. In the third case the optimization of the collector number was performed with the following boundary conditions: the system efficiency has to be highest for the year and the solar fraction in the summer months have to be higher than 90%.

In the second case when the number of collectors were reduced it can be concluded that in any orientation from East to West the number of collectors can be reduced by at least 42.9%. The system efficiency is increasing in this case from 3.92-7.55% to 10.44-13.9% and the investment costs decrease due to the lower number of panels.

In the third case the rational optimization of the solar collectors are done. By this optimization process the optimal number of collectors were determined for all three orientations. In every case the optimal number of collectors were 3. This means that the number of collectors were reduced, compared to the first case by 89.3% and 94.4% and compared to the second case by 81.3% and 85.7%. In this case the total solar coverage is not achieved, but the investment costs are drastically lower compared to the other cases.

#### REFERENCES

- [1] Directive 2010/31/EU of the European Parliament and of the Council of 19 May 2010 on the energy performance of buildings (recast)
- [2] URL: [http://www.met.hu/eghajlat/eghajlati\\_adatsorok/bp/Navig/Index2.htm](http://www.met.hu/eghajlat/eghajlati_adatsorok/bp/Navig/Index2.htm)
- [3] URL: <http://www.carpatclim-eu.org/pages/download/>
- [4] Efim G. Evseev, Avraham I. Kudish: The assessment of different models to predict the global solar radiation on a surface tilted to the south. *Solar Energy* 83, 377–388. 2009.
- [5] Reindl, D.T., Beckman, W.A., Duffie, J.A.: Evaluation of hourly tilted surface radiation models. *Solar Energy* 45, 9–17. 1990.
- [6] Szánthó Z., Némethi B., 2007. Measurement Study on Demand of Domestic Hot Water in Residential Buildings Proceedings of the 2<sup>nd</sup> IASME/WSEAS International Conference on Energy & Environment, pp. 68-73. Portorose, Slovenia, 15-17<sup>th</sup> May 2007. ISSN:1790-5095
- [7] S. A. Klein, W. A. Beckman, J. A. Duffie: A design procedure for solar heating systems. *Solar Energy* 18, 113-127. 1976.
- [8] John A. Duffie - William A. Beckman: *Solar Engineering of Thermal Processes*, Fourth Edition 2013. ISBN 13-978-471-69867-8
- [9] S. Armstrong, W. G. Hurley: A new methodology to optimise solar energy extraction under cloudy conditions. *Renewable Energy* 35., Issue 4., 780-787. 2010

# Sizing methods of domestic hot water recirculation systems

Kristóf Hargita\*, Zoltán Szánthó\*

\*Department of Building Service and Process Engineering, Budapest University of Technology and Economics, Hungary

[hargita.kristof@gmail.com](mailto:hargita.kristof@gmail.com), [szantho@egt.bme.hu](mailto:szantho@egt.bme.hu)

**Abstract**— the most common solution to ensure appropriate temperature at the taps in domestic hot water (DHW) systems, is to build a recirculation system. The annual heat consumption of DHW in modern buildings can exceed the heating's; in this heat consumption the heatloss of DHW system represents a vast majority. One mean of reducing losses could be the application of pipe in pipe recirculation. We've developed a sizing method for these systems. In a case study, we've investigated the costs of regular and 'pipe in pipe' setups, applying both the demanding German standard and the Hungarian practice of heat insulations. The cost of heat loss over the systems lifetime exceeds many times the investment cost of the insulation; it does not worth saving on it. Applying inline construction can decrease the operating costs as well, so it worth to take the additional investment costs.

## I. THE IMPORTANCE OF DHW RECIRCULATION SYSTEMS

In spacious buildings that have central DHW production and supply system, it can be of concern that after consumption pauses, opening a tap far from the DHW producing appliance, it takes a long time for the flow to reach the tap with its nominal temperature. The reason is that hot water – contained by the pipe before the consumption pause – cools down during the pause. This phenomenon causes several problems. First, from the aspect of comfort it is unpleasant, that the user has to wait for the cold water to leave the system. This could take a minute, even in a smaller residential household. Second, it is a waste of water and energy, thus, unnecessary cost. Third, it is hygienically objectionable, as stagnant water is present in the system for a longer period with appropriate temperature for bacterial growth (mainly legionella in drinking water systems). Releasing this fluid can endanger the consumer's health. Installing a central DHW recirculation system could give a solution to above problems. It keeps the water running continuously in the building, at the cost of heat and pumping energy.

Nowadays the enhanced thermal protection of buildings is of great importance. Accordingly, the heating energy consumption is drastically reduced, while the heat and electrical energy demands of DHW production and supply system stay at the same level. Figure 1. shows the heat demand of DHW production and heating, in an apartment house, depending on the number of apartments, along with the former and the present standards of thermal protection. Apparently, in buildings with proper insulation, the energy need of DHW deserves as much attention as of heating.

## II. BUILDUP TRADITIONS

In Hungarian practice, insufficient attention is paid on planning and operating of DHW systems. When designing, no detailed calculations are carried out neither for DHW consumption demands, nor for the dimensions of the DHW producing appliance and supply. In order, to make sure, that no consumer's complaint occurs, the equipments are significantly oversized and for this reason unrealistically high operational costs may present. In addition, the ill-considered designing method results in the following three syndromes, which together guarantee the high operational cost.

The pipes and elements of the system are fitted with heat insulation, with insufficient wall thickness (in Hungarian practice it is usually 13 mm). On one hand, this causes a slight decrease of investment cost, on the other hand, the heat losses are going to be relatively significant.

In the supply and the recirculation system, the hydraulic balance must be created. The common absence of this results that the flow increases on the shorter paths, while

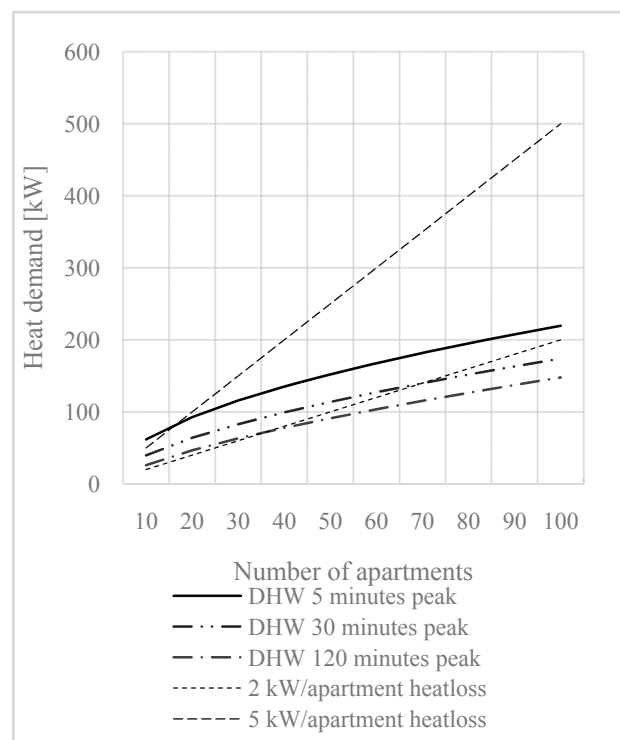


Figure 1. Heat demand for heating and produce of DHW



while decreases on the longer. In case of extreme cases, the flow could stop. The situation becomes even more serious by the fact, that in DHW recirculation systems higher flowrate would be needed on the longest, and lower on the shortest path, as the heat loss of pipes is replaced by the flow.

Since no sizing is made to determine heat losses and flowrates, worst case scenario the network is not balanced, in order to exclude consumer complaints, the recirculation pump will be oversized. This phenomenon may cause concerns later as well, when the supply system is properly insulated and balanced, so lower flowrate would be satisfying, but the circulation of this, with the earlier chosen pump is only possible at an inefficient operating point.

### III. SIZING METHODS FOR RECIRCULATION SYSTEMS

In Europe, for sizing DHW recirculation systems, the German standards and regulations are determinative. Earlier in Germany, the recirculation systems were designed by the DVGW W553 worksheet [1]. This defines for large systems a “detailed” and a “simplified” method, which are alternatives to each other. Applying the simplified method the main flowrate is calculated from the heat losses of the DHW supply system, assuming 2 K temperature drop from the starting point towards the taps. Since 2012 the sizing of DHW recirculation systems are regulated by the standard DIN1988-300:2012 [2] in Germany. The method is based on the W553, but it contains an innovation, the concept of the ‘admixture number’, which gives the possibility to determine the division of the main flowrate in another way. This way a better hydraulic resistance can be accomplished, while the criteria – that the temperature should not fall below a critical value of 55 °C after the DVGW W551 [3] – is realized. The hydraulic balance should be obtained in the system by both procedures.

Note that in Germany a standard exists about the proper thickness of heat insulation around pipes in HVAC systems. Earlier that was regulated by the “Heizungsanlagen-verordnung”, nowadays by the EnEV regulation. Essentially, it says that the pipe should be covered with the insulation having the wall thickness equal to the pipe diameter. By investigating the ASHRAE and ASPE [4][5] regulations, it could be seen, that they are not as sophisticated as the German standards. They only define some empirical number for heat losses, and a formula for calculating flow rate.

### IV. PIPE IN PIPE RECIRCULATION

By applying pipe in pipe recirculation by risers, an inner pipe is inserted to the DHW pipe, in which the recirculation flow comes back. The difficulty of this setup is that at the bottom of the riser the inner pipe has to be led out, and at the top of the riser the two pipes need to be hydraulically connected. Figure 2. shows a product of a specific manufacturer, but other solutions might be just as good. The material of the inner pipe is preferably some polymer, in order to maintain flexibility. There is a possibility to carry out 45° change of direction.

The benefits of the inline recirculation by riser are, that it demands less space, less wall and balk break-through, less and dimensionally smaller pipe, insulation and

banding. Besides, the heat loss of the system is significantly

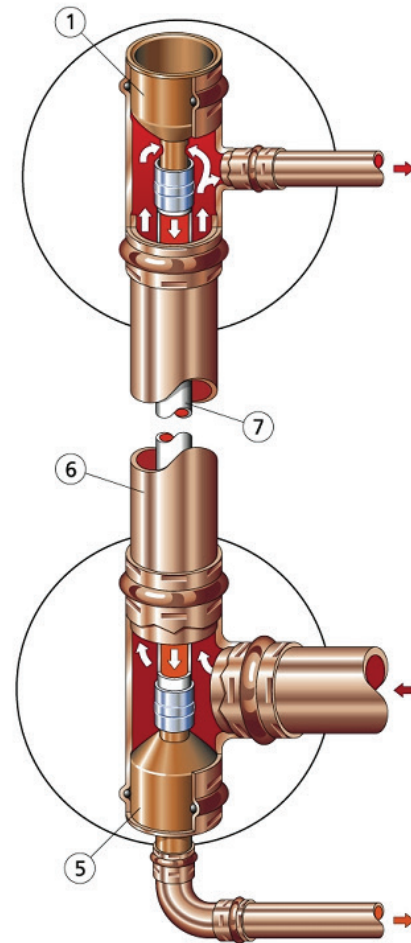


Figure 2. Pipe in pipe recirculation riser

lower, hereby the pump flow drops down as well. The disadvantage of the inline system is that special connectors are needed, which are not available for galvanized steel pipe systems. In case the system is constructed of a modern pipe system with press technology, from copper or stainless steel, the additional cost of these elements are relatively low. In Hungary it is not known, that a system like this had been carried out, probably as the specialty of it is believed to be too expensive.

We have established the mathematical model of an inline riser, refinements to German literature [6] and [7]. Consequently we have determined a design method for a complete system [8]. The processes taking place in the system are more complicated, than in the regular recirculation system, therefore the method is more complicated; it requires iteration.

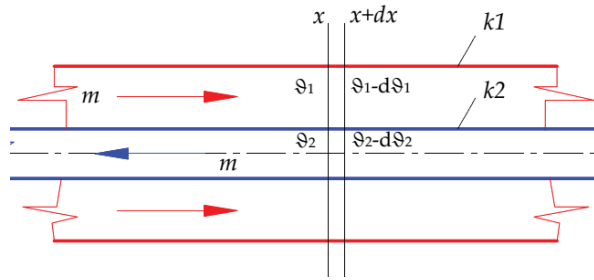


Figure 3. Mathematical model of an inline recirculation riser

#### V. MATHEMATICAL MODEL

Figure 3 shows the mathematical model of an inline riser. To determine the temperatures, we had to write two differential heat balances, one to the space between external and inner pipe, and the second one to the inner pipe.

$$\begin{aligned} \dot{m} \cdot c \cdot d\vartheta_1 &= -k_1 \cdot \vartheta_1(x) \cdot dx - \\ &\quad -k_2 \cdot (\vartheta_1(x) - \vartheta_2(x)) \cdot dx \end{aligned} \quad (1.)$$

$$-\dot{m} \cdot c \cdot d\vartheta_2 = k_2 \cdot (\vartheta_1(x) - \vartheta_2(x)) \cdot dx \quad (2.)$$

where:

$\dot{m}$ : flowrate of the riser [kg/s]

$c$ : specific heat of water [kJ/(kg K)]

$d\vartheta_1$ : cooling of water in the DHW pipe on a „dx” long section [°C]

$d\vartheta_2$ : cooling of water in the recirculation pipe on a „dx” long section [°C]

$k_1$ : heat transfer coefficient between DHW and ambience [W/mK]

$k_2$ : heat transfer coefficient between DHW and recirculation water [W/mK]

$\vartheta_1$ : temperature difference between DHW and ambience, on a „dx” long section

$\vartheta_2$ : temperature difference between recirculation water and ambience, on a „dx” long section

Equation 1. is the heat balance for the external pipe. It expresses that during the fluid's cooling period the heat flows into the inner pipe and to the ambience. Equation 2. refers to the “negative cooling” of the fluid, which gets the heat flow from the external pipe. To solve the differential equation system, we needed boundary conditions:

$$\vartheta_1(x = 0) = \vartheta_{10}. \quad (3.)$$

$$\vartheta_1(x = L) = \vartheta_2(x = L). \quad (4.)$$

where:

$L$ : length of the riser [m]

$\vartheta_{10}$ : riser inlet point ( $x=0$ ) the temperature difference between the DHW and the ambience [°C]

Equation 3. gives the inlet temperature of the riser, while Equation 4. refers to the fact, that temperatures are equal in the external and inner pipe at the end of the riser. To solve the equation system we needed to arrange them into a matrix form, and we replaced the constants with a constant matrix.

$$\begin{bmatrix} \vartheta_1' \\ \vartheta_2' \end{bmatrix} = \begin{bmatrix} -K_1 & K_2 \\ -K_2 & K_2 \end{bmatrix} \begin{bmatrix} \vartheta_1 \\ \vartheta_2 \end{bmatrix} \quad (5.)$$

The universal solution for this:

$$\underline{\vartheta} = C_1 \cdot e^{\lambda_1 x} \cdot \underline{s}_1 + C_2 \cdot e^{\lambda_2 x} \cdot \underline{s}_2 \quad (6.)$$

, where:

$C_1$ : first integration constant

$C_2$ : second integration constant

$\lambda_1$ : first eigenvalue of the matrix  $\underline{K}$

$\lambda_2$ : second eigenvalue of the matrix  $\underline{K}$

$\underline{s}_1$ : first eigenvector of the matrix  $\underline{K}$ :  $\underline{s}_1 = \begin{bmatrix} s_{11} \\ s_{12} \end{bmatrix}$

$\underline{s}_2$ : second eigenvector of the matrix  $\underline{K}$ :  $\underline{s}_2 = \begin{bmatrix} s_{21} \\ s_{22} \end{bmatrix}$ .

The integration constants may be calculated from the boundary conditions.

A riser consists of several sections, which have different geometries, thus, they have different heat transfer attributes. Therefore, it has become necessary to write differential equations to every section. With the help of boundary conditions we have connected the systems to each other, and it became possible to determine the deviation of temperatures (see Figure 4.).

It is not sufficient to design a whole system, to know how temperatures turn out on a single riser. We have to calculate flow rates on every section, in compliance with the criterion that the temperature can not drop under a minimum value. For this task we have developed an iterator program in Wolfram Mathematica [9], which solves the systems of differential equations, and calculates the temperatures in the system. The block diagram of the iteration is shown on Figure 5.

We start the iteration with an  $\dot{m}^{(0)}$  unrealistically high main flow rate, so the cooling is very small on the system. Next we calculate the heat loss of every section, assuming, that the pipesystem has the same temperature as of water, and we divide the main flowrate by the ratio of the heat losses, the section's flowrates are  $\dot{m}_i$ . After this, it is possible to calculate the cooling on every section ( $T_{i,start}$  and  $T_{i,end}$ ). We lower the main flow rate by an adequately small value, and stop the cycle, if the temperature becomes lower than  $T_{min}$  anywhere in the system. When the cycle stops, we have the nominal flow rate for every section in the system, so the pressure drops and the balancing values may be calculated.

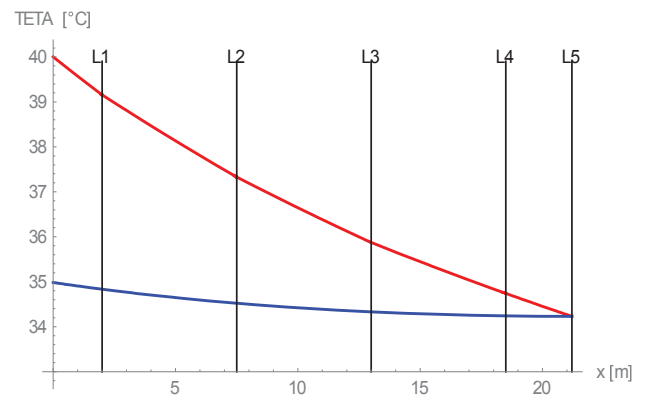


Figure 4. Temperatures of an inline recirculation riser

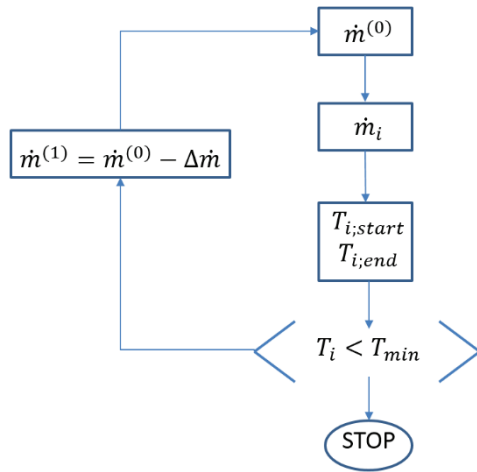


Figure 5. Block diagram for iterating the flow rates

Standards and regulations do not take into consideration the effect of convective heat transfer coefficient, they consider it with the value of infinity. If the flow velocity drops under drastically, the flow could change into laminar flow, and the convective heat transfer coefficient drops as well. Therefore we have investigated the effect of this phenomenon in case of an actual building. The calculation needs another iteration, which contains in itself the iteration above as well. As a result it was given, that the better the insulation of the pipe, the more it effects the convective heat transfer coefficient, the main flow rate (using German regulations approved insulation, 13 %), the pressure drop of the network (using German regulations approved insulation, 20 %), but it does not have much effect on the heat loss of the system (using German regulations approved insulation, 1-2 %).

## VI. CASE STUDY

We have been given the task of planning a 2x140 apartments in an apartment house in Budapest, where inline recirculation is going to be constructed [8]. We have prepared a case study, in which we investigated the investment and the operating costs, for four different cases:

Sizing by the DVGW, W553, with German regulation approved heat insulation.

Sizing by the DVGW W553, with the usual Hungarian heat insulation (13 mm).

Sizing by our own method and program, with inline recirculation, with German regulation approved heat insulation.

Sizing by our own method and program, with inline recirculation, with the usual Hungarian heat insulation (13 mm).

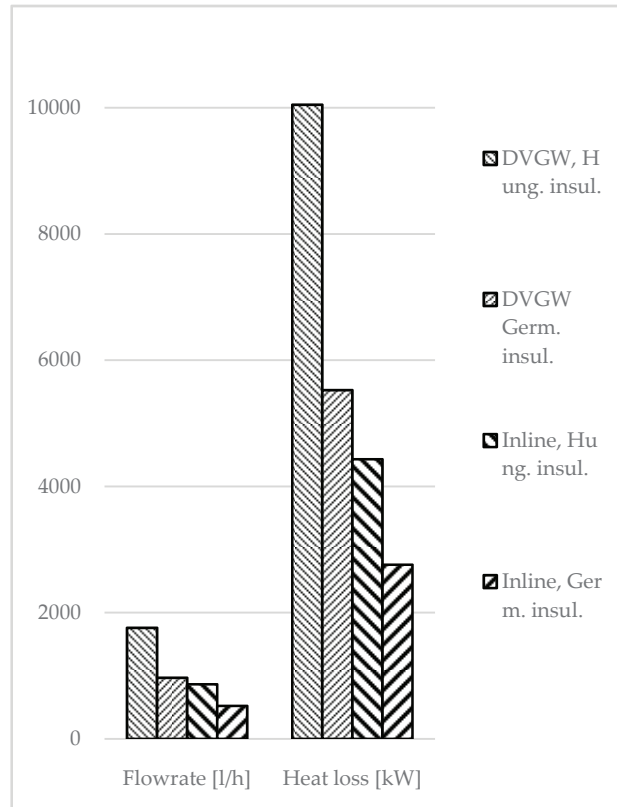


Figure 6. Main flow and heat loss of system alternatives

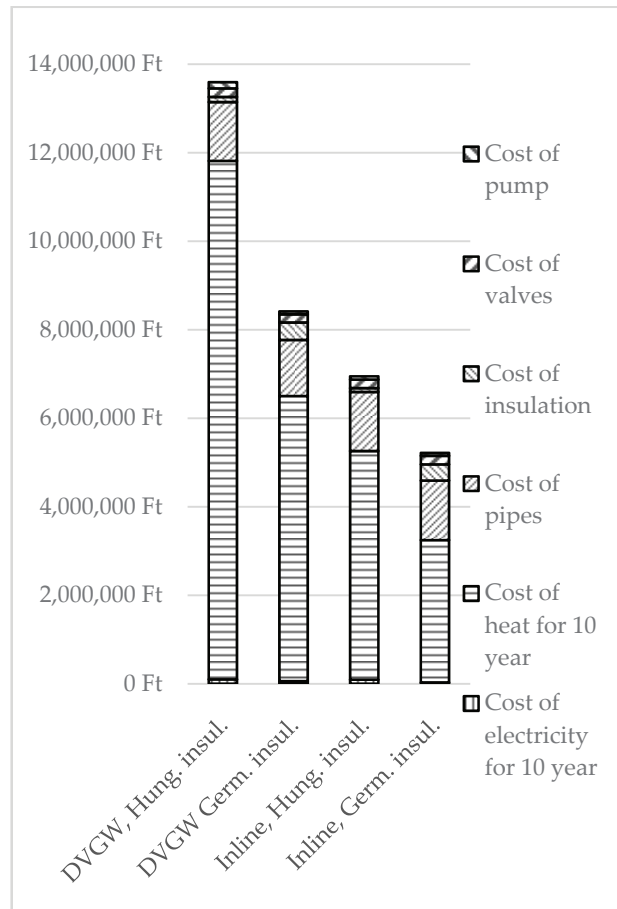


Figure 7. Total lifetime costs of system alternatives

The results of the study can be seen on Figure 6. as well as the 10 year operating costs and full investment costs on Figure 7. (We have used simplified economical calculation methods).

Figure 6. shows that by using the proper heat insulation the flow rate and heat loss drops by approximately 40-50 %. Our study has also shown, that keeping the heat loss small is vital, because supplying the heat takes 99 % of the operating costs [8]. On Figure 7. it is shown that the 10 year operating cost (mainly the cost of the heat) exceeds many times the investment cost of heat insulation, apart from which insulation was carried out. In conclusion, it is very important not to save on the amount of the heat insulation. Another fact from Figure 7. is that by applying inline recirculation instead of the regular, the operational cost drops to 50 %, while the investment cost stays almost at the same level.

#### SUMMARY

Developing [6] and [7] we have elaborated a computer program to design inline recirculation by risers system, and we applied it in case of an actual apartment house in Budapest. We have determined, that the effect of the convective heat transfer coefficient, in properly insulated systems is not significant compared to the heat loss and the pumping work of the system, although the precise calculation with it requires a large calculating capacity. We have established, that the investment cost of an inline recirculation system does not exceed the cost of a modern, regular system. Besides, according to the case study, the operating cost of an inline recirculation system is half the operating cost of a system, planned in the regular way. From the cost analysis of systems with different insulation it has come out, that the additional heat insulation returns approximately under a year for Hungarian financial conditions. In case of the actual building investigated, we will have the opportunity to make verification, measurements in the near future.

#### REFERENCES

- [1] DVGW (Deutscher Verein des Gas- und Wasserfaches) W553 worksheet, Bemessung von Zirkulationssystemen in zentralen Trinkwasser-Erwärmungsanlagen. Bonn, 1998
- [2] DIN1988-300:2012, Technische Regeln für Trinkwasser-Installationen – Teil 300: Ermittlung der Rohrdurchmesser. Berlin, 2012
- [3] DVGW (Deutscher Verein des Gas- und Wasserfaches) W551 worksheet, "Trinkwassererwärmungs- und Trinkwasserleitungsanlagen; Technische Maßnahmen zur Verminderung des Legionellenwachstums; Planung, Errichtung, Betrieb und Sanierung von Trinkwasser-Installationen", 2004
- [4] ASHRAE, HVAC Applications Handbook 2011, Chapter 50.5. US, Atlanta, 2011
- [5] A. Bhatia, B.E. Hot Water Plumbing Systems. Fairfax, Virginia, US : PDH Online, PDH Center, 2012.
- [6] Prof. Dipl.-Ing. Klaus Rudat, Analytische Untersuchung von Warmwasserverteilungssystemen mit strangweise innenliegenden Zirkulationsleitungen, HLH, Heizung, Lüftung/Klima, Haustechnik, Bd. 51., Nr. 11, Berlin, 1999
- [7] Sven Hiller: Eine vollständig thermodynamische Beschreibung von Trinkwarmwasserleitungen mit innenliegender Zirkulationsleitung, 2010
- [8] Kristóf Hargita, Diplomarbeit, Budapest, 2014
- [9] Wolfram Mathematica 10.0, © Copyright 1998-2014 Wolfram Research, Inc.

- [10] Nyers J., Garbai L., Nyers A.: "Analysis of Heat Pump's Condenser Performance by means of Mathematical Model". Int J. Acta Polytechnica Hungarica Vol. 11, No. 3, pp. 139-152, 2014.
- [11] Nyers J., Nyers A.: "Investigation of Heat Pump Condenser Performance in Heating Process of Buildings using a Steady-State Mathematical Model". I.J. Energy and Buildings. Vol. 75, pp. 523-530, June 2014.  
DOI: 0.1016/j.enbuild.2014.02.046



# Numerical investigation of offset jet attaching to a wall

Balázs Both\*, Zoltán Szánthó\*, Róbert Goda\*

\* Budapest University of Technology and Economics/Department of Building Service Engineering and Process Engineering, Budapest, Hungary

[both@epgep.bme.hu](mailto:both@epgep.bme.hu)

[szantho@egt.bme.hu](mailto:szantho@egt.bme.hu)

[goda@epgep.bme.hu](mailto:goda@epgep.bme.hu)

**Abstract**— In this paper an offset jet attachment is investigated applying tangential air distribution system, using numerical method. The attachment distance of the air jet – which significantly effects the ventilation characteristics in the occupied zone – was investigated as a function of offset ratio by numerically calculating the static pressure distribution on the wall, where the jet attachment happens.

Previously, several researchers investigated offset, attached jets. However tangential air distribution as a comfort type ventilation way and lower Reynolds numbers have not been considered. Besides, these previous investigations were made mostly on test facilities in infinitive (or semi-infinitive) spaces without air exhaust.

Three turbulence models were applied for the numerical simulation: standard and RNG  $k-\varepsilon$  model and SST  $k-\omega$  model. However the standard  $k-\varepsilon$  model seemed to be the most accurate turbulence model in the present work. The numerical results showed a very good agreement with previous results found in the literature.

## I. INTRODUCTION

To provide the required comfort parameters in closed areas it is necessary to distribute supply (primary) air in the occupied zone efficiently. The injected primary air jet induces secondary airflows in the ventilated space, so these primary and secondary airflows make an air distribution system [1]. Injected air jets and these distribution to the room play a very important role at each air distribution system. Tangential air distribution way is frequently used in several ventilated spaces. This type of air distribution can provide a pretty good comfort and ventilation effectiveness in rooms, where the draught risk is lower than in the other air distribution systems. In this case the air jet is injected to a surface in parallel (mostly this surface is a wall). Consequently, this jet adheres to the surface so an offset, attached jet is formed. After the attachment the air jet flows on the wall as wall air jet. The offset, attached and wall air jets play a very important role at tangential air distribution systems. As a result, it is needed to clear the main difference between offset and wall jets. At wall air jets the distance between the wall and the air inlet is zero and the jet is attaching to the surface right next to the wall. At offset air jets the distance between the wall and air inlet is higher than zero, so the air jet is attaching to the wall at a certain distance from air inlet. This distance is defined as attachment distance ( $y_a$ )

and the point, where it happens called as attachment point [2, 3, 4, 5]. One main advantage of applying these offset jets is that air jets can take longer ways till the occupied zone, so higher temperature differences can be applied at air inlet, so it yields lower volume flow rate to the room. The other main advantage is that ventilation characteristics can be designed in a more accurate and stable way [6].

One of the most important features of these offset jets is the attachment point, which effects the airflow characteristics in the room [6, 7]. The distance between the attachment point and air inlet is the attachment distance ( $y_a$ ). Process of the attachment can be featured by the followings. On Fig. 1, air flows out from an  $s_0$  sized slot with air velocity  $v_0$ . There can be seen a recirculation zone between the wall and the air inlet and the average pressure in this zone is less, than in the occupied zone ( $p_2 < p_1$ ), because there is no air injection from the wall. As a result, the Coanda-effect appears and then the offset air jet is attaching to the wall surface and flows as a simple wall jet [8].

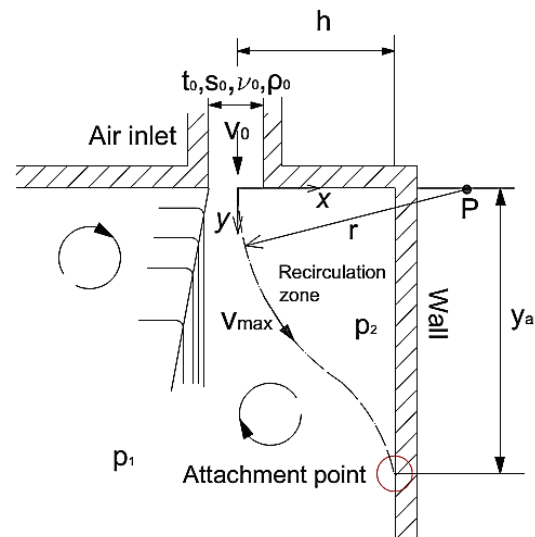


Figure 1. Sketch of an offset jet

Other important features for analysing offset jets are the distance between the wall and air inlet ( $h$ ), slot width ( $s_0$ ), slot length ( $L_0$ , which is perpendicular to the plane  $x-y$ ), air velocity at air inlet ( $v_0$ ) and the relative attachment distance ( $y_a/s_0$ ). Further parameters are the air density ( $\rho_0$ ), kinematic viscosity ( $\nu_0$ ) and the curvature of the air jet ( $r$ ). Geometry also plays an important role in the jet

attaching through AR (Aspect Ratio) and OR (Offset Ratio). AR can be defined as the ratio of the air diffuser length to the width ( $AR = L_0/s_0$ ), while OR is the distance between the wall and air inlet divided by the diffuser's width ( $OR = h/s_0$ ) [4, 5].

One of the earlier publications in this field of research is by Förthmann in 1934, who investigated plane and turbulent wall air jets [9]. The following decades brought several offset and wall air jet investigations. Sawyer [10] studied the attachment process of an air jet to a surface both theoretically and experimentally. He found that the attachment point is there, where the static pressure distribution on the wall has local maximum. This was also observed by other researchers [2, 3, 4, 8]. Other way of determination of the attachment point is observing the direction of airflow near the wall. In this case the attachment point is there, where the wall normal air velocity component is zero [4, 8, 11]. Nozaki et al. [4] determined the attachment streamline in the offset jet and the intersection of this streamline and the wall gives the attachment point. T. Magyar [12] investigated offset and wall air jets and these profiles, injected from circle air diffusers. He built a mathematical model of the jet and then performed experimental investigations on the jets.

In most of the investigations the air jet was injected in parallel to the wall, however Sarpkaya [13] used a curved surface and investigated the effect of curved geometry on jet flow. Rajaratnam and Subramanya [3] did water jet investigations. They found that there is an analogy between water and air jets, so they used an offset, parallel jet model. They also claimed that at higher Reynolds numbers ( $Re > 10^4$ ) geometry (OR and AR) has a significant effect on jet attaching to the wall. This was also verified by Sawyer [10], Pelfrey and Liburdy [11] and Bourque [14]. After the attachment point the air velocity profiles and the decay of maximum air velocity in the wall jet is very similar to the classical two-dimensional plane wall jets [11]. Nozaki et al. [4] showed that at higher offset ratios the air diffuser width has a minimal effect on the jet flow and the attachment process. Previous researchers like Nozaki et al. assumed that the pressure difference across the jet ( $\Delta p = p_1 - p_2$ ) which makes the axis of the injected air jet bend is constant. However, later Pelfrey and Liburdy [11] rejected this result.

Nozaki et al. showed that the attachment distance is almost independent from Re-number at the range  $2 \cdot 10^4 < Re < 7 \cdot 10^4$ , if  $AR = 8$ , and  $1.6 < OR < 16$ . If  $AR = 1, 2$  and  $3$ , respectively  $1.6 < OR < 16$  the effects of Re-number and side wall on the jet attaching is getting to increase, especially if AR is decreasing. This tendency was also verified by Nozaki [5], who found that if  $AR > 2$ , the attachment of the jet is independent from Re, while  $AR < 2$  Re will have a significant effect on the jet attachment. Pelfrey and Liburdy [11] showed that in case of  $Re > 10^4$  the attachment distance depends on mainly OR.

Most of the investigations were done in test facilities in laboratories, however the tangential air distribution system have not considered. Moureh and Flick [7] and Yu et al. [15] investigated the airflow in a slot ventilated space, which is similar to the tangential air distribution system, however these works do not deal with the attachment

distance and its determination. Few investigations used lower Reynolds-numbers, which would be very important from the aspect of comfort type ventilation applications.

The above investigations were mainly performed by using experimental and analytical methods. In case of applying numerical simulation (CFD = Computational Fluid Dynamics) the partial differential equations which describe the flow are solved using approximate methods. In fluid mechanics applications and HVAC systems finite volume method is commonly used [16]. The mathematical model of closed areas including the continuity equation, equation of movement, energy equation (if thermal processes are investigated), equation contamination of pollutants, etc. [17, 18]. In several engineering applications the flow is mostly turbulent, so it is needed to modelling turbulence with turbulence models. Several investigations have done in the recent years using numerical simulation, in order to investigate air jets. Driver and Seegmiller [19] used two-equation  $k-\epsilon$  turbulence models and compared these to experimental results. There was a pretty good correlation between the experimental and numerical data. Nasr and Lai [8] applied inhomogeneous numerical meshing in the computational domain. It is a well-known fact that near rounded faces, slots and complex geometries it is needed to apply thicker meshing, because the solution changes faster [16]. Nasr and Lai applied the standard  $k-\epsilon$ , RNG  $k-\epsilon$  and RS  $k-\epsilon$  turbulence models with power law, second order upwind and QUICK schemes. They found that the standard  $k-\epsilon$  model was more punctual than other turbulence models. Kechiche et al. [20, 21] numerically investigated a turbulent wall jet for lower Reynolds number (between  $7.3 \cdot 10^3$  and  $2.25 \cdot 10^4$ ) using  $k-\epsilon$  turbulence model. Moureh and Flick [7] have investigated a slot ventilated space using numerical and experimental methods. They used the two-equation  $k-\epsilon$  turbulence model and RSM model for predicting room ventilation characteristics for  $Re = 1.3 \cdot 10^5$ . Cao et al. [22] numerically investigated ceiling air jets and its effect for the ventilated space for  $Re = (1-4) \cdot 10^3$  range. SST  $k-\omega$  turbulence model was used because of the near wall effect with wall function and tetra elements.

The previous investigations were mainly performed in test facilities and did not consider the built-in circumstances and the exact air distribution system type. Furthermore, most of the investigations applied higher slot Reynolds numbers, which usually are not used in comfort type ventilation systems, because of thermal- and draught comfort problems. The attachment distance was mainly determined by the static pressure distribution on the wall, where the attachment process happens.

## II. MAIN INVESTIGATION AIMS

Due to the above, the following investigation aims can be stated.

- Determining the attachment distance by calculating the static pressure distribution along the wall using numerical method (CFD).

- Investigation of the attachment distance as a function of offset ratio using static pressure calculation on the wall by numerical method.

In order to realize these aims numerical simulation was applied and results were compared to previous works found in the literature.

### III. NUMERICAL METHOD

The numerical simulation was made by Ansys Fluent 12.1 CFD software, using a two-dimensional model (see the previous boundary conditions) at a certain Reynolds-number  $Re = 3 \cdot 10^3$  with different cell numbers in a  $3000 \times 2800$  mm domain size. Near the surface wall inflation was used, applying smooth transition with transition ratio 0.5, 6 layers and growth rate 1.5. Three different turbulence models were applied: Standard and RNG  $k - \epsilon$  models with wall function and SST  $k - \omega$  model. All of the turbulence models used Coupled numerical scheme, respectively QUICK, power law and second order upwind discretization.

It is very important to investigate the grid independence on an integral value because of the calculation time of the numerical model. Fig. 2 shows the maximum wall static pressure (as a surface integral value) as a function of cells. It can be seen that under  $10^5$  cells this integral value changes significantly, however over  $10^5$  cells this value is almost independent from the number of cells (grid resolution). In the present case it means 151236 cells with 7.5 mm max element size using tri and quad element types (as usual in 2D numerical models).

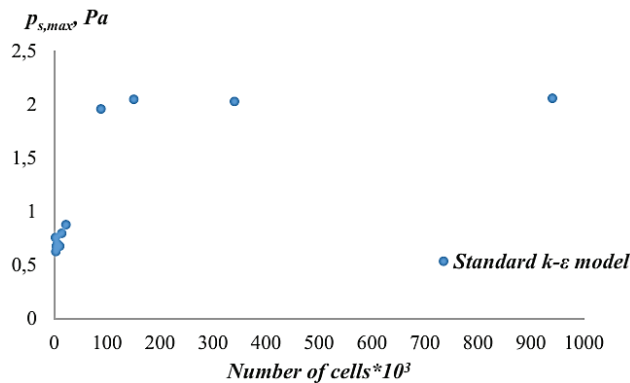


Figure 2. Grid independence investigation

The static pressure – which is an overpressure – distribution along the wall surface can be seen on Fig. 3.

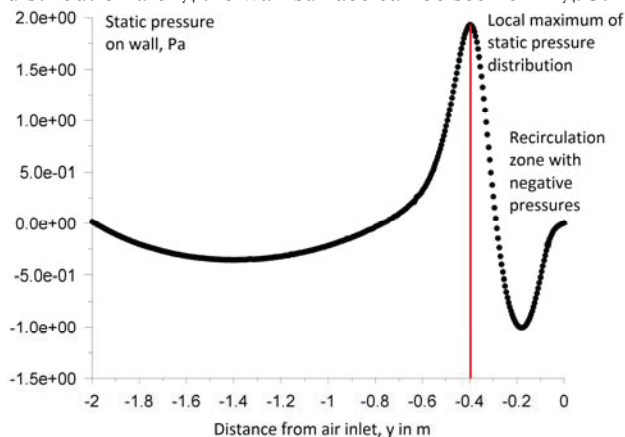


Figure 3. Static pressure distribution on wall

On Fig. 3 it is clear that in the recirculation zone the static pressure distribution has local minimum (negative static pressure values). Furthermore at the attachment point the static pressure distribution has a local maximum at  $y = y_a \approx -0.4$  m. And now let's compare the results with the literature.

Fig. 4 contains the numerically determined attachment distance as a function of OR on a constant slot Reynolds-number, compared with previous works. As the slot Reynolds-number has a negligible effect on attachment distance (as found in the literature), our result can be compared with previous works easily.

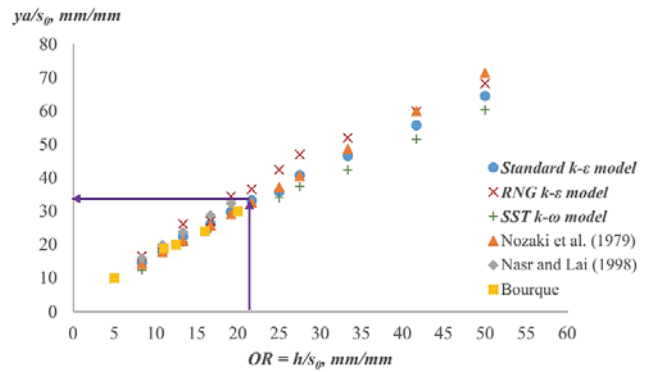


Figure 4. Relative attachment distance as a function of offset ratio

On Fig. 4 it is obvious that higher the offset ratio (OR), the longer the attachment distance is. In other words, the attachment of the injected air jet happens sooner if the air diffuser is closer to the wall. The numerical results used the standard  $k - \epsilon$  model, Coupled numerical scheme and power law discretization are closer to the previous investigations by other researchers. Otherwise, the RNG  $k - \epsilon$  model and SST  $k - \omega$  model gave a little bit higher difference from the literature results. Using the numerical results and literature data this value the relative attachment distance is  $y_a/s_0 \approx 34$  (Fig. 4).

Note that the previous result by other researchers did not consider the tangential air distribution. It means that the previous investigations were made at higher Reynolds-numbers than the tangential air distribution is used, however Reynolds-number has a minimal effect on attachment distance. By the way these investigations applied mostly horizontal air supply and test facilities without air exhaust. However, the present result in tangential air distribution system correlated with previous result well.

### IV. CONCLUSIONS AND SUMMARY

In this present work a wall bounded offset jet and its attachment were investigated applying numerical method.

Previous researchers mainly used static pressure determination on the wall to predict the attachment distance. In our work the static pressure distribution was calculated using CFD and then the attachment distance could be predicted. The relative attachment distance as a function of offset ratio at a certain slot Reynolds-number  $Re = 3 \cdot 10^3$  was plotted. Results showed a very good agreement with previous results in the literature. The relative attachment distance using the static pressure determination method was  $y_a/s_0 \approx 34$ .

In present work the standard  $k-\varepsilon$  model seemed to be the most accurate from the three applied turbulence models with Coupled numerical scheme and power law discretization. The attachment of the injected air jet happens sooner if the air diffuser is closer to the wall. The present result in tangential air distribution system correlated with previous results well.

#### ACKNOWLEDGMENT

The present research was supported by the Richter Gedeon Talentum Foundation.

The first author would like to thank the helpful advises to the supervisors of this research Dr. Zoltán Szánthó and Dr Róbert Goda.

#### REFERENCES

- [1] Magyar T.: Helyiségek légvezetési rendszerei és a hőérzeti méretezés kapcsolata. Szimpózium, Budapest, 1993. május, pp. 16 – 43.
- [2] Sushil Kumar Rathore, Manab Kumar Das: Comparison of two low-Reynolds number turbulence models for fluid flow study of wall bounded jets. *International Journal of Heat and Mass Transfer* 61, pp. 365 – 380, 2013.
- [3] Rajaratnam N.; Subramanya N.: Plane turbulent reattached wall jets. *Proceedings of the ASCE, Journal of the Hydraulic Division*, vol. 94, pp. 95 – 112, 1968.
- [4] Nozaki T; Hatta K; Nakashima M; Matsumura H.: Attachment flow issuing from a finite width nozzle. *Bull JSME*, vol. 22, pp. 340 – 347, 1979.
- [5] Tsutomu Nozaki: Attachment flow issuing from a finite width nozzle (report 4: Effects of aspect ratio of the nozzle). *Bulletin of the JSME*, Vol. 26, No. 221, November 1983, pp. 1884 – 1890.
- [6] Péntes Gy.: Sugárszellőzés alkalmazási lehetőségei. *ÉTI Évkönyv* 1977, pp. 330 – 339. ISSN 0133 – 4425.
- [7] J. Moureh, D. Flick: Airflow characteristics within a slot-ventilated enclosure. *International Journal of Heat and Fluid Flow* 26, pp. 12–24, 2005.
- [8] A. Nasr, J. C. S. Lai: A turbulent plane offset jet with small offset ratio. *Experiments in Fluids* 24(1998), pp. 47 – 57, Springer-Verlag, 1998.
- [9] Förthmann, E.: “Über turbulente Strahlausbreitung” (in German), *Ing. Arch. (Arch. Appl. Mech.)*, 5(1), 42-54. “Turbulent jet expansion” (English translation, March 1936), NACA Tech Memo, No. 789, 1934.
- [10] R. A. Sawyer: The flow due to a two-dimensional jet issuing parallel to a flat plate. *Engineering Department, Cambridge University. Journal of Fluid Mechanics*, Volume 9, Issue 04, December 1960, pp. 543 – 559.
- [11] Pelfrey J. R. R.; Liburdy J. A.: Mean flow characteristics of a turbulent offset jet. *Transactions of the ASME, Journal of Fluids Engineering*, vol. 108, pp. 82 – 88, 1986.
- [12] Magyar T.: Egy irányban határolt izotermikus levegősugár viselkedése zárt terekben. Műszaki doktori értekezés. Budapest, 1979.
- [13] Turgut Sarpkaya: The deflection of plane turbulent jets by convex walls. *Naval Postgraduate School*, 1968.
- [14] Bourque, C.: M.Sc. Thesis. University of Laval. Also *Aero. Quart.* 11, 201, 1959.
- [15] Hsin Yu, Chung-Min Liao, Huang-Min Liang, Kuo-Chih Chiang: Scale model study of airflow performance in a ceiling slot-ventilated enclosure: Non-isothermal condition. *Building and Environment* 42, pp. 1142–1150, 2007.
- [16] Kristóf Gergely: Áramlások numerikus modellezése. *Electronic book, BME* 2014. ISBN 978-963-08-1212-2. Availability: <http://www.ara.bme.hu/~kristof/CFDjegyzet/>, last viewed 26 January, 2015.
- [17] Sushil Kumar Rathore, Manab Kumar Das: Comparison of two low-Reynolds number turbulence models for fluid flow study of wall bounded jets. *International Journal of Heat and Mass Transfer* 61, pp. 365 – 380, 2013.
- [18] Magyar T., Goda R.: Laboratory modelling of tangential air supply system. *Periodica Polytechnica Ser. Mech. Eng.* Vol. 44, No. 2, pp. 207 – 215, 2000.
- [19] Driver D; Seegmiller H. L.: Features of a reattaching turbulent shear layer in divergent channel flow. *AIAA J* 23: pp. 163 – 171, 1985.
- [20] Jamel Kechiche, Hatem Mhiri et al.: Application of low Reynolds number  $k-\varepsilon$  turbulence models to the study of turbulent wall jets. *International Journal of Thermal Sciences* 43, pp. 201–211., 2004.
- [21] Jamel Kechiche et al.: Numerical study of the inlet conditions on a turbulent plane two dimensional wall jet. *Energy Conversion and Management* 45, pp. 2931–2949, 2004.
- [22] Guangyu Cao et al.: Modelling and simulation of the near-wall velocity of a turbulent ceiling attached plane jet after its impingement with the corner. *Building and Environment* 46, pp. 489 – 500, 2011.
- [23] Nyers J, Nyers L. “Monitoring of heat pumps” ‘Studies in Computational Intelligence’, Springer's book series, ISBN 978-3-642-15220-7 Vol. pp. 243, 573-581, Heiderberg, Germany. 2009.
- [24] J. Nyers Dr.Sci., S. Tomić Dr. Ec, „Financial Optimum of Thermal Insulating Layer for the Buildings of Brick” Symposium: 5th International Symposium on Exploitation of Renewable Energy Sources "EXPRES 2013", Subotica-Szabadka, Serbia. pp. 33-36. ISBN 978-86-85409-82-0



# Determination of optimal pipe diameters for radial fixed-track district heating networks

László Garbai, Andor Jasper,

Department of Building Service and Process Engineering, Budapest University of Technology and Economics, Hungary

garbai@epgep.bme.hu

jasper@epgep.bme.hu

**Abstract** - This paper presents the basics of Bellmann's dynamic programming, to be applied for radial fixed-track district heating networks. A decision-making model thereof is produced, and Garbai's scaling method [1] is applied in a new, narrower interval by using a tagging method well-known from computer science. So the sum of calculations to be performed is reduced considerably.

## I. INTRODUCTION

Public utilities in network systems perform very important tasks in the life of settlements. District heating systems represent a most sophisticated technology among public utility networks. They are highly asset-intensive, their development and operation are costly; at the same time, they play a major role in energetics as they provide space and opportunities for combined heat and power generation. 650 thousand apartments in Hungary, most of them built by using a system building technology in the course of the past few decades, are supplied with district heating. The economic optimization of the construction and operation of district heating networks can make district heating much cheaper. Zoltan Magyar, Zoltan Szantho deal with optimization of district heating systems in [17], [18], [19]. The request for optimization occurs in several fields in energy industry, relevant field to this paper is the implementation of heat pumps in district heating networks [13], [14], [15], [16]. Construction optimization refers to the specification of optimal pipe diameters.

Specification of optimal pipe diameters for district heating systems involves the selection of a conduit diameter for each section of the district heating system whereby the annual proportion of the investment cost of the network, the annual direct cost of operation, as well as the aggregate cost of hot water circulation and heat loss are minimized.

An efficient solution for this problem, effective from the engineering point of view and of substantial practical value, is still missing.

This problem arose in the 1960s and 1970s. Attempts in those times were characterized by a search for so-called analytic solutions. Diameters and costs were taken into consideration with continuous value series. The diameters yielded were rounded to standard by diverse heuristic procedures. The "distance" between the standard diameters thus yielded and the real optimum was left unexplored [5], [6], [7], [8], [9], [10], [11], [12]. Subsequent models were already characterized by best-first searches on sets of standard diameters using discrete diameter series and discrete cost functions. Extremum search was performed on discrete sets by various counting structures, such as the Branch and Bound method and dynamic programming [1], [2].

Theoretically, dynamic programming proved to be a stable and convergent method. When applying this method, however, the rapidity of convergence and hitting the global optimum were failed to be analyzed. Bellmann's optimality principle is used in our practice of applying this method. The state variable to connect stages of decision making at nodes, that is, junction points of mains and branch-off conduits, is pressure difference between the forward and return conduits. Most frequent division thereof can make the solution even more accurate. Search for a solution can also be taken as a task of trying to find an optimal route [1], [2].

This study presents a procedure based on dynamic programming, to guarantee convergence and finding the global optimum. The task is discussed with a systems theory and decision making theory approach; furthermore, efficiency of the method and error margins are discussed.

## II. TASK SPECIFICATION

Figure 1 shows the topology image, structure and basic features of a district heating network. The network presented is radial, consisting of consumers, conduit sections connecting consumers, and a circulation system (pump). Conduit sections consist of a forward and a return conduit each. Conduit sections are separated by nodes. Basic

geometric properties of conduit sections include conduit length and conduit diameter.

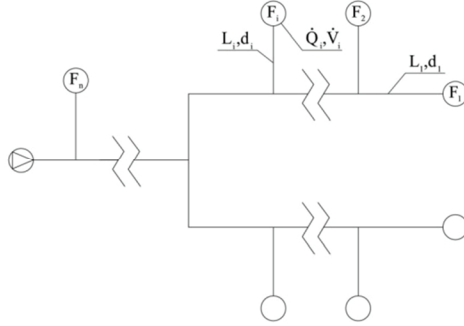


Figure 1. District heating network: an illustration

Legend:

- F consumer,
- L conduit length,
- d conduit diameter,
- $\dot{Q}$  heat demand,
- $\dot{V}$  hot water flow rate demand.

A graph shows the district heating network. A graph is a mathematical structure consisting of nodes and edges. The graph of a radial network is called a tree-structured graph. This graph serves for the hydraulic, thermal engineering, and mathematical modelling of district heating network design and operation.

The objective function of optimization:

$$C = f_1(d_1, d_2, \dots, d_n)a + f_2(\Delta p_p(d_1, d_2, \dots, d_n), \tau, e) \rightarrow \min!$$

where

- a annuity,
- $f_1$  investment costs,
- $f_2$  operating costs,
- $\tau$  operating time,
- e specific cost of electricity.

A graph-based modelling and optimization of district heating networks are presented by using so-called decision making systems. From a systems theory point of view, radial fixed-track district heating networks generally constitute diverging branch decision making systems [3], [4]. The simplest district heating networks form a serial system. A decision making system shows inputs and outputs, decision making variables, the transformation correlations linking them, and decision making results. The aim of decisions is to make decisions in function of the input and the required output of the system in order for the economic target function describing system operation to reach a minimum. Figure 3 shows a model of a decision making system in a white box representation.

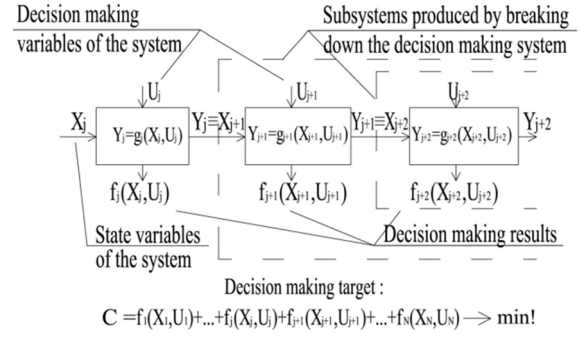


Figure 2. Decision making system illustration

Dynamic programming is a mathematical method to optimize series of interdependent decisions [1]. The criterion for each decision in the series of decisions is to satisfy the optimality principle of dynamic programming.

The original definition of the optimality principle states that:

”An optimal decision making series is always characterized by the fact that whatever the initial state and the initial decision is, subsequent decision(s) constitute an optimal decision making series compared to the new state resulting from the first decision and the initial state” [1]. Decision making systems are broken down into stages of decision making (subsystems).

According to the principle of optimality, decisions should be made by taking into consideration the options within the entire decision making process and should be optimal compared to the given state of the system. In the mathematical sense, our decisions satisfy a recursive function equation. The function equation of a serial system is as follows, using the notation of the general decision making process :

$$O(z_m) = \min_{u_m} \{f_m(z_m, u_m) + O(z_{m+1})\}. \quad (1)$$

And by introducing the state transformation to characterize given stage:

$$O(z_m) = \min_{u_m} \{f_m(z_m, u_m) + O(g(z_m, u_m))\} \quad (2)$$

By applying state transformation, the function equation will be a function of only the connection variable ( $z_m$ ) and the decision making variable ( $u_m$ ).  $O(z_m)$  is the so-called optimal function, containing optimal decisions associated with decision making stages in respect of each value of the connection variable  $z_m$ .

In decision making system optimization, node pressures (pressure differences)  $h_{jk}^*$  are taken as a series of discrete values located sufficiently densely. In the current stage of optimization, network parts  $O_{jk}(h_{jk}^*)$  of minimal cost are produced in function of the discrete values of node pressure  $h_{jk}^*$ , by an appropriate selection of an optional standard diameter  $d_{jk}^*$  which complies with the speed limits prescribed. When solving the function equation, costs of the network section up to stage  $jk$  are minimized by selecting values which, in the aggregate, yield a minimum figure, from the discrete empirical costs of the network section up to the (already optimized) stage  $jk+1$  (parametrically, in function of the discrete values of node pressure  $h_{jk+1}^*$ ), and those of the standard diameters  $d_{jk}$  and  $d'_{jk}$  of stage  $jk$ , reflecting all circumstances related to topology and laying.

Pipe networks can be optimized either by fixing or not fixing the input pressure (perhaps only by using an upper boundary to limit the input pressure). It does not constitute a theoretical and substantial methodological restriction for discrete dynamic programming if the value of the input pressure is prescribed.

At this point, in the first stage of the decision making system (and the last one in the sequence of optimization operations), the determination of pumping work is disregarded in cost calculations. From the discrete value series of input pressure  $h_{i_1}^*$ , constituting the input of this stage (as a parameter), the one coinciding with the prescribed input pressure is selected (such discrete value series can be compiled arbitrarily), and the last stage is optimized – the cost function  $O(h_{i_1}^*)$  is minimized only for this single value ( $h_{i_1}^* = \text{const.}$ ).

In the event that no input pressure is strictly prescribed, pumping costs are assigned to the first element of the decision making system in function of input pressure  $h_{i_1}^*$ , constituting the input to the first "box" (considered as a variable). After solving the function equation stated on the first "box", the optimal input pressure is also determined by comparing the optimal costs  $O(h_{i_1}^*)$  and by selecting the minimum cost.

It is conspicuous that in the successive solutions of the recursive function equation, all technical and economic requirements can be fully satisfied, and the topology, hydraulics and cost conditions of the network can be precisely analyzed simultaneously with optimization.

The success of optimization depends on increasing the breakdown frequency of pressure differences at nodes. Figure 3 provides a model for latticing pressure differences at nodes according to classic optimization, taking a simple network as an example (Figure 4).

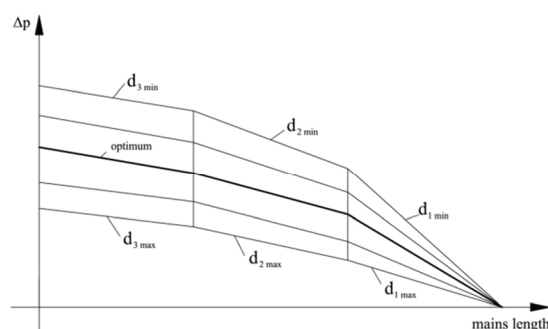


Figure 3. Lattice model of pressure differences at nodes

A minimum and a maximum diameter can be taken into consideration for each conduit section, with the optimal diameter expected to be somewhere in between. The upper and lower boundaries of the pressure figure are specified by the pressure losses calculated by using the minimum and maximum diameters, as shown in the figure. Latticing the nodes of the pressure figure will yield a graph on which the task of searching for the optimal route can be defined. The problem is the frequency of node selection within the graph. The following model can be applied for the size of the error possible to be committed. The optimum of the cost function should be estimated. Then a so-called unconditional optimization of the network should be performed, defining independently the standard conduit diameter for each conduit section where the investment cost, heat loss cost and flow cost of the section are minimal in the aggregate.

Then the pressure image of the network should be constructed and costs should be added up according to Figure 9.

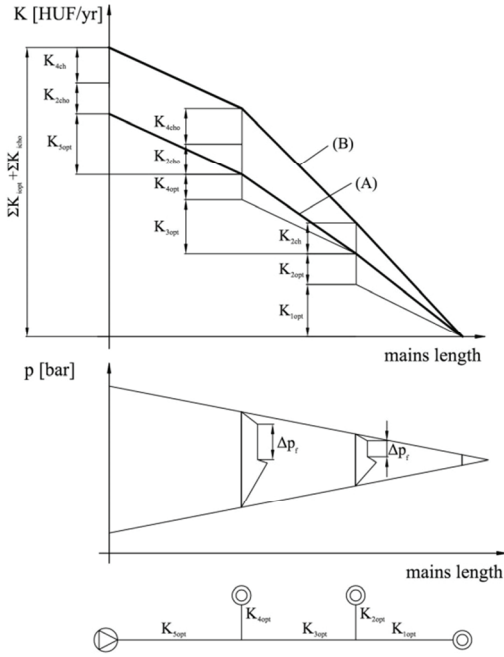


Figure 4. Pressure and cost figure of the network by system-independent optimization

In order to equalize pressures, stemming must be performed at the node in consumer branch-offs to adjust the required flow rates. Such stemming actions increase pumping costs. Curve (A) shows network costs, while curve (B) shows increased resultant costs arising from additional pumping due to stemming.

The optimum to be found in the set of standard pipe diameters cannot be smaller than the value of curve (A); and the exact optimum can be located between curves (A) and (B) if it exists at all. Let us try to find a solution between curves (A) and (B). Optimization should be performed using the optimal diameters defined according to independent optimums and their neighbours, by applying Bellmann's optimality principle and dynamic programming; to understand it more easily, on a serial system model similar to Figure 3.

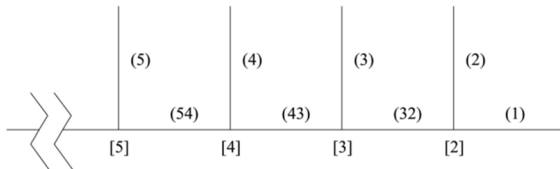


Figure 2. Network model for best-first search and positioning between curves (A) and (B)

Let the standard diameters to be taken into consideration for conduit sections (1) and (2) be as follows:

$$\{d_{(1),1}, d_{(1),opt}, d_{(1),3}\}, \{d_{(2),1}, d_{(2),opt}, d_{(2),3}\}$$

So-called recursive optimization functions should be generated by tagging assigned to section (2) as follows:

$$O_{(2)1}(d_{(2)1}) = \min_{d_{(1)i}} \{K_{(2)1}(d_{(2)1}) + K_{(1)i}(d_{(1)i})\}$$

$$O_{(2)2}(d_{(2)2}) = \min_{d_{(1)i}} \{K_{(2)2}(d_{(2)2}) + K_{(1)i}(d_{(1)i})\}$$

$$O_{(2)3}(d_{(2)3}) = \min_{d_{(1)i}} \{K_{(2)3}(d_{(2)3}) + K_{(1)i}(d_{(1)i})\}$$

where:

$$i = 1, 2, 3$$

Recursive optimality functions should be generated by tagging assigned to section (3), using the partial optimums  $O_{(2)}$  previously yielded as follows:

$$O_{(3)1}(d_{(3)1}) = \min_{d_{(32)j_i}} \{K_{(32)j}(d_{(32)j}) + K_{(3)1}(d_{(3)1}) + O_{(2)i}(d_{(2)i})\}$$

$$O_{(3)2}(d_{(3)2}) = \min_{d_{(32)j_i}} \{K_{(32)j}(d_{(32)j}) + K_{(3)2}(d_{(3)2}) + O_{(2)i}(d_{(2)i})\}$$

$$O_{(3)3}(d_{(3)3}) = \min_{d_{(32)j_i}} \{K_{(32)j}(d_{(32)j}) + K_{(3)3}(d_{(3)3}) + O_{(2)i}(d_{(2)i})\}$$

where:

$$i = 1, 2, 3 \quad j = 1, 2, 3$$

The procedure is continued in a recursive fashion and optimal functions are stored in the meantime. In each stage of decision making, an optimal diameter structure is associated with three possible branch-off diameters. In each stage of decision making,  $3 \times 3 = 9$  cost variants should be compared in respect of each tag. When reaching the pump, optimization is performed for the last 3 tags. The previous optimal tag is associated with each tag, and both the optimal diameters and the optimal pressure image can be called in by moving backwards. If the cost function yielded does not proceed below curve (B), then there is no network with better costs than the concatenation of system-independent optimums.

### III. CONCLUSIONS

Specification of optimal pipe diameters for district heating systems involves the selection of a conduit diameter for each section of the district heating system whereby the annual proportion of the investment cost of the network, the annual direct cost of operation, as well as the aggregate cost of hot water circulation and heat loss are minimized.

An efficient solution for this problem, effective from the engineering point of view and of substantial practical value, is still missing. This paper presented a procedure based on dynamic programming, to guarantee convergence and finding the global optimum. The task is discussed with a systems theory and decision making theory approach. Calculations were performed for fifty hungarian district heating networks. Compared to the common design method our optimization



method resulted in 4-5% cost saving. This improved variant of the dynamic programming described in the present paper have multiplied the speed of the calculation. With optimums independent of the system its possible to estimate the exact boundaries between which the optimum lies. This is the most important result of our paper as no constraints were determined by other researchers before. We have also proven that less calculation capacity is needed with the labeling method.

## REFERENCES

- [1] Garbai, L., Dezső, Gy.: Flow in Building Engineering Conduit Systems (in hungarian), Műszaki Könyvkiadó, 1986
- [2] Belmann, R.E.: Dynamic Programing. Princeton University Press, Princeton 1962.
- [3] Aris, R., Nemhauser, G.L., Wilde, D.J.: Optimization os Multistage Cycle and Branching System by Serial Procedures, A.I.Ch.E. Journal 10(6), (1964), pp.913-919, doi: 10.1002/aic.690100626
- [4] Garbai, L.: District heating (in hungarian), 2012. ISBN: 978-963-279-739-7
- [5] Phetteplace, G.: Optimal Design of Piping Systems for District Heating, CRREL Report 95-17, 1995. [http://www.crrel.usace.army.mil/library/crrelreports/CR95\\_17.pdf](http://www.crrel.usace.army.mil/library/crrelreports/CR95_17.pdf)
- [6] Xiang-li L., Duanmun L., Hai-wen S.: Optimal design of distrect heating and cooling pipe network of seawater-source heat pump, Energy and Buildings 42 (2010), pp. 100-104. doi:10.1016/j.enbuild.2009.07.016
- [7] Jamsek, M., Dobersek, D., Goricanec, D., Krope, J.: Determination of Optimal District Heating Pipe Network Configuration, WSEAS Transactions on Fluid Mechanics, Issue 3, Volume 5, July 2010, pp. 165-174. ISSN:1790-5087
- [8] Tol H. I., Svendsen S.: Improving the Dimensioning of Piping Networks and Network Layouts in Low-Energy District Heating Systems Connected to Low-Energy Buildings: A Case Study in Roskilde, Denmark, Energy, Volume 38, Issue 1, February 2012, pp. 276–290., doi:<http://dx.doi.org/10.1016/j.energy.2011.12.002>
- [9] Hlebnikov, A., Dementjeva, N., Siirde, A.: Optimization of Narva District Heating Network and Analysis of Competitiveness of Oil Shale CHP Building in Narva, Oil Shale, 2009, Vol. 26, No. 3 Special, pp. 269–282. doi: 10.3176/oil.2009.3S.09
- [10] M. H. Afshar, A. Afshar, M. A. Mariño, Hon. M. ASCE: An Iterative Penalty Method for the Optimal Design of Pipe Networks, International Journal of Civil Engineerng. Vol. 7, No. 2, June 2009, pp. 109-123.
- [11] Wang, W., Cheng, X., Liang, X.: Optimization modeling of district heating networks and calculation by the Newton method; Applied Thermal Engineering 61 (2013) 163-170; <http://dx.doi.org/10.1016/j.applthermaleng.2013.07.025>
- [12] Sakawa, M., Matsui, T.: Fuzzy multiobjective nonlinear operation planning in district heating and cooling plants; Fuzzy Sets and Systems 231 (2013) 58 – 69; doi:10.1016/j.fss.2011.10.020
- [13] Nyers J., Tomic S., Nyers A. : “ Economic Optimum of Thermal Insulating Layer for External Wall of Brick ”. International J. Acta Polytechnica Hungarica Vol. 11, No. 7, pp. 209-222. 2014.
- [14] Nyers J., Nyers A. : “ Investigation of Heat Pump Condenser Performance in Heating Process of Buildings using a Steady-State Mathematical Model ”. International J. Energy and Buildings. Vol.75, pp. 523–530, June 2014.DOI: 0.1016/j.enbuild.2014.02.046
- [15] Nyers J., Pek Z.: "Mathematical Model of Heat Pumps' Coaxial Evaporator with Distributed Parameters " InternationalJ. Acta Polytechnica Hungarica Vol.11, No.10, pp.41-57, 2014.
- [16] Nyers J., Kajtar L., Tomic S., Nyers A.: “ Investment-savings method for energy-economic optimization of external wall thermal insulation thickness”. International J. Energy and Buildings. Vol.86, pp. 268–274, 2015. <http://dx.doi.org/10.1016/j.enbuild.2014.10.023>
- [17] Magyar Z. – Petitjean, R.: Energy Saving of District Heated Flats from the Recondition of the Heating System in Hungary, ASHRAE Transactions 108 Part 2, 2002, pp. 575-579.
- [18] Harmati, N., Folic,R., Magyar, Z.: Energy performance modelling and heat recovery unit efficiency assessment of an office building, Thermal Science International Scientific Journal, 2015. <http://thermalscience.vinca.rs/online-first/1363>,DOI: 10.2298/TSCI140311102H
- [19] Determining the optimal schedule of district heating, Periodica Politechnica Ser. Mech. Eng. VOL.44 No. 2. Pp.285-300. (2000.)

# Building energy performance improvement from the aspect of envelope upgrading

N. Harmati\*, R. Folić\* and Z. Magyar\*\*

\* University of Novi Sad, Faculty of Technical Sciences/Department of Civil Engineering, Novi Sad, Serbia

\*\* Budapest University of Technology and Economics/Department of Building Energetics and Building Services, Budapest, Hungary

[harmati@uns.ac.rs](mailto:harmati@uns.ac.rs), [r.folic@gmail.com](mailto:r.folic@gmail.com), [magyar@egt.bme.hu](mailto:magyar@egt.bme.hu)

**Abstract** - This investigation presents a detailed analysis in an effort of building energy performance improvement from the aspect of building envelope influence on the annual heating and cooling demand. The aim is to indicate methods of performative intervention for envelope improvement and to offer architects and practitioners useful information in decision-making considering the early desing stage of new buildings or rehabilitation of existing office buildings. A comparative analysis was performed among the monitored building and calculated heating and cooling demands from the multi-zone thermal model calibrated in EnergyPlus engine. Findings from the dynamic simulations indicated the influence of exterior glazing parameters on the annual heating and cooling demand of the multi-zone building model.

## I. INTRODUCTION

The investigation presents a detailed analysis in an effort of building energy performance improvement from the aspect of building envelope influence on the annual heating and cooling demand. The aim is to indicate methods of performative intervention for envelope improvement and to offer architects and practitioners useful information for decision-making in the early desing stage of new buildings or rehabilitation of existing office buildings.

Annual energy demand for heating and cooling was calculated in the function of three principal parameters: window to wall ratio (WWR), window geometry (WG) and glazing properties (U-value, SHGC, VT). The Best Case Scenario for WWR and WG was determined in the function of visual comfort maintenance (daylight quality) and glazing ratio reduction in offices via numerical simulations in Radiance engine. A comparative analysis was performed among the monitored building and calculated heating and cooling demands from the multi-zone thermal model calibrated in EnergyPlus engine. Findings from the dynamic simulations indicated the influence of glazing properties (U-value, SHGC, VT) on the annual heating and cooling demand of the multi-zone building model.

## II. METHODOLOGY AND MATERIALS

In order to determine the heating and cooling loads a multi-zone thermal model was constructed of the B+Gf+9

level reference office building, shown in Fig. 1. Each thermal zone was assigned with internal load properties typical for a large office building. The thermal zones were formed and named according to their function and position in the building. According to the investigation phases and complexity of the model and simulation processes, five programs were applied for this study, which are the following:

1. Autodesk Revit Architecture – 3D model design [1]
2. Autodesk Ecotect Analysis and Desktop Radiance – Solar analysis and advanced daylight simulation [2, 3]
3. Sketchup Make – Multi-zone thermal model construction [4]
4. Open Studio – Integration of multi-zone thermal model properties; construction, materials, occupancy, internal loads and schedules [5]
5. EnergyPlus – dynamic energy simulation [6]

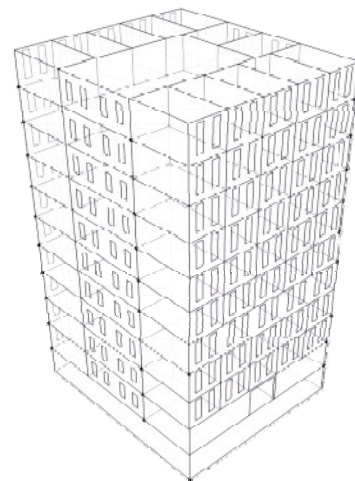


Figure 1. Reference office building

The location and climate data were imported from the global climatological database Meteonorm 7. [7] The location of the building is Novi Sad, Latitude = 45.333°, Longitude = 19.850°, Altitude = 84 m and Climatic zone = III, 3. The imported data are the following: Radiation model = Default (hour); Temperature model = Default

(hour), Tilt radiation model = Default (hour) (Perez), Radiation: New period = 1986-2005, Temperature: New period = 2000-2009. Building orientation is 30° counter-clockwise from North axes.

The research included the monitoring of a 10 level reference office building through a period for three months in winter and two months in summer period of 2014 in order to assess and evaluate its energy performance in a temperate climate. Daily energy consumption was recorded in the sub-station while indoor mean air temperature and illumination intensity were monitored with digital instruments.




Indoor illumination, daylight quality and visual comfort of occupant were analyzed in numerous researches devoted to energy performance assessment of buildings in different climate conditions. [8, 9, 10, 11, 12, 13, 14, 22] Thermal and lighting simulations in a total energy perspective were investigated in previous researches applying energy modelling. [15] Envelope glazing's transmittance dependence on the solar radiation in order to reduce building energy demand was investigated respectively from various approaches. [16, 17]

### III. MODELING OF BUILDING ENVELOPE IN THE FUNCTION OF DAYLIGHT INTENSITY

#### A. WWR and WG application

The quality of daylight influences occupant comfort improves environmental quality and affects the health and productivity of occupants. Furthermore the building envelope's glazing ratio (WWR) affects the total annual energy demand for heating and cooling. The research involves the analysis of glazing geometry (WG) as a significant criterion of envelope optimization from the visual comfort aspect. Indoor illumination dispersion is analyzed for three geometric shapes as presented in Table I.

TABLE I.  
WINDOW GEOMETRIES APPLIED FOR DAYLIGHT ANALYSIS

Square	Horizontal rectangle	Vertical rectangle
a x a 	a x b 	a x b 


The WG's from Table I were applied for five WWR's: 20 %, 25 %, 30 % and baseline model's 50 % and 90 %. From the conducted on-site daylight intensity monitoring it was concluded that the 50 % WWR with clear glass does not meet the visual comfort standards in offices.

#### B. Advanced daylight simulation setup in Radiance

The daylight simulation setup and image rendering was conducted via detailed setup in Radiance Control Panel (CP). The rendering settings for the simulation are presented in Table II Interior daylight dispersion was simulated using three reflections with medium lighting detail and image quality. Simulated illumination scale was set from 0-1000 lx.

The daylight intensity analysis and daylight dispersion required numerous simulations which depended on the analyzed period, time, sky conditions and zone orientation. The period setup for the simulation was the 15th of every second month within intervals of 4h to determine the daylight intensity in offices at 8.00h, 12.00h and 16.00h on an annual basis. Visual comfort is satisfied if the lighting intensity holds a constant value between 350 and 500 lx throughout occupied hours. The lighting quality was demonstrated through daylight dispersion analysis including 720 simulations.

TABLE II.  
RENDERING SETTINGS IN RADIANCE CP

Illumination scale	Render settings	
	Run identifier:	RCP
	Display type:	Illuminance [lx]
	Max. Reflections:	3
	Lighting detail:	Medium
	Lighting variability:	Medium
	Image quality:	Medium
	Scale:	1000
	Scale division:	10

Window frames were disregarded in the simulations. The calculation of daylight factor (DF) is performed in zone centre points as BRE DF calculation for WWR of 20%, 25%, 30%, and base case 50%. The total number of performed simulations was 16, and the calculated DF's determined the final decision of WWR selection for the optimal building envelope. Two modes were simulated for electric lighting: on/off mode and dimming switch mode. The simulations presented the annual percentage of unnecessary usage of electric lighting in the building according to each orientation. Illumination sensors were determined in geometric centre points of zones. The on/off mode and the dimming switch mode adjusted the illumination intensity always to fulfil the minimal requirement of 350 lx.

#### C. Results

The Best Case Scenario considering the illumination intensity detectors were integrated in the offices, as stated previously. If lighting level in the center zone point falls below 350 lx the sensors automatically turn on electric lights or switch to dimming mode. Findings indicated best performance if dimming mode is applied. In conclusion, considering the minimal daylight factor (DF) and annual percentage of unnecessary usage of electric lighting the adopted scenarios of WWR for vertical WG are presented in Table III.

TABLE III.  
DAYLIGHT FACTOR CALCULATION WITH PHOTOELECTRIC DIMMING

East Offices	South Offices
30 % WWR	25 % WWR
1.97 DF	2.05 DF
69% Ann. Elect. reduction	70% Ann. Elect. reduction
West Offices	North Corridor
30 % WWR	20 % WWR
1.78 DF 66%	1.89 DF
Ann. Elect. reduction	67% Ann. Elect. reduction

#### IV. ENERGY SIMULATION SETUP

##### A. Construction, occupancy and operation schedules

The building envelope applied in the simulation was selected and applied according to the thermal insulation requirements. It was improved in order to reduce the heat transfer coefficient, U-value, where the existing exterior walls had 2.32 W/(m<sup>2</sup>K). Furthermore it was recorded that the existing exterior glazing (37.5%) also has a significant U-value, 2.788 W/(m<sup>2</sup>K). The modified exterior wall construction adds 140 mm expanded polystyrene to the exterior construction including finishing work with portland cement mortar resulting in significant U-value reduction of 0.22 W/(m<sup>2</sup>K), which meets the prescribed requirements of the Serbian and European standards. [18, 19, 20]

Internal gains from occupants were assigned in OpenStudio in the "people definition" dialog. The number of occupants and internal gains were implemented in the energy simulation setup by the following steps:

1. Expectable number of occupants was calculated – possibility analysis
2. Occupied office areas were calculated
3. Unoccupied areas were calculated

##### B. Applied glazing types and parameters

Glazing types were applied according to window properties (parameters: U-value, SHGC, VT) as shown in Table IV. The selection of glazing types was among windows with 1.3 and significantly low 0.296 U-values with high and low SHGC coefficients respectively. [21] The energy simulation will indicate the heating and cooling demands and assess the influence of window parameters.

TABLE IV.  
SIMULATION SCENARIOS AND WINDOW PROPERTIES

Scenario	Windows
W1	Dual pane, Pilkington Optifloat clear
W2	Dual pane, Pilkington Energy Adv., Ag, Low-E, #3 Surface
W3	Trip-pane, One pane with Sun-Stop coating and Ag
W4	Trip-pane, Pilkington Planar + Optifloat + Optitherm
Parameters	
W1	U-value 1.3 W/(m <sup>2</sup> K); SHGC 0.50; VT 0.73
W2	U-value 0.296 W/(m <sup>2</sup> K); SHGC 0.756; VT 0.77
W3	U-value 1.056 W/(m <sup>2</sup> K); SHGC 0.338; VT 0.63
W4	U-value 0.7 W/(m <sup>2</sup> K); SHGC 0.26; VT 0.52

#### V. RESULTS

##### A. Annual energy demands

The annual heating and cooling demand of the four Scenarios is shown in Fig. 2 and Fig. 3. Scenario W2 with the lowest U-value and highest SHGC coefficient had the highest cooling and lowest heating demand (total 221 MWh/a, 65 kWh/m<sup>2</sup>/a). Scenario W3 with higher U-value and low SHGC coefficient presented opposite results, higher heating demand and lower cooling demand (total 156 MWh/a, 46 kWh/m<sup>2</sup>/a). W4 Scenario with 0.7

W/(m<sup>2</sup>K) U-value compared to W2 Scenario with 0.296 W/(m<sup>2</sup>K) could not be predicted if the SHGC coefficient is neglected since it has the most significant impact on the heating and cooling performance. W4 Scenario (0.7 W/(m<sup>2</sup>K), SHGC 0.26) had a total annual demand of 132 MWh/a, 38 kWh/m<sup>2</sup>/a. W2 Scenario (0.296 W/(m<sup>2</sup>K), SHGC 0.756) had a total annual demand of 221 MWh/a, 65 kWh/m<sup>2</sup>/a. The annual energy demand reduction was 41% which was significantly affected by the low SHGC coefficient. The VT value was 0.5 for which the Radiance simulations and WWR/WG analysis was performed, which qualified the W4 Scenario as the most preferable. The total energy demand for the Best Case Scenario compared to the reference building can be reduced roughly by 83% in case of annual heating. Considering cooling demands the results have slight deviation.

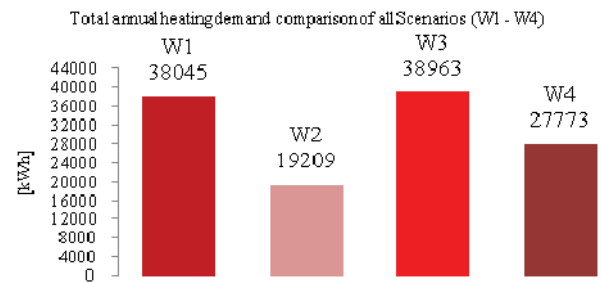


Figure 2. Annual heating demand (W1-W4)

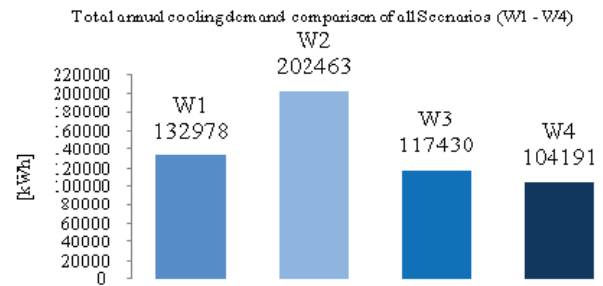


Figure 3. Annual cooling demand (W1-W4)

##### B. Evaluation and discussion

In order to determine the Best Base Scenario for WWR and WG the findings were elaborated in four simulation categories:

1. Illumination dispersion analysis (advanced lighting simulation, visual comfort),
2. Daylight factor calculation (visual comfort),
3. Photoelectric lighting simulation (electricity reduction),
4. solar exposure analysis (radiation gains).

Findings indicated that window height contributes to deeper daylight dispersion in the indoor environment which results in achieving qualitative natural illumination in offices. Photoelectric lighting simulation was applied in order to reduce the electricity requirement for the building by 70% in case of dimming mode. For the climatic conditions on the territory of Novi Sad the Best Case Scenario adopted windows W4 from the energy efficiency aspect since it matched the criteria which



included the following definitions: possibly lower U-value than defined in regulations, low SHGC coefficient due to high internal gains (equal or below 0.3) and high VT value in case of qualitative illumination (above 0.5). the energy performance results of the Best Case Scenario is compared with the reference building expenses in Table V below.

TABLE V.  
ENERGY PERFORMANCE COMPARISON

Reference FTS office-tower (2012)			
	Heating energy [kWh]	Cooling, lighting and equipment electricity [kWh]	
Sum	378784	203810	
[kWh/m²/a]	110	59	
Indoor Environment	Unsatisfied	Unsatisfied	
Best Case Scenario – W4			
	Heating energy [kWh]	Cooling energy [kWh]	Energy demand for lighting and equipment [kWh]
Sum	27773	104191	106330
	prEN 15251:2014; air ventilation amount + 37325 (for heating) + 7330 (for cooling)		
[kWh/m²/a]	19	32	31
Indoor Environment	Satisfied	Satisfied	Satisfied

## VI. CONCLUSION

The investigation presented the significance on the reduction of annual energy performance of building envelope's thermal properties and the application of adequate windows in the function of climate conditions and building type. WWR and WG can be analyzed from the aspect of daylight intensity distribution in order to offer performable results without neglecting indoor environmental quality in offices. The WWR per single office was decreased from 50% to 30% and 25% per single office exterior wall area depending on the orientation. Thermal comfort parameters are included in the further directions of investigation in the function of minimizing annual heating and cooling loads, yet maintaining a comfortable indoor environment.

## ACKNOWLEDGMENT

This paper is a part of the research that is performed within the project "Development and application of contemporary procedures for design, construction and maintenance of buildings" founded by the University of Novi Sad, Faculty of Technical Sciences, Department of Civil Engineering and Geodesy in 2015.

## REFERENCES

- [1] Autodesk Revit Architecture, 2013, <http://www.autodesk.com/products/revit-family/overview>
- [2] Autodesk Ecotect Analysis, 2013, <http://usa.autodesk.com/ecotect-analysis/>

- [3] Desktop Radiance, 2013, <http://radsite.lbl.gov/deskrad/download.htm>
- [4] Sketchup Make, 2013, <http://www.sketchup.com/buy/education-licenses>
- [5] Open Studio, 2013, <http://openstudio.nrel.gov>
- [6] Energy Plus, 2013, <http://apps1.eere.energy.gov/buildings/energyplus>
- [7] Meteonorm 7, 2014, <http://meteonorm.com/en/downloads>
- [8] D.H.W. Li, "A review of daylight illuminance determinations and energy implications," *Applied Energy*, vol. 87, pp. 2109–2118, 2010.
- [9] I.T. Dogrusoy, M. Tureyen, "A field study on determination of preferences for windows in office environments," *Building and Environment*, vol.42, pp. 3660–3668, 2007.
- [10] K. Konis, "Evaluating daylighting effectiveness and occupant visual comfort in a side-lit open-plan office building in San Francisco, California," *Building and Environment*, vol. 59, pp. 662–677, 2013.
- [11] A. Roetzel, A. Tsangrassoulis and U. Dietrich, "Impact of building design and occupancy on office comfort and energy performance in different climates," *Building and Environment*, vol. 71, pp. 165–175, 2014.
- [12] A. Nabil, J. Mardaljevic, "Useful daylight illuminance: a replacement for daylight factors," *Energy and Buildings*, vol. 38, pp. 905–913, 2006.
- [13] N. Harmati, Z. Magyar, "Energy consumption monitoring and energy performance evaluation of an office building," *Proceeding of the Fifth German-Austrian IBPSA Conference BauSim*, Aachen, pp. 115–122, 22–24.09.2014.
- [14] N. Harmati, Z. Magyar and R. Folić, "Building energy performance evaluation from the comfort aspect," *Proceedings of the International Congress E-nova on FH Burgenland*, Pinkafeld, 13–15.11.2014.
- [15] F. Goia, M. Haase and M. Perino, "Optimizing the configuration of a facade module for office buildings by means of integrated thermal and lighting simulations in a total energy perspective," *Applied Energy*, vol. 108, pp. 515–527, 2013.
- [16] J.T. Kim, M.S. Todorovic, "Tuning control of buildings glazing's transmittance dependence on the solar radiation wavelength to optimize daylighting and building's energy efficiency," *Energy and Buildings*, vol. 63, pp. 108–118, 2013.
- [17] M.S. Mayhoub, D.J. Carter, "The costs and benefits of using daylight guidance to light office buildings," *Building and Environment*, vol. 46, pp. 698–710, 2011.
- [18] Official gazette RS no. 61/2011, Rules on conditions for the contents and manner of certificate issuance of energy performance for buildings, 2011.
- [19] Directive 2012/27/EU of 25 October 2012 on Energy Efficiency (amending Directives 2009/125/EC and 2010/30/EU and repealing Directives 2004/8/EC and 2006/32/EC (1)), Official Journal of the European Union No. L 315, vol. 55, pp. 1–56, 2012.
- [20] European Standards: prEN 15251 Annex B; Basis for the criteria for indoor air quality and ventilation rates; Recommended design ventilation rates in non-residential buildings, pp. 32–35, 2014.
- [21] Pilkington, 2014 <http://www.pilkington.com/de-de/de/architects>
- [22] N. Harmati, Z. Magyar, "Influence of glazing properties on the annual heating and cooling energy demand in buildings," 6<sup>th</sup> International Building Physics Conference, Turin, 14–17.06.2015., unpublished.
- [23] Nyers J., Tomic S., Nyers A.: "Economic Optimum of Thermal Insulating Layer for External Wall of Brick". I J Acta Polytechnica Hungarica Vol. 11, No. 7, pp. 209–222. 2014.

# Distributed mathematical model of the heat pump's evaporator with boundary condition

Jozsef Nyers Dr. Sci <sup>\*,\*\*</sup>, Jozsef Tick Dr. habil<sup>\*</sup>, Zoltan Pek PhD student<sup>\*</sup>

<sup>\*</sup> University Obuda Budapest, Hungary

<sup>\*\*</sup> VTŠ Subotica, Department of Energy, Subotica, Serbia

e-mail: [nyers@uni-obuda.hu](mailto:nyers@uni-obuda.hu)

[pekszoli@tippnet.rs](mailto:pekszoli@tippnet.rs)

EXPRES 2015 march 19-21

**Abstract**—the aim of this article is to present the heat pump evaporator's mathematical model with distributed parameters and boundary conditions. Additionally, applying the model is simulated behavior of the evaporator. The boundary conditions contain the heat transported fluid, the throttle valve and the compressor. The mathematical model consists of the refrigerant's balance differential equations, the equations of viscous friction coefficient, the convective heat transfer, and the state-state equation of refrigerant R134a. The heat transport fluid - well water is described by differential equations while throttle aperture and compressor with algebraic equations. For the solution of mathematical model an iterative numerical procedure was applied. Simulation results were obtained in numerical form and are presented graphically.

**Keywords**— evaporator; heat pump; mathematical model; distributed parameters; boundary conditions.

## Nomenclature

$\dot{m}$	Mass flow rate [ $kg/s$ ]
$\alpha$	Convective heat transfer coefficient [ $W/m^2/^\circ C$ ]
$\lambda$	Conductive heat transfer coefficient [ $W/m/^\circ C$ ]
$C_p$	Specific heat, $p = \text{const}$ [ $J/kg/^\circ C$ ]
$t, T$	Temperature [ $^\circ C$ ], [ $K$ ]
$dt$	Temperature difference [ $^\circ C$ ]
$f$	Function of viscous friction [ $-$ ]
$A$	Cross section area of flow [ $m^2$ ]
$di$	Latent heat [ $J/kg$ ]
$q$	Heat flux, performance [ $W$ ]
$Re$	Reynolds number [ $-$ ]
$Pr$	Prandtl number [ $-$ ]
$Fr$	Fraud number [ $-$ ]
$C$	Coefficient [ $s/kg^2/m$ ]
$\rho$	Density [ $kg/m^3$ ]
$\delta$	Thickness [ $m$ ]
$d$	Diameter [ $m$ ]
$w$	Velocity [ $m/s$ ]
$i$	Specific enthalpy [ $J/kg$ ]
$R$	Gas constant [ $J/kg K$ ]
$V$	Work Volume [ $m^3$ ]
$x$	Vapor quality [ $-$ ]
$p$	Pressure [ $Pa$ ]

Subscripts and superscripts

$w$	water
$f$	refrigerant (Freon)
$i$	input
$o$	output
$c$	critical
$v$	volumetric
$k$	critical
$eva$	evaporator
$com$	compressor
$con$	condenser
$h$	long-stroke

## I. INTRODUCTION

The evaporator is a very important component of the heat pump. In the evaporator heat transfer takes place between refrigerant and heat source fluid.

The efficiency of heat exchange in the evaporator is largely depends on the structural details and from external influences. Mathematically, intensity of heat exchange was taken using the convective heat transfer coefficient. Mathematically, the impact of external influences is taken over the boundary conditions.

Physically, components that exhibit an external influence on the evaporation of refrigerant in the evaporator are: throttle valve, compressor and fluid as a heat source.

Mathematically, some components represent boundary conditions. Boundary conditions are equations of the throttle valve, compressor and fluid as a heat source.

Since is examined the steady operation mode of the heat pump therefore the heat transfer process in the evaporator as well steady, does not depend on time. Governing equations that describe the evaporation of refrigerant in the evaporator are ordinary differential equations with distributed parameters. Differential equations are one-dimensional, as a function of the length but do not depend on time. For description of the thermal behavior of the refrigerant additional is necessary to apply equations of state. The equations of state are algebraic equations.

Boundary condition or external influence of the heat transport fluid is also one-dimensional ordinary differential equation with distributed parameters. The boundary condition equations of the throttle valve and the compressor are algebraic equations with lumped parameters.

Therefore the created mathematical model with distributed parameters for the description of heat transfer during evaporation in the evaporator consists of ordinary differential equations for the refrigerant and the transport fluid heat. Other boundary conditions, throttle valve and compressor, were described by algebraic equations with lumped parameters.

In the evaporator, evaporation takes place and the overheating of the refrigerant and therefore the mathematical model has two parts. Governing equations for the two parts are the same but the physical parameters of the refrigerant are different for vaporizing and superheating part. Changing parameters in the governing equations takes place if the vapor quality equal to  $x = 1$ . This is the case when the complete refrigerant liquid has evaporated and transferred in saturated vapor.

Since mathematically, the problem is "two-points", on the one side of the evaporator is throttle valve on the other side the compressor. Solving the model is possible using one of the iterative numerical mathematical processes.

## II. PHYSICAL MODEL OF THE EVAPORATOR WITH EXTERNAL IMPACT

Structurally, the considered evaporator is a coaxial tube heat exchanger. From thermal aspect, in the evaporator the heat transfer is performed between the refrigerant and the well water. In the observed case, refrigerant Freon R134a flows inside the evaporator tubes, while the cooled mass - the well water - flows inside the shell of evaporator.

In the evaporator, the parallel pipes are connected with the baffles. The baffles are placed perpendicular to the pipe bundle at a distance of about 150 mm in the direction of the tube axis. Water flows between the baffles like a sinusoid.

The evaporator works most efficiently when the full length of parallel pipes is filled with refrigerant which still contains the liquid phase. The quantity of evaporated refrigerant depends on the compressor capacity; the temperature and the mass flow rate of well water respectively.

The thermo-expansion (TEX) valve doses an adequate quantity of refrigerant into the evaporator. This valve uses the sensors monitors the temperature and the pressure of the outlet refrigerant from the evaporator. Based on the measured temperature and pressure, the valve carries out optimal dosing of the refrigerant.

In case of a refrigerant quantity deficit, the shorter length of the pipes evaporates the liquid phase of refrigerant, and in the remaining part of the evaporator

flows only vapor which superheats. The heat transfer of the Freon's' vapor phase is multiple times lower than of the liquid phase. The vapor of the refrigerant in the dry section superheats.

Over-dosing of the refrigerant means that the liquid phase cannot evaporate and some quantity of the liquid phase leaves the evaporator. This phenomenon reduces the refrigeration effect, for example the performance of the heat pumps' evaporator. Interpretation: non-evaporated liquid phase evaporates in the compressor. Consequently, hydro hammer can happen in the compressor. In the correct operation mode from the evaporator dry vapor flows out, superheating up to 4 °C.

The evaporator is connected to the compressor. From the aspect of the evaporator, the compressor only sucks out the superheated vapor from the evaporator. From the aspect of compressor, the compressor using mechanical work compresses the vapor which primarily increases the temperature on the adequate level. The compression is unfortunately accompanied with intensive increase of the pressure as well.

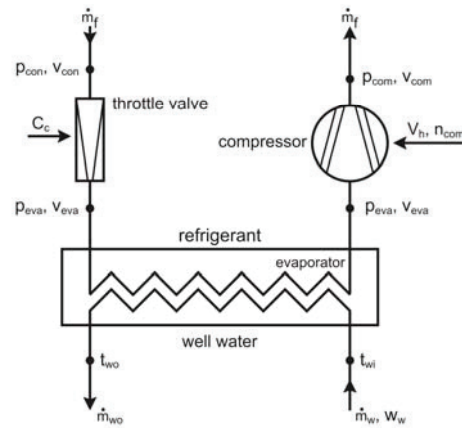


Figure 1.  
The physical model of the heat pumps' evaporator with the system parameters

## III. DISTRIBUTED MATHEMATICAL MODEL OF THE EVAPORATOR WITH BOUNDARY CONDITIONS

### A. GOVERNING EQUATIONS OF REFRIGERANT

#### a. Balance equations of the refrigerant

Mass conservation

$$\frac{\partial(\rho \cdot w)}{\partial z} = 0 \quad \rho \cdot w \equiv \dot{m} = \text{const.} \quad (1)$$

Impulse conservation

$$\frac{\partial(\rho \cdot w \cdot w + p)}{\partial z} + f(x) = 0 \quad (2)$$

Energy conservation

$$\frac{\partial(\rho \cdot w (w \cdot w / 2 + i))}{\partial z} - q(x) = 0 \quad (3)$$

b. Energy balance equation of the pipe wall using the energy conservation law

$$C_{cv} \cdot (T_w - T_c) - C_{cf} \cdot (T_c - T_f) = 0 \quad (4)$$

## B. AUXILIARY EQUATIONS OF REFRIGERANT

a. State equations of the refrigerant R 134a

The equations are applicable at the following conditions:

$$0.60 < T_r = T/T_c < 0.96$$

$$0.5 [\text{bar}] < p < 25 [\text{bar}]$$

$$T_{max} = 500 [\text{K}]$$

$$T_c = 374.21 [\text{K}]$$

$$p_c = 40.5 [\text{bar}]$$

$$p_r = p/p_c$$

b. The balance equation according to Wagner

$$\ln p_r = \frac{1}{T_r} \cdot \left[ A_1 \cdot (1 - T_r) + A_2 \cdot (1 - T_r)^{B1} + A_3 \cdot (1 - T_r)^{B2} + A_4 \cdot (1 - T_r)^{B3} + A_5 \cdot (1 - T_r)^{B4} + A_6 \right] \quad (5)$$

c. The parameters of the saturated refrigerant vapor

Specific enthalpy of the mixture

$$i = i' + x \cdot (i'' - i') \quad (6)$$

Specific internal energy of the mixture

$$u = u' + x \cdot (u'' - u') \quad (7)$$

Specific volume of the mixture:

$$v = v' + x \cdot (v'' - v') \quad (8)$$

d. State equation of R134a according to Martin - Hou for the superheated area

$$p = \frac{R \cdot T}{V - b} + \sum_{i=2}^5 \frac{A_i + B_i T + C_i \exp(-KT/T_{crit})}{(V - b)^i} \quad (9)$$

Where:

$$b = 2.99628 \cdot 10^{-4} [\text{m}^3/\text{kg}]$$

$$K = 5.475$$

e. Specific enthalpy of the Freon vapor

$$i(T_r, v) = i_o + (p \cdot v - R \cdot T) + D_1 \cdot T + D_2 \cdot T^2/2 + D_4 \cdot \ln T + E_1/z + E_2/2z + E_3/3z + E_4/4z + e^{-kT_r} \cdot (1 + k \cdot T_r) \cdot (G_1/z + G_2/2z^2 + G_4/4z^4) \quad (10)$$

f. Pressure drop in the single-phase and the bi-phase of refrigerant  $f(x)$

Friedel's [2] mathematical model of pressure drop is used in the area of single-phase and bi-phase evaporation as well.

$$\frac{\Delta p}{dz} = \Phi^2 \cdot \left( \frac{dp}{dz} \right)_f \quad (11)$$

Pressure drop factor of the liquid phases

$$\left( \frac{dp}{dz} \right)_f = \frac{4 \cdot \lambda_f \cdot G^2}{2 \cdot D \cdot \rho_f} \quad (12)$$

Where:

- $\lambda_f$  friction factor according to Blasius for the liquid phase
- $\Phi^2$  characteristics of the friction factor in bi-phase flow

g. Latent heat as a function of the evaporation temperature

$$di = a_o + a_1 \cdot t_{fo}^1 + a_2 \cdot t_{fo}^2 \quad (13)$$

Where the constants of the refrigerant R 134a are:

$$a_o = 200.5965715$$

$$a_1 = -0.709168$$

$$a_2 = -0.00596796$$

h. Evaporative heat transfer coefficient of the refrigerant

Kandlikar's improved mathematical model was used for the determination of the evaporative heat transfer coefficient of refrigerant inside the pipe. The same model was used for single-phase and bi-phase refrigerant as well. The result is taken as the maximum value of the calculated two.

$$\alpha_{tp} = \max [\alpha_n, \alpha_c] \quad (14)$$

i. Heat transfer coefficient of the convective area

$$\alpha_n = 0.6683 \cdot Co^{-0.2} \cdot (1 - x)^{0.8} \cdot \alpha_{lo} \cdot f[Fr_{lo}] + 1058 \cdot Bo^{0.7} \cdot (1 - x)^{0.8} \cdot F_{FL} \cdot \alpha_{lo} \quad (15)$$

j. Heat transfer coefficient of the bubble area

$$\alpha_c = 1.136 \cdot Co^{-0.9} \cdot (1 - x)^{0.8} \cdot \alpha_{lo} \cdot f[Fr_{lo}] + 667.2 \cdot Bo^{0.7} \cdot (1 - x)^{0.8} \cdot F_{FL} \cdot \alpha_{lo} \quad (16)$$

## C. BOUNDARY CONDITIONS

a. Equation of the well water which flows through the evaporator, based on the energy conservation

$$\pm w_v \cdot \frac{\partial T_w}{\partial z} + C_w \cdot (T_w - T_c) = 0 \quad (17)$$

Mathematical model of the heat transfer coefficient of well water according to Hausen

$$\alpha_w = 0.0222 \cdot Re_w^{0.6} \cdot Pr_w^{0.33} \cdot \frac{\lambda_w}{d_k} \quad (18)$$



- $Re_w$  Reynolds number of well water
- $Pr_w$  Prandtl number of cooled mass - well water
- $d_k$  Outside diameter of pipe

#### b. Equation of the throttle valve

The pressure drop due to flow through the throttle aperture is calculated using the Darcy-Weissbach relation.

$$\Delta p = p_{con} - p_{eva} = C_c \cdot w^2 \quad (19)$$

Throttling aperture is adjustable. In the equation for pressure drop throttle is regulated by coefficient  $C$ . Coefficient  $C_c$  is

$$C_c = \xi(geom) \cdot \frac{\rho}{2} \quad (20)$$

Where

- $\xi$  (geom) coefficient of the local resistance to flow depends on the geometry of the aperture
- $\rho$  the density of the refrigerant in the flow cross-section of the aperture

Value of the coefficient  $0 < C_c < C_{c\max}$

If the coefficient is equal to zero, the aperture is fully closed and the mass flow rate is zero if the coefficient maximum aperture is totally opened and the mass flow rate is maximum.

#### c. Equation of the compressor

The mechanism of the compressor is with piston and clearance volume- dead space.

The clearance volume of dead space

$$V_c = V_h \cdot C_c \quad (21)$$

Where:

- $V_h$  working volume of the piston
- $C_c$  coefficient of the clearance volume (3-7)%

The total volume of the cylinder

$$V = V_h + V_c \quad (22)$$

Volume of the expanded superheated vapor from dead space

$$V_{exp} = V_c \cdot \frac{v_{eva}}{v_{com}} \quad (23)$$

Volume of the sucked vapor quantity from the evaporator

$$\Delta V = V - V_{exp}$$

$$\Delta V = V_h + V_c - V_c \cdot \frac{v_{eva}}{v_{com}}$$

$$\Delta V = V_h + V_h \cdot C_c - V_h \cdot C_c \cdot \frac{v_{eva}}{v_{com}}$$

$$\Delta V = V_h \cdot \left(1 + C_c - C_c \cdot \frac{v_{eva}}{v_{com}}\right) \quad (24)$$

Mass of the sucked vapor from the evaporator is for one rpm of the compressor.

$$m = \frac{\Delta V}{v_{eva}} = \frac{V_h}{v_{eva}} \cdot \left(1 + C_c - C_c \cdot \frac{v_{eva}}{v_{com}}\right) \quad (25)$$

Mass flow rate of the superheated and compressed vapor by the compressor.

$$\dot{m} = m \cdot n_{com} = \frac{V_h}{v_{eva}} \cdot \left(1 + C_c - C_c \cdot \frac{v_{eva}}{v_{com}}\right) \cdot n_{com} \quad (26)$$

Compression of the superheated vapor is carried by polytropic

$$\frac{v_{eva}}{v_{com}} = \left(\frac{p_{com}}{p_{eva}}\right)^{1/n} \quad (27)$$

Exponent of the polytropic compression

$$(izoterma) 1 < n < \frac{C_p}{C_v} \quad (adiabata)$$

Mass flow rate of the superheated vapor through the compressor

$$\dot{m} = \frac{V_h}{v_{eva}} \cdot \left(1 + C_c - C_c \cdot \left(\frac{p_{com}}{p_{eva}}\right)^{1/n}\right) \cdot n_{com} \quad (28)$$

Where:

- $v_{eva}$  vapor specific volume on the end of evaporator
- $v_{com}$  vapor specific volume on the end of compression
- $p_{eva}$  vapor pressure on the end of evaporator
- $p_{com}$  vapor pressure on the end of compression
- $n_{com}$  rpm of the compressor
- $C_p$  specific heat of the vapor at  $p = \text{const.}$
- $C_v$  specific heat of the vapor at  $v = \text{const.}$

#### IV. NUMERICAL METHOD

Mathematical model consists of system coupled differential equations with boundary conditions. The boundary conditions are algebraic equations to describe the behavior of throttle valve and the compressor and differential equation of well water.

For solving the mathematical model the numerical recursive procedure Runge-Kutta and iterative Mac Adams were applied. The procedure of Runge-Kutta is used only for getting initial solutions. Mac Adams procedure converge the initial solutions using iterative manner to the accurate values. Namely, the recursive procedure Runge-Kutta solves only one-point boundary problems; in our case, the problem is two-points. The system of the differential equations with two-point boundary conditions is solved by an iterative procedure, one of these is Mac. Adams. The obtained results are numerical and presented visually in graphical form. Graphics are visible in Figure 2 and 3.

## V. SIMULATION RESULTS

The obtained results are based on the created mathematical model and numerical methods. These results are presented in the Figures 2, and 3.

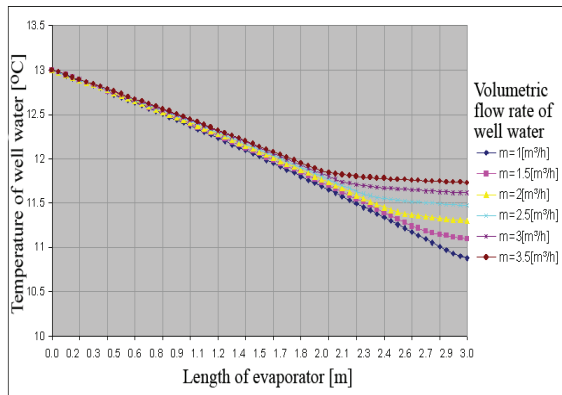


Figure 2.  
Well water temperature in the evaporator as a function of the pipe length

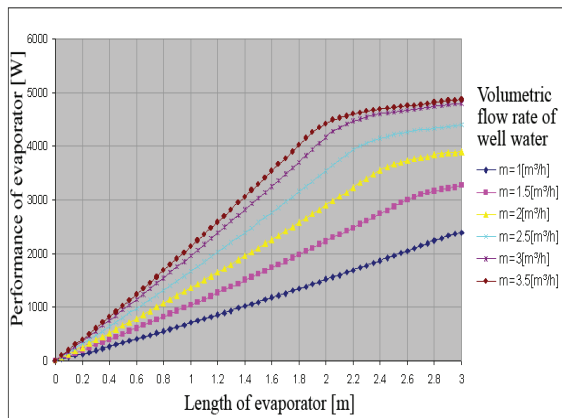


Figure 3.  
Evaporator's thermal performance as a function of the pipe length

## VI. CONCLUSION

- The stationary mathematical model of the evaporator consists of the system coupled differential equations and the explicit and implicit non-linear algebraic equations,
- the model is one-dimensional with distributed parameters, for steady-state operation mode,
- Solving the mathematical model is possible only numerically,
- The applied numerical procedure is iterative.
- The accuracy of the mathematical model depends largely on the applied heat transfer coefficient of both streaming fluids,
- Based on the tested five models, Kandlikar's heat transfer coefficient model of the refrigerant proved the most appropriate. [4],
- With increasing the well water's mass flow rate: Decreases the length of evaporation, increases the refrigeration capacity of the evaporator, the

quantity of superheated vapor increases and tends asymptotically towards a constant value, by increasing the mass flow rate of well water, the water temperature decreases.

## References

- [1] Martin J. J., Hou Y. C.: Development of an equation of state for gases, AIChEJ, 1955, 1: 142.
- [2] Satish G. Kandlikar: Heat transfer and fluid flow in mini-channels and micro-channels, Mechanical Engineering Department, Rochester Institute of Technology, NY, USA.
- [3] Fridel L.: Improved Friction Pressure Drop Correlations for Horizontal and Vertical Two-Phase Pipe Flow, European Two-Phase Flow Group Meeting, (1979), Ispra, Italy, June, Paper E2.
- [4] Róbert Sánta: „The Analysis of Two-Phase Condensation Heat Transfer Models Based on the Comparison of the Boundary Condition” Acta Polytechnica Hungarica Vol. 9, No. 6, 2012, pp. 167-180.
- [5] Yi-Yie Yan, Hsiang-Chao Lio, Tsing-Fa Lin: ”Condensation heat transfer and pressure drop of refrigerant R-134a in a plate heat exchanger” I. J. of Heat and Mass Transfer Vol. 42 (1999), pp. 993-1006.
- [6] Imrich Bartal, Hc László Bánhidi, László Garbai: ”Analysis of the static thermal comfort equation” Energy and Buildings Vol. 49 (2012), pp. 188-191.
- [7] Garbai L., Méhes Sz.: Energy Analysis of Geothermal Heat Pump with U-tube Installations. IEEE International Symposium CFP 1188N-PRT EXPRES 2011. Proceedings, pp. 107-112. Subotica, Serbia. 11-12 03. 2011.
- [8] Nyers J., Garbai L., Nyers A.: “Analysis of Heat Pump's Condenser Performance by means of Mathematical Model”. I. J. Acta Polytechnica Hungarica, Vol. 11, No. 3, pp. 139-152, 2014.
- [9] Nagy Károly, Divéki Szabolcs, Odry Péter, Sokola Matija, Vujicic Vladimir: "A Stochastic Approach to Fuzzy Control", I.J. Acta Polytechnica Hungarica, Vol. 9, No 6, 2012, pp. 29-48. (ISSN: 1785-8860).
- [10] Kajtár L., Hrustinszky T.: Investigation and influence of indoor air quality on energy demand of office buildings. WSEAS Transactions on Heat and Mass Transfer, Issue 4, Volume 3, October 2008. 219-228 p.
- [11] László Kajtár, Miklós Kassai, László Bánhidi: Computerised simulation of the energy consumption of air handling units. 2011. Energy and Buildings, ISSN: 0378-7788, (45) pp. 54-59.
- [12] László Kajtár, Levente Herczeg: Influence of carbon-dioxide concentration on human wellbeing and intensity of mental work. Bp. 2012. Időjárás, Quarterly Journal of the Hungarian Meteorological Service, Vol. 116 No.2 april-june 2012. p. 145 – 169. ISSN 0324-6329.

# The effect of thermal insulation of an apartment house on thermo-hydraulic stability of the space heating system

Mária Kurčová\*

\* Slovak University of Technology in Bratislava, Faculty of Civil Engineering,  
Department of Building Services, Slovakia  
e-mail: maria.kurcova@stuba.sk  
EXPRES 2015

**Abstract** - The contribution aims investigation of the effect of decreased thermal losses of an apartment house due to thermal insulation of external opaque building constructions and replacement of transparent constructions. It emphasizes the effect of thermal characteristics of the external constructions on functionality of the existing heating system in the building, and the related requirements on renovation of the heating system in order to ensure hydraulic stability of the system and thermal comfort of the inhabitants.

**Key words** – insulation, space heating, hydraulic stability

## I. INTRODUCTION

The construction of apartment buildings started expanding in 1950 in Slovakia. Best technologies and procedures available were used in the construction process that time. External constructions were being made from materials with the thermal characteristics corresponding to the regulations and standards valid in the time of their construction.

Currently, the standard STN 73 0540 is valid since 1<sup>th</sup> January 2013. There are four values of thermal resistance given in the standard: minimum, normalized, recommended and target [12].

The requirements on minimum level of thermal insulation of building constructions, in terms of heat transfer coefficient (U-value), has become stricter comparing to the values valid in 1964 and 1977. This implies an energy saving potential after refurbishment of 50 to 60 %.

The main objective is to analyse the effect of thermal insulation of the apartment house envelope on the heat loss, and subsequently the effect of the change in the heat loss on hydraulic balance of the heating system from the thermo-hydraulic stability point of view. Based on this analysis, the convenience of different types of control valves applied in the existing heating systems in buildings after renovation is to be determined from their function and construction parameters point of view.

## II. MATHEMATICAL MODEL

The method is based on a parametrical study of the effect of the change in thermal characteristics of building envelope on thermal heat loss, and of the effect of the volume flow rate of the heating medium on pressure conditions in the heating system and on hydraulic stability, by own mathematical calculation tool created in Microsoft Excel®.

A mathematical model of thermo-hydraulic stability was created in order to be applied on the apartment houses investigated (see Fig. 1).

Following applies to the mathematical model [3, 4]:

- for each node of the heating system a so called “node rule“ applies, which expresses the balance of the flows from one node to another,
- for each radiator circuit, a so called “circuit rule“ applies, which expresses the balance of pressures causing circulation of the heating medium, i.e. the balance of active pressure gradients and passive pressure gradients (pressure losses),
- for each radiator and heated space, the balance of proportional heat flows supplied by the heating medium into the radiator, proportional flows emitted into the heated space by the radiator and proportional heat losses of the heated space, applies.

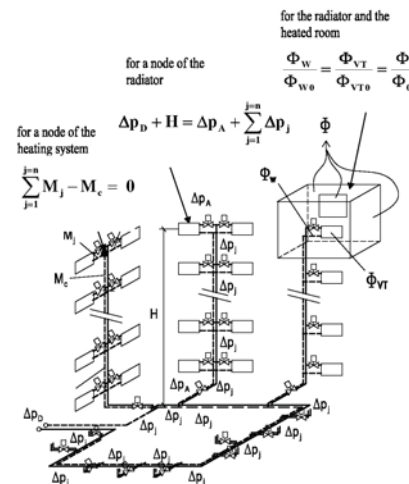


**Fig. 1** Mathematical and physical model of thermo-hydraulic stability for the apartment house

Description:  $M_j$  – volume flow to a node (kg/s),  $M_c$  – volume flow from a node (kg/s),  $\Delta p_D$  – pressure difference at the connection to the heating system (Pa),  $H$  – effective uplift (Pa),  $\Delta p_A$  – pressure loss of the valves (Pa),  $\Delta p_j$  – pressure loss of a section of the distribution network (Pa),  $\Phi_W$  – immediate thermal flow of the radiator (W),  $\Phi_{VT}$  – immediate thermal output of the radiator (W),  $\Phi$  – immediate thermal loss of the room (W),  $\Phi_{W0}$  – calculation heat flow supplied to the radiator (W),  $\Phi_{VT0}$  – calculation thermal output of the radiator (W),  $\Phi_0$  – calculation heat loss of the room (W)

**Tab.1** Thermal characteristics of the envelope constructions of the two apartment houses

Construction	Heat transfer coefficient U (W/(m <sup>2</sup> .K))	
	Original house	Refurbished house
External walls	1.09	0.28
Roof	0.83	0.17
Ceiling of the	2.83	0.75

underground floor		
Transparent constructions	2.7	1.2

The buildings investigated in this experimental study are two eight-floor buildings with an unheated underground floor, located next to each other in Bratislava. The apartment house referred to as “original” has its building constructions in original conditions. The apartment house referred to as “refurbished” has external walls, the roof and the ceiling of the underground floor insulated and the old windows have been replaced by new ones. Thermal characteristics of both buildings are listed in **Tab.1**.

In both buildings the heating system is with two pipes and bottom uniflow distribution – Tichelmann. The heating system is directly connected to district heating. In the original house there are high-resistance valves installed before each radiator, set on low pressure loss. On each raisers there is a combination of pressure difference controller with a balancing valve. Stop valves are installed at the connection to the heating system (connection to the heating system is the point, where the primary network enters the building and becomes the heating system in the building). In the refurbished apartment house, there are also high-resistance valves installed before each radiator, set on high pressure loss. On each raiser there are spherical valves, at the connection to the heating system there is a combination of pressure difference controller and a balancing valve. Both heating systems are with hydraulic balance.

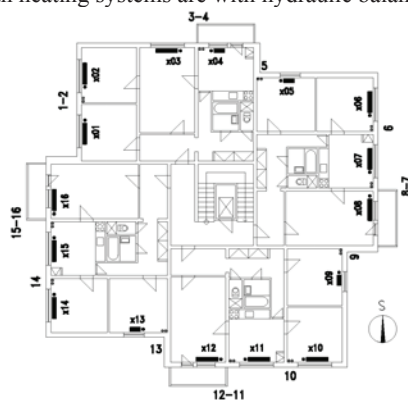


**Fig. 2** Plan of a typical floor

### III. THE EFFECT OF REFURBISHMENT ON THERMAL LOSSES

After refurbishment of the envelope constructions, the thermal characteristics of the building have changed, as shown in **Tab. 1**. In **Fig. 2** are the results of the calculation for the whole building and for a reference (typical) room in accordance with STN EN 12831 for the original house and for the refurbished house, respectively [10]. The refurbishment of the envelope constructions is given for two variants: for a typical refurbishment (insulation of external walls and replacement of windows, and for a complex refurbishment (insulation of external walls, replacement of windows, insulation of the roof and insulation of the underground floor).

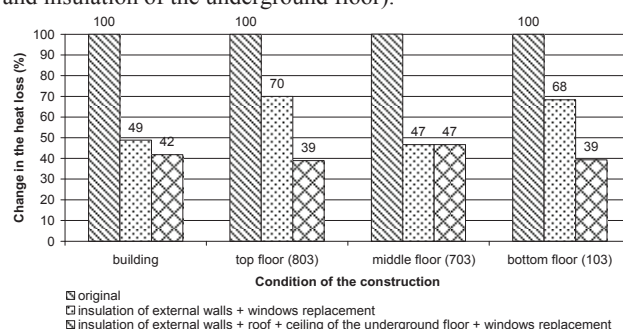


**Fig. 3** Change in the building heat loss and a reference room on the top, middle and lowest floor

From **Fig. 3** it can be seen that after implementation of the energy saving measures the change in thermal losses of the rooms located on typical floors is of the same magnitude as for the whole building. After insulation of external walls and replacement of transparent constructions, the thermal losses decrease by about 50 %. However, the thermal losses of the rooms located on the top and the bottom floor decrease by only about 30 %. After additional thermal insulation of the roof and the ceiling of the underground floor, the thermal losses of the top and the bottom floor also decrease by 60 %. Thus, the rooms located in the middle of the building, the rooms located at the top and at the bottom, and also the building as a whole, have the same decrease in thermal losses after complex thermal insulation.

From the comparison of the effect of the respective energy saving measures applied on the envelope it can be seen that it is not correct to base the calculation of the heat loss decrease only on the heat loss calculated for the whole building, but it is important also to check the heat loss of each room, which can differ significantly, depending on the location in the building. The most frequent energy saving measures – insulation of external walls and replacement of old windows – decrease the heat loss on the middle floor to 50 %, however, on marginal floors the decrease can be only to 70 %. Taking this into consideration, it can be either assumed that the heat loss to be only 70 % on each floor, or that the heat loss decreased to 50 % and subsequently to replace the radiators on the top and on the bottom floors. However, both of these two approaches are non-profitable. Therefore, in the refurbishment process it is necessary to insulate also roof and ceiling of the underground floor in order to make the decrease in heat loss uniform throughout the building, which is important in the process of design and correction of the heating system. Otherwise, the heat loss of the rooms located on the marginal floors may not be fully covered by the heat output of the radiators.

### IV. THE EFFECT OF REFURBISHMENT ON PRESSURE CONDITIONS IN THE HEATING SYSTEM

Taking into account that the heating system is directly connected to district heating, it is not possible to decrease the heat flow transferred by the heating system by decreasing the temperature gradient of the heating system. Such a measure would require high investments and operation costs. Therefore, it is suggested that the adjustment of the transferred heat flow to the actual heat loss of the object of the building is realized by changing the volume flow rate of the heating medium proportionally, in the proportion as defined in the previous section, thus to 70 % or to 50 %.

Setting of the thermal losses to the changes in the temperature of outside air is performed on the heat source, by means of equithermic curve, thus by changing the temperature of the heating medium.

The thermo-hydraulic stability of the heating system is affected by:

- the temperature of the heating medium by means of the effective uplift,
- the volume flow rate of the heating medium by means of pressure losses.

In the process of refurbishment, the system has to be designed so as the change in the abovementioned parameters affects the thermo-hydraulic stability as little as possible. Since the distribution system remains the same and the effective uplift in the heating system is given by the construction height of the building, the only means of assuring the thermo-hydraulic stability is regulation valves.

The calculation of the pressure conditions was performed for the heating system on the top floor (indicated as 803 in **Fig.**



2), based on relationships thoroughly described in the literature [2, 3, 5].

The values of effective uplift, obtained from the equithermic curve for the temperature gradient of the heating medium of 90/70 °C and for the indoor air temperature of 20 °C [7], are given in Tab. 2. In the calculation, the effective uplift ratio of  $u = 0.5$  (the value commonly used by designers) and of  $u = 1.0$  (the real effective uplift in the heating system) was assumed.

**Tab. 2** Effective uplift for the radiator on the top floor at the height of 20.5 m above the reference plane

$\theta_{ac}$ (°C)	$\theta_p$ (°C)	$\theta_v$ (°C)	$\Delta\theta$ (°C)	$\theta_s$ (°C)	$\varepsilon$ (-)	$H_{u=1}$ (Pa)	$H_{u=0.5}$ (Pa)
-11	90.0	70.0	20.0	80.0	0.622	2502	1251
-4	77.2	61.8	15.5	69.5	0.567	1766	883
0	69.6	56.7	12.9	63.2	0.531	1378	689
4	61.7	51.3	10.3	56.5	0.491	1019	510
8	53.3	45.5	7.7	49.4	0.447	696	348
13	39.4	35.5	3.9	37.5	0.360	280	140

$\theta_{ac}$  – temperature of the outside air (°C),  $\theta_p$  – temperature of the supplied heating medium (°C),  $\theta_v$  – temperature of the return heating medium (°C),  $\Delta\theta$  – difference between the supply and return temperature of the heating medium (°C),  $\theta_s$  – mean temperature of the heating medium (°C),  $\varepsilon$  – coefficient expressing change in the density of the heating medium (-),  $H_{u=1}$  – effective uplift at the value of  $u = 1.0$  (Pa),  $H_{u=0.5}$  – effective uplift at the value of  $u = 0.5$  (Pa)

The pressure conditions, occurring in the heating system, are calculated for the following valves:

- low-resistance valves before radiators, closing valves at the bottom of risers and at the connection to the heating system – the pressure gradient at the connection to the heating system is variable - the evaluation was done for the pressure difference of 4 kPa and 12 kPa, respectively, pressure loss of the pipe network is  $\Delta p_p = 4332$  Pa at 100 % volume flow rate,  $\Delta p_p = 2132$  Pa at 70 % volume flow rate,  $\Delta p_p = 1163$  Pa at 50 % volume flow rate,
- high-resistance valves before the radiators – the pressure gradient at the connection to the heating system is constant - the pressure gradient at the connection to the heating system kept constant at 10 kPa, pressure loss of the pipe network is  $\Delta p_p = 4332$  Pa at 100 % volume flow rate,  $\Delta p_p = 2132$  Pa at 70 % volume flow rate,  $\Delta p_p = 1163$  Pa at 50 % volume flow rate,
- for a static hydraulic balance of the heating system – high-resistance valves with a pre-set, located before the radiators, balancing valves with a pre-set, located at the bottom of risers, a pressure difference controller, located at the connection to the heating system – the pressure gradient at the connection to the heating system is constant - the pressure difference at the connection to the heating system is kept constant, 13 kPa, pressure loss of the pipe network is  $\Delta p_p = 7332$  Pa at 100 % volume flow rate,  $\Delta p_p = 3337$  Pa at 70 % volume flow rate,  $\Delta p_p = 1763$  Pa at 50 % volume flow rate,
- for a dynamic hydraulic balance of the heating system – high-resistance valves with a pre-set and a temperature controller, located before radiators, balancing valves and pressure difference controllers, located at the bottom of risers and at the connection to the heating system – vertical piping was evaluated - pressure gradient at the bottom of risers is kept constant at 7 kPa, pressure loss of the pipe network is  $\Delta p_p = 1656$  Pa at 100 % volume flow rate,  $\Delta p_p = 798$  Pa at 70 % volume flow rate,  $\Delta p_p = 459$  Pa at 50 % volume flow rate.

The pressure conditions on the radiators in the heating system with valves before radiators, for the four cases investigated in this study, are in Figs. 5 and 6.

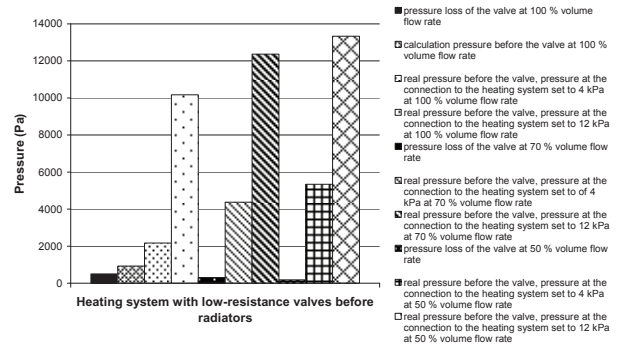


**Fig. 5** Pressure conditions on the radiator in the heating system with low-resistance valves before radiators

From the graph in **Fig. 5** it can be seen that before the refurbishment at 100 % volume flow rate of the heating medium, the calculation pressure loss of the valve and the calculation pressure before the valve are virtually the same (columns 1 and 2). However, in the reality the pressure before the valve relative to the pressure loss of the heating system is much higher (column 3) due to the high effective uplift. Column 4 shows that the destabilisation of the pressure gradient at the connection to the heating system causes an increase of the pressure before the radiator valve to the extent that the valve cannot cope with, resulting in a significant disbalance of the system. The situation is further exacerbated by decreasing the volume flow rate in consequence of thermal insulation of the building, when the difference between the pressure loss on the valve (columns 5 and 8) and the pressure before the valve (columns 6, 7 and 9, 10) grows significantly. For this reason, low-resistance valves are no more suitable for current heating systems. Moreover, assuring constant pressure at the connection to the heating system is necessary.

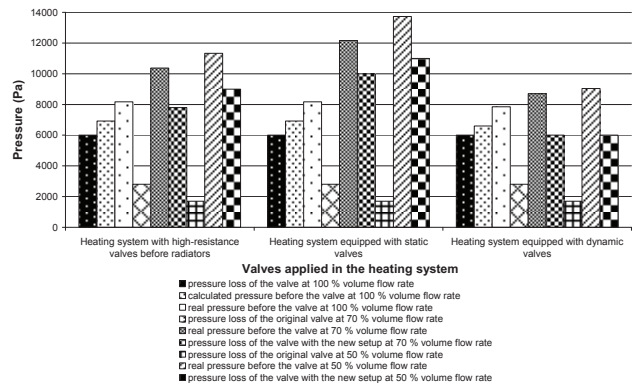


**Fig. 6** Pressure conditions on the radiator

In **Fig. 6** it can be seen that when using high-resistance valves, the influence of effective uplift on the pressure conditions before the valve is negligible (columns 2 and 3). When the volume flow rate is decreased, the pressure loss of the heating network, as well as the pressure loss of the valve before the radiator (columns 4 and 7), decrease, and the system becomes unbalanced from the hydraulic conditions point of view (columns 5 and 8). The difference between the pressure loss of the valve before the radiator and the pressure before the valve increases even more after installation of balancing valves (static valves – they work in a way similar to the pipe network) at the bottom of risers (columns 5 and 8 - solution 2). Therefore, after insulation of building envelope and the subsequent decrease of the volume flow rate, it is necessary to change the pre-set of the valve before the radiator (if the valve construction allows to do so) or to replace the valve for a more suitable one (columns 6 and 9). If the pressure before the valve is as high that the valve is not able to cope with it, it is

necessary to split the heating system to two separate hydraulic sections (solution 3) and to install a balancing valve in combination with a pressure difference controller at the bottom of risers.

## V. THE EFFECT OF REFURBISHMENT ON THERMO-HYDRAULIC STABILITY OF THE HEATING SYSTEM

The variations in the volume flow rate through the heating system in result of thermal insulation of the envelope affect the pressure conditions in the heating system, and thereby the thermo-hydraulic stability of the heating system. The extent of this effect can be quantified by the degree of hydraulic stability  $X$ , expressed through the volume flow rate or through the pressure difference (pressure gradient) [1, 4]:

$$X = \frac{M}{M_0} \quad (-) \quad (1)$$

$$X = \left( \frac{\Delta p}{\Delta p_0} \right)^{0.5} \quad (-) \quad (2)$$

$M$  – immediate volume flow rate of the heating medium through

a section of the heating system (kg/s),

$M_0$  – calculation volume flow rate of the heating medium through a section of the heating system (kg/s),

$\Delta p$  – immediate pressure difference referring to the corresponding section of the distribution network (Pa),

$\Delta p_0$  – calculation pressure difference referring to the corresponding section of the distribution network (Pa).

The degree of hydraulic stability compares the actual immediate condition with the calculated condition. The degree of hydraulic stability of at least 0.7 is recommended for two-pipe heating systems [3].

By decreasing the volume flow rate of the heating medium in consequence of thermal insulation of the apartment house to the value of 70 % or 50 % of the original calculation volume flow rate, the degree of hydraulic stability, calculated in accordance with the equation (1), will be 0.7 and 0.5, respectively. In the former case, the boundary value is still reached, but in the latter case the degree of hydraulic stability indicates an unstable heating system.

**Tab. 3** Degree of hydraulic stability of the heating system before and after renovation

Valves in the heating system	Degree of hydraulic stability X (%)			
	Variation of the volume flow rate			
	Original valves		Valves with new setting	
	70 %	50 %	70 %	50 %
A1) system with low-resistance valves before radiators – pressure gradient of 4 kPa	0.78	0.58	-	-
A2) system with low-resistance valves before radiators – pressure gradient of 12 kPa	0.45	0.33	-	-
B) system with high-resistance valves before radiators	0.70	0.50	0.99	0.997
C) system with static hydraulic balance	0.69	0.52	0.997	0.99
D) system with dynamic hydraulic balance	0.55	0.48	0.99	0.97

Formulation of the degree of hydraulic stability through volume flow rates in accordance with equation (1) does not consider the way the heating system is balanced. On the other hand, the degree of hydraulic stability expressed through pressure gradients in accordance with equation (2) takes into account also the influence of the heating system and its components. Therefore, it is more efficient to calculate the degree of hydraulic stability based on equation (2). The degree of hydraulic stability, calculated based on the pressure gradients in the heating system for different types of valves in the system before and after refurbishment of the heating system (replacement of valves before the radiator), is listed in Tab. 3.

From **Tab. 3** it can be seen that by decreasing the volume flow rate of the heating medium in consequence of thermal insulation of the building, without any intervention to the heating system, a required degree of hydraulic stability of  $X \geq 0.7$  is achieved only in case with high-resistance valves (case B). After the refurbishment of the heating system by replacement the low-resistance valves with high-resistance valves and by changing the setting of pressure gradients of the existing high-resistance valves or eventually by replacement of the valves, the degree of hydraulic stability of the existing heating system increases above 0.9. Increasing of the degree of hydraulic stability has a positive effect of uniform distribution of the volume flow rates among the radiators.

## VI. CONCLUSION

In the present contribution, thermal and hydraulic conditions are analysed for heating systems of two apartment houses, one being in the original condition and the other being after refurbishment of building constructions, the refurbishment having a significant effect on thermal losses of the object and subsequently on hydraulic conditions and hydraulic stability of the heating system. On the basis of analysis the effect of change of thermal characteristics of the building envelope on thermal losses of the building, and subsequently the effect of the decrease in thermal losses on hydraulic conditions in the heating system from thermo-hydraulic stability point of view, it can be concluded that a refurbishment of the envelope constructions of the building has to be followed by a refurbishment of the heating system. After the refurbishment, it is necessary to replace the low-resistance valves by high-resistance valves. The installation of the high-resistance valves results in an increased degree of hydraulic stability. A constant pressure gradient has to be set at the connection to the heating system, by installing a pressure difference controller in combination with a balancing valve. By following these recommendations, an energy saving of 40 to 50 % can be achieved.

## REFERENCES

- [1] ANDREAS, U., WINTER, A., WOLFF, D.: Regelung Heiztechnischer Anlagen, VDI-Verlag, Düsseldorf, 1985. ISBN 318 400 6905
- [2] BURKHARDT, W., KRAUS, R.: Projektierung von Warmwasserheizungen. 7 Auflage. Oldenburg Industrie Verlag, München, 2006.
- [3] PEKAROVIČ, J.K., PETRÁŠ, D., LULKOVIČOVÁ, O., TAKÁCS, J.: Vykurovanie. II. diel. SVŠT, Bratislava, 1994. ISBN 85-230-94
- [4] PETITJEAN, R.: Total hydronic balancing. 2nd Edition. Responstryck, Boras, 1997.
- [5] ROOS, H.: Hydraulik der Wasserheizung. 5. Auflage. Oldenburg Verlag, München, 2002. ISBN 3-486-26521-6
- [6] CHMÚRNÝ, I.: Stavebná tepelná technika. Tepelná ochrana budov. Jaga, Bratislava, 2003. ISBN 80-88905-27-3
- [7] ŠULCOVÁ, D.: Otopové křivky. Příloha časopisu Topin. Technické vydavatelství, Praha, 1999.
- [8] PETRÁŠ, D., KONKOL, R., REPKA, N.: Energetický úsporné opatrenia v bytových domoch. Zb. I. medzinárodná konferencia Nové trendy a technológie v komplexnej obnove bytových domov. STU Bratislava, 2007, str. 71-75.
- [9] STN EN 12 831 Vykurovacie systémy v budovách. Metóda výpočtu projektovaného tepelného príkonu. 2004 .
- [10] STN 73 0540 Tepelné technické vlastnosti stavebných konštrukcií a budov. Názvosloví. Požiadavky a kritéria. 1964.
- [11] STN 73 0540-2 Tepelná ochrana budov. Tepelno-technické vlastnosti stavebných konštrukcií a budov. Časť 2: Funkčné požiadavky.2012

# Experimental investigations of indoor climate parameters a swimming pool during summer operation period

R. Turza, Belo B. Furi\*

\* Department of Building Services, Faculty of Civil Engineering STU in Bratislava, Bratislava, Slovakia

e-mail: [robert.turza@stuba.sk](mailto:robert.turza@stuba.sk), [belo.furi@stuba.sk](mailto:belo.furi@stuba.sk)

EXPRES 2015

**Abstract** - Number of indoor swimming pools and wellness centers currently is growing, it is necessary to concern on parameters of their indoor environment. These parameters are necessary for the design of HVAC systems that operate in these premises. In indoor swimming pool facilities, the energy demand is large due to ventilation losses with the exhaust air. Since water is evaporated from the pool surface, the exhaust air has a high water content and specific enthalpy. In this publication measurements of indoor climate parameters and the calculation of water evaporation in pools are described.

**Key words** - swimming pool, measurement, water evaporation, temperature, relative humidity, air velocity

## I. INTRODUCTION

This paper deals with the topic of hygro-thermal climate in indoor swimming pool. Ventilation in these places ensures mainly the hygienic function. A ventilation device provide internal environment for people to feel comfortable in the swimming pool, protecting their health by eliminating pollutants and finally keep the technology in run and protects the building structure. Indoor swimming pools belong to premises with high moisture production, respectively water vapor, where the relative humidity in this area is usually between 60 to 80 % and in rare cases even more.

Indoor swimming pools are water bodies designed for recreational or competitive swimming, diving and other water sports that require swimming or aquatic exercise. Indoor swimming pools make use artificial environment with technological elements (filtration, ventilation equipments, pumps, dosing of chemicals, etc.). Water temperature depends on pool type. In table 1 are described design water temperatures for different pool types. The water temperature affects the heat and mass transfer between water and human body. Because of evaporation of the film of water on the unclothed body additional heat is lost. Therefore to minimize feel of cold, air temperature should be 2 K to 4 K (min. 1 °C according to [6]) above the water temperature, but not above 34 °C [4, 5]. Relative humidity in swimming pool hall should be within the range 40 ÷ 65 %. Air flow velocity in the zone of stay should be below 0,2 m/s.

The water evaporation is a natural process and it is a critical energy parameter in design and control system. The forecast of water evaporation from swimming pools by its reliable calculation is required for accurate projection of HVAC systems. In order to eliminate condensation on cold surfaces in a swimming pool, water vapor has to be removed by HVAC system and on the other hand water in the pool has to be heated to compensate the heat lost by evaporation. According to statistics, 70 % of energy loss in swimming pools goes to water evaporation.

TABLE I.  
WATER TEMPERATURES IN INDOOR SWIMMING POOL

Basin	Water temperature according to edict 72/2008 [5] (°C)	Water temperature according to VDI 2089 [4] (°C)
swimming	18 ÷ 26	28
non-swimming	28	28
relax	40	36
kids up to 36 months kids older 36 months	30 ÷ 36 28 ÷ 32	32

Water evaporation rate to its complex and stochastic nature is nearly impossible to predict. In the literature is available wide variation in correlations for predicting water evaporation and energy consumption.

TABLE II.  
WATER EVAPORATION RATE EQUATIONS

Author	Equation
Dalton (1802)	$m_e = C(p_w^* - p_a)$
Box (1876)	$m_e = 0,0000778 \cdot (p_w^* - p_a)$
Carrier (1918)	$m_e = \frac{(0,089 + 0,40782x) \cdot A_w (p_w^* - p_a)}{l_e}$
Himus a Hinchley (1924)	$m_e = 0,0000258(p_w^* - p_a)^{1,2}$
Rohwer (1931)	$m_e = 0,08(\theta_a - \theta_w + 3)^{1,2}(p_w^* - p_a)$
Boelter et al. (1946)	for $\Delta x < 0,008$ $m_e = 5,71 \cdot \Delta x$
	for $0,008 < \Delta x \leq 0,016$ $m_e = 4,88(-0,024 + 4,05795 \cdot \Delta x)$
	for $\Delta x > 0,016$ $m_e = 38 \cdot 2 \cdot (\Delta x)^{0,25}$



TABLE II  
WATER EVAPORATION RATE EQUATIONS

Author	Equation
Leven (1969)	$m_w = 0,00000945(p_s^* - p_i)^{0,5}$
Biasin a Krumme (1974)	$m_w = -0,059 + 0,000079(p_s^* - p_i)$
Harsen a Mathisen (1990)	$m_w = 3 \cdot 10^{-5} \cdot v^{1,5} (e^{0,06 \Delta t_s} - \varphi_i e^{0,06 \Delta t_i})$
Smith et al. (1993)	$m_w = \frac{0,76(0,089 + 0,0782v)(p_s^* - p_i)}{l_i}$
Tang et al. (1993)	$m_w = 35 \cdot (\Delta x)^{-0,27}$
Pauken (1999)	$m_w = a \left( \frac{p_s - p_i}{1000} \right)^b$ $a = 0,074 + 0,0979 \cdot v + 0,02491 \cdot v^2$ $b = 1,22 - 0,19 \cdot v + 0,038 \cdot v^2$
Santori (2000)	$m_w = \frac{(0,00407 \cdot v^{0,5} \cdot L^{0,2} - 0,01107 \cdot L^{0,5})(p_s^* - p_i)}{P_i}$
Al-Shamiri (2002)	$m_w = (0,12083 \cdot v^{1,43}) \left( \frac{p_s^* - p_i}{1000} \right)^{0,454}$
Shah for unoccupied pools (2002)	$C=40 \text{ pre } \Delta p < 0,02$ $C=35 \text{ pre } \Delta p > 0,02$ $m_w = C \cdot \rho_i \cdot (p_i - p_s)^{0,5} (x_s - x_i)$
Shah for occupied pools (2004)	$m_w = \left( 0,113 - \frac{0,0000175}{N} + 0,000059(p_s^* - p_i) \right)$
Tang a Etzion (2004)	$m_w = 3600 \cdot (0,2253 + 0,24644 \cdot v) \frac{(p_s^* - p_i)^{0,42}}{l_i}$
ASHRAE (2007)	$m_w = 0,000144(p_s^* - p_i)$
VDI 2089 (1994)	$m_w = \beta(p_s^* - p_i)$
VDI 2089 (2000, 2010)	$m_w = \frac{\beta}{RT}(p_s^* - p_i)$

## II. MEASUREMENTS

For performing experimental measurement was selected the THERMAL CORVINUS in periphery of Velky Meder, Slovakia. This facility is located in Dunajská Streda County, 65 km from Bratislava. Swimming pool uses thermal water from two sources. THERMAL CORVINUS in Velky Meder is yearlong open with nine pools with water temperature of 26-38 °C.



Figure 1. Indoor swimming pool, Velky Meder [7]

Measurements were carried out in the indoor swimming pool (Fig. 1), which is yearlong open. The hall serves as a small family water park, where beside the indoor swimming pool with asymmetrical shape with swimming and relaxing activities, is also a whirlpool, children's pool with pool elements and yearlong operated 2 waterslides. Declared properties of the indoor swimming pool are water temperature 30 °C, water area 291.4 m<sup>2</sup> and depth of 1.2 m, the whirlpool water temperature 33 °C, water area 19.65 m<sup>2</sup> and depth of 0.6

m, children's pool with water elements water temperature 30 °C, water area 20.00 m<sup>2</sup> and depth 0.4 m.



Figure 2. Measuring instruments Comet S3541, S0111, Testo 451, 445 [8, 9]

For long-term measurements of microclimate inside the swimming pool hall and the outside air were used data logger Comet S3541 (Fig. 2), thermo- and hygrometer with temperature measuring range -30 ÷ +70 °C with an accuracy ± 0.4 °C, with a resolution of 0.1 °C. Relative humidity measuring range is 0 – 100 %, with an accuracy of ± 2.5 % (5-95%) and with a resolution of 0.1 %. Also was used measuring instruments Comet S0111 (Figure 2), thermometer with extern probe, for measuring outside temperature. Measuring temperature range is -30 ÷ +70 °C with an accuracy of ± 0.2 °C and with a resolution of 0.1 °C.

For instant measurements of microclimate inside the swimming pool hall were used measuring instruments Testo 451 and 445 (Fig. 2). Measuring instrument Testo 451 has the measurable range of air temperature -40 ÷ +70 °C with an accuracy ±0,1 °C and resolution 0,1 °C, relative humidity range 0 ÷ 100 %, with an accuracy ±2,0 % (2 ÷ 98 %), and resolution 0,1 % and air flow velocity range 0,2 ÷ 60 m/s with an accuracy ±0,1 °C and resolution 0,1 °C. Measuring instrument Testo 445 has the measurable range of air temperature of -50 ÷ +150 °C with an accuracy ±0,2 °C and resolution 0,1 °C, relative humidity 0 ÷ 100 %, with an accuracy ±2,0 % (2 ÷ 98 %)



and resolution 0,1 % and air flow velocity 0,0 ÷ 10 m/s with an accuracy  $\pm 0,03$  m/s and resolution 0,01 m/s.

### III. MEASUREMENTS INSIDE THE SWIMMING POOL

During the days 09. - 22.07.2013 were made measurements of temperature and humidity in the occupation zone (1 m from ground) inside the swimming pool and outside air temperature. Inside the hall was used data logger Comet S3541 with the set of record interval every 5 min and outside data logger Comet S0111. With this could be evaluated air temperature and relative humidity values inside the covered swimming pool.

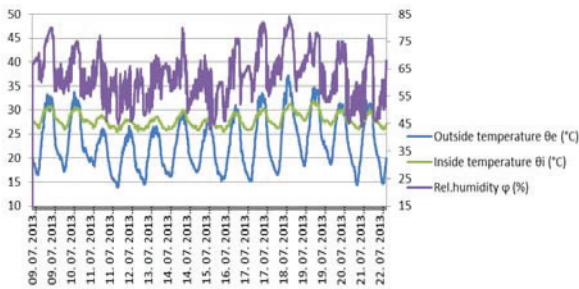


Figure 4. Time course of air temperature and relative humidity in swimming pool in 9.7-22.7.2013

In the figure (**Fig. 3**) you can see the behavior of hydro-thermal microclimate in swimming pool in summer period of 2013. The average inside air temperature was 27,9 °C and the relative humidity 62,5 % and the average outside air temperature 23,1 °C.

During the day 04.-08.08.2014 were made measurements of temperature and humidity in the occupation zone (1 m from ground) inside the swimming pool and outside air temperature. Inside the hall was used data logger Comet S3541 with the set of record interval every 5 min and outside data logger Comet S0111. With this could be evaluated air temperature and relative humidity values inside the covered swimming pool.

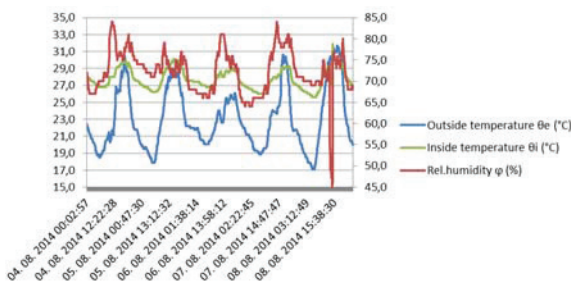


Figure 5. Time course of air temperature and relative humidity in swimming pool in 4.8-8.8.2014

In the following **Fig. 4** you can see the behavior of hydro-thermal microclimate in swimming pool in summer period of 2014. The average inside air temperature was 27,7 °C and the relative humidity 72,2 % and the average outside air temperature 23,0 °C.

### IV. MEASUREMENTS OF AIR FLOW VELOCITY

During the days 04 ÷ 08.08.2014 were performed measurements of the temperature and air velocity at the water level (0,1 m above this level) and in the occupation zone (1,5 m above this level) at 4 measuring spots using a measuring instrument Testo 445. With this the device could be evaluated the flow of air, or more precisely the air flow velocity (**Fig. 5**). On these days was the average air temperature in the swimming pool 29 °C and the air velocity 0,15 m/s. These temperature and air velocity, however, were also affected by external weather conditions, ie. action of wind pressure (air movement) through the windows and doors.

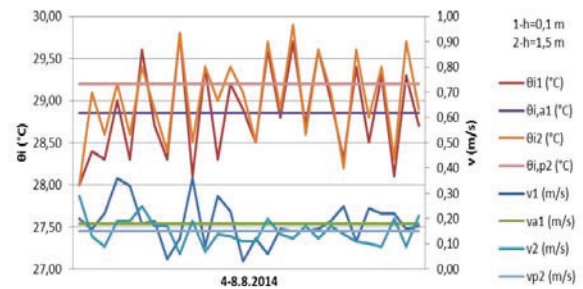


Figure 3. Time course of air temperature and relative humidity in swimming pool in 4.8-8.8.2014

### V. WATER EVAPORATION CALCULATION

After these measurements was made also calculations of water evaporation. Numerous empirical correlations have been presented for unoccupied or occupied swimming pools. I have choose 2 mainly used formulas used in Slovakia. First one is according to [4] and the another one is according to [1, 2]. As can be seen the main difference between these methodologies is the calculation of the coefficient of transmission of moisture, respectively the mass transfer coefficient  $\beta$  on which depends the energy demand of the pool hall. While according to [4] the coefficient is fixed for different types of swimming pools, according to the methodology [1, 2] this factor depends also on the speed of the airflow over the surface.

The mass flow of evaporated water  $m_w$ :

- according to [1,2]:

$$m_w = \beta_p \cdot (p_{p(\theta_w)} - p_{p(\theta_a)}) \cdot A_h \quad (\text{kg/s})$$

$$\beta_p = f(\text{swim min gpool type, air flow velocity})$$

- according to [4]:

$$m_w = \frac{\beta}{R_v \cdot T} \cdot (p_{p(\theta_w)} - p_{p(\theta_a)}) \cdot A_h \quad (\text{kg/s})$$

$$\beta_p = f(\text{swim min gpool type})$$

where:

$\beta_p$  – coefficient of evaporation according to the vapor pressure difference above the water and the surrounding air ( $\text{kg}/(\text{m}^2 \cdot \text{s} \cdot \text{Pa})$ )

$\beta$  – coefficient of mass transfer ( $\text{m/h}$ ),

$R_v$  – specific gas constant for water vapor ( $J/(kg.K)$ ),  
 $T$  – arithmetic mean of water and air temperature (K),  
 $p_{v(\theta_w)}$  – saturation pressure of water vapors at water temperature (Pa),  
 $p_{v(\theta_i)}$  – water vapor pressure of the swimming hall air (Pa),  
 $A_h$  – water area ( $m^2$ ).

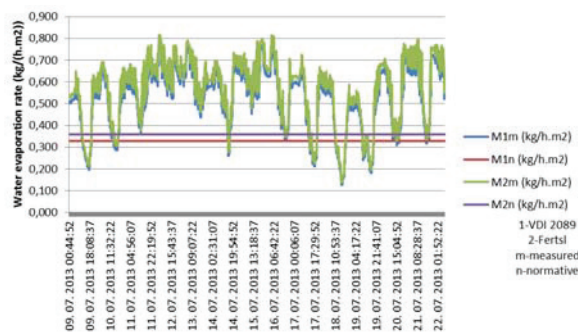


Figure 6. Time course of water evaporation rate in swimming hall in 9.-22.7.2013

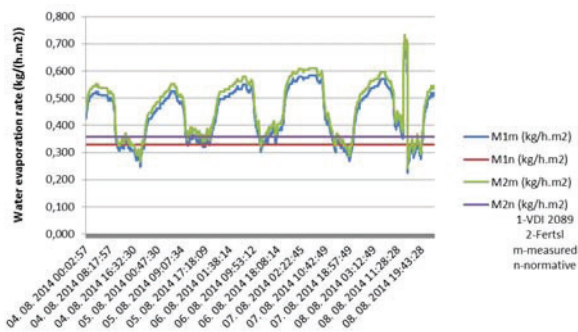


Figure 7. Time course of water evaporation rate in swimming hall in 4.-8.8.2014

In the following diagrams (**Fig. 6, 7**) are compared water evaporation rates from the surface based to the unit area of water level. The water evaporation rate of the two methodologies are calculated with the real measured values (index m) and with the standard values  $\theta_w = 30\text{ }^{\circ}\text{C}$ ,  $\theta_i = 32\text{ }^{\circ}\text{C}$ ,  $\varphi_i = 65\%$ ,  $w = 0,2\text{ m/s}$  (index n). The following diagram shows that the results from each methodology have very similar.

## VI. CONCLUSIONS

During the summer time were made measurements of hydro-thermal microclimate in the indoor swimming pool in Thermal Corvinus Velký Meder. This paper

presents the results of these measurements. During the measurements was also used natural ventilation through open windows and doors. In consequence of this, inside air temperature depended on the temperature of the external environment. Therefore it was not permanently secured required level of air temperature, which should be at least  $2\text{ }^{\circ}\text{C}$  higher from the water temperature. Relative humidity in the swimming pool was below the required level 65%. The exception was side of the swimming pool with toboggans, where the relative humidity was affected by significant water spilling due to slipping on the water slides. In 2014 was rainy weather during the measurements and because the opened windows and doors was the relative humidity in the swimming hall over the required level 65%. During this measurements were sort of complains, because the feel of sultriness. Solution of this could be elimination of additional moisture by closing doors and windows and running the HVAC system with better regulation.

Air flow velocity above the water level was met, except some occasion, which could be eliminated by closing doors and windows.

In this paper was presented also calculation of water evaporation from water level according to 2 methodologies. The values were similar. Despite of this it would be appropriate to verify these measurements and do lab or simulation tests to prove which formula is more accurate.

## VII. REFERENCES

- [1] FERSTL, K., Vetrание a klimatizácia priestorov s vyššou produkciou vlhkosti, SSTP, Bratislava, 2001
- [2] FERSTL, K., MASARYK, M., Prenos tepla, STU, Bratislava, 2011, ISBN 978-80-227-3534-6
- [3] Turza, R., Teplovzdušné vetranie krytej plavárne, Diplomová práca, STU, Bratislava, 2011
- [4] VDI 2089, Building services in swimming baths – Indoor pools
- [5] Edict of Ministry of Health SK 72/2008
- [6] Edict of Ministry of Health SK 259/2008
- [7] Thermal Corvinus, Veľký Meder, <http://www.thermalcorvinus.sk>
- [8] Comet, <http://www.cometsystem.cz>
- [9] Testo, <http://www.testo.sk>
- [10] Kajtár L., Hrustinszky T.: Investigation and influence of indoor air quality on energy demand of office buildings. WSEAS Transactions on Heat and Mass Transfer, Issue 4, Volume 3, October 2008. 219-228 p.
- [11] Nyers J., Kajtar L., Tomic S., Nyers A.: "Investment-savings method for energy-economic optimization of external wall thermal insulation thickness". International J. Energy and Buildings. Vol.86, pp. 268–274, 2015. doi.org/10.1016/j.enbuild.2014.10.023
- [12] Nyers J., Tomic S., Nyers A.: "Economic Optimum of Thermal Insulating Layer for External Wall of Brick". I J Acta Polytechnica Hungarica Vol. 11, No. 7, pp. 209-222. 2014.
- [13] K Dabis, Z Szánthó: Control of Domestic Hot Water production is instantaneous heating system with a speed controlled pump, 6<sup>th</sup> International symposium "EXPRES 2014 VTS." Subotica, Serbia, 2014. pp. 101-106. ISBN 978-86-85409-96-7.

# Revealing the costs of air pollution caused by coal-based electricity generation in serbia

F.E. Kiss\* and Đ.P. Petković\*\*

\* University of Novi Sad/Faculty of Technology, Novi Sad, Serbia

\*\* University of Novi Sad/Faculty of Economics, Subotica, Serbia

ferenc1980@gmail.com; pegy@ef.uns.ac.rs

**Abstract**— The aim of this research was to determine the costs of damages caused to the environment by emissions released in the life cycle of electricity generated in the Serbian coal-fired power plants.

Data on direct emissions released from power plants were obtained from the Electric Power Industry of Serbia, while life cycle inventory data of up- and downstream processes of electricity were taken from the Ecoinvent v. 2.0 database. Serbia-specific damage costs factors of local and regional pollutants were determined with the EcoSense software which is based on the Impact Pathway Approach method. The assumed damage costs of greenhouse gas emissions are 0.025 EUR·kg<sup>-1</sup> CO<sub>2</sub> equivalent based on literature review.

Research results indicate that costs of environmental damages caused by airborne pollutants and greenhouse gases emitted from Serbian coal-fired power plants were 3.6 billion EUR in 2011, or in average 0.13 EUR·kWh<sup>-1</sup>. Results have revealed substantial differences in the power plant specific damage costs (0.10–0.24 EUR·kWh<sup>-1</sup>). This highlights the possibility for significant reductions in external costs by improving the electric efficiencies and implementing more efficient emission control devices.

**Keywords:** external costs, electricity, lignite, coal, life cycle, Serbia.

## I. INTRODUCTION

Coal-fired thermal power plants (TPPs) are an important source of emissions of many pollutants which cause considerable damage to the environment such as the degradation of ecosystems or human – made structures and health effects [1]. Costs arising from these damages are in general not, or not adequately, reflected in the price of electricity; thus, they represent external costs<sup>1</sup>. If such costs exists but are not adequately considered when making decisions a non-optimal allocation of resources leading to welfare losses may occur [2]. The importance of including external costs – to obtain the true social cost of activities – in economic analysis is agreed, at least at the theoretical level [3].

Previous study revealed that the damage caused to the environment as a direct result of air pollution caused with electricity production in the EU-27 countries was between 66 and 112 billion EUR [4]; with the country-

specific damage costs of electricity production between 0.018 and 0.059 EUR·kWh<sup>-1</sup> [5].

The magnitude of the environmental damage caused by national electricity systems depends on many factors, including the fuel mix for electricity generation, the efficiency of the power plants, the use of pollution abatement technology, and the location of the power plants [5]. Electricity production in Serbia overwhelmingly relies on lignite (ca. 70%), a type of coal with low calorific value and high moisture and sulphur content. This characteristic of the Serbian electricity system give rise to concerns about its environmental impact and related externalities. Different approaches are available for reducing externalities, ranging from the development of new technologies and technical solutions to the use of fiscal instruments, or the imposition of emission limits [6]. In order to analyze the cost effectiveness of these options, however, the decision makers require data on costs and benefits of the various options. Consequently, identification, quantification and finally monetization of the external effects of electricity generation are necessary.

A previous study has estimated the costs of air pollution caused by Serbian coal-fired power plants [7]. The assessment was limited to the environmental damage caused by direct emissions from the power plants. This approach is in accordance with the generally accepted view that in the life cycle of electricity the power plant i.e. fuel combustion has the most severe environmental consequences. However, up- and downstream processes (e.g. fuel production chain, production of required infrastructure, waste disposal) may also have significant impacts on human health, natural and built environment [8].

Therefore, the aim of this research is to quantify the damage costs resulting from air pollution caused by emissions released in the entire life cycle of electricity generated in Serbian coal-fired power plants.

## II. METHOD AND MATERIALS

### A. Coal-fired power plants in Serbia

The study includes the assessment of environmental damage cost of electricity produced in six Serbian coal-fired power plants operated by the Electric Power Industry of Serbia. The total net output capacity of these power plants is 3,936 MW with an annual electricity

<sup>1</sup> Damage cost is the cost incurred by repercussions (effects) of direct environmental impacts (for example, from the emission of pollutants) such as the degradation of land or human - made structures and health effects. Note that external costs are related to, yet different from environmental damage costs. External costs are the not yet internalized part of the environmental damage costs.



TABLE I.  
ELECTRIC CAPACITY AND ANNUAL PRODUCTION OF ELECTRICITY AND HEAT IN SERBIAN COAL-FIRED POWER PLANTS (2011)\*

Name of the TPP**	abbrev.	Net output electric capacity (MW)	Electricity generation (MWh·a <sup>-1</sup> )	Thermal energy generation (MWh·a <sup>-1</sup> )	Location of the TPP
TPP "Nikola Tesla A"	TENT A	1,502	11,388,893		Obrenovac
TPP "Nikola Tesla B"	TENT B	1,160	7,637,326		Obrenovac
TPP "Kolubara"	TEK	245	1,448,950		Lazarevac
TPP "Morava"	TEM	108	521,132		Svilajnac
TPP "Kostolac A"	TEK A	281	1,702,100	302,573	Kostolac
TPP "Kostolac B"	TEK B	640	4,454,000		Drmno
Total		3,936	27,152,401	302,573	

Notes: \* Thermal power plants located on the territory of Kosovo and Metohija with overall electric capacity of 1,235 MW are out of the scope of this research; \*\* TPP stands for Thermal Power Plan.

production of 27,152 GWh in 2011, or around 70% of electricity produced in Serbia [9]. The remaining ca. 30% of annual electricity production is related to hydropower plants. Electricity generated in hydropower plants has negligible environmental impact arising from life cycle airborne emissions [10]; therefore, the results of this research are also a good proxy for the total damage costs caused by electricity generation in Serbia.

Table 1 gives an overview of power plants covered by the research. Detailed data on the technical characteristics of Serbian coal-fired power plants are available on the webpage of the Electric Power Industry of Serbia [11].

#### B. General approach

In the first step, quantities of airborne emissions released in the entire life cycle of electricity are determined using the Life Cycle Inventory (LCI) analysis method. In the second step, the pollutant specific damage cost factors are determined using the Impact Pathway Approach (IPA). Finally, in the third step, the environmental damage cost (DC) is calculated using (1).

$$DC = \sum_{i=1}^n E_i \cdot C_i \quad (1)$$

where:  $E_i$  – Emission quantity of pollutant  $i$  in the life cycle of the electricity (in kg·MWh<sup>-1</sup>);  $C_i$  – Damage cost factor of pollutant  $i$  (in EUR·kg<sup>-1</sup> emission);  $n$  – Number (type) of airborne pollutant covered with the analysis.

#### C. LCI analysis of electricity generated in coal-fired power plants

Damage cost valuation is based on the results of LCI analysis which include information on emissions released during the entire life cycle of electricity generated from coal. Since damage costs factors are available for only a few pollutants, the analysis was limited to the following greenhouse gases (GHGs) and airborne pollutants: CO<sub>2</sub>, CH<sub>4</sub>, N<sub>2</sub>O, NH<sub>3</sub>, NMVOC (non-methane volatile organic compounds), SO<sub>2</sub>, NO<sub>x</sub> (nitrous oxides), PM<sub>2.5</sub> (particles with diameter bellow 2.5 µm), PM<sub>2.5-10</sub> (particles with diameter between 2.5 µm and 10 µm) and PM<sub>10</sub> (particles with diameter bigger than 10 µm).

The processes studied in this life cycle assessment can be divided into four main subsystems: *i*) coal mining, *ii*) coal transportation, *iii*) coal combustion in power plants, i.e. electricity generation, and *iv*) treatment of coal ash. A detailed description of material and energy flows

associated with each of the four life cycle subsystems, as well as a more detailed description of the production technologies and the calculation procedure is available in our previous report [10]. A concise description of the investigated subsystems and processes is provided below.

*i) Coal mining.* The six Serbian thermal power plants consumed ca. 39 million Mg of coal with an average energy content of 7.5 MJ·kg<sup>-1</sup> in 2011 [10]. The required quantities of coal were provided by opencast lignite mines in Kolubara and Kostolac [9, 10]. In these mines coal is obtained by surface mining which involves fracturing and removing the overlying soil and rock (i.e. overburden), breaking the coal by blasting or mechanical means, and loading the coal for transport to its final destination.

Environmental impacts of coal mining include emissions released during mining operations, and emissions released in the life cycle of mining infrastructure. LCI data of coal excavation from opencast mines are available from the Ecoinvent v. 2.2 LCI database. The respective process is „Lignite, at mine/RER“ and refers to the excavation of 1 kg coal from the average opencast lignite mine in Europe. The process contain information on emissions associated with *a*) manufacture, maintenance and demolition of machinery and equipment required for coal mining; *b*) life cycle of diesel fuel and electricity required for the operation of water pumps and machinery, and *c*) field emissions of particles (PM<sub>10</sub>) and CH<sub>4</sub>. Emissions associated with coal preparation (washing and crushing) are not included in the process; thus, their potential environmental impacts are not considered in this study.

*ii) Coal transportation.* Data on coal transportation modes and distances are obtained from the officials of the Electric Power Industry of Serbia and they refer to the situation in 2011. In general, coal is transported to the power plants by conventional freight trains and/or conveyor belts. In this study the potential environmental impacts of transportation with conveyor belts are not considered due to data constraints and their suspected small environmental impact.

The inventory assessment for the transportation subsystem includes emissions associated with transportation of coal by train between the boundaries of the coal mining and power generation subsystems. Life cycle inventory data of coal transport with electric trains is described in the Ecoinvent database: „Operation, coal



TABLE II.  
QUANTITY OF COAL REQUIRED BY THE SERBIAN TPPS AND COAL TRANSPORTATION MODES

TPP	Transported quantity of coal (Mg)	Departure point	Arriving point	Distance in one direction	Transported quantity (Mg·km)	Transport mode
TENT A	16,515,699	Vreoci	Obrenovac (city)	32 km	1,057,004,736	Freight trains
TENT B	10,832,201	Vreoci	Obrenovac (near Skela)	38 km	823,247,276	Freight trains
TEK	2,197,248	Vreoci	Veliki Crljeni	5 km	21,972,480	Freight trains
TEM	662,202	Vreoci more places	Svilajnac Svilajnac	147 km average 30 km	74,828,826	Freight trains
TEK A	2,800,559	Kostolac	Kostolac	n.a.	n.a.	Conveyor belts
TEK B	6,048,221	Kostolac	Kostolac	n.a.	n.a.	Conveyor belts

freight train, electricity/CN". The process refers to coal transport with electric trains in China; thus, it was necessary to adopt it to the Serbian situation by changing the electricity supply system data [10]. LCI of the transportation process also includes emissions associated with railway infrastructure which are available from the Ecoinvent LCI database as well. Relevant data for the quantification of environmental impacts associated with coal transportation subsystem are summarised in Tables 2 and 3.

iii) *Electricity generation in power plants.* The inventory assessment of the electricity generation subsystem includes emissions released during the combustion of coal and emissions released during the construction, maintenance and demolition of power plant infrastructure. The Electric Power Industry of Serbia provides information on annual emissions of four pollutants, namely CO<sub>2</sub>, SO<sub>2</sub>, NO<sub>x</sub> and PM [12]; thus, the assessment is limited to the environmental impacts of these airborne emissions. The document does not provide information on particles size distribution. However, information in this regard is necessary since size of the particles is of a crucial relevance in damage costs assessment. In this research we follow the

recommendation of Röder et al. [13] who suggested the following size distribution of particles emitted from power plants equipped with electrostatic precipitators: 83.1% are particles with diameter below 2.5 µm (PM<sub>2.5</sub>), 7.1% are particles with diameter bigger than 10 µm (PM<sub>10</sub>) and the rest are particles with diameter between 2.5 µm and 10 µm (PM<sub>2.5-10</sub>). TPP specific direct emissions of CO<sub>2</sub> and classical pollutants are summarized in Table 3.

Inventory of emissions released during the construction, maintenance and demolition of power plant equipment and infrastructure is available from the Ecoinvent database. Same database provided LCI data of cooling water used in TPPs (see Table 3).

iv) *Coal ash treatment.* Coal ash is the unburned material that remains after coal is burned to generate electricity. Ash content of dry coal varies in a significant range from 2-60% depending on the coal type [14]. According to Röder et al. [13] in average 0.189 kg ash is formed after each kg of lignite burned in Serbian power plants. Based on the annual coal consumption in Serbian TPPs in 2011, the annual ash production is estimated to be 7.3 million Mg. In this study it is assumed that ash from lignite combustion is used as a backfilling material

TABLE III.  
LIFE CYCLE INVENTORY OF ELECTRICITY GENERATED IN SERBIAN TPPS (DATA REFER TO 1 MWh OF ELECTRICITY)

	Life cycle phase	Unit	TENT A	TENT B	TEK	TEM	TEK A*	TEK B	Average	LCI data from Ecoinvent
I.	Coal mining									
	- lignite	kg	1.45E+03	1.42E+03	1.52E+03	1.27E+03	1.40E+03	1.36E+03	1.44E+03	(a)
II.	Coal transportation									
	- rail transport	Mg·km	9.28E+01	1.08E+02	1.52E+01	2.85E+02	0.00E+00	0.00E+00	7.55E+01	(b)
	- rail infrastructure	Mg·km	9.28E+01	1.08E+02	1.52E+01	2.85E+02	0.00E+00	0.00E+00	7.55E+01	(c)
III.	Power plant									
	- emissions									
	PM	kg	6.42E-01	2.54E-01	1.28E+00	6.05E+00	8.86E-01	1.56E+00	8.36E-01	
	PM <sub>2.5</sub>	kg	5.33E-01	2.11E-01	1.06E+00	5.03E+00	7.36E-01	1.30E+00	6.95E-01	
	PM <sub>2.5-10</sub>	kg	6.27E-02	2.47E-02	1.25E-01	5.91E-01	8.64E-02	1.52E-01	8.17E-02	
	PM <sub>10</sub>	kg	4.57E-02	1.81E-02	9.11E-02	4.32E-01	6.29E-02	1.11E-01	5.95E-02	
	SO <sub>2</sub>	kg	1.11E+01	8.72E+00	1.05E+01	2.08E+01	3.04E+01	2.20E+01	1.36E+01	
	NO <sub>x</sub>	kg	1.90E+00	1.84E+00	1.80E+00	1.77E+00	1.89E+00	1.95E+00	1.88E+00	
	CO <sub>2</sub>	kg	1.10E+03	1.07E+03	1.05E+03	1.14E+03	1.35E+03	1.11E+03	1.11E+03	
	- infrastructure	p.	1.18E-08	1.18E-08	1.18E-08	1.18E-08	1.18E-08	1.18E-08	1.18E-08	(d)
	- water consumption	m <sup>3</sup>	4.24E+01	4.24E+01	4.24E+01	4.24E+01	4.24E+01	4.24E+01	4.24E+01	(e)
IV.	Coal ash treatment									
	- coal ash	kg	2.74E+02	2.68E+02	2.86E+02	2.40E+02	2.64E+02	2.57E+02	2.72E+02	(f)

Notes: (a) Lignite, at mine/RER; (b) Modified Operation, coal freight train, electricity/CN see Section C; (c) Transport, freight, rail/RER; (d) Lignite power plant/RER; (e) Water, cooling, unspecified natural origin/m<sup>3</sup>; (f) Disposal, lignite ash, 0% water, to opencast refill/CS. \* Of the overall environmental flows related to TPP "Kostolac A" 85% are allocated to electricity and 15% to heat co-product according to the principles of energy allocation (ISO 14040:2006).

in opencast mines. Environmental flows associated with ash disposal in the Serbian TPPs are described in the „Disposal, lignite ash, 0% water, to opencast refill/CS” process of the Ecoinvent database.

#### D. Pollutant specific damage cost factors

Pollutant specific damage costs (except GHGs) were calculated using the EcoSenseWeb v. 2.0 software tool [15] which is based on the Impact Pathway Approach (IPA) [15]. The IPA methodology was originally developed in the 1990s in a collaborative programme, ExternE, between the European Commission and the US Department of Energy to quantify the damage costs imposed on society and the environment due to energy use [16]. „The IPA starts with the specification of the quantities of the relevant pollutants emitted and the location of the pollution source. In the next step, using appropriate atmospheric dispersion models the concentration changes of pollutants in all affected regions are calculated. In the following step, the cumulated exposure from the increased pollutant concentration and the associated impacts (damage in physical units) from this exposure are calculated using a set of predefined exposure-response functions. These impacts are then weighted and aggregated into external costs using both, market and non-market valuation techniques“ [17]. EcoSenseWeb considers impacts of different airborne pollutants on human health, crops yield, building materials, and biodiversity. The IPA cannot yet provide quantification for all types of damage caused by airborne pollution, particularly those relating to ecosystems [4].

The environmental damage caused by emission of gases other than GHGs is affected by the location of emission. For example, the damage caused by NO<sub>x</sub> emission in Europe can vary in a significant range from 1.33 EUR·kg<sup>-1</sup> to 16.95 EUR·kg<sup>-1</sup> depending on the country of origin [15]. Site-specific damage costs factors for pollutants emitted from the territory of Serbia were calculated with the EcoSenseWeb. Serbia specific damage costs factors were also used to evaluate the environmental damage caused by emissions emitted outside Serbia (e.g. emissions associated with the construction of mining machinery). This simplification was necessary since it is not possible to determine the exact location of pollution sources in the life cycle of electricity. Furthermore, it was expected that most of the damage caused by electricity is due to the combustion of

coal; thus, this approximation, which mainly affects up- and downstream processes, will have a very limited impact on the overall damage costs of electricity.

GHGs mix globally in the atmosphere; therefore, the damages are spread around the world and are unaffected by the location of emissions. Thus, instead of complex modelling we used literature data to propose a damage cost factor for CO<sub>2</sub> and other GHGs. Maibach et al. [18] have performed a detailed and comprehensive review of recent studies calculating the damage costs associated with greenhouse gas emissions. Although, the results of studies display a large spread, indicating the high level of uncertainty still attached to this approach, Maibach et al. [18] came out with a central damage cost value of 25 EUR·Mg<sup>-1</sup> CO<sub>2</sub>. In this study we adopted this value for the assessment of damage caused by CO<sub>2</sub> emissions. The damage costs for other greenhouse gases (i.e. CH<sub>4</sub> and N<sub>2</sub>O) are calculated by multiplying the damage cost factor of fossil CO<sub>2</sub> with the global warming potential factor of CH<sub>4</sub> and N<sub>2</sub>O. The global warming potential factors of CH<sub>4</sub> and N<sub>2</sub>O are 23 and 296, respectively [19].

Emission specific damage costs factors used in the assessment are summarized in Table 4.

### III. RESULTS AND DISCUSSION

In 2011 annual costs of environmental damages caused by airborne pollutants and greenhouse gases released in the life cycle of electricity generated in Serbian coal-fired power plants were 3.6 billion EUR (Table 5). This should be regarded as the lower limit to real damages due to reasons listed in the Introduction part and Section D.

Health impacts dominate the damages quantified in the study (ca. 75% of total; Table 5); in particular, mortality due to primary and secondary particulates caused by SO<sub>2</sub> emissions. These damages only partially occur within Serbia due to atmospheric transport of pollutants. For some air pollutants, in particular particulates with diameter below 10 µm, NO<sub>x</sub> and SO<sub>2</sub>, atmospheric dispersion is significant over hundreds to thousands of km; thus, both local and regional effects are important. In fact, a detailed analysis of the results obtained with EcoSenseWeb v. 2.0 revealed that only 14% of total damages caused by emission of classical pollutants (all emissions apart from GHGs) released from TENT A are on the territory of Serbia. Apart from Serbia the three most affected countries are Italy (ca. 12% of the total

TABLE IV.  
DAMAGE COST FACTORS OF AIRBORNE POLLUTANT

Airborne emission	Damage caused to (in EUR·Mg <sup>-1</sup> ):					Estimation method:
	Human health	Crops	Buildings	Biodiversity	Total	
PM <sub>2.5</sub>	13,111	0	0	0	13,111	Calculated value (EcoSenseWeb v2.0)
PM <sub>2.5-10</sub>	547	0	0	0	547	Calculated value (EcoSenseWeb v2.0)
PM <sub>10</sub>	547	0	0	0	547	Calculated value (EcoSenseWeb v2.0)
SO <sub>2</sub>	6,221	-22	234	90	6,524	Calculated value (EcoSenseWeb v2.0)
NO <sub>x</sub>	4,934	316	49	374	5,673	Calculated value (EcoSenseWeb v2.0)
NM VOC	715	78	0	-26	766	Calculated value (EcoSenseWeb v2.0)
NH <sub>3</sub>	9,149	-226	0	1,289	10,212	Calculated value (EcoSenseWeb v2.0)
CO <sub>2</sub>	n.a.	n.a.	n.a.	n.a.	25	Literature review
CH <sub>4</sub>	n.a.	n.a.	n.a.	n.a.	575	Literature review
N <sub>2</sub> O	n.a.	n.a.	n.a.	n.a.	7,400	Literature review

damage) and Romania (ca. 11% of the total damage) and Hungary (ca. 6% of the total damage). Similar results were obtained for other Serbian TPPs as well.

Climate change costs caused by GHG emissions are responsible for ca. 21% of total external costs (Table 5). Climate change costs are related almost solely to CO<sub>2</sub> emitted from power plants. Damage caused in building materials and biodiversity loss due to acidification and eutrophication contribute less than 5% to overall external costs. The positive impact of electricity generation on crops yield (Table 5) can be explained with the fertilizing effect of SO<sub>2</sub>. This should be considered as a positive externality of electricity generation from lignite fuel.

Table 6 shows the relative contribution of life cycle phases to the overall damage caused by electricity. Up- and downstream emissions, i.e. all emissions in the life cycle of electricity systems except emissions released during the combustion of lignite used for the electricity generation, contribute less than 2% to the overall damage caused by electricity. The negative influence of up- and downstream processes are almost entirely related to coal mining. The zero effect of coal ash treatment subsystem can be explained with the limitations of the applied Ecoinvent LCI dataset which includes only water and soil emissions, i.e. emissions which were not considered in this research. Due to huge fuel masses to be burned, lignite power plants are generally placed next to the lignite mines. This explains the small share of the coal transportation processes in the total damage costs of electricity from lignite.

Fig. 1 shows the damage costs of electricity in the investigated coal-fired power plants in Serbia. The average damage caused to the environment due to electricity production in coal-fired power plants was estimated at 0.13 EUR·kWh<sup>-1</sup>. TPP specific damage costs vary in a significant range from 0.10 EUR·kWh<sup>-1</sup> (TENT B) to 0.24 EUR·kWh<sup>-1</sup> (TEM). Substantial difference between the results can be explained with different electric efficiencies of Serbian power plants, the use of pollution abatement technology, and the location of the plant itself with respect to population centres, agricultural land, etc. Variability in damage costs can be partially

explained with differences in chemical composition and heating value of lignite used for electricity generation in different power plants. In 2011 the average heating value of lignite used by different power plants varied between 6.8 MJ·kg<sup>-1</sup> and 8.7 MJ·kg<sup>-1</sup> [10].

Relative contributions of airborne pollutants to the total damage cost are presented on Fig. 2. Contribution of SO<sub>2</sub> to total external costs is prevailing over other emissions, making around 65% of total external costs of lignite based electricity. The SO<sub>x</sub> emissions from lignite combustion are a function of the sulphur content of the lignite and the lignite composition (i.e., sulphur content, heating value, and alkali concentration) [20]. Besides the relatively large sulphur content of Serbian lignite (up to 1.58 wt.% on dry basis [21]) one of the main reasons of relatively high SO<sub>2</sub> emissions are the inefficient and old abatement technology or the lack of treatment of flue gases. CO<sub>2</sub> emissions contribute with ca. 21% to the total damage caused by emissions released in the life cycle of coal-based electricity (Fig. 2). NO<sub>x</sub> and PM emissions vary in significant range. This can be explained with different fuel composition, boiler design and combustion conditions, and different extension of installation and efficiency of emission control devices in the investigated TPPs.

#### IV. CONCLUSIONS

Annual costs associated with air pollution caused by coal-based electricity generation in Serbia were 3.6 billion EUR in 2011. This should be regarded as the lower limit of real environmental damages since *i)* not all the damages related to air pollution were accounted for; *ii)* the assessment did not include environmental impacts associated with emissions to water and soil.

The average damage cost of coal-based electricity was estimated at 0.13 EUR·kWh<sup>-1</sup>. It is clear that the present retail prices of electricity in Serbia (0.04-0.13 EUR·kWh<sup>-1</sup>) do not adequately reflect the social costs of electricity generation. Consequently, stakeholders do not get accurate price signals that are necessary to reach decisions about the socially optimal use of resources.

Results revealed substantial differences in the power

TABLE V.  
DISTRIBUTION OF TOTAL DAMAGES BETWEEN IMPACT CATEGORIES (EUR)

Impact category	TENT A	TENT B	TEK	TEM	TEK A	TEK B	Total
Damage to human health	9.872E+8	5.161E+8	1.294E+8	1.077E+8	2.570E+8	7.322E+8	2.730E+9
Crop yields loss	4.326E+6	3.154E+6	5.221E+5	6.790E+4	-5.076E+4	6.904E+5	8.709E+6
Damage to buildings	3.088E+7	1.650E+7	3.714E+6	2.607E+6	8.877E+6	2.341E+7	8.599E+7
Biodiversity loss	1.988E+7	1.156E+7	2.394E+6	1.349E+6	4.282E+6	1.221E+7	5.167E+7
Global warming impact	3.210E+8	2.109E+8	3.910E+7	1.527E+7	4.237E+7	1.269E+8	7.555E+8
Total	1.363E+9	7.582E+8	1.752E+8	1.270E+8	3.125E+8	8.955E+8	3.632E+9

TABLE VI.  
ANNUAL COSTS OF DAMAGE CAUSED TO THE ENVIRONMENT DUE TO ELECTRICITY GENERATION IN SERBIAN TPPS IN 2011 (EUR)

Life cycle phase	TENT A	TENT B	TEK	TEM	TEK A	TEK B	Total
Coal mining	1.943E+7	1.274E+7	2.585E+6	7.791E+5	2.375E+6	7.116E+6	4.503E+7
Coal transportation	4.611E+6	3.591E+6	9.586E+4	6.471E+5	0.000E+0	0.000E+0	8.946E+6
Power plant	1.339E+9	7.418E+8	1.725E+8	1.255E+8	3.101E+8	8.884E+8	3.578E+9
Coal ash treatment	0.000E+0	0.000E+0	0.000E+0	0.000E+0	0.000E+0	0.000E+0	0.000E+0
Total	1.363E+9	7.582E+8	1.752E+8	1.270E+8	3.125E+8	8.955E+8	3.632E+9

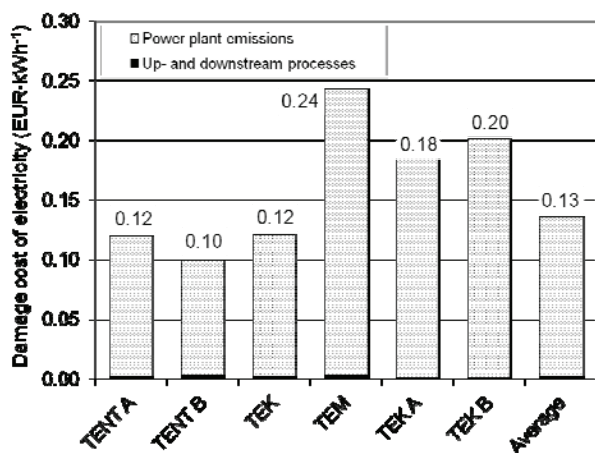


Figure 1. Power plant specific damage costs in 2011 (EUR-kWh<sup>-1</sup>)

plant specific damage costs (0.10–0.24 EUR-kWh<sup>-1</sup>). This highlights the possibility for significant reductions in external costs by improving the electric efficiencies and implementing more efficient emission control devices. Actions should be taken in order to reduce SO<sub>2</sub> emissions from power plants since these emissions are responsible for ca. 65% of total damages caused by electricity generation in the Serbian coal-fired power plants.

#### ACKNOWLEDGMENT

This research was supported by the Hungarian Academy of Sciences within the framework of the Domus Programme (Contract no.: DSZ/34/2013).

#### REFERENCES

- [1] M. Sevenster, H. Croezen, M. van Valkengoed, A. Markowska, and E. Dönszelmann, "External costs of coal - Global estimate," Delft, CE Delft, 2008.
- [2] R. Friedrich, P. Bickel, eds., "Environmental external costs of transport," Springer, 2001.
- [3] P. Bickel, S. Schmid, W. Krewitt, R. Friedrich, External Costs of Transport in ExternE, IER, Stuttgart, 1997.
- [4] M. Holland and A. Wagner (ed.) "Revealing the costs of air pollution from industrial facilities in Europe," EEA Technical report No 15, 2011.
- [5] European Environmental Agency, "EN35 External costs of electricity production," Available online at: <http://www.eea.europa.eu/data-and-maps/indicators/en35-external-costs-of-electricity-production#toc-1> [accessed 12/09/2014]
- [6] J.V. Spadaro, and A. Rabl, "External costs of energy: application of the ExternE methodology in France - Final Report," 1998.
- [7] F. Kiss and P. Preiss, "External Costs of Electricity Generation in Serbian Coal-Fired Power Plants," Proceeding of International Conference "Power Plants 2014", pp. 364–373, 2014.
- [8] D. Bennink, F. Rooijers, H. Croezen, F. de Jong, and A. Markowska, "VME Energy Transition Strategy: External Costs and Benefits of Electricity Generation," Delft, CE Delft, 2010.
- [9] Electric Power Industry of Serbia, "Technical Report for the Year 2012," Available online at: [http://www.eps.rs/TehnickiIzvestaji/TEH\\_Godisnjak2011\\_SR.pdf](http://www.eps.rs/TehnickiIzvestaji/TEH_Godisnjak2011_SR.pdf) [accessed 08.12.2013]
- [10] F. Kiss, "Real costs of fossil electricity generation in Serbia – study on environmental and economic interdependencies," Project

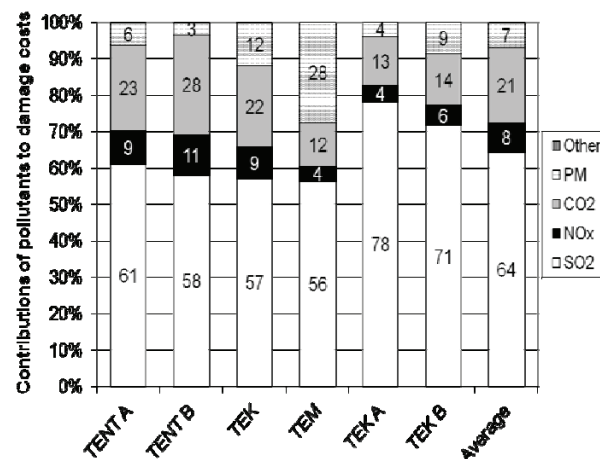


Figure 2. Relative contributions of specific emissions to the life cycle damage cost of electricity (%)

financed by the Hungarian Academy of Sciences (DSZ/34/2013), 2014.

- [11] Electric Power Industry of Serbia, "Technical Characteristics of Thermal Power Plants," Available online at: <http://www.eps.rs/Eng/Article.aspx?lista=Sitemap&id=70> [accessed 09.06.2014]
- [12] Elektroprivreda Srbije, "Izveštaj o stanju životne sredine u JP Elektroprivreda Srbije za 2012. godinu," Beograd, Serbia.
- [13] A. Röder, C. Bauer, R. Dones, "Kohle: Sachbilanzen von Energiesystemen," Final report No. 6 ecoinvent data v2.0. Volume: 6. Swiss Centre for LCI, PSI. Dübendorf and Villigen, Switzerland, 2008.
- [14] B. Németh, "Szénermelés, felhasználás fizikája," Jegyzet, PTE Fizikai Intézet; Környezetfizika, Pécs, Hungary. Available online at: <http://www.physics.ttk.pte.hu/pages/munkatarsak/nemetb/KorFiz-I-7-szen.pdf> [16.12.2012]
- [15] P. Preiss, R. Friedrich, and V. Klotz, "Report on the procedure and data to generate averaged/aggregated data," NEEDS Project: deliverable No. 1.1 - RS 3a IER, University of Stuttgart, 2008.
- [16] European Commission, "ExternE - Externalities of Energy – Methodology 2005 Update," Office for Official Publications of the European Communities, Luxembourg, 2005.
- [17] F. Kiss, Đ. Petković, "External Cost of Electricity from Different Energy Sources – a Life Cycle Perspective," Proceeding of the 5th IEEE International Symposium on Exploitation of Renewable Energy Sources – EXPRES 2013, Subotica, Serbia, March 21–23, 2013, pp. 70–75, 2013.
- [18] M. Maibach et al. "Handbook on estimation of external costs in the transport sector," Produced within the study Internalisation Measures and Policies for All external Cost of Transport (IMPACT) Version 1.1, Delft, 2008.
- [19] IPCC 2011, "Climate Change 2001: The Scientific Basis. Contribution of Working Group I to the Third Assessment Report of the Intergovernmental Panel on Climate Change," Cambridge University Press, Cambridge, United Kingdom and New York, NY, USA, 2001.
- [20] V. Jovanović, M. S. Komatina, "NO<sub>x</sub> and SO<sub>2</sub> emission factors for Serbian lignite Kolubara," Thermal Science, 16.4, 2012, pp. 1213–1228, 2012.
- [21] D. Životić, K. Stojanović, I. Gržetić, B. Jovančević, O. Cvetković, A. Šajnović and G. Scheeder, "Petrological and geochemical composition of lignite from the D field, Kolubara basin (Serbia)," International Journal of Coal Geology, 111, pp. 5–22, 2013.



# Detailed analytical method for ventilation energy consumption investigation

Miklos Kassai\*, Laszlo Kajtar\*

\* Budapest University of Technology and Economics/Department of Building Service Engineering and Process Engineering, Budapest, Hungary  
kas.miklos@gmail.com  
kajtar@epgep.bme.hu

**Abstract**—In our time the explosive spread of the air conditioning systems herein the air handling units is a global phenomenon. Based on the 2002/91/EC, the Directive on the energy performance of buildings (EPBD) it is important to determine the expected energy consumption of the building during the designing period of the HVAC systems. The energy consumption of air handling units and the energy saved by heat recovery units can be determined by two methods. In the case of operating ventilation systems the actual consumption data can be exactly determined by measurement. There are imperfections in the actual available national and international regulations for calculating the energy consumption of ventilation systems. Our research focuses to work out a detailed analytical method to calculate the saved energy of the heat recovery units integrated in ventilation systems.

## I. INTRODUCTION

In our time the explosive spread of the air conditioning systems herein the air handling units is a global phenomenon [1]. With the help of them such air parameters can be supplied in the spaces of the building which can provide the pleasant comfort sensation of the people or the easy operation of the installed technology. Previously the main consideration of the tenders for the reviewing of air-conditioning system designs and constructing was the investment cost. The importance of energy efficient operation and quality management is higher and higher. One of the ways to decrease the investment cost is the neglecting of the accessory costs, and the low quality of the material. All these raise the energy consumption and the opportunity of the uneconomical operation. To supplant these disadvantageous effects, the „Life Cycle Cost” principle is taken into consideration during the reviewing of the tenders. On this wise the investment and operation costs are together taken into consideration for the whole operation period of the equipment [2]. The operation costs include the energy consumption of the air handling unit, the maintenance cost, the cost of the preservation and the annuity cost. In this case the importance of the quality management and the energy efficient operation is higher than focusing only for the investment cost. The spread of this attitude is especially important, because the „low energy buildings”, the „super low energy buildings” and the „passive buildings” are coming to force in the immediate future [3-4]. In additional the statistical data attest that the active cooling is applied by residential and public buildings more and more. By these buildings the

ventilation proportion is significantly increased in the whole energy consumption. There are similar problems by the operation of thermal insulated buildings. In this case the energy consumption of the ventilation system is a major proportion of the energy consumption of whole building services [5].

The objective of 2002/91/EC Directive is to promote the improvement of the energy performance of buildings within the EU countries, taking into account outdoor climatic and local conditions, as well as indoor climate requirements and cost-effectiveness [6]. In the case of many buildings the 100% fresh air in HVAC systems results a significant increasing in the building cooling/heating loads. For such systems, it is necessary to use energy recovery systems to reduce this load. The operating objective of the energy recovery systems is to use the exhaust air of the room to pre-condition the outdoor air. By this way a substantial amount of energy is recovered which reduces the overall HVAC energy consumption. The development of energy recovery systems has led to improved performance and capability in recovering both sensible and latent energy. Enthalpy energy exchangers that utilize a porous membrane as the heat and moisture transfer surface is one device that can recover both sensible and latent energy [7]. Energy recovery systems are commonly used in HVAC systems nowadays. They reduce the operation costs for conditioning ventilation air by both decreasing the required energy to the condition air and auxiliary energy consumption. Significant energy savings from these systems have been shown in several situations. There are many types of energy recovery systems which are now cost effective in a wide range of ventilation designs. These systems include heat or enthalpy wheels, flat plate exchangers (heat/enthalpy), or runaround glycol loops. The operation and performance of these systems is well described in literature.

Air conditioning consumes large share of energy of the total energy use by the whole society. About 20–40% of the overall energy consumption of HVAC system is consumed for ventilation air-conditioning in most commercial buildings. In buildings that require 100% outdoor air to meet ventilation standards (e.g. hospitals), this fraction can be even higher (e.g. 50–60%). Without energy recovery, ventilation air increases energy consumption of buildings since outdoor air must be cooled or heated to bring it close to the indoor thermal comfort conditions [78]. Air-to-air heat and energy recovery systems can be operated in buildings to precondition the supply air by using the exhaust air energy to reduce the

HVAC energy consumption [9]. This also reduces the size of heating and cooling facilities when the indoor air quality is satisfactory.

In our research using these experimental data with the ambient temperature, enthalpy duration curves and the mentioned ambient temperature-enthalpy graph [10], detailed mathematical expressions are presented to calculate and compare the annual energy consumption and energy saved by air-to-air heat recovery and energy recovery units.

## II. METHOLOGIES

Calculation of heating and cooling energy consumption it is necessary to take account of variation of ambient air parameters (temperature, humidity and enthalpy) that vary in daily and season period. The developed calculation procedure is introduced in the article by a fresh air supply air handling unit (AHU). The connection diagram can be seen of a fresh supply air handling system with heat recovery on Figure 1. The signs of the figure are the following: HR: Heat recovery unit, PH: Pre-heater, AH: Adiabatic humidifier, C: Cooler, RH: Re-heater, V: Ventilator.

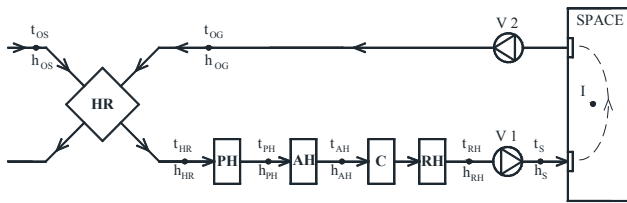


Figure 1. The connection diagram of the ventilation system.

During the energy calculations it is important to take into consideration the order of the air handling elements and the air handling processes. During the operation of the air handling units the air handling processes can be best demonstrated by the Mollier h-x chart [11]. Some parameters are given such as the temperature and relative humidity of ambient air in the sizing state conditions ( $t_{OS}; \varphi_{OS}$ ), the supply air that enters the room ( $t_S; \varphi_S$ ) and the outgoing air that leaves the room ( $t_{OG}; \varphi_{OG}$ ). To perform the energy calculations it is necessary to know the supply air volume flow and the density of the supply air. The values of indoor air parameters depend on the air distribution of the room and are shown between the supply air and outgoing parameters. The energy analysis is not influenced by the indoor air parameters. Figure 2. shows in Mollier h-x chart [11] the process of heat recovery („OS-HRS”) pre-heating („HRS-PH” section), the adiabatic humidifier („PH-H” section) and the re-heating („H-RH” section) in the dimensioning phase in winter time.

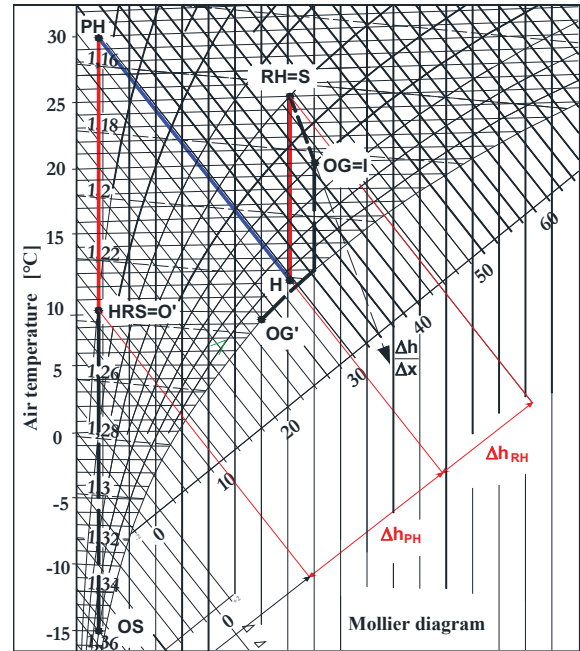


Figure 2. Air handling processes at Mollier diagram in the dimensioning state in winter time.

During the change of the ambient air state the pre-heater heats up the air up to the constant enthalpy line that is determined by the adiabatic humidifier, therefore the ambient enthalpy duration curve has to be used to define the energy consumption of heating [12]. On the ambient enthalpy duration curve (Figure 3.) the above mentioned air state parameters in the dimensioning phase are also shown as well as their changes as the ambient air enthalpy varies during the heating season. The areas of the ambient enthalpy duration curve that represent the energy consumption of the pre-heater and the re-heater can be accordingly drawn. Throughout the calculation of the energy consumption of heating the supply and outgoing air parameters were assumed to be constant during the heating season. This approximation was also applied for the supply and outgoing parameters in the dimensioning phase for the cooling season in the summer.

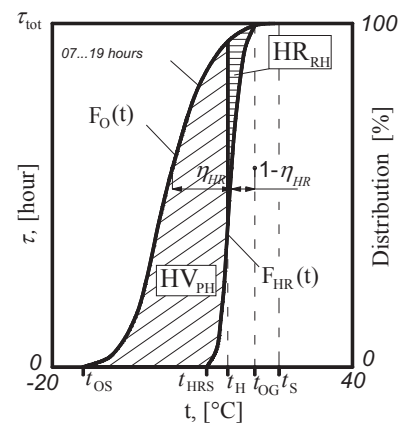


Figure 3. The areas on the ambient enthalpy duration curve that represent the energy saved of heat recovery unit in winter.

On Figure 3. can be seen the areas that proportional to the daytime (07-19 hours) heating energy saved of heat recovery unit in the ventilation system. In compliance with it the physical and mathematical equations were determined to calculate the energy saved of heat recovery for the heaters. Energy saved of the heat recovery for the pre-heater:

$$Q_{HR-PH} = c_{pa} \cdot \rho \cdot \dot{V} \cdot \left[ \int_{t_{OS}}^{t_H} F_o(t) dt - \int_{t_{HRS}}^{t_H} F_{HR}(t) dt \right] [\text{kJ/year}] \quad (1)$$

where  $c_{pa}$  specific air capacity of the air in kJ/kg°C,  $\rho$  is the air density in kg/m<sup>3</sup>,  $\dot{V}$  is the air volume flow in m<sup>3</sup>/h,  $F_o(t)$  is the ambient temperature duration curve (07-19 hours) in h°C,  $t_H$  is the air temperature after the adiabatic humidifier in °C,  $t_{OS}$  is the ambient temperature in sizing state in winter in °C,  $F_{HR}(t)$  is temperature duration curve based on the heat recovery efficiency in h°C,  $t_{HRS}$  is the air temperature after the heat recovery unit in °C.

Energy saved of the heat recovery for the re-heater:

$$Q_{HR-RH} = c_{pa} \cdot \rho \cdot \dot{V} \cdot \left[ \int_{t_H}^{t_{OG}} F_{OS}(t) dt - \int_{t_H}^{t_{OG}} F_{HR}(t) dt \right] [\text{kJ/year}] \quad (2)$$

where  $t_{OG}$  is the outgoing air temperature the leaves the space in °C.

Analyzing the cooling energy consumption the calculation procedure is similar in the summer time. The dimensioning phase for the summer period is specified by the regulations (Figure 4.). The average temperature of the surface of cooling coil ( $t_{ST}$ ) is about 13-14°C.

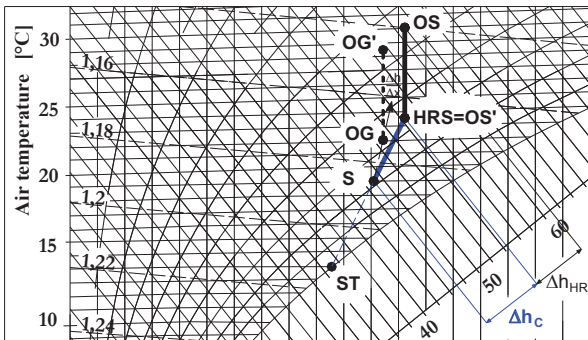


Figure 4. Cooling process on the Mollier h-x chart in the dimensioning phase in summer time.

In light of the above mentioned data the area proportional to the energy consumption of the cooling coil can be drawn in the ambient enthalpy duration curve. In consideration of the fact that there is condensation on the

surface of the cooling coil, the ambient enthalpy duration curve was used to determine the annual energy consumption of the cooling coil (Figure 5.).

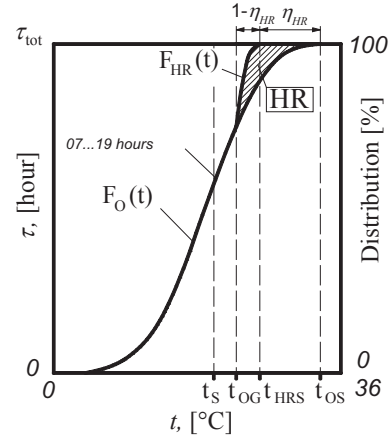


Figure 5. The area on the ambient enthalpy duration curve that represents the energy consumption of the cooling coil.

Energy saved of the heat recovery for the cooling coil:

$$Q_C = c_{pa} \cdot \rho \cdot \dot{V} \cdot \left[ \int_{t_{OG}}^{t_{OS}} [1 - F_o(t)] dt - \int_{t_{OG}}^{t_{HRS}} [1 - F_{HR}(t)] dt \right] [\text{kJ/year}] \quad (3)$$

### III. RESULTS AND DISCUSSION

Good agreement between the experimental and developed detailed analytical results is archived. For proving right of the theoretical method, measured energy consumption data of separated years (2002, 2005 and 2006) were used in the case of two hotel building complexes and an office building. In the selected years the operation characteristic and the caseload of the buildings was average correlate with the building type. On the basis of the underlying six independent measured energy consumption data the difference of the calculated and the measured energy consumption values was between -11,7 and +11,7 % (Table 1). During our research the data of 30 pieces of various constructed air handling units were used.

TABLE I.  
The measured and the calculated energy consumption

	Measured value	Calculated value	Difference [(C-M)/M]
	[kWh/m <sup>2</sup> year]	[kWh/m <sup>2</sup> year]	[%]
Office building (2002)	426	476	11,7
Office building (2005)	539		-11,7
Hotel 1 (2005)	437	455	4,1
Hotel 1 (2006)	444		2,4
Hotel 2 (2005)	441	422	-4,3
Hotel 2 (2006)	418		0,9

Furthermore, in our research work a theoretical comparative analysis was made between two cases too. During our analysis the saved energy of two air handling units were determined for heating and cooling seasons and

the volume flow rate of the air was 3000 m<sup>3</sup>/h and the efficiency of the heat recovery was 70%. The reference model was a model for fresh air supplied air handling unit. The energy analysis was fulfilled using meteorological data for Budapest. The elements of the AHUs are presented in Table 2.

TABLE II.  
Elements of the AHUs.

	HR	PH	AH	RH	C
AHU 1	X	X		X	X
AHU 2		X		X	X

The annual energy saved by the heat recovery unit for heating and cooling seasons has been calculated with the developed method. The saved energy in the case of AHU 2 in heating case is about 23 000 kWh/year and for cooling season was 1100 kWh, comparing the results with AHU 1 which does not include heat recovery unit.

#### IV. CONCLUSIONS

The results show that the saved energy with the heat recovery unit in heating case was about 23 000 kWh/year and for cooling season was 1100 kWh. The annual energy saved is a significance proportion. The developed method is suitable for analyzing the energy saving of the various constructed air handling units. In this manner an optimal decision can be made in the design phase. By choosing the lowest energy consumed air handling unit, a significant energy saving (30-60%) can be achieved during the whole lifetime of the system.

#### ACKNOWLEDGMENT

This research was financially supported by "Sustainable Energy Program" of BUTE Research University (TAMOP-4.2.1/B-09/1/KMR-2010-0002), Budapest, Hungary.

#### REFERENCES

- [1] Jeff B, Explaining the spread of residential air conditioning, 1955–1980, *Explorations in Economic History* 45 (2008) 402–423.
- [2] Magyar T (2003) *Principle of air duct design and application*. Budapest, Hungary p. 3./23-24.
- [3] Mikko N, Carey JS (2005) Life cycle assessment of residential ventilation units in a cold climate, *Building and Environment*, p.15-27.
- [4] Yaw A, Robert W B, Carey JS (2005) Cost-Effective Design of Dual Heat and Energy Recovery Exchangers for 100% Ventilation Air in HVAC Cabinet Units, *ASHRAE Transactions*, Volume 111, Part 1, ISSN 0001-2505, p. 858-863.
- [5] Kjell F, William L (2005) *Calculate ventilation Life Cycle Cost and Count on Savings*, Business Briefing: Hospital Engineering & Facilities Management.
- [6] Official Journal of the European Communities, Directive 2002/91/EC of the European Parliament and of the Council of 16 December 2002 on the energy performance of buildings, 4.1.2003, p. 1/65-71.
- [7] ASHRAE, (2005) *ASHRAE Handbook-Fundamentals*, American Society of Heating, Refrigerating and Air Conditioning, Engineers Inc., Atlanta.
- [8] T. Poós, M. Örvös, L. (2013) Legeza Development and Thermal Modeling of a New Construction Biomass Dryer DRYING TECHNOLOGY 31:(16) pp. 1919-1929.
- [9] M. Fauchoux, C.J. Simonson, D.A. Torvi, (2007) The effect of energy recovery on perceived air quality, energy consumption and economics of an office building, *ASHRAE Trans.* 113 (2) p. 437–449
- [10] L. Kajtár, M. Kassai, L. Bánhidi, (2012) Computerised simulation of energy consumption of air handling units. *Energy and Buildings* 45, p. 54–59.
- [11] Heinz E (1998) Einführung in die Klimatechnik, Erläuterungen zum h-x Diagramm, ISBN 3 8027 2371 6, p.10.
- [12] J. Nyers Dr.Sci., S. Tomić Dr.Ec.: „Financial Optimum of Thermal Insulating Layer for the Buildings of Brick” Conference: 5th International Symposium on Exploitation of Renewable Energy Sources "EXPRES 2013", At Subotica-Szabadka, Serbia
- [13] Robert Kiss (1980) Data for ventilation, Technican Publisher. Budapest, ISBN 963 10 3152 7, p. 207-208.



# Expansion of the photovoltaic solar power plants in the Romanian electric energy industry

István Vallasek

MTA-KAB: Renewable Energetics Work-team CLUJ - Romania

e-mail:ivallasek@ gmail.com

**Abstract – In the present paper we intend to summarize the results in Romania of the industrial use of one of the most promising renewable energy resources – the solar energy – mostly in the field of production of electric energy, which is of crucial importance in all branches of the national economy, as well as in the energy consumption of the population.**

**Key words:** solar photovoltaic power plant, installed capacity, cost of photovoltaic solar energy

## I. INTRODUCTION

The realization of the more and more intensive utilization of renewable energy resources is being a great challenge in the 21st century energetics. The main reason for this is the most probable dwindling of the supply of fossil energy resources (mineral oil, natural gas, coal) as well as the obvious safety problems of nuclear power plants. The basic principles of the EU energy policy are laid down in the Lisbon Treaty. The aims of this policy are supported by market basis means (taxes, support, commercial system of carbon dioxide emission ), by the development of energy technologies (mostly the technologies increasing energy efficiency, the ones using renewable energy sources, and the low emission carbon dioxide technologies ) and finally by communal financial means.

Besides, in December 2008 the EU accepted a number of measures in order to decrease its contribution to global warming and to guarantee the power supply. The renewable energy sources such as wind-power, solar energy (thermal energy and electric power), water-power as well as geothermal- and biomass energy are an alternative of crucial importance as against fossil fuel. Harnessing these sources not only helps to reduce the quantity of green house effect gas which appears during the production and consumption of energy, but also contributes to decrease the dependency of the EU member states on importing fossil fuel (first of all mineral oil and natural gas). [1], [6].

## II. THE PHOTOVOLTAIC EFFECT AND THE PRODUCTION OF ELECTRIC CURRENT BY USING SOLAR ENERGY

Nowadays, besides the quickly spreading of the wind-power plants, the small and large photovoltaic solar power plants represent one of the most dynamically growing area of the environmentally friendly electric energy production. For the time being their capacity is placed on the scale 1kW-500 MW and they can be

divided into two large groups: grid-connected and autonomic (stand alone) power generating systems. In the case of the latter the generated electric power has to be stored compulsorily in accumulator batteries. H. Bequerel discovered the photovoltaic effect in 1839, but more than a century passed until its practical application. The first solar cell based on silicon was produced in 1953 (Pearson, Fuller and Chapin – Bell Laboratories). The first space technological application of the solar cells was the energy supply system of the American satellite Vanguard-1, but following the great mineral oil crisis in 1972, the ground applications started to develop quickly as well. At the beginning of the 21st century the volume of solar cell production shows an exponential development (fig.1.) [2].

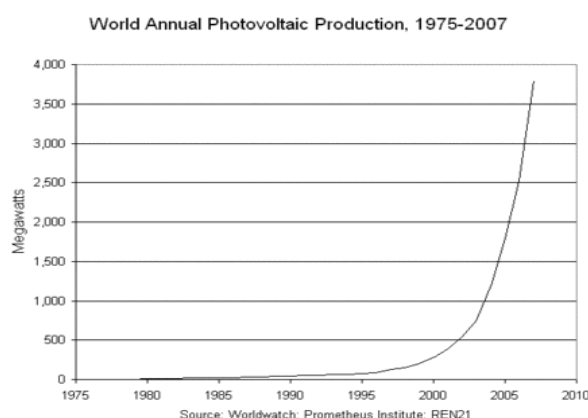


Figure 1. World Annual Photovoltaic Production, 1975-2007  
Source: Worldwatch, Prometheus Institute, Ren21

In the past 5 years the installed capacity of the photovoltaic systems located in the world has increased by 39% on the average besides the significant drop in prices (down by 20 % yearly) of solar cells. As a result of the most intensive research and development activity another promising tendency is the expectable growth of the degree of efficiency of solar cells. At present the net efficiency of the distributed amorphous silicon-basis solar cells is only 4-6% their price being 2,5–3 USD/Wp, yet the efficiency of the crystalline silicon basis solar cells is 14-16% their price being 3-3,5 USD/Wp [4]. In 2012 researchers of Fraunhofer Institute (Freiburg – Germany) developed layered structured solar cells with 43% efficiency. Their industrial mass production could give the photovoltaic branch a great impetus. According to the 2014 data at the end of the year 2013 the electric current producing capacity of the branch reached a 139 GW value on a world scale (fig. 2.)

### III. SPREADING OF THE PHOTOVOLTAIC POWER PLANTS IN ROMANIA

Since 1st January 2007 Romania has become member of the European Union, thus in the energy policy it has to apply the EU regulations concerning the widely spreading of the renewable energy resources. Besides, the National Action Plan (PNAER – June 2010) [3] concerning the energetical utilization of renewable energy sources has been worked out. In Romania the major part of the energetic resources (oil, gas, coal, uranium ore ) is available only in a limited quantity, however the country has an important potential in the field of renewable energy sources (solar-, water- wind-, geothermal and biomass).

Solar PV Total Global Capacity, 2004–2013

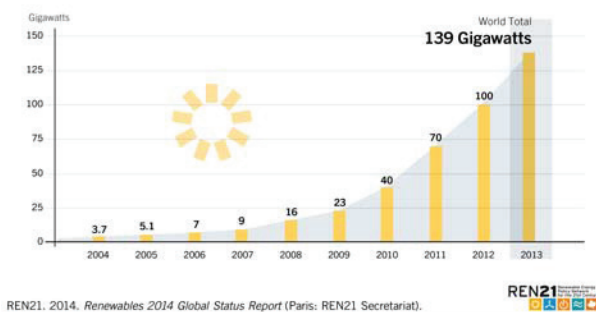


Figure 2. Solar PV Total Global Capacity 2004-2013.

Source: Renewables 2014 Global Status Report, Ren21, Paris

The major objective of the energetic strategy of the country is framing a well-balanced energy mixture which could ensure the competitiveness of the energetic branch, the safety energy supply of the national economy, the wide and efficient exploitation of the inner resources (coal, water and nuclear energy, renewable energy sources), as well as the protection to a greater extent of the healthy environment. By 2010 the scheduled 33% renewable proportionate part of the electric energy production of the country was successfully implemented (20,2TWh, meaning 35,2%), mostly due to the contribution of water-plants (74%), wind plants (22%), and plants using biomass (4%). However, the photovoltaic proportionate part was negligible. The profitable utilization of wind power showed an unexpected explosion-like development between 2010–2013. The growth of the installed output: 7 MW (2008), 14 MW (2009), 462 MW (2010), 982 MW (2011), 140 MW (April 2012), 2000 MW (2013). Wind power parks have been built near the Black Sea in Dobrogea region – the one built in Fantanele – Cogealac is the largest in Europe with 600 MW installed output –, on the Plateau in Moldova and in the south – western part of the country, in the Valley of Timiș.

In the European relation the local conditions and potentiality of Romania, as far as the available solar energy potential is concerned, are favourable, the yearly average value of solar radiation – similar to Hungary – is between 1100-1300 kWh/m<sup>2</sup> (fig.3). According to surveys the photovoltaic potential of solar energy in Romania is 6 TWh/year which is equal to 6000 MWp output.

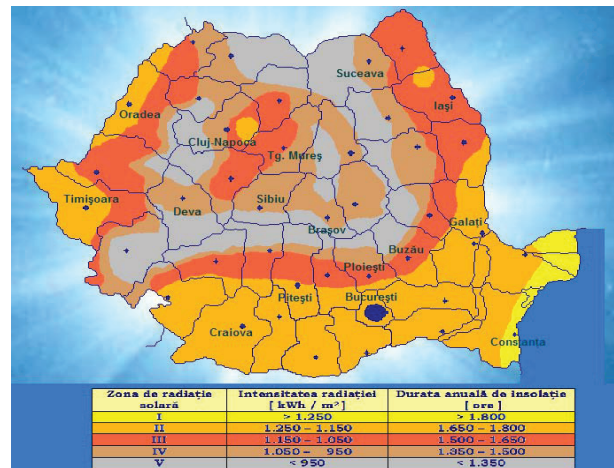


Figure 3. Solar Energy map of Romania.

Source: [www.ministerulmediului.ro](http://www.ministerulmediului.ro)

In the period 2011-2014 a significant number of photovoltaic power plants were built or reached the phase of implementation all over the country. According to the data released by Transelectrica company in September 2014, in Romania the installed output of the power plants based on renewable energy reached the value of 4725 MW, out of which 2805 MW in case of wind – power plants, 1245 MW in photovoltaic solar power plants, 574 MW in small water-power plants and 101 MW can be found in biomass basis power plants. Forecasts predict that in the period 2014-2105 the installation of another 2500 MW capacity is to be expected. Comparing the facts it can be said that for the time being the output of the reactors of the nuclear power plant in Cernavoda is 2x706 MW, the total output of the 259 water power plants of Hidroelectrica Society is 6462 MW, the total output of all the power plants in the country is near 23000 MW. According to the main objective of the National Energetic Strategy (being under processing), by 2020 Romania may be after Denmark the second energetically independent country in Europe.

In Transylvania until August 2012 photovoltaic power plants were built in the following localities: In Satu-Mare county: Satu Mare 6 MW, Mădăraș 0,14 MW, Cămin 0,05 MW, Carei 0,011 MW. In Maramureș county: Oncești 2,91 MW, In Bihor county: Oșorhei 2,97 MW, Nojorid 2,97 MW, Salonta 3 MW. In Timiș county: Gătaia 4x8 MW, Sînnicolaul Mare 7 MW and 2x2 MW, Deta 4 MW, Buziaș 1 MW, Lovrin 2x2 MW, Făget 2 MW, Giulvăz 7,36 MW, Remetea Mică 3 MW, Dudeștii Vechi 2 MW, Săcălaz 0,97 MW, Drăgășina 4 MW, Moșnița Nouă 3 MW. In Caraș-Severin county: Iabłanița 0,05 MW, Berzasca 0,05 MW. In Bistrița-Năsăud county: Lechința 2x3 MW, 2,6 MW, 2,4 MW, Bistrița 1,35 MW. In Alba county: Pianu de Jos 5 MW, In Cluj county: Codor 5 MW, Dej 5,8 MW and 4,5 MW, Moldovenești 3,6 MW, 2 MW, Săcuieu 5 MW. In Mureș county: Stejeriș 5 MW, Tîrgu Mureș 7 MW, Chirileu 3,2 MW. In Sibiu county: Copșa Mică 2,2 MW, Sarosuț pe Târnave 2,97 MW, Șura Mică 2 MW, Ocna Sibiului 3,8 MW, Racovița 1 MW, Hosman 3 MW, 1,2 MW. In Brașov county: Codlea 3,5 MW, 1 MW and Feldioara 5,45 MW, 1 MW.





Figure 4. Izvoarele 50MW Photovoltaic power plant in Romania (Giurgiu county)

In the southern counties of Romania, where the number of sunny hours is greater, more photovoltaic power plants can be found the maximum output of which being superior to 10 MW: Izvoarele 50 MW and 20 MW, Segarcea 48 MW, Slobozia 45 MW, Bălteni-Contești 48 MW, Dumbrava 23 MW and 13 MW, Grojdibodu 10 MW. As represented in the centralised map of photovoltaic power plants [5], the total number of solar power plants in August 2012 was 203. In March 2014 the number of grid-connected photovoltaic power plants was significantly improved, it reached 411. The cost of installed photovoltaic power plants is about 2-2,5 million euro/MW.



Figure 5. The largest photovoltaic power plant in the country was built in Livada (Satu-Mare county). Source: www.napelem.lap.hu, June, 2013.

In 2013 other photovoltaic power plants were opened in different counties of Transylvania: Sebiș (Arad county) 15 MW, Tureni (Cluj county) 0,9 MW, Vinga (Arad county) 1 MW, Livada (Satu Mare county) 48 MW (fig. 5.), Săcășeni (Satu Mare county) 1 MW, Medieșul Aurit (Satu Mare county) 5 MW, Doba (Satu Mare county) 5 MW, Agriș (Satu Mare county) 5 MW, Botiz (Satu Mare county) 9,7 MW, Sălărd (Bihar county) 3,75 MW.

Further photovoltaic investments are being planned in different localities of Transylvania: Cluj, Sfântu

Gheorghe, Baraolt, Bistrița, Lăzarea, Olari, Pilu, Luduș, Vladimirescu, Târnăveni.

Good example for the earlier significant realizations is the photovoltaic energy supply system of END-IBO chocolate manufacture in Remetea (Harghita county) (fig. 6). The system, installed in 2009 covers the needs of the entire industrial production process and of the building itself, and being connected with the national energy network, the produced energy surplus is fed into it. Its output is 8,8 kWp. [2].



Figure 6. Industrial photovoltaic power plant in Remetea (Harghita county) Source: [4].

#### IV. CONCLUSIONS

Using environmentally friendly renewable energy sources photovoltaic power plants could be a promising solution in the field of electric energy production. At present the further development of the area with nearly 140 GW installed output altogether depends on the decrease in prices of solar cells, on the increase of their efficiency as well as on the applied financial support system of the different countries.

#### REFERENCES

- [1.] VALLASEK I. (2013): A megújuló energiaforrások hasznosításának helyzete Romániában, A Magyar Tudomány Napja Erdélyben – *Műszaki Tudományok Szakosztály Konferenciája, Kolozsvár*, 2013. november 23.
- [2.] VALLASEK I. (2013): Fotovillamos energiatermelés Romániában és az Európai Unió néhány tagállamában, EMT-ENELKO (2013): Nemzetközi Energetika - Elektrotechnika Konferencia, Nagyszeben, 117–122 old.
- [3.] \*\*\* 2010: Planul național de acțiune în domeniul energiei din surse regenerabile (PNAER), București, 3–87. old.
- [4.] VALLASEK I. (2013): Fotovillamos áramtermelés Romániában, Magyar Energia Szimpózium, Budapest, 2013. 09. 26.
- [5.] \*\*\* (2012): Harta proiectelor fotovoltaice din Romania, Fabrica de Cercetare
- [6.] \*\*\* (2011): Beneficiile energiei regenerabile, Uniunea Europeană - Direcția Generală Energie, Luxemburg, 1–23 old.
- [7.] Jozsef Nyers, Zoltan Pek: "Mathematical Model of Heat Pumps' Coaxial Evaporator with Distributed Parameters" International J. Acta Polytechnica Hungarica Vol.11, No.10, pp.41-57, 2014.

# Green and more green information technology

Imre Petkovics\* and Ármin Petkovics\*\*

\*Assistant professor, The Faculty of Economics Subotica, Department of Business Informatics and Quantitative Methods, Subotica, Serbia

\*Professor for Applied Studies, Subotica Tech - College of Applied Sciences, Department of Informatics, Subotica

\*\* PhD student, Department of Networked Systems and Services, Budapest University of Technology and Economics

[peti@ef.uns.ac.rs](mailto:peti@ef.uns.ac.rs), [peti@vts.su.ac.rs](mailto:peti@vts.su.ac.rs), [petkovics@hit.bme.hu](mailto:petkovics@hit.bme.hu)

**Abstract**—Energy efficiency is generally the most important aspect for the information technology (IT) sector. The average utilization of IT firms' data centers is varying from 5-15% and there is not much space for improvement. As utilization of cloud computing (CC) data centers are around 35-70%, therefore the cloud-based IT/software utilization is often considered as green. The Power Usage Effectiveness (PUE) values that should be met by CC servers are decreasing year by year which also serves the protection of the environment by offering greener IT. The utilization of the dissipated thermal energy from the data centers for heating purposes can further decrease the carbon emission of the IT infrastructure. Moreover, leading CC service providers are encouraged to use renewable energy sources to offer more environment friendly services and to lower their costs.

## I. INTRODUCTION

By 2030 CC data centers will be responsible for 18% of the world's total energy consumption as forecasted by a recent study [1]. This fact is not negligible even from the environmental pollution point of view; however, CC providers are not primarily driven by the reduction of their ecological footprint but by the lowering of operational costs. Fortunately, in this case, the two goals converge and they meet in the concept of green cloud. Its realization obviously means the development and implementation of green data centers [2].

These days cloud services' energy efficiency is receiving particular attention in research centers and the academia [3]. The topic is very actual and it is noticeable that providing energy efficient software brings new problems to the scene which can be solved only by further investments and by changes in the services of the CC providers. There is a new attribute to describe software products designed to run in the cloud: the aforementioned energy efficiency [4].

Authors of [5] depicted the high-level components of CC (see Figure 1.), noting that "cloud computing environment is a large cyber-physical system consisting of electrical, mechanical and IT systems running a variety of tasks on a multitude of server pools and storage devices connected with multitier hierarchy of aggregators, routers and switches".

Majority of the companies use different servers, operating systems, databases and software which are making them difficult to manage. This problem can be resolved by virtualization, but the high variance their workload and the changing IT resource requirements makes it hard to achieve higher savings.

A company's peak-load level determines the quantity of physical resources which are, in the vast majority of the

time, underutilized. However at CC providers the peak-load levels of the customers does not coincide with each other; rather they are distributed so their utilization can reach notably higher values.

For thousands of interconnected computers in a cloud data center it is a big challenge to migrate the VMs among physical servers dynamically. This can be done with different virtualization platforms.

The disencumbered servers are turned off, resulting in further energy saving. The degree of energy saving can be well estimated based on the following findings.

A well-known early study from 2007 [6] discusses that the total power used by servers in U.S. "represented about 0.6% of total U.S. electricity consumption in 2005. When cooling and auxiliary infrastructure are included, that number grows to 1.2%". Another paper from 2011 [7] contains information that 2008 demand (in U.S.) "was approximately 69 billion kilowatt-hours (1.8% of 2008 total U.S. electricity sales) and that it may be technically feasible to reduce this demand by up to 80% (to 13 billion kilowatt-hours) through aggressive pursuit of energy efficiency measures". A recent study [8] discusses that migrating all business applications in the U.S. to the cloud could reduce their energy consumption by 87%.

After a short introduction to CC our paper will discuss the green operation of the CC data centers, the possibilities of application of renewable energy sources and the utilization of the dissipated energy for diverse purposes.

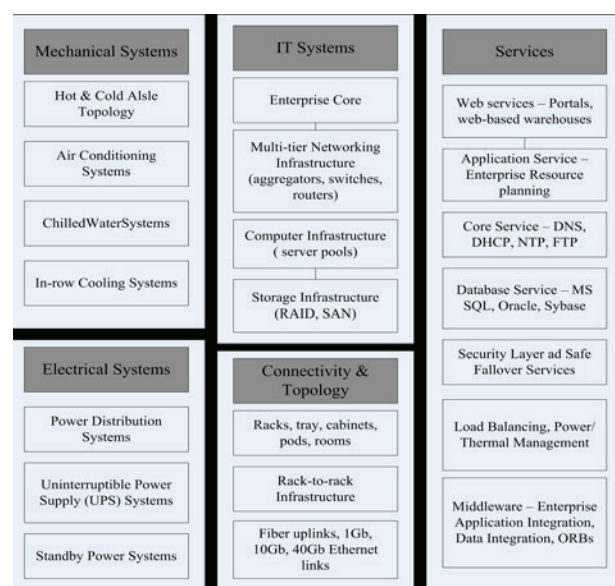


Figure 1: High-level components comprising cloud computing environment [5]



## II. CLOUD COMPUTING

Cloud computing is a fairly old concept (originating from MIT professor, John McCarty in 1961, as a computing utility) implemented by contemporary tools to use computer resources (hardware, software, platform, database servers, application, software package) over the Internet and those about service-level understanding of the processing and payment [9]. "The appearance of CC has been influenced by numerous factors such as the internet, the bandwidth of communication lines (speed of transfer), standardization and virtualization of computer hardware, service orientation of applicative software, the global economic crisis, etc." [10]. Globally CC offers the next three services (Figure 2. [11]):

1. *Software as a Service (SaaS)*. This is software on demand (or software rent) via the Internet for using it on a thin client (web browser) on all computers and mobile platforms.
2. *Platform as a Service (PaaS)* means the rent of computation platform (platform on demand) with necessary software of special use (developmental environments, i.e. programming languages, different libraries of development environments, tools and services) for application development.
3. *Infrastructure as a Service (IaaS)* is the rent of basic computer hardware in the form of virtual machines and networks [12].

From the aspect of publicity of usage, the deployment models are:

- *Private cloud*: The cloud infrastructure is dedicated for exclusive use to a single organization with a large number of workers/end users.
- *Community cloud*: The type of cloud service that provides services for a specific group of users or organizations with common interest.
- *Public cloud*: The type of cloud deployment that offers services to any consumer for open use over the public Internet.
- *Hybrid cloud*: This design of cloud deployments presents a composition of two or three types of cloud deployment models (private, community, or public) [13].

There are many advantages of CC: there are no capital expenditure into hardware and premises for equipment,

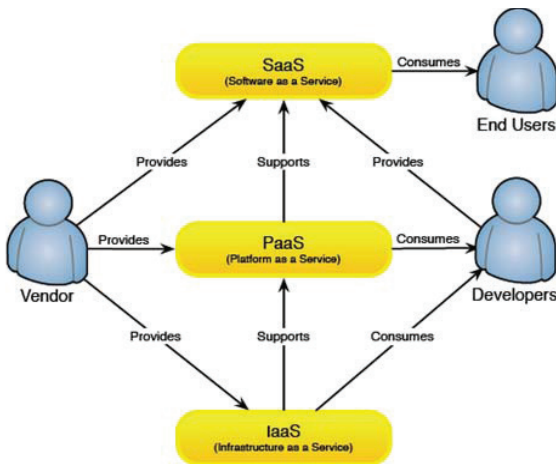


Figure 2. CC services

no costs for software (purchase, licensing and update), reduced energy costs (power supply and cooling), low costs of usage, pay-per-use model of billing, rapid elasticity of services, ubiquitous network access, location-independent resource pooling, identity management and access control, etc.

There are some renowned skeptics with their fears and drawbacks about the application and use of CC: problem of service transferability between suppliers, limited number of services, poor offer of software solutions in cloud, lack and rigidity of SLAs, immature technology, availability of services and bottlenecks in transfer, the likelihood of troubles halting the service is great (the type of service is very complex), and so on.

The conceptual model of physical realization of CC services in Figure 3. [14] shows how the data centers' servers are allocating virtual machines with suitable resources for the diverse needs of many different users. They do this with the help of a virtualization platform.

The power usage effectiveness (PUE) is one of the most important indicators for cloud computing (and other) data centers' functionality, especially to express their power efficiency. If the value of PUE is 2.0 that mean that for every watt of IT power, another additional watt is consumed to distribute power and to cool the IT equipment. Ideal value of the PUE would be a little above 1.0, when nearly all of the energy is used for computing.

Google calculates PUE by the following formula [15]:

$$PUE = \frac{ESIS + EITS + ETX + EHV + ELV + EF}{EITS - ECRAC - EUPS - ELV - ENet1}$$

The abbreviations are the following:

**ESIS** - Energy consumption for supporting infrastructure power substations feeding the cooling plant, lighting, office space, and some network equipment

**EITS** - Energy consumption for IT power substations feeding servers, network, storage, and computer room air conditioners (CRACs)

**ETX** - Medium and high voltage transformer losses

**EHV** - High voltage cable losses

**ELV** - Low voltage cable losses

**EF** - Energy consumption from on-site fuels including natural gas & fuel oils

**ECRAC** - CRAC energy consumption

**EUPS** - Energy loss at uninterruptible power supplies

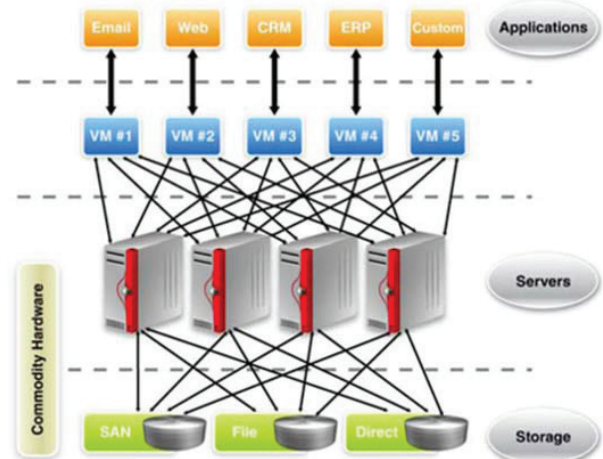


Figure 3. Physical realization of CC [14]

(UPS) which feed servers, network, and storage equipment

**ENet1** - Network room energy fed from type 1 unit substitution

### III. TOWARDS GREENER CLOUD COMPUTING

#### A. Decreasing the PUE value of data centers

Keeping PUE values around 1.1-1.2 would result in around 40% saving compared to classical CC data centers. With the following techniques, one can further improve (lower) the PUE values:

#### B. Energy consumption of IT equipment

- a. Cloud computing data centers can comprise even thousands or tens of thousands of server machines. Those servers may be far from energy uniformity, and that may be the key source to energy inefficiency in cloud computing environment.
  - a. *Solution 1*: using energy-proportional servers in data centers.
  - b. *Solution 2*: dynamic migration of VMs among physical servers and turning off idle servers using Dynamic Voltage/Frequency Scaling (DVFS) approach
- b. Energy inefficiency of the disks
  - a. *Solution*: applying CCD devices
- c. Servers still consume electric energy and have to be cooled even when they are turned off, because the embedded card controllers are always active, as they are used to wake up the servers.
  - a. *Solution*: -This issue does not have a solution published yet. Our idea for this question is to deploy small passive RFID elements which will be in charge for waking up servers from sleep mode. They are called passive elements because they are obtaining their energy for operation from the wake-up electromagnetic waves that are sent them when they have to act. The energy demand and thus the efficiency of such wireless wake-up methods for cloud data centers are quite hard to judge without real-life simulation.

#### C. Energy consumption of Cooling and Air Conditioning

- d. Inefficiencies of Cooling and Air Conditioning systems - cooling is responsible approximately for 30% of the overall energy cost of the cloud environment.
  - a. *Solution 1*: better server and rack arrangement for CC data centers
  - b. *Solution 2*: continuously controlling the temperature of the equipment, and using demand-driven, variable frequency drive (VFD) fans to match variable heat loads

c. *Solution 3*: increasing the temperature in the data center: instead of 20-22 degrees, 26-28 degrees of Celsius can be suitable [16]

d. *Solution 4*: using liquid-cooling or evaporative cooling [17] instead of only ventilators - as these cooling techniques are more efficient thus are cheaper to operate

e. *Solution 5*: finding the right geographical location in order to benefit from ambient cooling (cold air or water)

#### D. Power supply and the energy waste of multiple power conversions

- e. Enhancing supply-safety and the usage of green energy sources
  - a. *Solution 1*: data centers have to be connected to two or more separate grids: one or more renewable power grids, and the generic “grid” power, see Figure 4. [18]
- f. Multiple power conversion losses (because the need for multiple power conversions in the power distribution system for data centers) - main AC power supply from the grid is usually first converted to DC to charge the battery backup system whose output by inverter converted to AC power again, and this energy is then distributed to the data center’s hardware (Figure 4. [18])

#### Power Supply

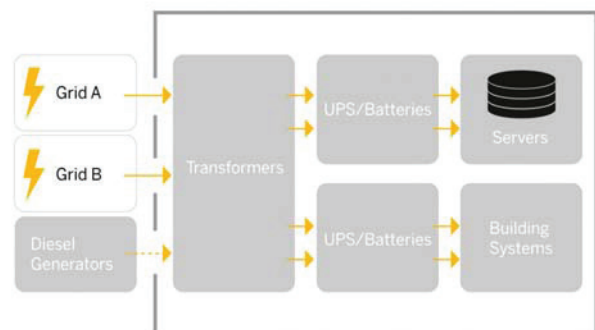


Figure 4. Power supply of SAP Data Centers [18]

a. *Solution 1*: using highly efficient transformers and inverters with continuous operation control.

#### E. Renewable energy sources and utilization of the dissipated energy

All CC providers tend to use renewable energy sources. Most of them have long-term contracts with companies who are providing green energy obtained from sunlight or wind power. The proportion of renewable energy usage from the overall power consumption is highly differing among CC services providers. All the data centers of SAP use renewable energy [19] so they rightly claim that their cloud services can be considered

fully “green”. One should note that SAP is momentarily one of the minor cloud providers so its energy demand is much less than those of the big players on the market. One of the biggest cloud services providers, Google obtains 35% of its energy needs from renewable sources. The liquid-cooled data centers’ rapid spread is expected in the near future, because on the one hand they result in large cost savings, on the other hand, the dissipated energy can be used for heating at the data centers other premises or for the same purpose at the nearby offices and residential buildings [20], [21], [22]. The huge advantage of liquid-cooling is that there is no need for fans inside the servers, resulting in 30% saving on cooling. What is even more significant, these types of servers result in no or just very slight warming of their surroundings, which results in an additional 30% on server-cooling costs. Liquid-cooled servers could be deployed in server racks more densely and processor overclocking can be applied without any concerns [23].

#### IV. CONCLUSION

As both the number of cloud computing users and providers are growing at a rapid pace (are said to be doubled in every five years according to the literature), the energy consumption of data centers, their operational efficiency, possibilities to reduce dissipation and the recycling of the released heat energy have become areas of intensive research. Our paper aimed to give an insight and overview of this important scientific and technical problem group, pointing to the possible ways of development and opportunities for better solutions in the topic.

#### REFERENCES

- [1] S. Srivastava, P. M. Khan, R. Beg, "Energy Efficient Approach For Cloud To Improve Environmental Effect", *International Journal of Software Engineering Research & Practices* Vol.4, Issue 1, April, 2014., pp. 14-19., ISSN: 2231-2048
- [2] V. P. Viradia, C. M. Bhatt, H. S. Jayswal, "Green Cloud: Implementation and Adoption of Green Data Center", *Proceedings of the Second International Conference on "Emerging Research in Computing, Information, Communication and Applications"*, ERCICA 2014, ISBN:9789351072621, Elsevier Publications 2014., pp. 163-167.
- [3] G. Procaccianti, S. Bevin, and P. Lago, "Energy efficiency in cloud software architectures," in *Proceedings of the 27th Conference on Environmental Informatics - Informatics for Environmental Protection, Sustainable Development and Risk Management*, vol. 1. Shaker Verlag GmbH, 2013, pp. 291–299.
- [4] G. Procaccianti, P. Lago, G. A. Lewis, "Green Architectural Tactics for the Cloud", *WICSA 2014*, pp. 41-44
- [5] A. Uchechukwu, K. Li., Y. Shen, "Energy Consumption in Cloud Computing Data Centers", *International Journal of Cloud Computing and Services Science (IJ-CLOSER)*, Vol.3, No.3, June 2014, pp. 145-162., ISSN: 2089-3337
- [6] J. Koomey, "Estimating Total Power Consumption by Servers in the U.S. and the World", Oakland, CA, Analytics Press, 2007
- [7] Masanet, E., Brown, R.E., Shehabi, A., Koomey, J.G., and B. Nordman (2011). "Estimating the Energy Use and Efficiency Potential of U.S. Data Centers." *Proceedings of the IEEE*. In press. DOI: 10.1109/JPROC.2011.2155610
- [8] E. Masanet, A. Shehabi, L. Ramakrishnan, J. Liang, X. Ma, B. Walker, V. Hendrix, P. Maanthe, "The energy efficiency potential of cloudbased software: A u.s. case study," *Laurence Berkeley National Lab, Berkeley, California, Tech. Rep.*, June 2013.
- [9] I. Petkovic, P. Tumbas, "Temptation of the Past in the Shape of Clouds – Cloud Computing", in *Hungarian, IKT2010*, Dunaujvaros, Hungary, 2010, p. 190-199.
- [10] I. Petkovics, Á. Petkovics, "ICT Ecosystem for advanced Higher Education", *SISY 2014, IEEE 12th International Symposium on Intelligent Systems and Informatics • September 11–13, 2014, Subotica, Serbia*, ISBN: 978-1-4799-5996-9
- [11] G. Briscoe, A. Marinos, "Digital ecosystems in the clouds: towards community cloud computing", *Conference paper, Originally presented at IEEE International Conference on Digital Ecosystems and Technologies*, 1-3 June 2009, Istanbul.
- [12] I. Petkovic, Dj. Petkovic, A. Tesic, E. Suljovic, "Value network of Cloud Computing Service Ecosystem", *TTEM Journal*, ISSN 1840-1503, Vol.8, No.4, 2013, pp.1689-1698.
- [13] I. Petkovics, P. Tumbas, P. Matković, Z. Baracska, "Cloud Computing Support to University Business Processes in External Collaboration", *Acta Polytechnica Hungarica*, ISSN 1785-8860, Vol. 11, No 3, 2014., pp. 181-200.
- [14] Broadcom Corporation, "Meeting the Five Key Needs of Next-Generation Cloud Computing Networks with 10 Gb", *E-White Paper*, July, 2009.
- [15] Google, "Efficiency: How we do it - Measuring efficiency", <http://www.google.com/about/datacenters/efficiency/internal/>, referenced at Feb. 03, 2015.
- [16] Google, "Efficiency: How we do it - Temperature control", <http://www.google.com/about/datacenters/efficiency/internal/#temperature>, referenced at Feb. 07, 2015.
- [17] "Evaporative cooling: Engineering's second server room", case study, *The Cambridge Green Challenge*, online: <http://www.environment.admin.cam.ac.uk/resource-bank/case-studies/energy-and-carbon-reduction/evaporative-cooling-engineerings-second>, referenced at Feb 06, 2015
- [18] SAP Data Centers, "How a Data Center Works", [http://www.sapdatacenter.com/article/data\\_center\\_functionality/#details-aside-90](http://www.sapdatacenter.com/article/data_center_functionality/#details-aside-90), referenced at Feb. 03, 2015.
- [19] SAP Data Centers, "Zero Emissions", <http://www.sapdatacenter.com/article/zero-emissions/>, referenced at Feb. 05, 2015.
- [20] Gizmodo, "Seattle Wants to Heat Itself Using Waste Heat From Data Centers", 10/17/13, <http://gizmodo.com/seattle-wants-to-heat-itself-using-waste-heat-from-data-1446977944>, referenced at Feb. 05, 2015.
- [21] M. LaMonica, "IBM liquid-cooled supercomputer heats building", <http://www.cnet.com/news/ibm-liquid-cooled-supercomputer-heats-building/>, referenced at Feb. 06, 2015.
- [22] Reuters, "Underground data center to help heat Helsinki", <http://www.cnet.com/news/underground-data-center-to-help-heat-helsinki/>, referenced at Feb. 05, 2015.
- [23] P. Rubens, "Liquid Cooling Gaining in Popularity Again", <http://www.enterprisenetworkingplanet.com/datacenter/liquid-cooling-making-a-comeback.html>, referenced at Feb. 06, 2015.



# Tribological characteristics of bio lubricants

M. Stojilko<sup>\*</sup>, D. Golubović<sup>\*\*</sup>, D. Ješić<sup>\*\*</sup>

<sup>\*</sup> NIS Gaspromneft, Novi Sad, Serbia, e-mail: miles.ns@gmail.com

<sup>\*\*</sup> Faculty of Mechanical Engineering in East Sarajevo, Republic of Srpska, e-mail: dusan.golubovic54@gmail.com

**Abstract** - Vegetable oils and animal fats are used for lubrication before the discovery of crude oil. With the advent of petroleum and petroleum products, mineral base oils are more accessible and cheaper than the plant. Development of lubricants is going in the direction of mineral base oils. However, in recent years, as a consequence of the increasing environmental pollution and reduction of reserves of crude oil, have intensified the development of a large number of environmentally friendly lubricants. Environmentally friendly lubricants are rapidly biodegradable and non-toxic to living organisms. The most important raw materials for the formulation of environmentally friendly lubricants are vegetable oils, as well as their modified esters. The paper presents the tribological properties of vegetable oils, which was compared with the tribological properties of mineral oil.

## I. INTRODUCTION

The interest in environmentally acceptable lubricants is growing from year to year, especially in areas where, on the application of mineral oil can cause damage to the environment, such as oil losses in motor saws, agricultural, forestry and construction machinery, railway and tram switches, outboard motor boats, formwork oil in construction, steel ropes and chains, as well as other flow lubrication where the lubricant in the overall amount remains in the environment.

Previous studies in this area have shown that vegetable oils can replace some of the mineral due to their inherent biodegradability, and excellent lubricity. In addition, vegetable oils are renewable resource or a renewable natural resource. Research in the field of application of biodegradable oils indicate that vegetable oils have advantages and disadvantages compared to mineral oils:

- Advantages: non-toxicity, biodegradability, good lubricity, high flash point, high viscosity index and low volatility
- Disadvantages: poor oxidation stability, poor low-temperature characteristics, or poor flowability, poor hydrolytic stability and high cost price compared to mineral oil

Typical characteristics of the vegetable and mineral base oil are shown in Table 1. The vegetable oils are triglycerides, which are a complex mixture of fatty acids with different chain lengths and number of double bonds. Triglycerides are rapidly biodegradable and have excellent lubricity properties. However, their thermal, oxidative and hydrolytic stability are limited. Lubricants

based on vegetable oils are suitable only for relatively lower working temperature not exceeding 70 °C.

Table 1: Typical characteristics of different base oils

Characteristics	Vegetable oil	Mineral oil
Lubricity	high	low
Oxidation Stability	poor	very good
Index viscosity	excellent	good
Hydrolytic Stability	low	high
Stickiness	high	low
Saturation hydrocarbons	unsaturated	saturated
Flash point	very good	good
Low-temperature properties	poor	good
Miscibility with mineral oil	good	-
The tendency to swell seals	slightly	mildly
Impact of the paint	no effect	no effect
Tendency to the formation of sludge	poor	good

## II. EXPERIMENTAL

The tests should show the difference that exists between mineral lubricants and based on vegetable oils in terms of their technical characteristics, or their ability additive and are therefore subject to these tests, as starting materials, used the following base oils. As a mineral oil base oil is taken which is used for the production of mineral lubricant for lubrication. This mineral base oil in the following text will be marked as MIN 30, and is set to such a viscosity corresponding to a viscosity of vegetable oil from rapeseed, which is designated as the REP 30. Physico-chemical characteristics MIN 30 and REP 30 are shown in Table 2. For this test was taken as vegetable oil from rapeseed oil, which is pressed from a non extraction method. Pre tribological testing of oil samples was evaluated solubility of anti-wear additives. The additive is well-dissolved in the oil. Only after these tests carried out was started with a series of tests specified below.

Table 2. Physical and chemical characteristics of the oil used in the experiment

Physical and chemical characteristics	Units	MIN 30	REP 30	Methods
Density at 20°C	g/cm <sup>3</sup>	0,8903	0,92	ISO 3675
Kinematic viscosity at 40°C	mm <sup>2</sup> /s	29,15	34,07	ISO 3104
Kinematic viscosity at 100°C	mm <sup>2</sup> /s	5,3	7,84	ISO 3104
Index viscosity		98	213	ISO 2909
Flash point	°C	207	322	ISO 2952



Pour point	$^{\circ}\text{C}$	- 15	-8	ISO 3016
Neutralization number	mgKOH/g	0,007	0,3	ISO 6618

### III. EQUIPMEN AND TEST METHODS

#### Four ball test - Wear

The test resistance to wear is performed by the standard method ASTM D4172. This test demonstrates the efficacy of protection against wear, or used for determining the resistance of lubricating film on the load in mixed and mild boundary lubrication conditions. Basic test element consists of four balls that are in the shape of a regular tetrahedron immersed in the test oil. Three balls are fixed in the carrier by means of rings and submerged in the oil. The fourth balls is attached to the bracket that together with it rotates around a vertical axis, with 1500 rpm, Figure 1. The load of 40 kg is transmitted through the upper rotating balls resting evenly on three balls. Test duration was 60 minutes at a temperature of  $65^{\circ}\text{C}$ . After the test is measured by the diameter of the wear surface (which is in the form of a calotte) of the lower three stationary balls, and the result is expressed as the mean diameter in mm wear. Wear beads is a direct indicator of resistance lubricating film on the load; What is the value of the mean diameter less resistance lubricating film is higher and inversely.



Figure 1: Four ball apparatus

#### Four ball test - Extreme Pressure

Test the ability to withstand extreme pressures is performed the standard method ASTM D 2783, on the device with four balls. The difference from the previous test of wear is that the load is gradually increased until scuffing or welding beads, Figure 2. EP-four ball is used to determine the load that the lubricant may be submitted, or to measure the strength of the lubricating layer in the boundary lubrication conditions (EP properties). Basic test element consists of four balls, which are in the form of a regular tetrahedron immersed in an oil to be tested. The upper balls rotates at a constant speed around a vertical axis, touching the other three balls fastened to the base of the tetrahedron. With specific load balls, test takes 10 seconds. The load is increased until the balls are

not welded. The load at which the bead welds is expressed as a point of welding expressed in Newtons (N). What is the value of the welding point, the greater the strength of the lubricating film.

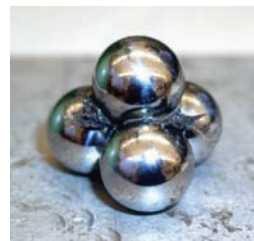


Figure 2: Welded steel balls

### IV. TEST RESULTS

Measured values obtained in a device with four balls of rapeseed (REP 30) and mineral oil (30 MIN) can be found in Tables 3 and 4 and shown in the diagram in Figure 3 and 4.

Table 3: Carrying capability extremely high pressures

Participation additives (%)	REP 30 (N)	MIN 30 (N)
0,0	1400	1400
0,2	1500	1600
0,4	1900	1700
0,6	2000	1800
0,8	2000	1900
1,0	2200	1900
1,2	2200	1900
1,4	2200	1900
1,6	2200	1900
1,8	2400	1900
2,0	2400	1900

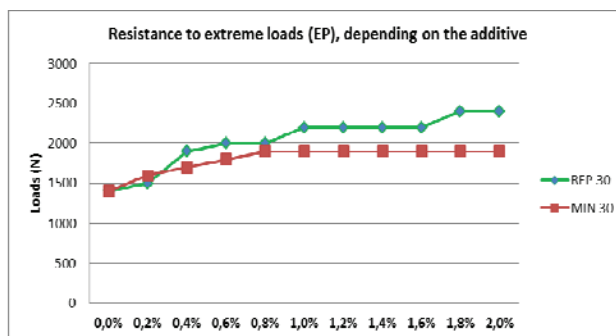


Figure 3: Resistance to extreme loads

Table 4: Resistance to wear

Participation additives (%)	REP 30 (mm)	MIN 30 (mm)
0,0%	0,66	0,87
0,2%	0,62	0,81
0,4%	0,57	0,76
0,6%	0,55	0,72
0,8%	0,55	0,64
1,0%	0,51	0,61
1,2%	0,48	0,57
1,4%	0,47	0,48

1,6%	0,43	0,40
1,8%	0,40	0,40
2,0%	0,38	0,40

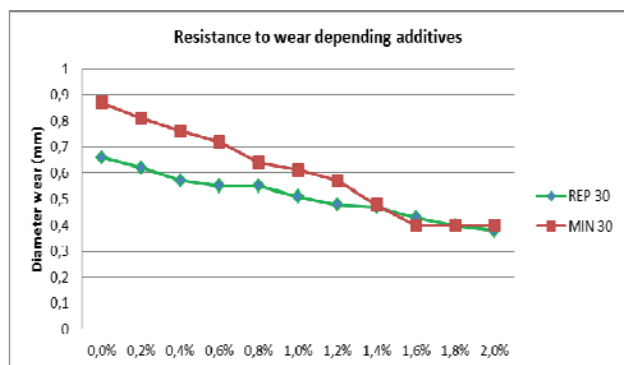


Figure 4: Resistance to wear

Test results of tribological characteristics (size wear and withstand high pressures) of mineral base oils (MIN 30) and vegetable oils (REP 30) are shown in Tables 3 and 4, and to facilitate analysis are also shown diagrammatically in Figures 3 and 4.

During the testing was done additives and anti-wear additives to withstand the extreme pressures and shock loads in the amount of 0.2%. After each addition of additives, laboratory testing was performed on a standard device with four balls. The first measurement was with pure base oils without additives.

When testing the resistance to extreme loads (Table 3 and Figure 3) you can see the influence of additives on vegetable and mineral base oil. Already in the share of 0.4% additives can be seen better efficacy in rapeseed oil. Further adding additives were given the better characteristics of rapeseed oil. With addition of 0.8% of additives, the values obtained for the rapeseed oil of 2000N, and 1900N for the mineral oil. The further addition of additives in mineral base oil had no effect, the balls are permanently welded at a load of 1900N. However, with further addition of rapeseed oil additives it was effective up to 1.8% when the maximum load of 2400 N.

When testing the resistance to abrasion (Table 4 and Figure 4) we can see the impact of additive tear on vegetable and mineral base oil. Already at the first addition of the additive of 0.2% can be observed in the efficiency of the additive as rapeseed oil as well as in the mineral base oil. For mineral base oils by adding 1.6% additive achieves the maximum result and further additives have no effect. The additive in the amount of 2.0% rapeseed oil achieves the maximum value, minimum value or tear in diameter of 0.38 mm.

## V. CONCLUSION

Test of resistance to wear and high pressures were carried out on the device with four balls ("four ball" test). Abrasion testing was carried out according to the method

ASTM D 4172. The test is done with a load of 400 N, number of revolutions of movable balls of 1500 min<sup>-1</sup>, at oil temperatures of 65°C for a period of 60 minutes.

Test of resistance to extreme pressures was performed according to ASTM D 2783 on the unit with four balls ("four ball"). The load is gradually increased until the moment scuffing balls. This load is the maximum value that investigated the oil may be submitted until the moment of scoring.

The results show much better tribological properties of rapeseed oil (REP 30) in relation to the mineral base oil (MIN 30) and much better able to withstand the extreme pressures and shock loads and better wear resistance.

## REFERENCES

- [1] Bartz W.J., Ekotribologija, XXXVI stručno znanstveni skup Maziva 2003, Rovinj, Separat No. 347.
- [2] Stojilković M.: Research application of ecological oils in the tribological systems, Doctoral dissertation, 2014.
- [3] Stojilković M., Golubović D., Ješić D.: Ecotribology Aspects in the Lubricants Application, EXPRES 2014. Subotica
- [4] Stojilković M.: Primena maziva, NIS a.d., Beograd (2011)
- [5] Stojilković M.: Podmazivanje motornih vozila, YUNG, Beograd (2002)
- [6] Stojilković M., Pavlović M.: Utjecaj maziva na okoliš, XXXVIII stručno znanstveni skup Maziva 2007, Rovinj
- [7] Stojilković M., Vukolov D., Kolb M.: Tribološka ispitivanja biorazgradivih ulja, Stručno znanstveni skup Maziva 2013, Rovinj
- [8] Golubovic, D., Kovač, P. i dr.: Wear intensity of different heat treated nodular cast irons, Journal of Metallurgy, Vol. 53, January/March, 2012.
- [9] Sovilj, B., Sovilj-Nikic, I., Golubovic, D., Jesic, D.: The effect of specific relationship between material and coating on tribological and protective features of product, Journal of Metallurgy, Vol. 53, January/March, 2012.
- [10] Jesic, D., Sovilj, B., Sovilj-Nikić, I.: Measurement methodology of characteristics and election of materials of elements of tribomechanical systems, Metalurgija, April/June, 2011.
- [11] Ridderikhoff H., Horvath P.: Razmatranje utjecaja zaštite zdravlja, okoliša i sigurnosti pri izboru baznih ulja za industrijska maziva, XXXVI strucno znanstveni skup Maziva 2003, Rovinj, Separat No. 356.
- [12] Hewstone R.K., Spiess G.T., Handling, reuse and disposal of used lubricating oils, Institute of Petroleum, Petroleum review, \*ISSN\* 0020-3076, 1988
- [13] Marin AG., Petre I., Bogatu L.: Vegetable oils in engine lubricants formulation, Serbiatrib 07, 10th International Conference on Tribology, 2007.
- [14] Linda McGraw, "Biodegradable Hydraulic Fluid Nears Market", April 19, 2000, USA Agricultural Research Service.
- [15] Nyers J., Nyers A.: "Investigation of Heat Pump Condenser Performance in Heating Process of Buildings using a Steady-State Mathematical Model". I.J. Energy and Buildings. Vol. 75, pp. 523–530, June 2014. DOI: 0.1016/j.enbuild.2014.02.046
- [16] Nyers J., Nyers A.: "Hydraulic Analysis of Heat Pump's Heating Circuit using Mathematical Model". 9rd IEEE ICCCI International Conference" Proceedings-USB, pp 349-353, Tihany, Hungary. 04-08. 07. 2013. ISBN 978-1-4799-0061-9

# Experimental and investigating of different engineering materials

A. Nagy, B. Dudinszky

\*Budapest University of Technology and Economics, Department of Building Service and Process Engineering, H-1111 Budapest, Műgyetem rkp.3-9. Tel: (1)-4631119, e-mail: [drnagyandras@freemail.com](mailto:drnagyandras@freemail.com), <http://www.epget.bme.hu>

**Abstract**-The damage in structures caused by repetitive load can originate in the material fatigue appearing at stress-concentrate places. Depending on the value of the load number which causes the damage done by fatigue it can talk about low cyclic fatigue caused by cumulative plastic strain or high cyclic fatigue caused by purely elastic stress. The dimensioning methods [2,3] which take into consideration the above mentioned phenomenon based on experimental data. This article summarizes the most important results of the investigation done on low cyclic fatigue specimens as well as the conclusions which can be drawn from them. The aim of the experiments is to reveal the actually utilizable elastic stress range between tensile and compression yield stress belonging to different tensile strains. The results of the experiments provide the basic data for dimensioning structures exposed to low cyclic fatigue taking into account the Bauschinger-effect.

## I. INTRODUCTION

The development of the information technology parallel to numerical methods (BEM & FEM) made it possible to determine precisely the elastic-plastic load carrying capacity of steel-structures, by other words, to realize more economic and safer structures utilizing better the engineering material. The above mentioned numerical methods use ideal elastic-plastic or linear stiffening material laws in majority of cases. The criterion limit of load carrying capacity is determined at static load as  $p_{0,2}$  belonging to 0,2% plastic deformation, at repeated load it is the shakedown load ( $2R_{eH}$ ) meaning the double of yield strengths. Experience gained from our previous test results [1] that is at vicinity of stress concentrating cross-sections on pressure vessels (for instance, flanges, tube connections, man-holes or supports as well as at critical areas of closing heads) behavior of engineering material inclines from the above mentioned simple material laws, so the criterions derived from them, among others the load carrying capacity should be revised. Applying strain gauges measurements around stress-concentrating cross-section it can be testified that structures can stand static loads without damages that cause bigger deformations than 0,2% plastic deformation. At the same time it is proved that under proportionally increasing cyclic load the compression yield strength of the applied engineering materials as well as the utilizable elastic stress range

belonging to the elastic-plastic shakedown are not constant but their actual value changes by significant measure as a function of prestressing. Conclusions derived from test results correlate with explanations found by other research fellows [2,3] who deduced the mentioned phenomena on the „Bauschinger-effect” observed at engineering materials. Investigating the related literature it can be stated that several researchers are dealing with the Bauschinger-effect in our days [4-7] but it is rare to take it into consideration at dimensioning structures on strength.

## II. EXPERIMENTAL INVESTIGATION OF THE BAUSCHINGER EFFECT USING FATIGUE SPECIMENS MADE OF DIFFERENT ENGINEERING MATERIALS

Damages caused by repeated load at different structures basically can be deduced on fatigue of the engineering material at stress concentrating places. The damage by fatigue can come into being as low cycle damage owing to accumulation of plastic deformations or as high cycle damage resulted by stresses within the elastic limit stress. Dimensioning methods [2,3] taking into consideration the above mentioned phenomena are based on the test results. This chapter presents the most important results of our low-cycle tests on fatigue specimens parallel to conclusions that can be deduced from them. The tests were carried out on room temperature with specimens made of carbon and stainless steels. The aim of the tests was to determine the range of elastic-stresses that can be utilized [assigned in Fig.2. with  $\sigma^E(\varepsilon)$ ] in case of the different elastic-plastic tensile displacements and compression yield stress limits belonging to them. Test results serve as basic data at dimensioning structures on low-cycle fatigue taking into consideration the Bauschinger effect.

### A. Test results and conclusions

These were manufactured fatigue test specimens both from carbon and stainless steels to investigate the characteristics of the engineering material followed by heat treatment to eliminate residual stresses. Tests were carried out on room temperature at the Department of

Material Science and Technology using MTS 810 type compression-tension tensile tester equipped by programme-controlling (see Fig 2). During the tests specimens, previously heat treated to eliminate residual stresses, were loaded up to different levels of tensile elongation then subjected to compression. Correlation of stress-elongation was registered by fine displacement register having 8mm measuring base (see Fig.1.). Results of tests are presented in Fig.3-12. The interpretation of strength characteristics presented in the following figures can be seen in Fig.2. Figure 3,5,7,9,11. show the results of tensile/compression tests carried out until various tensile elongation, whereas Figure 4,6,8,10,12 illustrate the resultant stress-strain diagram determined from the measurement points and values of compression yield stress function of tensile elongation. As shown in Figure 3, the compression yield stress was defined by stress values  $\sigma_{p(50)}(\epsilon)$ ;  $\sigma_{p(100)}(\epsilon)$ ;  $\sigma_{p(200)}(\epsilon)$  belonging to deviations from the unloading straight lines  $\Delta\epsilon = 50\mu\text{strain}$ ;  $\Delta\epsilon = 100\mu\text{strain}$  and

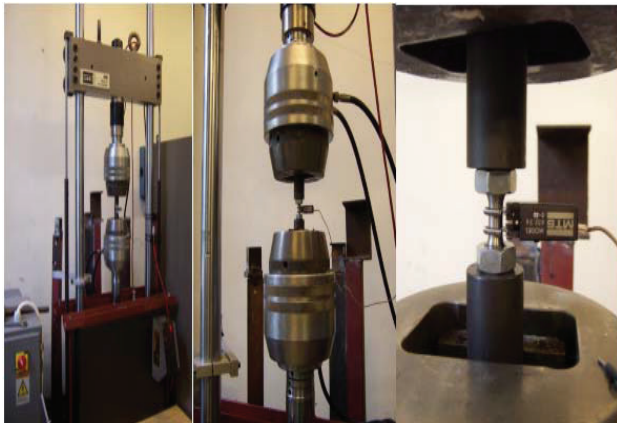


Fig.1. MTS 810 type compression-tension tensile tester equipped by fine displacement register.

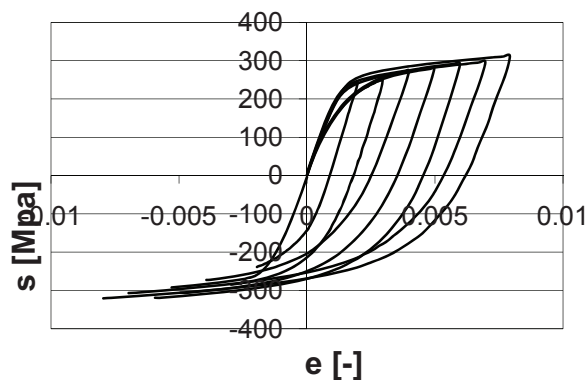


Fig. 3. Stress-strain characteristic curves at different tensile elongations in case of 1.4301 type engineering material.

$\Delta\epsilon = 200\mu\text{strain}$ . The figures also show the utilizable elastic stress  $\sigma_{50}^E(\epsilon)$ ;  $\sigma_{100}^E(\epsilon)$ ;  $\sigma_{200}^E(\epsilon)$  belonging to the different tensile elongations. As figures suggest, the compression yield stress of carbon steels is not invariable, its numerical value changes (decreases) significantly depending on the tensile elongation. Utilizable elastic tension as shown in figures is not invariable, either; in the case of the carbon steel under investigation, it decreases with increasing elongation and its value is lower than what the literature assumes ( $2R_{eH}$ ). Based on specimen tests it can be stated that the compression yield strength is significantly changed both at carbon steel and at alloyed steel so that its value usually decreases as the tensile relative strain increases. Further on the elastic stress utilizable range is not constant either. In case of the tested carbon steel by increasing strain its value decreases and numerically it is less than the literature presume ( $2R_{eH}$ )

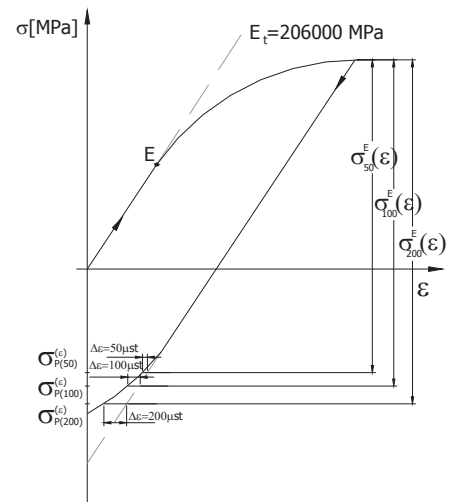


Fig.2. Defining the elastic-stress range to utilize applying different preload

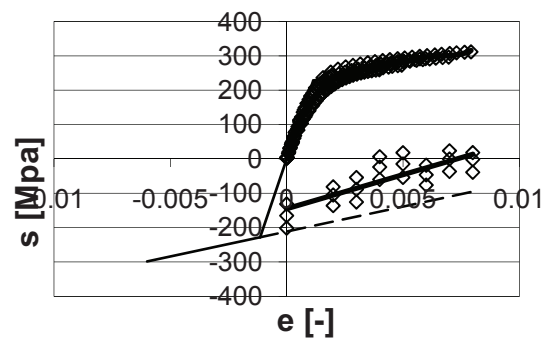


Fig. 4. Resultant stress-strain characteristic curve and compression yield stress in the function tensile strain in case of 1.4301 type engineering material.



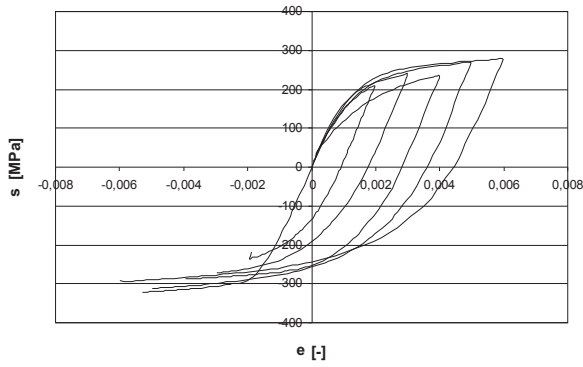


Fig. 5. Stress-strain characteristic curves at different tensile elongations in case of 1.4541 type engineering material.

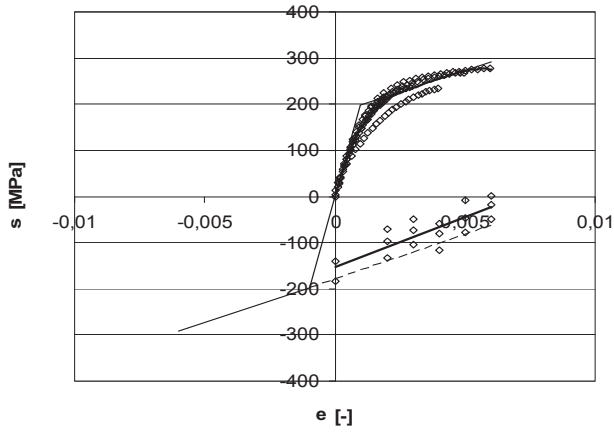


Fig. 6. Resultant stress-strain characteristic curve and compression yield stress in the function tensile strain in case of 1.4541 type engineering material.

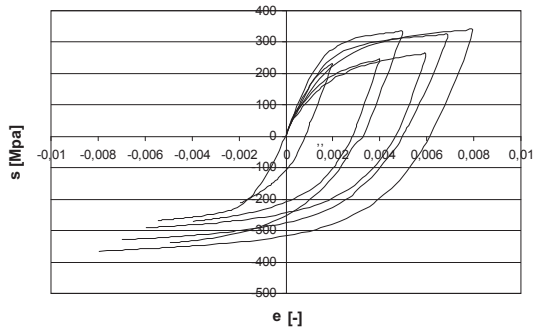


Fig. 7. Stress-strain characteristic curves at different tensile elongations in case of 1.4571 type engineering material.

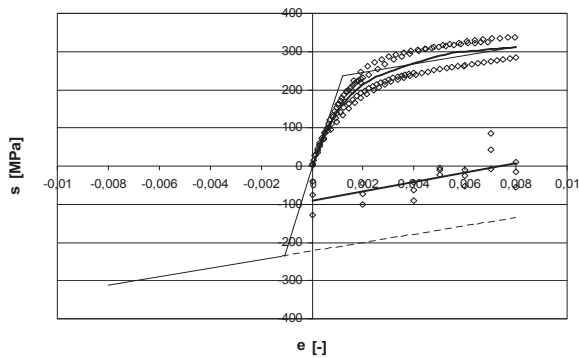


Fig. 8. Resultant stress-strain characteristic curve and compression yield stress in the function tensile strain in case of 1.4571 type engineering material.

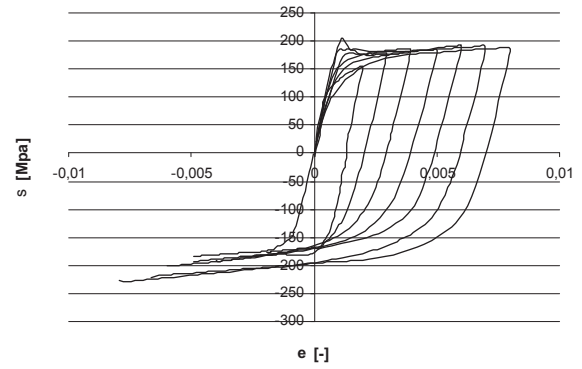


Fig. 9. Stress-strain characteristic curves at different tensile elongations in case of P235 type engineering material.

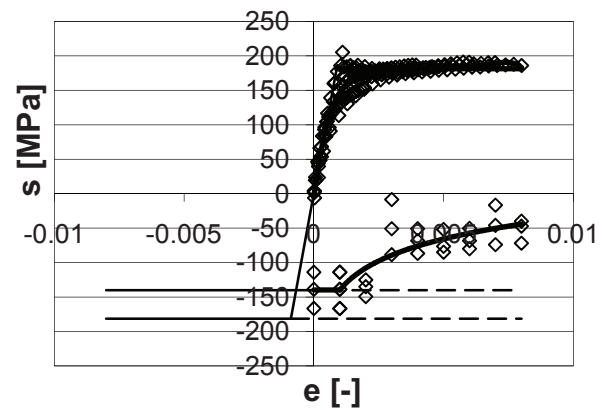


Fig. 10. Resultant stress-strain characteristic curve and compression yield stress in the function tensile strain in case of P235 type engineering material.

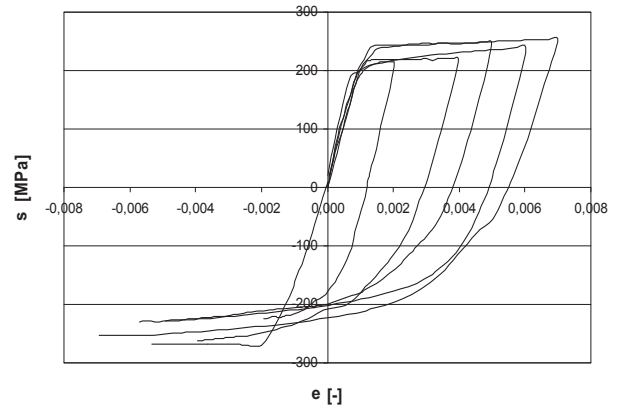


Fig. 11. Stress-strain characteristic curves at different tensile elongations in case of P275 type engineering material.

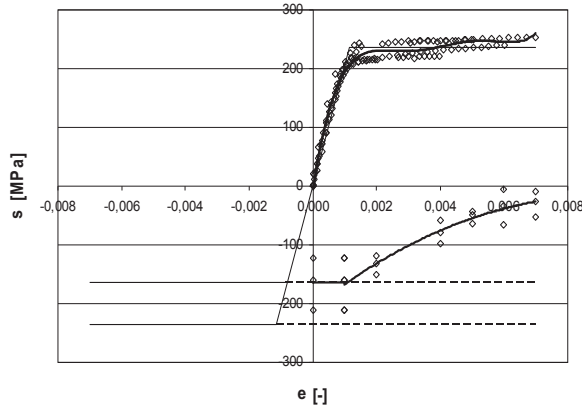


Fig.12. Resultant stress-strain characteristic curve and compression yield stress in the function tensile strain in case of P275 type engineering material.

### B. Structural tests

In the present case, our structural investigations aim at a demonstration of the *Bauschinger effect*, that is, the determination by measurement of compression yield stress that obtains on unloading period. The purpose of the experiments is to decide in what way the numerical values of strength characteristics (tensile/compression yield stress) measured on a specimen exposed to a single-axis force are affected by the multi-axis situation that obtains in the real structure and by the interaction of elastic/plastic regions. In order to perform the experiments, it was a straightforward option to use round plates since surface distributed loading results in a primarily dangerous bending-stress state in all cross-sections of a round plate. Another advantage of the choice of round plates was the possibility of an easy and geometrically accurate application of strain gages.

The next step of preparations for the experiment was the determination of geometrical sizes and the load (internal pressure) values belonging to them. For that purpose, using the  $(\sigma - \varepsilon)$  material law defined from the specimen measurements, we made calculations with the finite element program *COSMOS/M 2.9*. The purpose of those calculations was to determine the thickness values and the diameter of the round plate to be measured and the pipe welded to it such that, starting from the centre of the round plate, a significant area of plastically yielding zone should come about as the load increases. On the other hand, on unloading period, plastic yield flow of the opposite direction should also be produced. This would probably occur if the elastic stress decrease occurring in the unloading period is larger than the utilizable elastic stress shown in Figures 3. In the case of size relations and load values fulfilling the above requirements, plastic flow in the opposite direction on unloading can be registered by strain-gages applied radially and tangentially on the round plate (see Fig. 16.). The numerical value of the compression yield stress  $\sigma_p(\varepsilon)$  can be obtained, knowing the earlier measured stress-strain diagram and the elastic stress state of the round plate, by the following formula:

$$\sigma_p(\varepsilon) = \sigma(\varepsilon) - \Delta p \cdot \Delta \hat{\sigma}_e(\varepsilon) \quad (1)$$

where

- $\sigma(\varepsilon)$  is the stress value of the material law curve belonging to the elongation at the point under investigation,
- $\Delta p$  is the pressure drop value belonging to the yield flow in the opposite direction (on unloading) at the point under investigation, and
- $\Delta \hat{\sigma}_e(\varepsilon)$  is the equivalent stress per unit load at the point under investigation.

On the basis of the foregoing, we have performed a series of calculations and found that, as shown in Figure 13, for nominal diameter  $DN = 300\text{ mm}$ , round plate thickness,  $s_F = 10\text{ mm}$ , and cylinder thickness  $s_K = 8\text{ mm}$ , at pressure  $p = 2,2\text{ MPa}$ , a continuous plastic flow region appears on the external surface of the round plate, within a circle of  $r = 100\text{ mm}$ , measured from the central point. Figure 13 also shows equivalent strains  $\varepsilon_e$  for various pressure values, as given by finite element calculations, as a function of radial coordinates. The figure suggests that at the connection of the cylindrical jacket and the round plate, due to local bending stresses, a significant amount of plastic strains can be observed. Figure 14 illustrates the utilizable elastic stress  $\sigma^E(\varepsilon)$  that belongs to loading the flat plat under investigation by  $p = 2,2\text{ MPa}$  and decrease of equivalent elastic stress on unloading, as a function of the radius. Analysing the figure, we can see that within a circle of  $r = 70\text{ mm}$  measured from the centre, plastic elongation in the opposite direction (that is, a flow) can be expected to occur on unloading.

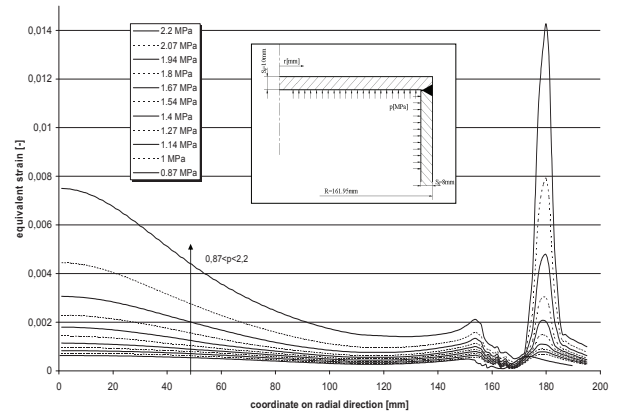


Figure 13. Equivalent strain distribution along the radial direction at different loads

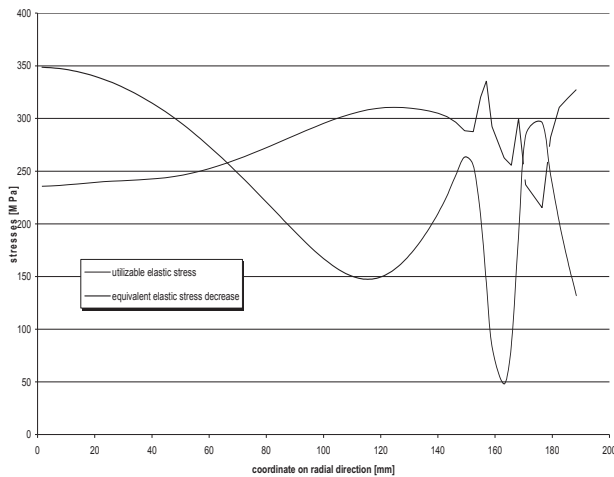


Fig. 14. The utilizable elastic stress and equivalent elastic stress decrease along coordinate on radial direction



Fig.15. Experimental test device

To complete the experiments we have developed the experimental strain gage that is shown on Figure 15. After finishing the experiments according to the above mentioned criteria the changes in compression yield stress were determined in the function tensile stress. Figure 16. Illustrates the variations of values among the obtained results in case of 1.4301 type engineering material. On this Figure the black dots demonstrate the changes in compression yield stress in the function tensile strain deriving from the round plate which is in multiaxial stressed state. The empty circles show those deriving from the specimen.

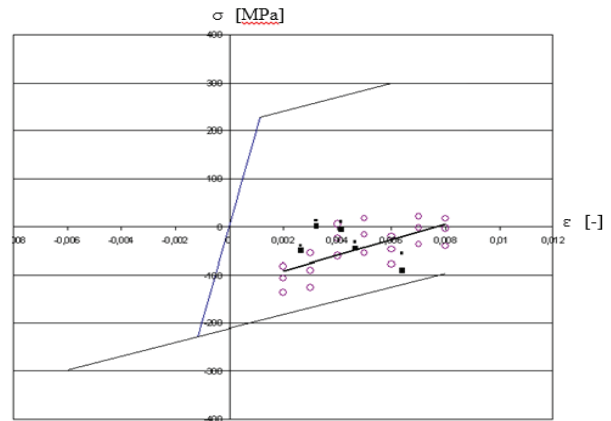


Fig.16. The variations of compression yield stress measured on a round plate and a specimen in case of 1.4301 type engineering material

Based on the experiments it can be stated (see Figure 16.) that there is a good accordance between the compression yield stress measured on the construction and the one measured on the specimens. It follows from the above findings that the compression yield stress measured on the specimen and the numeric values of the utilizable elastic stress considered to be the characteristic of the material can be applied when examining the load index of complex structures.

## REFERENCES

- [1] Nagy, A., Székelyhidi, E.: Dimensioning on repeated load stress concentrating places by taking into consideration the Bauschinger effect. Proceedings of the Fourth Conference on Mechanical Engineering. Technical University of Budapest. 2004. május 27-28.
- [2] Jiang, N., Zhen, B.P. Xu: Study on control limits of secondary stress strength in pressure vessels. Int. J. Pres. Ves. & Piping 76 (1999.) 711-714.
- [3] Thumser, R., Bergmann, J. W., Vormwald, M.: Residual stress fields and fatigue analysis of autofrettaged parts. Int. J. Pres. Ves. & Piping 79 (2002.) 113-117
- [4] Sketon, R. P., Maier, H. J., Christ, H. J.: The Bauschinger effect, Masing model and the Ramberg-Osgood relation for cyclic deformation in metals. Material Science and Engineering A 238 (1997.) 377-390.
- [5] Chun, B. K., Jim, J. T., Lee, J. K.: Modeling the Bauschinger effect for sheet metals part I. theory. Int. J. Plasticity 18 (2002.) 571-595.
- [6] Jen-Terng Gau, Gary, L. Kinzel: An experimental investigation of the influence of the Bauschinger effect on springback predictions. Journal of Material Processing Technology 108 (2001.) 369-375.
- [7] Fusahito Yoshida, Takeshi Uemori, Kenji Fujiwara: Elastic-plastic behaviour of steel sheets under in-plane cyclic tension-compression at large strain. Int. J. Plasticity 18 (2002.) 633-659.
- [8] Varga, L.: Design of optimum high pressure monobloc vessels. Int. J. Pres. Ves. Pip. 48 (1): 93-110 1991

# COP of refrigerants in heat pumps

Jozsef Nyers<sup>\*</sup>, Daniel Stuparic<sup>\*\*</sup>, Arpad Nyers<sup>\*\*\*</sup>

<sup>\*</sup>Obuda University Budapest, Becsi ut 96, 1034 Budapest, Hungary

<sup>\*\*\*</sup>Budapest University of Technology & Economics, Budapest, Muegyetem rkp. 3-5

<sup>\*\*</sup> VTS Subotica, M. Oreskovica 16, Serbia

E-mail: [nyers@uni-obuda.hu](mailto:nyers@uni-obuda.hu); [sdanijel@vts.su.ac.rs](mailto:sdanijel@vts.su.ac.rs); [nyarp@yahoo.com](mailto:nyarp@yahoo.com)

EXPRES 2015

March 19-21. 2015

**Abstract**–The aim of this paper is to examine the COP and the applicability of certain refrigerants, which are used today in refrigeration systems, such as R410A, R404A and R407C. Special attention was given to refrigerants R134a and R1234yf. Because of the higher GWP (1430) of the R134a, researches have begun in a world scale, which of the cooling agents could serve as a substitute. In the USA it has been announced that from 2017 the R1234yf will be in use for automobile air conditioning systems, instead of the R134a. However Mercedes has proved that the use of R1234yf is dangerous due to flammability. In addition R1234yf has low COP when compared to other popular refrigerants. Due to the flammability and low values of COP, it has been proven that R1234yf cannot replace the R134a in heat pump systems. It should only be used in small quantities in very low power refrigerators.

---

**Keywords** -COP, refrigerant, R1234yf, R134a, diagram.

---

## Nomenclature

q [W]	Heat flux
P [W]	Power
COP [-]	Coefficient of performance

## Subscripts and superscripts

Con	Condenser
com	Compressor
max	Maximal
e	Evaporation
c	Condensation

## I. INTRODUCTION

Recently, on a global scale, there is a majordilemma, which chemical compounds could be used as a replacement for the refrigerant R134a, the replacement refrigerant of the former R12 (CH<sub>2</sub>Cl<sub>2</sub>).

At that time the criteria for replacing the R12 with a new refrigerant was its chlorine (Cl) content; it had to be zero.

The R134a met this and also the other major thermal criteria. However recently has come to expression not only the Cl content, but also the value of the refrigerants' global warming potential (GWP). GWP is the number which defines, how many times does a certain refrigerant increase the risk of global thermal atmosphere loading compared to the CO<sub>2</sub>.

In the case of R134a, GWP is 1430 for 100 years, ie. it has 1430 increased risk due to the green house effect of the atmosphere for 100 years than CO<sub>2</sub>.

Beginning from 2017, the car industry in USA will switch to the new refrigerant R1234yf in their air conditioners instead of the currently used R134a. But Europe is in the process of testing the refrigerant R1234yf, especially the Mercedes car industry. During their practical experiments, they discovered the tragically bad characteristics of this new refrigerant, which is its flammability.

The test was done by blowing the refrigerant R1234yf on the warm engine, which ignited the R1234yf, and in the end all the engine was on fire. In this paper we analysed the COP and the thermal characteristics of the mentioned refrigerant R1234yf. The COP of some other widely used refrigerants was also determined, as well as of the R1234yf.

The COP of a refrigerant is the ratio between the heat flux in the condenser, and the power output of the compression. The COP was determined for the same conditions: evaporation temperature of 5°C, isentropic compression ( $s=\text{const}$ ), and the condensation temperature by increments of 5 °C. The COP was investigated for the following refrigerants: R 134a, R 410A, R 404A, R 407C and R 1234yf.

The numerical results are shown in a 2D graphic form – the COP as a function of the condensation temperature.

## II. THE PHYSICAL MODEL

### A. Physical model of refrigerant R134a

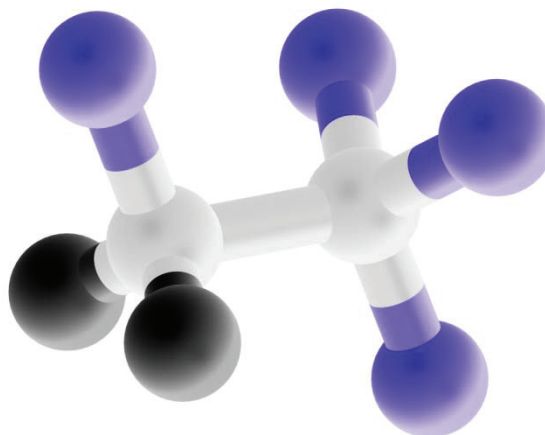


Figure 1. 3D physical representation of R134a  
by Wikipedia



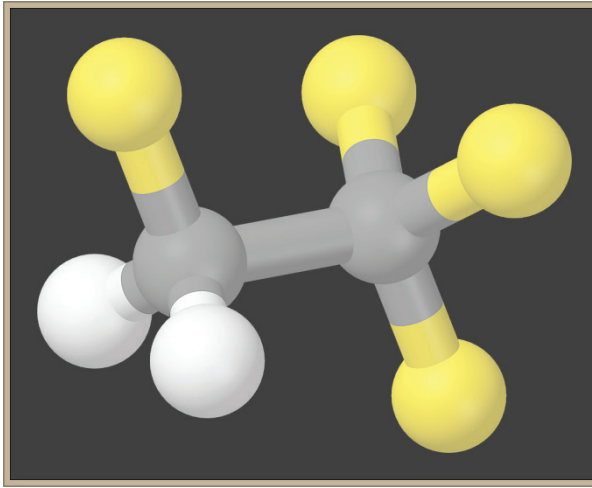


Figure 2. 3D physical representation of R134a by Wikipedia

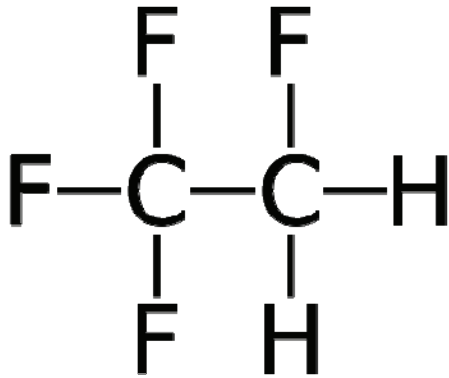


Figure 3. 2D presentation of tetrafluoroethane R134a by Wikipedia

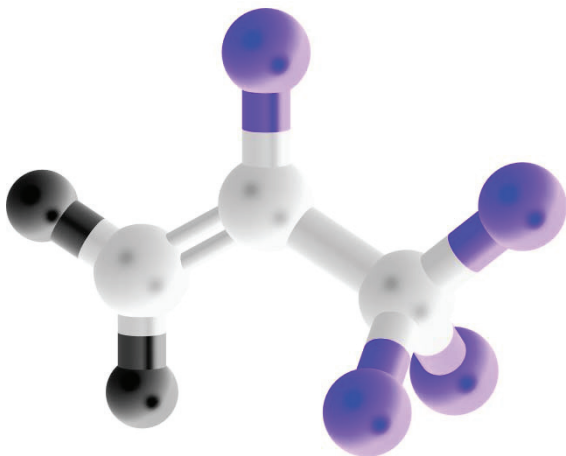


Figure 4. 3D presentation of R1234yf by Wikipedia (Ben Mills)

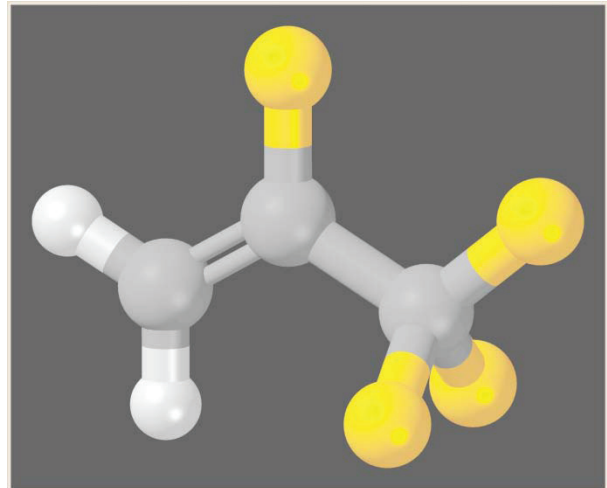


Figure 5. 3D presentation of R1234yf by Wikipedia (Ben Mills)

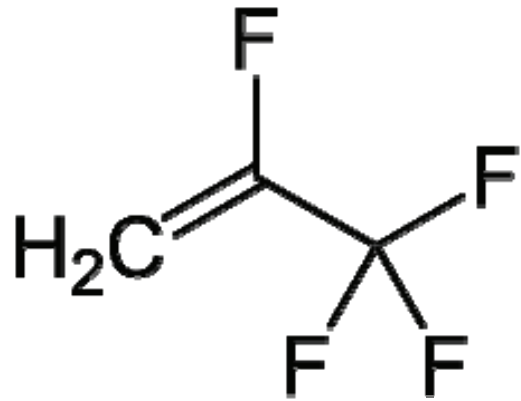


Figure 6. 2D presentation of R1234yf by Wikipedia (Ben Mills)

### III. MATHEMATICAL MODEL

The mathematical model in this case is a very simple relation. COP of specific refrigerants is the ratio of the heat flux, which is exchanged in the condenser between the refrigerant and the fluid used for transporting the heat, and the power output at the compressor accounting for the refrigerant vapor compression.

$$\text{COP}_{\max} = \frac{q_{\text{con}}}{P_{\text{com}}}$$

Heat flux in the condenser

$$q_{\text{con}} = i_{\text{con4}} - i_{\text{con3}}$$

Power used for the compression of refrigerant vapor:

$$P_{com} = i_{com3} - i_{com2}$$

$$i_{con3} = i_{com3}$$

Where:

- $i_{com2}$  superheated vapor enthalpy at the compressor input
- $i_{com3}$  superheated vapor enthalpy at the compressor output
- $i_{con3}$  superheated vapor enthalpy at the condenser input
- $i_{con4}$  condensate enthalpy in the condenser

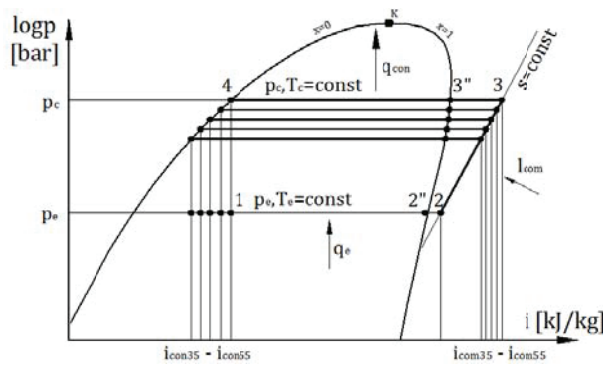


Figure 7. logp-i diagram of cooling process

The determined COP for the specific refrigerants is the maximal ideal COP, since the calculations are carried out as if the compression was isentropic. During the isentropic compression the least amount of mechanical work is spent per time unit. It is the ideal compression mechanism. However, during a real compression, the power spent during the compression is a few percent higher, which in turn lowers the COP proportionally.

#### IV. SIMULATION

##### A. About the simulation

The data for determining the required power of the isentropic compression and the resulting amount of heat flux from the condenser for the investigated refrigerants were calculated using the software package "SOLKANE Software" from the internet. SOLKANE Software does not contain the refrigerant R1234yf, therefore the data for the mechanical work and heat flux in this case were taken from its logp-i diagram.

The investigated refrigerants are: R 134a, R 404A, R 410A, R407C i R 1234yf.

##### B. Initial data of the simulation

The simulation was carried out using the following initial parameters:

- evaporation temperature  $t_e = 5^\circ\text{C}$
- condensation temperature  $t_c = (35; 40; 45; 50; 55)^\circ\text{C}$
- temperature of superheating  $\Delta t = 5^\circ\text{C}$
- isentropic compression  $s = \text{const}$ .

#### V. THE RESULTS

##### A. Analytical results

Based on data for the required power of the isentropic compression, and the obtained amount of heat flux, the  $\text{COP}_{\max}$  was calculated for the condensation temperatures specified below. The calculated data are shown in the table:

$T_{\text{con}} [^\circ\text{C}]$	$\text{COP}_{\max} [-]$				
	R134a	R404A	R407C	R410A	R1234yf
35	9,02	8,28	8,33	8,40	6,25
40	7,56	6,94	7,07	7,07	5,24
45	6,54	5,89	6,10	6,06	4,47
50	5,74	5,05	5,33	5,24	3,85
55	5,09	4,33	4,70	4,57	3,33

Table 1.  $\text{COP}_{\max}$  of certain refrigerants

##### B. Numerical results

The numerical results obtained by simulation are presented graphically in Figures3,4.

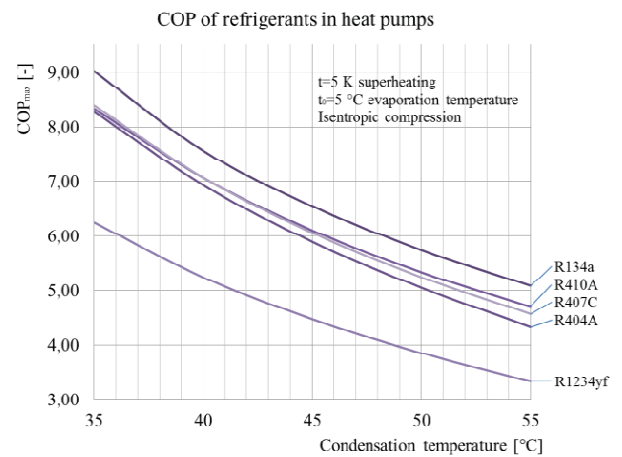


Figure 3. COP of refrigerants as a function of condensation temperature

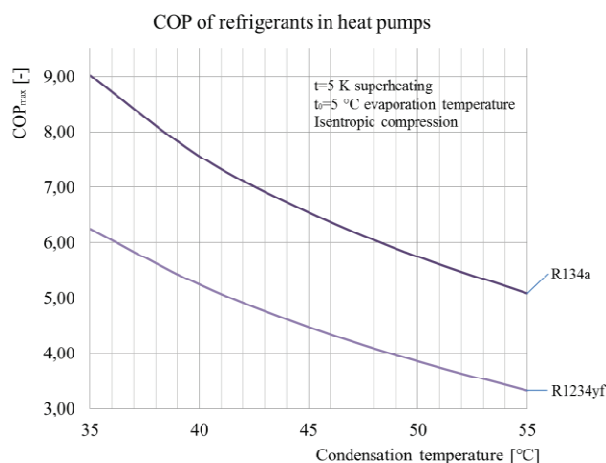


Figure 4. COP<sub>max</sub> of refrigerants R134a and R1234yf as the function of condensation temperature

## VI. CONCLUSIONS

Based on the results and analysis can be concluded that:

- Due to the high flammability of R1234yf, it has a very high risk, with strong limitations in applicability,
- R1234yf could possibly be applicable in low power refrigerators, in small quantities,
- In the USA the replacement of R134a to R1234yf in automobile air conditioners is predicted to 2017,
- Mercedes has proved with an experiment on a car engine, that risk of fire is present when R1234yf escapes from the air conditioner and ignites due to the heat of the warm engine,
- In addition to flammability, R1234yf has a very low COP when compared to other refrigerants, especially to R134a,
- R134a at the condensation temperature of 35°C has 45%, while at 55°C has 50% percent higher COP than the R1234yf,
- Due to flammability and its low COP R1234yf is not applicable in heat pumps.
- Heat pumps for heating-cooling of buildings have much greater power, which means that the quantity of the refrigerant should be much higher than in automobile air conditioners. Due to the large amounts, the risk of fire is tremendous.
- Advantage of R1234yf is its low GWP value. GWP is 4 in a timescale of 100 years, compared to the CO<sub>2</sub>
- However due to the low COP of 1234yf, energy consumption during cooling increases, which in turn means an increased total GWP.

## REFERENCES

- [1] Ray Galvin: Thermal upgrades of existing homes in Germany: The building code, subsidies, and economic efficiency. *Energy and Buildings*, Volume 42, Issue 6, June 2010, Pages 834–844.
- [2] Meral Ozel: Cost analysis for optimum thicknesses and environmental impacts of different insulation materials. *Energy and Buildings*, Volume 49, June 2012, Pages 552–559.
- [3] Surapong Chiraratananon, Vu Duc Hien: Thermal performance and cost effectiveness of massive walls under thai climate, *Energy and Buildings*, Volume 43, Issue 7, July 2011, Pages 1655–166.
- [4] Nyers J., Garbai L., Nyers A. :“Analysis of Heat Pump's Condenser Performance by means of Mathematical Model”. *International J. Acta Polytechnica Hungarica*, Vol. 11, No. 3, pp. 139-152, 2014.  
<http://dx.doi.org/10.1016/j.enbuild.2014.10.023>
- [5] Nagy Károly, Divéki Szabolcs, Odry Péter, Sokola Matija, Vujicic Vladimir: "A Stochastic Approach to Fuzzy Control", *I.J. Acta Polytechnica Hungarica*, Vol. 9, No 6, 2012, pp. 29-48. (ISSN: 1785-8860).
- [6] Kajtár L., Hrustinszky T.: Investigation and influence of indoor air quality on energy demand of office buildings. *WSEAS Transactions on Heat and Mass Transfer*, Issue 4, Volume 3, October 2008. 219-228 p.
- [7] László Kajtár, Miklós Kassai, László Bánhidi: Computerised simulation of the energy consumption of air handling units. 2011. *Energy and Buildings*, ISSN: 0378-7788, (45) pp. 54-59.
- [8] László Kajtár, Levente Herczeg: Influence of carbon-dioxide concentration on human wellbeing and intensity of mental work. Bp. 2012. *Időjárás, Quarterly Journal of the Hungarian Meteorological Service*, Vol. 116 No.2 april-june 2012. p. 145 – 169. ISSN 0324-6329.
- [9] K Dabis, Z Szánthó: Control of Domestic Hot Water production is instantaneous heating system with a speed controlled pump, 6<sup>th</sup> International symposium “EXPRES 2014 VTS.” Subotica. Serbia, 2014. pp. 101-106. ISBN 978-86-85409-96-7.
- [10] Saša R. Pavlovic, Velimir P. Stefanović , Dragan Kuštrimović: Review of Heat Transfer Fluids for Concentrating Solar Collectors. “EXPRES 2014 VTS.” Subotica. Serbia, 2014. pp. 90-96. ISBN 978-86-85409-96-7.

# Simulation of the nuclear power plant cooling using the TEG

A. Szente<sup>\*</sup>, I. Farkas<sup>\*\*</sup> and P. Odry<sup>\*\*\*</sup>

<sup>\*</sup> Paks Nukleár Power Plant, Paks, Hungary

<sup>\*\*</sup> College of Dunaújváros/Computer Engineering, Dunaújváros, Hungary

<sup>\*\*\*</sup> Polytechnic of Subotica/Electrical Engineering, Szabadka, Serbia

[szentea@npp.hu](mailto:szentea@npp.hu), [imka26@gmail.com](mailto:imka26@gmail.com), [odry@appl-dsp.com](mailto:odry@appl-dsp.com)

**Abstract**—it has been shown in recent years that there is a great need for additional security measures to be taken in high security systems in case of occurrence of unanticipated events. A Nuclear Power Plant is exactly such kind of a sophisticated system. Thou, before we begin to work on improving the overall security of a system, we have to familiarize ourselves with the type of event that causes the issue during an unanticipated event. For this we need a well-constructed simulation. The fortification of the removal of decay heat following the subcritical stage of a reactor shutdown forms a significant portion of the workings of a nuclear power plant. The lack of such a measure could lead to a catastrophic meltdown (Fukushima 2011). The necessary electrical energy for this process under normal conditions is supplied by the primary (national and home power grids) and secondary (diesel generators) electrical supply systems. One of the key factors of the insurance of higher plant safety could be the application of a third diverse decay heat removal ensuring system. The solutions that we came up with were based on the observations of the Paks Nuclear Power Plant's VVER440 type reactor cores, thou it could be reflected to any similar working nuclear power plant type.

## I. THE BASICS OF NUCLEAR POWER PLANT COOLING

Once the adequate boric concentration is reached during shutdown the reactor needs to be cooled down, and kept at a desirable temperature. During cooldown on the one hand the heat stored in the structure as well as the decay heat generated by the active zone needs to be removed.

During the first stage of the process, it's necessary to set the prescribed temperature difference of 60 °C in the primary circuit-pressurizer, using the cooling of the pressurizer. Naturally, this implies that the pressure in the primary circuit needs to be lowered. Later, besides the cooling of the primary circuit it's important to constantly keep this difference.

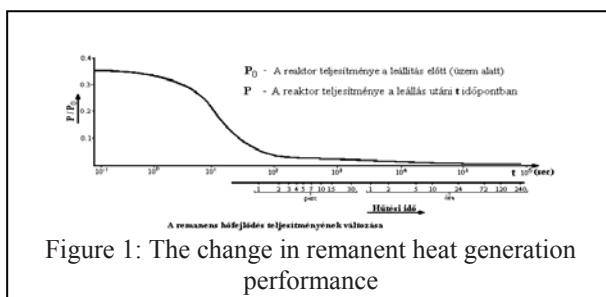


Figure 1: The change in remanent heat generation performance

Due to the constant pressure lowering in the primary circuit, the hydro-accumulators need to be disengaged from the primary circuit once a  $p_1 < 75$  bar pressure is reached, also as the primary circuit is being cooled, it's pressure needs to be let out by releasing the nitrogen (in order to avoid any risk of brittle fracture). Once we reach a pressure of  $p_1 \leq 20$  bar's during the depressurization of the primary circuit, the steam cushion in the pressurizers needs to be changed to nitrogen. In order to minimize the necessary quantity of nitrogen, it's imperative that the pressurizers are to be filled to their maximal capacity ( $L_{YP10} = 7.5 \pm 0.5$  m) before the administration of nitrogen. In the following the precise level in the pressurizers should be kept particularly in mind, because the changes in that significantly affect the primary circuit pressure. (Due to the continuous primary circuit cooling, the constant level in the pressurizer can only be ensured if the drop in volume is substituted continuously with water, unlike the power stage, where according to the average temperature we let the level change, namely we keep a constant volume of water.) The  $\Delta T = 60$  °C between the primary circuit and the pressurizer needs to be kept at until  $T_1 \leq 150$  °C, following which it's needs to be lowered to  $\Delta T = 30$  °C.

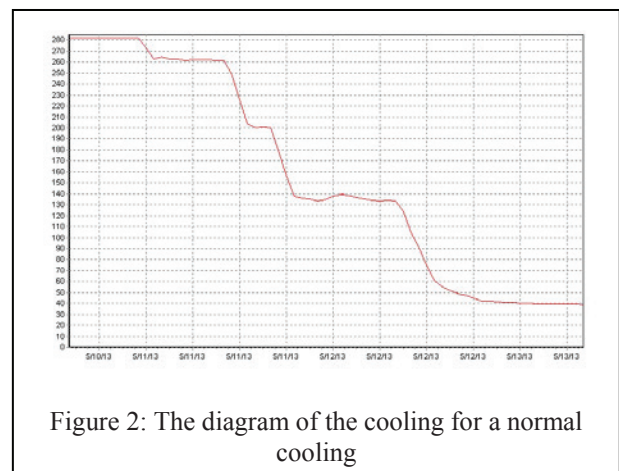


Figure 2: The diagram of the cooling for a normal cooling



Attention needs to be paid during the set of the cooling speed, so as the maximum allowed is not exceeded, therefore it must be approached from below. In the case of huge supply tanks and big primary circuit temperature differences the exceed can easily occur. The cooling must be carried out by the subtraction of steam from the fresh steam collector until  $T_1 = 140\text{ }^{\circ}\text{C}$  is reached. The condensate condensed in the technology condenser is returned back to the secondary supply tank. In the last third of the water-steam cooling the heating of the supply containers should be gradually reduced to ensure the temperature step between the primary - secondary circuit.

While above  $T_1 > 190\text{ }^{\circ}\text{C}$  it's advisable to avoid a too high active zone pressure difference, an FKSZ needs to be shut down. Because of the even cooling of primary circuit pipes, the shutdown FKSZ needs to be restarted ( $T_1 = 175$  and at  $160\text{ }^{\circ}\text{C}$ ) once we stopped an operator. Once  $T_1 < 150\text{ }^{\circ}\text{C}$  is reached the speed of cooling drops significantly, because the  $\Delta T$  between the supply water and the primary circuit is pretty low. Once a stable value of below  $150\text{ }^{\circ}\text{C}$  is reached, the system should be switched from steam – water to water – water cooling. To do this the GF, fresh steam lines, fresh steam collectors, and the cooling system should be completely filled with feed water. Before the start of the filling, prevention of inadvertent defense operations must take place, the security of the GF's need to be paralyzed on the BER panel, because  $L_{GF} > L_{Néveleges} + 600\text{ mm}$  excludes the upload path. The speed of the filling needs to be set in such a way that it's minimum 3.5h's. At this stage of the cool-down the migration from the (Lépcsőzetes Indítási Programok) LIP II should be checked. The switch to this program also means that some elements of the ZÜHR systems are no longer needed now, in fact their trigger could lead to adverse consequences, and therefore, they should be staggered.

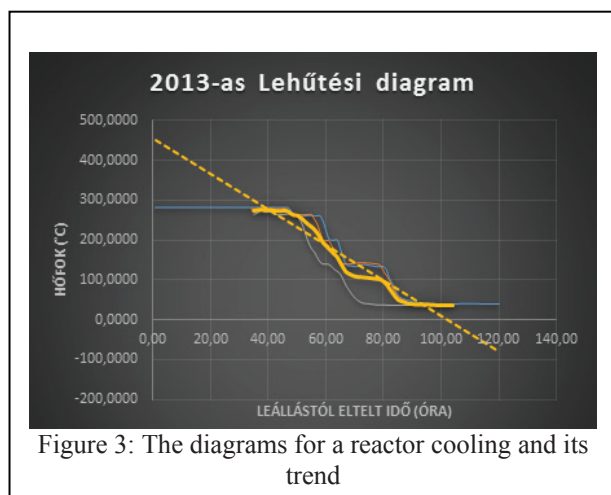


Figure 3: The diagrams for a reactor cooling and its trend

(E.g., Under pressure, still closed, but cooled reactor, if the TH pumps are started even if for a false signal, we can go beyond the allowed pressure of the brittle temperature in seconds, or the sprinkler system starts for a wrong signal, since on this primary temperature it's

unlikely that even in the event of a broken pipe the pressure of the containment reaches the limit.) Since the amount of heat removal is steadily declining over the filling, care should be taken that the primary circuit does not warm up to above  $150\text{ }^{\circ}\text{C}$ .

After filling the secondary side, the cooling must continue on a water - water mode of operation using five FKSZ while  $T_1 < 100\text{ }^{\circ}\text{C}$  is reached. The secondary side circulation is ensured by chilling pumps. If the primary circuit average temperature is below  $100\text{ }^{\circ}\text{C}$ , the FKSZ's need to be stopped by detaching the earlier used two loops. Secondary side steam generators that have been taken out of the plant loops should not be excluded, ensuring their intense chilling. Their detachment should be carried out at  $T_{GF\text{ fail}} \leq 40\text{ }^{\circ}\text{C}$  but no later than before the reactor is depressurized. If the difference in temperature between the pressurizer and the added water is  $\Delta T < 80\text{ }^{\circ}\text{C}$  the cooling of the pressurizer can be continued by using supplement pumps.

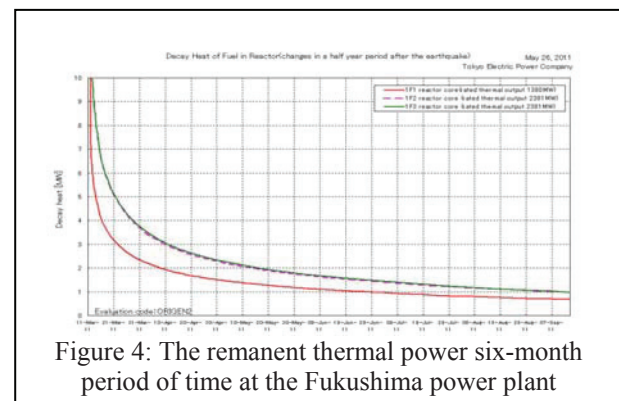


Figure 4: The remanent thermal power six-month period of time at the Fukushima power plant

## II. THE SIMULATION OF THE COOLING

In order to be able to analyze the task, in the first step let's see how large this energy is. The codes that use numerical methods to estimate the remnant heat (decay heat) (Melcor, Relap 1-2-3, Trac, Origen) are capable to model the state with a precision of 3-5%.

### A. The simulation of remnant heat

Using MATLAB R2013a with numerical methods we simulated (figure 5.), a  $T_0 = 335$  days constantly operational  $P_0 = 1485\text{ MWt}$  („Megawatt thermal”) heat energy producing reactor, it's remnant heat 10 days following it's shutdown (864000s) is shown on figure 6. It can be seen that this value even after ten days is more than 3MWt.



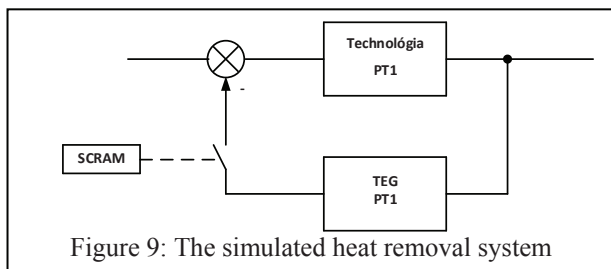


Figure 9: The simulated heat removal system

The thus constructed MATLAB model can be seen on figure 10, while the cooling curves are shown on figure 11. The “minima” function that does not allow the temperature to climb above 300 °C, has to have at least a  $Y = \frac{0.0015}{7005 \cdot 0.1}$  transfer function. Increasing the time constant does not affect the shape of the curve it determines the availability of electric power that can be extracted from the TEG, while the proportional transfer component has effect on the slope of the cooling.

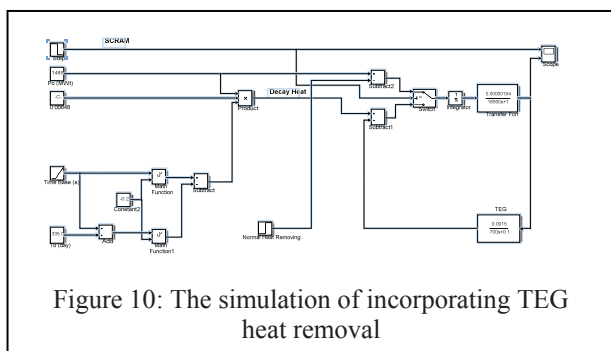


Figure 10: The simulation of incorporating TEG heat removal

#### D. TEG as a residual heat-absorber

The increase of storage capacity can be resolved by the storage of electricity generated by the TEG's in batteries (figure 12).

During the campaign, the heat produced is continuously "there" in a time period after SCRAM as well in the form of stored heat, so during the residual heat removal's critical stage of 2-3 days the multiple amount of charger (conditioning) power could be removed from the batteries to maintain the circulation. Each plant has a battery-supported DC rail (220V or 24V), so building that will not be an additional cost.

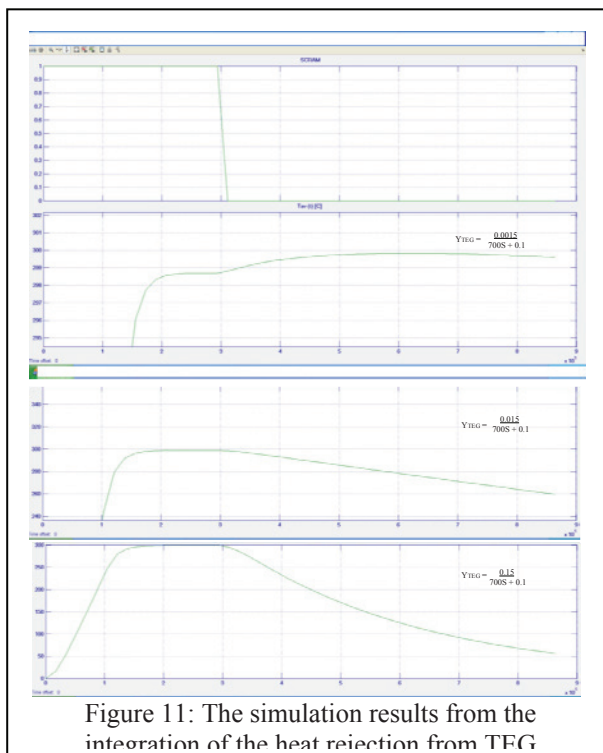


Figure 11: The simulation results from the integration of the heat rejection from TEG

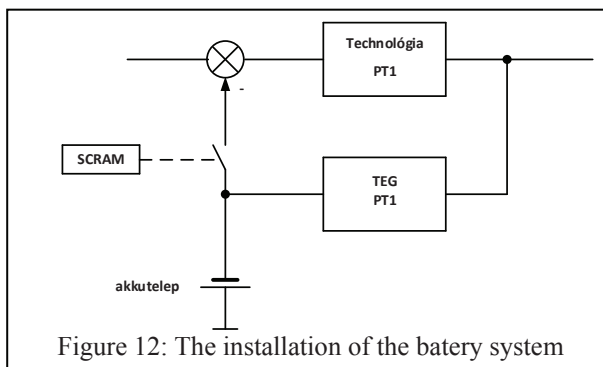


Figure 12: The installation of the battery system

#### SUMMARY

In this article we have tried to show how is it possible to simulate processes taking place in an abandoned nuclear power plant. As you can see this can be resolved perfectly using MATLAB. We have outlined the theoretical possibility of usage of residual heat removal using a third, diverse way method. In further studies we try to put more emphasis on the fine tuning of the simulated system and to clarify the physical realization of the possibilities.

#### REFERENCES

- [1] M. Ragheb: Decay heat generation in fission reactors, 3/22/2011
- [2] A. Szente, I. Farkas and P. Odry: *The application of Thermopile Technology in high Energy Nuclear Power Plants*, Expres 2014
- [3] <http://www.tecteg.com/>
- [4] Piotr Dziurdzia, AGH University of Science and Technology in Cracow, Poland: *Modeling and Simulation of Thermoelectric Energy Harvesting Processes*

# Technological features of biogas plants using mixed materials

L. Tóth\*, J.Beke\*, Z. Bártfai\*\*, I. Szabó\*\*, G. Hartdégen, I. Oldal\*\*, Z. Blahunka\*\*

Szent István University, Hungary, 2100 Gödöllő, Páter K. u. 1.

\* Institute of Process Engineering, \*\* Institute of Mechanics and Machinery  
[toth.laszlo@gek.szie.hu](mailto:toth.laszlo@gek.szie.hu) , [beke.janos@gek.szie.hu](mailto:beke.janos@gek.szie.hu) , [bartfai.zoltan@gek.szie.hu](mailto:bartfai.zoltan@gek.szie.hu)  
[szabo.istvan@gek.szie.hu](mailto:szabo.istvan@gek.szie.hu) , [oldal.istvan@gek.szie.hu](mailto:oldal.istvan@gek.szie.hu) , [blahunka.zoltan@gek.szie.hu](mailto:blahunka.zoltan@gek.szie.hu) ,

**Abstract—** The most ecological and environmentally sensible way of the utilisation of biomass is the biogas production. The applied technologies are basically mesophile and thermophile methods, or the mixture of them. The applicable, effective energy production technology for biomass always depends on the input materials. Incineration is a wide-spread technology, mainly for the primer biomass. Fermentation is applied for those of secondary and tertiary materials that need post-treatment because of the environmental requirements (infection, ground water damage etc). Materials utilised for biogas production are no harmful for the environment, moreover the residues can be used as nutrient in the plant production technologies.

**Key words:** biogas, sewage sludge, fermentation, foam formation

## I. BACKGROUND

Biogas plants use a wide variety of primer materials such as whole corn silage, root crops, seed crops residues etc. that make the operation of the biogas plant more stable as their structure is mainly constant in time. A biogas plant is quite similar to a ruminant animal. For example in the feeding of cows the so called TMR (TOTAL MIXED RATIO) system is used, that means the same composition of the feeds are used during the whole season. The stomach flora adapt to the feed and able to transform rapidly the desired quantity. The biogas plant we studied within the frame of our research project applies different kind of input materials as a mixture. The mixing ratio also differs from the usual. In agricultural circumstances biomass is used as primer and waste from animal husbandry as sounder material is used for biogas production. When the composition of the materials is almost constant, and the material supply is continuous the operation of the biogas plant is acceptable. The other kind of technology is based on fermentation of sewage sludge from waste water plants. The constitution of the input material is also constant, but max 10% deviation can be accepted. In the examined technology the ratio of the sewage sludge is 55-60% (respect to the dry matter). The

sewage sludge as an input material comes from 8-10 settlements and the consignments differ very much from each other. 10% of the total amount of input materials is waste from food industry. Having an up-to-date computer based control system, the electric power production of the biogas plant is approximately 2,0 MW (see Figure 1.)

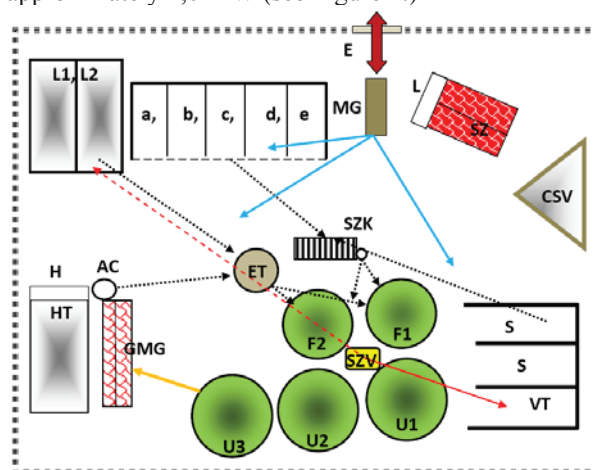


Figure 1. Scheme of the biogas plant

E = Main entrance, L = Logistics station, SZ = Social facility, MG = Weighing of the input material, CSV = rainwater tank, a, b, c, d, e = Temporary storage, S = Silage storage, VT = Separated storage of end product, L1, L2 = End storage of the liquid material (lagoons), ET = Pre-storage and mixer for liquids SZK = mixing, and chopping of solids H = Hygienisation, HT = Storage, GMG = Gas motors, F1, F2 = Digester, U1, U2, U3 = Second digester, SZV = Pump station and separation, AC = disinfectant (autoclave)

Mixture and the chopping of the input materials (cow manure, corn silage) take place in the SZK, from where will be filled to the F1 or F2 digesters. First mixing of the liquid manure, sewage sludge and other liquid materials happens in the heated pre-storage bunker (ET). According to the EEC hygiene regulation, pasteurising for min. 1 hour (hereby for 4 hours) at a temperature of 70°C is prescribed. Pasteurising process of the following materials take place in HT:

- food waste
- fat
- cooked oil
- fat coming from grease traps

One of the most important criterions in the profit oriented biogas plants for the stable electric and heat energy production is the continuous biogas supply for the gas motors. Such companies have an obligation of



pre-announcing the production of the electric power for the next 24 hours. In the case of any deviation sanction occur (more than 20% deviation causes 15-18% price reduction).

The biggest technological problem in the investigated biogas plant is the foaming of the digesters. One of the targets of our research work is to discover of the possible reasons of this undesirable phenomenon. Rich literature sources can be found for this kind of operational problem, but the practical experience for the solution is quite limited.

## II. SEWAGE SLUDGE

The average ratio of the sewage sludge utilisation in the existing biogas plants is 10-15%. In our case the value of 40-50% is quite perspective for the agricultural soil resource management and the energy receiving aspect as well. According to the 50/2001. (IV. 3.) Regulation only well prepared sewage sludge can be utilised in the agricultural production. The sewage sludge utilisation is a subject to authorisation.

Nowadays 58-60% of the total amount is placed on agricultural lands, 20-22% is placed on landfills, 1-2% is incinerated, and the rest is utilised on an unknown way. According to the previous plans in 2015 390.000 tonnes of sewage sludge will be utilised in the agriculture a year. Fermentation of the sewage sludge results energy saving, and the specific expenses of the sewage sludge cleaning process will also decrease. The fermented sewage sludge as the end product in the biogas plant can be placed without environmental problems. This could improve the quality of life, and the ecological condition of the environment.

## III. POSSIBLE REASONS OF THE FOAMING

According to the results of some research (Kougias et al, 2014) foaming is a quite common technology problem. In 16 biogas plants investigated by them, the average duration of foaming was 1-21 days while 20-50% of the gas quantity was lost.

The main reasons for the foaming problem in the Lemvig biogas plant (Denmark) was the composition of the input material and the insufficient mixing as well. According to their measurements the communities of bacteria don't have effect on foaming, meaning the indifference of the filamentous bacteria to the foam formation in the co-substrate based reactor. At the same time they confirm that filamentous bacteria, especially *Gordonia* species and *Microthrix parvicella* facilitate foaming in sewage sludge fermentation technologies.

Their articles emphasize the organic overloading and subsequently the accumulation of acetic acid as the cause of foam formation in wastewater sludge digesters (corresponding to Boe et al.).

Moreno-Andrade et al. (2004) performed a research with 10% starting value of sewage sludge that was increased continuously for 30 days. During the start up of the plant the sewage sludge was recirculated, and the pH value was set-up by lime.

According to McCarty the sewage sludge as a substrate contains all the necessary nutrients for the bacteria. 60-75% of the dry content of sewage sludge is organic

material. In the mesophilic range 12-13 days are needed for the decomposition of the sewage sludge having 70% organic matter content. Under 50% of organic matter content the anaerobic decomposition is not economic.

Oláh et al. emphasize that direct charging of the organic matter into the reactor can cause the overload. In this case intensive foaming may occur within 30 minutes and the methane content of the biogas decrease as well.

## IV. THE MOST IMPORTANT FACTORS OF FOAMING AND SOLUTIONS (BASED ON LITERATURE):

- Composition of the organic matter should be constant, that helps to develop a well-balanced microbiological population (max. 4kg/day/m<sup>3</sup> dry material).
- The best value of the C/N ratio is 15-30/1. When the level of nitrogen is low the carbon elaboration decreases-, while too much nitrogen reduces the methane production.
- Methane-producing bacteria live best under neutral to slightly alkaline conditions. Under anaerobic conditions, the pH will normally take on a value of between 7 and 7.5 (less than 6,8 can be harmful). In the presence of fermentative anaerobic organisms the optimal pH value is 4,5-6,3.
- The optimal dry matter content is 6-15 % in the case of mechanical mixing. Continuous mixing is needed in order to maintain process stability and improving the efficiency within the digester.
- Fluctuation of the temperature reduces the methane development.
- Optimal temperature of the mesophilic bacteria is 35-40 °C.
- Dry matter content determines the load of the reactor. Quantity and the concentration together give the correct information.
- Volatile acids, the HCO<sub>3</sub> alkalinity and the ammonium concentration must be determined.
- Volatile acid concentration is less than 1000 mg acetic acid/l equivalent
- FOS/TAC value: 0,3-0,4 is good, but depends on the system. 0,2-0,3 is good in the second digester and the lagoon. When the value is less than 0,2 there is a lack of organic matter. Above 0,4 the organic matter content is too much.
- Air intake is needed for hydrogen sulphide oxidation (admissible content is 2-2,5% of the gas)

Applied materials for producing biogas in the investigated plant:

- corn silage
- cow manure
- liquid manure
- sewage sludge (from 12 waste water plants)
- food residues
- oil-, and fat sludge
- expired food ( cold cuts, ice cream, chips)

The most important factors affecting the anaerobe digestion:

- fresh inoculums

- constitution and concentration of the input material
- solids retention time, and the system load by the organic matter
- temperature, mixing and flowing compliance
- exclusion of toxic matter

In order to keep the desired efficiency, controlling some of the above mentioned factors (load, temperature, mixing) the operator is able to intervene, but changing the features of the substrate (chemical, microbiological constitution, toxic components) is complicated or sometimes impossible.

Discovering the real problem in the investigated plant, as a first step the constitution of the input material was examined with a special focus on energy and ash content. At the beginning of the research project we established a target: preparing recipients to create optimal inputs for the reactors.

Determining parameters are:

- C/N
- FOS/TAC
- pH

Components are introduced in Table 1. Components are signed  $J_e$ . The desired ratio can be reached by changing the ratio of the components considering the reactor dry matter (SZA) capacity, and the load (SZA/kg).

Table 1.

Calculating table for the appropriate components ratio

Matter/ Feature	Dimension	A		B		C.. etc..		$\Sigma_{imp.}$	$\Sigma J_e_{imp.}$
		kg	$J_e^*$	kg	$J_e^*$	kg	$J_e^*$		
C/N	ratio								15-25
SZA	(%)								8-12
pH									6,5-7,8
TAC CaCO <sub>3</sub>	(mg/l)								13000
FOS acetic acid equivalent	(mg/l)								3000
FOS/TAC	ratio								2,1-3,0
KOI	(mg/l)								3000
NH <sub>3</sub> -N	(mg/l)								1600
Phosphate	(mg/l)								10,5-12

#### A. Calculating example:

$J_e$  = feature determination e.g.: C/N

Materials weigh separately and sum total (kg)

$$\Sigma kg_{imp.} = Akg + Bkg + Ckg + \dots = \Sigma kg$$

Features separately and sum total (C/N)

$$\Sigma J_e_{imp.} = (Akg \cdot A J_e + Bkg \cdot B J_e + Ckg \cdot C J_e + \dots) / (Akg + Bkg + Ckg + \dots) = \Sigma J_e \text{ (sum C/N)}$$

Calculation must be fulfilled for all the used input materials every time, when feeding the reactor and always if any changes occur.

#### V. FEATURES OF SEWAGE SLUDGE

Results of energetic and chemical tests of 3-3 samples (chosen from all the 12 input materials coming from different waste water plants) can be studied on figures 3-8. Dry matter content of the samples differs very much, but the C content is almost the same.

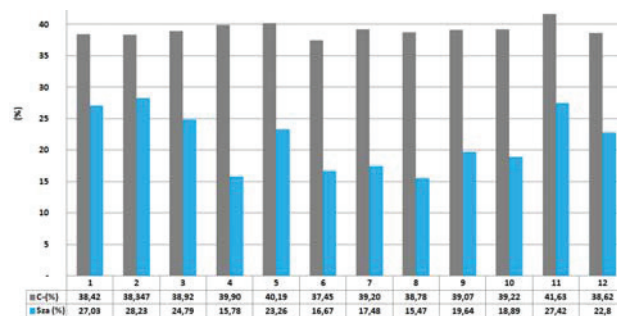


Figure 3. Dry matter content of the samples

Significant difference can be found in the pH value and the C/N ratio of the samples. It is a big problem and intervention needed to make a better balance.

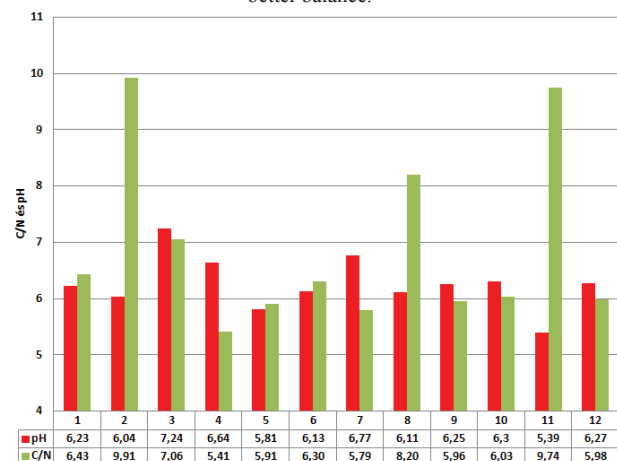


Figure 4. pH value and C/N ratio (average)

During the fermentation process C and the dry matter content decreases in the reactors. Compensation of the difference in the C/N ratio was carried out by manure and corn silage dosage. Because of the F2 digester operated using more sewage sludge, the dry matter content and the C/N ratio was disadvantageous, and the foaming was more intensive there (see Figure 5.).

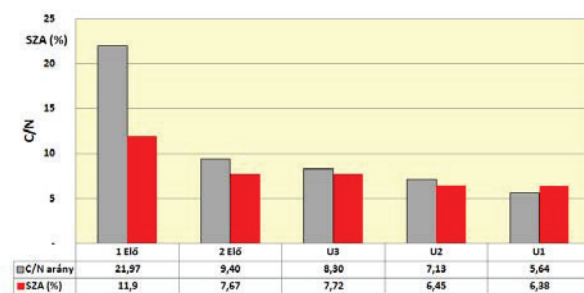


Figure 5. Changing the C/N ratio and the dry matter content in the reactors

Features of the other input materials were also tested. Significant difference was detected in the dry matter content, but they have more advantageous C/N ratio than the sewage sludge (see Figure 6.).

Feeding of the reactors can be realised from different sources, as the pre-storage bunker (ET), chopper (SZK) and the autoclave (AC) (see Figure 1.). All the reactors can be supplied by the central pump from all the mentioned sources. This can be important in the case of foaming.

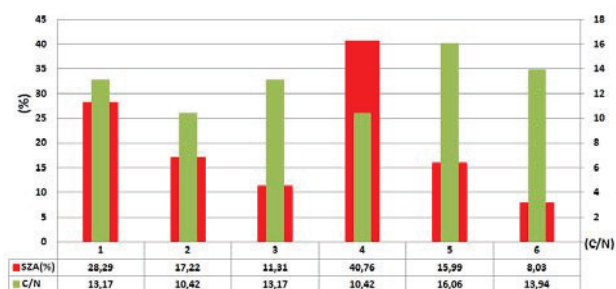


Figure 6. Features of the other materials

1) food residues, 2) liquid manure, 3) oil-, and fat sludge, 4) manure, 5) expired food ( cold cuts, ice cream, chips) 6) cooked oil.

## VI. UTILISATION OF THE END PRODUCT

With the help of the pump the substrate can flow from the second digesters to the separator, from where the liquid phase flows to the lagoon, and the solid phase goes to the concrete bunkers (VT).

Some quantity of the solid residues -as have a high energy content- can be re-used in the fermentor in order to increase the C content. The dry end product can be used as nutrient on the fields or can be composted. Also some quantity of the liquid from the lagoon can be used to help for pre-mixing (in order to control the dry content).

According to the current regulations the liquid end product (digestate) must be handled as liquid manure and may be spread out to the fields only one time a year. It must be ploughed into the soil. Problems of this procedure are:

- plants are not able to utilise the so much quantity
- sometimes nutrients are not available when plants need

The high moisture content is an advantage of spreading the liquid end product, and it can help am lot in doughty. Other economical advantages can also be mentioned as digestate may substitute fertilisers, can be used well on sand soil (0,5-0,7GWh/year electric capacity ensure digestate for 1,0-1,2 ha plough land).

## VII. EFFECT OF THE SEWAGE SLUDGE AND THE SAND CONTENT OF THE MANURE

Sewage sludge and manure contain significant quantity of sand (quartz sand). As the particulars are abrasive very much, the sand content is disadvantageous for the technical equipments (mainly for the chopper, and mixers). Sand stays at the bottom of the lagoon. This must be considered when using the digestate as diluents. Only precipitated digestate can be used for dilution!

The intensive abrasion makes serious problem in the chopper operation (figure 7.). Hammers were rapidly, that cause inappropriate chopping. Fibrous material reduces the mixing efficiency that causes less gas production.



Figure 7. Abrasion of the hammers

A-original hammer, B-one month operated hammer, C-two months operated hammer

Strengthen of the edges (e.g. welding using hard metal) is suggested to avoid the intensive abrasion of the hammers.

## VIII. EFFECT OF THE MIXERS

The digesters (F1, F2) have three same sized moveable mixers, and a bigger fix mixer. The second digesters (U1, U2, U3) have three, same sized moveable mixers. The vertical position of the smaller mixers can be changed, and they can be turned with 60 degrees from left to right.

Mixers play an important role in homogenisation. Optimal streamline inside the reactors supports the adequate heat exchange for the heating pipeline that is needed for ensuring the homogeny reactor temperature. According to our monitoring the mixing process is inappropriate. Finding the optimal adjustment of the mixers modelling and simulation of the mixing process was performed. 135 variations were analysed. In a next article, we report on the modeling of mixing.

## IX. RESULTS

During the 5 months research project our effort oriented to find the optimal feeding of the reactors. Ad hoc breakdowns of the system and sometimes stoppages of the needed input material supply resulted unwanted delays (see Figure 8.).

Application of the simulation resulted moderated foaming, and the number of the malfunctions of the system reduced. The specific gas production, relative to the input material increased (see Table 2.). During three months the electric capacity value grown from 61,2 % to 68,7 %.

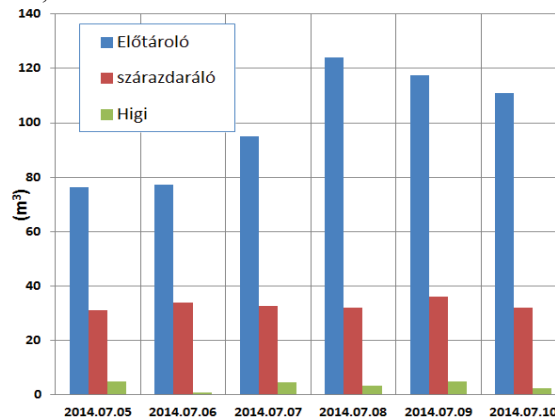


Figure 8. Fed materials

(blue-pre-storage, brown-solid chopper, green-autoclave)

This proves our targets and the benefits of the research work that would be sensible to continue in order to optimise the applied technology.

Table 2. Electric power capacity of the system

Rated capacity MWh/month	Effective capacity (MWh/month)	Calculated cap. from inputs** (MWh/month)	Calculated cap. from inputs * MWh/month)
1480,56	592,2	1017,6	916,2
100%	40,0%	68,7%	61,2%

## X. SUMMARY

This article dealt with an operational segment of a biogas plant. As far as we can prognosticate biogas plants will be wide spread in the near future in Hungary as the concept is supported by the Government. Furthermore the concept of settling biogas plants nearby wastewater treatment plants is supported by the European Union. Biogas plant can be established in the area of a wastewater treatment plant, but the idea of serving a biogas plant by at least 2-3 sewage treatment plants seems to be more effective and economic. Usually the most important problems derive from the great variety of the input materials and the very much difference in content of them. Foaming is maybe the most serious malfunction. Operation without any troublesome can be observed mainly where recipes are used in the technology based on laboratory tests, focusing all the critical parameters and features of the input materials. If feeding is consistent, then the specific gas production ( $\text{m}^3$  gas/kg input material) increases. In Hungary the annual sewage production is

500.000 t, and only 20% is utilised for biogas production. A significant amount is sent to landfills, although the anaerobic digestion is the best solution considering the ecological and economical aspect. The end-products of the biogas plants are energy (electric and heat as well) and good quality manure that can be used well in the plant production technologies.

## LITERATURE

- [1.] A. Zehnsdorf, L. Moeller, K. Görsch, V. Beer. Bernburg, 2010 Schaumbildung in Biogasanlagen, Hemholtz, Zentrum für Umweltforschung UFZ, 30. November
- [2.] Bayerische Landesanstalt für Landwirtschaft (LfL). (2006). Biogastechnologie zur umweltverträglichen Flüssigmistverwertung und Energiegewinnung in Wasserschutzgebieten, (<http://www.LfL.bayern.de/publikationen/>)
- [3.] Esteves S- Miltner M-Fletch S: Folyamatos ellenőrzési útmutató a biogáz és biometán üzemek megfelelő működtetéséhez  
Gruber, W. (2007). Biogasanlagen in der Landwirtschaft. Aid infodienst Verbraucherschultz, Ernährung, Landwirtschaft e.V. Bonn. 1453.
- [4.] Kardos L. A szennyvíztelepi biogáz termelő fermentációs folyamatok nyomon követése kémiai és biokémiai módszerekkel  
PhD dolgozat, ELTE, 2012
- [5.] Koppe, P. - Stozek, A. - Neitzel, V.: Municipal waste eater and sewage sludge  
in Rehm, H. J. and Reed G: Biotechnology, Volume. 11a. Environmental Process, p. 337-
- [6.] Kougias P. G., Boe K., Thong S. O, Kristensen L. A. and Angelidaki I.: Anaerobic digestion foaming in full-scale biogas plants: a survey on causes and solutions ISWA publishing 2014,
- [7.] Kovács at al ( 2003): A szennyvíziszap-kezelés és hasznosítás jogi, gazdasági, műszaki, környezetegészségügyi



# Energy efficiency as a precondition of sustainable tourism

Slavica Tomić \*, Aleksandra Stoiljković \*\*

\* University of Novi Sad, Faculty of Economics in Subotica, Serbia

\*\* University of Novi Sad, Faculty of Economics in Subotica, Serbia  
tomics@ef.uns.ac.rs

**Abstract—** Tourism is growing faster than the world economy. Despite of numerous economic benefits of tourism development, tourism activities have numerous negative consequences. The most important negative impact of tourism is on the environment. Tourism extensively used water and energy and produces large amounts of waste. UNWTO showed that tourism is responsible for 5% of the worldwide carbon dioxide emissions. The main polluters are transportation and accommodation. The concept of energy efficiency in tourism is based on the knowledge of people about the need to preserve the environment and existing energy sources.

## I. INTRODUCTION

The environmental pollution is one of the problems that engage the attention of world public. Waves of scientific and technological progress are present in all spheres of individual and social life and make it easier. On the one hand are unimagined possibilities of science and technology but on the other hand increased concern about the negative consequences. Man is the only being in the biosphere that is able to cancel the terms of their own survival. A man proves its power to reign over nature often destroying and disrupting its balance. In addition to the many positive results of scientific and technological progress, there are many negative effects on the environment and the survival of the planet. Spending significant quantities of energy depletes limited resources and the discharge of harmful substances into the environment affect the degradation of the environment.

Tourism has a great share of environmental pollution and especially in the wasting of energy resources. In an effort to develop the tourism industry countries often neglected the need to protect the environment and save energy.

The solution should be sought in the context of sustainable development. The basis of this type of development is to achieve economic and social goals while preserving the environment and resources for future generations. [13] Sustainable is every type of tourism that permanently contributes to the protection and improvement of the environment, natural and created resources, cultural values and integrity of the local community. So, tourism and sustainable development are two mutually dependent and conditioned phenomena. [1] But the idea of sustainable development was preceded by

a long practice of unsustainable development.

## II. ENERGY EFFICIENCY IN TOURISM

The frequency of use of the concept of energy efficiency is not in proportion to its true understanding. The concept of energy efficiency is based on the knowledge of people about the need to preserve the environment and existing energy sources.

The European Union in 2007 set a strategic goal of reducing primary energy consumption by 20% until 2020. In the literature this goal is called 20-20-20, means that the 20% increase use of renewable energy compared to conventional sources, reduce the level of greenhouse gases by 20% and 20% increase the efficiency of energy use.

Every individual, every company and every country should act towards savings. Great hopes are placed in the possibility of saving in buildings, [8] which, according to the latest data, consume about 40% of the energy in the EU.

Energy efficiency can be viewed from two aspects : first aspect is related to the energy efficiency of buildings and equipment, and other, which includes measures and ways of behavior that lead to energy efficiency.

Energy efficient building is one that the application of certain rules of construction occur significant energy savings. Installation of equipment and devices that save energy brings not only saving money but, more importantly, increase the value of the building in case of sale. When accessing the installation of such equipment and devices, it is important to do so gradually favoring those with the shortest period of return on investment (payback). Investments in energy-efficient equipment bring an average savings of 20%. [11] Measures that lead to energy efficiency are all measures and regulations or changes in the behaviors which lead to the reduction of energy consumption, for example, the use of renewable energy sources instead of non-renewable, replacing inefficient appliances that consume more energy to those who are efficient, heating insulation. Energy efficiency does not imply a decline in the quality and standards of living, comfort or economic activities. [10]

Although achieving energy efficiency in the tourism industry is very complex, these aspects of energy efficiency are applicable in the field of tourism. It applies to all stakeholders in tourism supply and tourism demand.

As a participant in the tourism supply can be regarded hotel industry as its subsystem, as well as equipment used in hotels and other tourist facilities in order to provide services to tourists. On the other hand it is necessary to create educated tourist demand, which will result in energy-efficient behavior of tourists.

Energy efficiency of the tourism sector is one of the steps which seek to achieve sustainable development of tourism as a global phenomenon.

Today, the business volume of tourism equals or even surpasses oil export business, food products or automobiles. Tourism has become one of the major players in international commerce, and represents at the same time one of the main income sources for many developing countries. [20] The size of the industry itself makes it important to consider the impact of tourism on the environment. It is important to understand the impacts because tourism products, in addition to anthropogenic, are highly dependent on the natural attractiveness. Tourism in the last six decades is one of the largest and fastest-growing sector, as evidenced by figures, whether it is as an indicator used the total number of international tourists or total tourism consumption. If we look at the chart below, which shows the upward trend of the total number of international tourists in the period between 1950- 2014, we can see that the number of tourists in the world increased 45.5 times, and exactly in this period, tourism is experiencing the greatest expansion. If we look at long-term forecasts of the World Tourism Organization, we will see that in the projected period to 2030, expects further growth in international tourism, at an average annual rate of 3.3%, which represents an average increase of 43 million international tourists a year.

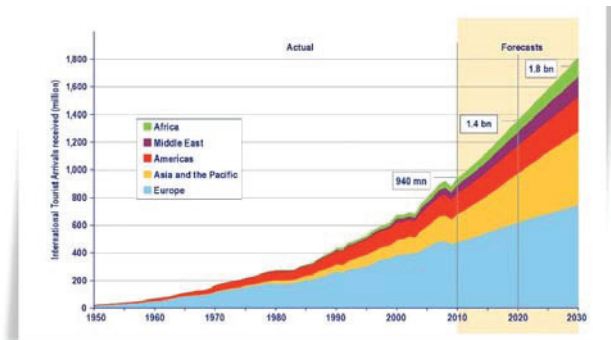


Figure 1. Actual trend and forecast 1950-2030.

Source :

[http://dtxtg4w60xqpww.cloudfront.net/sites/all/files/pdf/unwto\\_highlights\\_14\\_en\\_hr\\_0.pdf](http://dtxtg4w60xqpww.cloudfront.net/sites/all/files/pdf/unwto_highlights_14_en_hr_0.pdf)

The data shown are telling us that this is an important segment which should be given great attention, just because more tourists consume more energy. Tourists consume energy, water, emit CO, CO<sub>2</sub>, HC, NO, wastewater, solid waste. According to the one study, tourist results in more environmental loads than local people (for example, the amount of solid waste discharge per tourist is 1.95 kg per day that of per local people is 1.18 kg). [9] It is necessary to affect the tourists

themselves, to create awareness of the importance of sustainable tourism development. Support by tourists in creating sustainable tourism is one of the most important, because tourism is made of people.

When we talk about types of energy expenditure, which have the greatest importance in tourism, first that needs to be mentioned is transport. The development of various means of transport is one of the most important factors that created the phenomenon of mass tourism. Before that, travel to distant destinations was very difficult and very time consuming. With the development of transport means a large number of long haul destinations become physically and economically accessible to a large number of tourists. A major influence on the occurrence was low cost airline and a large number of regular airlines due to the introduction of direct flights that connect much emitive and receptive country. Tourism has experienced expansion and diversification to become one of the largest and fastest growing sectors in the world economy just as the development of means of transport, which contributed to the development of new destinations, primarily in Asia, and a growing share of Africa and the Middle East, which, along with the traditional tourist favorites, Europe and North America, are becoming available and contribute to the expansion of tourism. This is important to note because transportation is the largest consumer of energy in tourism (and there's no tourism without travel). 75% of the energy used in tourism is used on arrival at the destination and return from the destination. [11] The transport sector is the largest emitter of CO<sub>2</sub> and other harmful gases (GHG - Greenhouse Gases). More than 70% of CO<sub>2</sub> emissions in the tourism sector emerged during transport, and 40% of CO<sub>2</sub> emissions of the total amount come from the use of air transport. [4]

Air transport, as the most dominant form of transportation, is the largest consumer of energy when we talk about the different means of transport. Travelling by air requires significant amounts of fossil fuels, whose combustion causes the greenhouse effect in the atmosphere. Aviation makes 2-3% of the world's use of fossil fuels, with more than 80% of the consumption of civil aviation. The contribution of aviation to global emission of CO<sub>2</sub>, according to forecasts, will grow for 3-7% by 2050. [9] The following chart shows the share of individual modes of transport in international tourism in 2013, according to UNWTO.



Figure 2. Inbound tourism by mode of transport, 2013.

Source :

[http://dtxtg4w60xqpww.cloudfront.net/sites/all/files/pdf/unwto\\_highlights\\_14\\_en\\_hr\\_0.pdf](http://dtxtg4w60xqpww.cloudfront.net/sites/all/files/pdf/unwto_highlights_14_en_hr_0.pdf)

The given graphical display shows clearly that dominant share is air traffic, followed by road traffic, while the share of rail and water traffic are marginal. However, it is anticipated the development of rail transport in the future, because congested road traffic. Air traffic affects the emission of greenhouse gases the most, and the transition to the use of rail transport in addition to the problem of traffic congestion is also one way of reducing these emissions. If only one third of tourist trips with air travel are oriented towards rail transport, if infrastructure allows it, there would be cost reduction of CO<sub>2</sub> emissions around 8% (in the EU). Divert 20% of car traffic on the railway would reduced emissions of CO<sub>2</sub> by 4 to 5%.[4]

Previously stated that the transport largest energy consumer in tourism, but also the largest emitter of harmful gases. Estimates indicate that more than 80% of the energy used in tourism comes from non-renewable sources of energy. [2] It is therefore necessary to review and improve the traditional concepts of transport and energy required for its implementation, which, for the most part, derived from crude oil and oil products. Technical innovations tourist transport can be one of the most important factors to achieve energy-efficient transport and also entire tourism. They may consist of improving fuel efficiency, the use of alternative fuels, the introduction of renewable energy sources, as the primary source for energy in transport, as well as developing a completely new means of transport. [15]

After transport, tourism segment that consumes the most energy are accommodation facilities that tourists are staying in, and then the various tourist activities that require the use of energy. Energy efficiency experienced its first broad deployment in the accommodation sector. Hotel companies are among the first in the world to realize the benefits of energy efficiency of their buildings, primarily financial benefits, due to the reduction of expenditure for consumed energy. The energy crisis in the 70s of the twentieth century, put the builders in front of a new challenge - to design a building that is energy efficient, primarily with a goal of reducing "wasting" energy. Hotels were the most suitable for the implementation of such projects, thanks to their energy complexity, because hotels of all categories of accommodation have the highest average energy consumption per visitor. This is because hotels include energy-intensive facilities, such as bars, restaurants, swimming pools and more spacious rooms. Of all categories of accommodation, it is considered that camps account for the lowest energy consumption per night. [5]

In the commercial and institutional sectors, hospitality is ranked as one of the largest consumers of energy and therefore is loaded with proportional energy costs. But it's also a fact that those costs can be effectively controlled than all operating costs. And most importantly, the degree of reduction of these costs affect the final financial result, increasing profits and makes the hotel cost significantly more competitive by allowing focus on the customer and occupancy

In addition, with the same beneficial savings we achieve the following: [12]

- improving the level of comfort and satisfaction of the guests;
- addition to the aesthetics and content;
- reduce maintenance costs and failures of systems;
- increasing the life of the equipment and the value of buildings;
- improving corporate culture and awareness;
- reducing emissions that affect climate change.

The cost of the energy consumption in hotels continental type range from an average of 15-18% of the total operating cost of the hotel and are on the second place (behind labor costs). [12]

Within the hospitality sector, energy costs may only be a small percentage of turnover, but reducing them can directly increase revenue without the need to increase sales. Money saved on energy goes straight to the bottom line which makes businesses more competitive. The implementation of simple energy efficiency measures can also increase levels of staff and customer comfort as well as improving general morale. [17]

The next pie charts to the right show where hotels use most energy and where the biggest savings can be made: in heating, lighting, hot water, and catering.

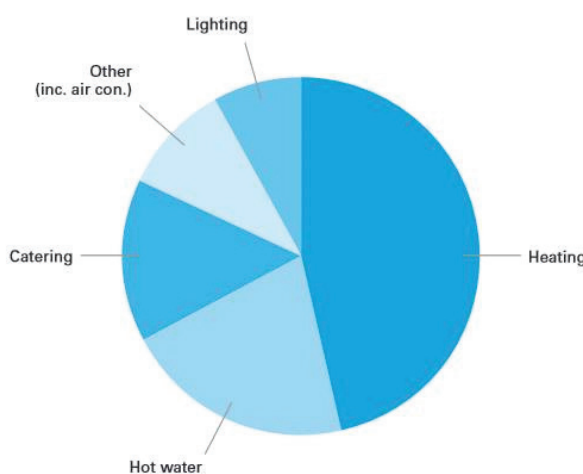


Figure 3. Breakdown of energy use within the average hotel

Source :

[http://www.carbontrust.com/media/39220/ctv013\\_hospitality.pdf](http://www.carbontrust.com/media/39220/ctv013_hospitality.pdf)

Building energy efficient and environmentally friendly hotel buildings can be significantly more expensive than conventional construction, but it is necessary to take into consideration benefits that the construction of hotel facilities according to the standards of energy efficiency brings over the lifetime of the object.

The most important principles in the construction of energy-efficient and environmentally-friendly hotel are: [12]

- the use of energy-efficient apparatus
- the use of environmentally sustainable materials
- use of recycled materials
- use materials manufactured, according to the standards, with reduced or without chemical toxicity
- positioning the subject at the adequate sunlight exposure
- installation of insulating material on the outer walls respecting the principles of thermal bridges
- installation of thermal regeneration devices.

The following illustrates two examples written by Hannes Lütz (Product Manager, CentraLine). [18] The first example shows the possibilities to reduce costs in hotels, through the reduction of energy consumption in the guest rooms. Another example refers to the technique of monitoring energy consumption in the hotel, whereby, using these techniques do not make direct energy savings, but indicates where it is possible to achieve the appropriate improvements.

### III. FIRST EXAMPLE

This is the ideal situation:

1. If the room is not used, the temperature is maintained at a low "night" mode, supply of fresh air is turned off, and turned off the lights and TV
2. When a guest application, the room is maintained at a "standby" temperature and the minimum amount of fresh air is injected
3. When the presence of the guest IS detected (either by presence sensors, either through the hotel card) provides the normal supply of fresh air, the temperature is maintained at a normal level of comfort, and light will turn on if the outside IS too dark
4. **Aspirating** fan in the bathroom will automatically increase the speed if the increased moisture is in the bathroom or if it is turned on manually by guest (over the five-minute timer)
5. Room switches to standby temperature and the minimum amount of fresh air, if the customer opens a window
6. Room switches to standby temperature and the minimum amount of fresh air, if the guest leaves the room. Light and TV are turned off.
7. Room switches to night temperature and zero amount of fresh air when a guest checks out and pays the bill.

Calculations of cost savings show that a simple timer program for heating rooms can save even more than 40% compared to the radiator valve. Automation standby / presence can reduce costs by an additional 5-10%, depending on the given temperature and standby time.

Clever integration of room automation system in reservations, as foreseen in the CentraLine will reduce the work effort of staff to zero, because of the automatic link between both systems. These reservations systems are connected in various ways with Centralin systems, building automation, and not only for climate control, but the power supply and shutters.

### IV. SECOND EXAMPLE

This is the ideal situation:

1. Power consumption is periodically monitored in various parts of the hotel, such as swimming pool, kitchen, restaurant, guest rooms;
2. Heat energy is monitored by a single rooms in order to detect open doors or windows;
3. The consumption of hot water is monitored in order to notice leaking valve in the guest rooms or elsewhere;
4. The amount of cooling energy consumed in conference rooms and guest rooms can be measured, for possible user charges;
5. Comparison of curves energy consumption from day to day can lead to the identification of irregular events which may lead to a reduction in energy consumption;
6. Finding the primary consumers and their minimization.

Energy monitoring, by itself, does not make direct energy savings, but also allows hoteliers to see where and when energy is consumed, and thus enable to make appropriate improvements.

Application of the above examples in practice, the hotel may directly or indirectly affect significantly reducing operating costs of the hotel. There are other opportunities to reduce operating costs, such as reducing staff or services, which has a direct negative impact on guest satisfaction, and leads to a decrease of reservations.

It is important to note that the use of techniques of improving energy efficiency and control techniques can reduce consumption and waste of energy to the hotel without affecting comfort.

A copy of the reference object UNICOM Ltd. in the hospitality and tourism: [18]

1. Hotel Park, Ruma
2. Hotel IN, Novi Beograd
3. Zlatiborska Noć, Bela Zemlja, Užice
4. Institut Dr.Simo Milošević, Igalo
5. Banja Junaković
6. Hotel Hyatt Regency, Beograd
7. Hotel Grand, Kopaonik
8. Premijum Aqua, Vrdnik
9. Kragujevac Plaza TC
10. Master Centar, Novosadski sajam.



Green innovation in tourism (the planet Earth Summit 2012) may contribute to the implementation of the concept of sustainable development and at the same time achieve energy efficiency for tourist companies. Green innovation, among other things, led to the reduction of costs, increase revenues, create new jobs and more efficient use of energy resources. Promoting the use of green innovation, aims to protect the natural environment, but also the development of the tourism industry by increasing the competitiveness of companies and destinations and improve the experience of tourists.[7]

Problems which prevent faster progress in this area are insufficient awareness of tourists who often are not willing to pay premium prices for "sustainable tourism experience." Problems that prevent faster progress in this area are insufficient awareness of tourists who often are not willing to pay premium prices for "sustainable tourism experience." According to research, 33% of households in deciding on the place of vacation takes into account environmental factors, 40% of tourists are ready to pay more to stay in an eco hotel. Insufficient funding of small and medium-sized enterprises, as well as the lack of integration between key sectors, ie tourism, transport, energy and environment, also hinder progress.

Green innovations are not necessarily linked with a significantly increased costs of companies. The aim is to analyze and detect those opportunities and solutions that require the lowest cost, [6] but which will enable the tourist growth is separated from the negative impact on the environment and will allow more efficient use of resources. So, with adequate investment, tourism in the future may become even more profitable, but at the same time environmentally friendly. With more than one billion participants in international tourism it is important, more than ever, that green innovation become a catalyst for sustainable development in tourism

UNWTO with the support of the European Agency for Competitiveness and Innovation has developed an application "Energy Solutions for hotels" (HES), which calculates the energy needs of the hotel, costs and return of capital. Data collected by HES applications are focused on small and medium hotels EU because they are usually less engaged in the field of environmental protection. The goal is to get at hotels greater energy savings of 20% and the use of renewable energy to 10%.

Tourism has several motives that should lead him towards achieving energy efficiency.

The obligation of tourism is to be friendly to the respective nature, which is its main resource.

Another reason is certainly profit. Tourism, like any other economic activity, is profit-oriented. Measures to be taken to ensure energy efficiency, initially may require significant investment, but long term it returns.[3] The savings achieved in energy consumption becomes quickly evident.

The third reason is the moral nature. Tourism has an impact on the general public. To a large extent, this branch of the economy and symbolizes the efforts of one country has in its functioning. Promoting energy

efficiency through the field of tourism contributes to increasing the awareness of the public and tourist visitors and shows how one country to invest in this area and how much care about their environment.

The economic benefits of sustainable tourism and increasing energy efficiency

Tourism products and services which are based on sustainable tourism bring various economic benefits for all stakeholders. Some of these advantages are:

*a) Economic development opportunities*

The fact that tourism is at the forefront of the global industry talks about the significant potential to increase revenues, the impact on national income, gross domestic product, employment, development of underdeveloped areas. Improve tourism multiple returns to all stakeholders, from employees, satisfied customers over to the state itself. Foreign tourists bring significant foreign currency incomes.

*b) Comfort of tourists*

Basic goal of tourist activities is to ensure guests a pleasant and interesting stay. Modern tourists wants to escape from everyday life, asphalt and noise, to experience excitement, authentic experience, to have fun, learn and takes care of the environment (concept 6 E - escape, experience, entertainment, excitement, education, ecology ). Tourist facilities that are energy efficient and using more resource efficient technologies not only provide the required level of comfort for tourists, but also can increase the quality of the stay at the hotel.

*c) Increased productivity*

Orientation of hotels and other tourist facilities to promotion of sustainable tourism, brings benefits to employees in this area. Better working conditions provide reduced health problems, and thus absence from work. Studies have shown that green business facilities in addition to saving energy, increase employee productivity by 30%, and sick leave are reduced by 80%. Instruct its employees on energy management plans and their involvement in its implementation will further motivate them. With a sense of belonging to a team, employees will become more successful and productive.

*d) Competitive advantage*

Sustainable design allows tourist facilities to differentiate against the competition and even increase its market share by focusing on the segment of tourists with a high level of environmental awareness. Examples show that promote performance in the market as a "green hotel" often leads to a significant increase utilization of capacity.

*e) Higher profits*

You cannot do business responsibly [14] with thinking that is making a profit only purpose of business. But achieving greater employee productivity, more efficient use of resources and energy, reducing costs related to energy, increasing occupancy of buildings, and therefore increase market share have resulted in the ultimate positive effect of the increased profits. Hotels that succeed in their quest to increase energy efficiency,

thus realizing higher profits and market share, and get to market value.

#### V. CONCLUDING REMARKS

Improving energy efficiency in tourism and lowering costs imposed as a necessary choice. Improving energy efficiency in tourism and lowering costs imposed as a necessary choice. It emits additional positive effects and benefits. The most direct positive impact is on the environment which is the primary resource for tourism. Natural catastrophes which are a consequence of climate change is increasingly affecting the awareness of the necessity of changes in behavior, which among other things includes the rationalization of energy consumption. This is a chance for tourism through activities on energy efficiency programs further enhances its attractiveness.

#### REFERENCES

- [1] Bartoluci, M. (2013). Upravljanje razvojem turizma i poduzetništva, Školska knjiga, Zagreb.
- [2] Conrady, R. and Buck, M. (eds), (2010). Trends and Issues in Global Tourism 2010. Springer- Verlag Berlin Heidelberg.
- [3] Croucher, M. (2012). What is important when modeling the economic impact of energy efficiency standards, Utilities Policy 22.
- [4] Ćurčić, Lj., Stepanov, J., Aleksić, D., Štrbac, S. (2009). Interakcija između turizma i klimatskih promena. EnE09 Zbornik radova 5. regionalne Konferencije „Životna sredina ka Evropi“. Ambasadori životne sredine i Privredna komora Srbije, Beograd, 16-20. <http://ambassadors-env.com/wp-content/uploads/Zbornik-radova-EnE09.pdf>
- [5] Gössling S., Peeters, P., Ceron, J.-P., Dubois, G., Patterson, T., Richardson, R. (2005). The eco-efficiency of tourism. Ecological Economics, 54(4), 417-434.
- [6] Janusz, G., Bajdor, P. (2013). Towards to Sustainable Tourism – Framework, Activities and Dimensions, IECS .
- [7] Khademvatani, A., Gordon, D. (2013). A marginal measure of energy efficiency: The shadow value, Energy Economics, 38.
- [8] Kosorić, V. (2013). Ekološka kuća, GK Beogra, 2008.[4] John A. Laitner, An overview of the energy efficiency potential, Environmental Innovation and Societal Transitions, 9.
- [9] Kuo, N.-W., Chen, P.-H. (2009). Quantifying energy use, carbon dioxide emission, and other environmental loads from island tourism based on a life cycle assessment approach. Journal of Cleaner Production, 17, 1324-1330.
- [10] Laitner, J. (2013). An overview of the energy efficiency potential, Environmental Innovation and Societal Transitions, 9.
- [11] Maksin, M. [et al.]. (2009). Menadžment prirodnih i kulturnih resursa u turizmu, Univerzitet Singidunum, Mladost grupu, Beograd.
- [12] Pavlović, D. (2008). Energetska efikasnost u hotelskoj industriji: put u korporativno građanstvo. Acta turistica nova 2 (2),155-179.
- [13] Perišić-Živadinov, I. (2009). The environmental and economic impact of sustainable hotels. Ekonomska istraživanja, 22(2), 98-110.
- [14] Sloan, P., Legrand, W., Chen, J. (2009). Sustainability in the Hospitality Industry, Principles of Sustainable Operations, Elsevier, Great Britain.
- [15] Zotz, A. (2010). The role of Tour Operators in Climate Change Mitigation. Institute for Integrative Tourism and Development, Wien.
- [16] [http://www.climalptour.eu/content/sites/default/files/Tour\\_Operators\\_EN.pdf](http://www.climalptour.eu/content/sites/default/files/Tour_Operators_EN.pdf)
- [17] [http://www.carbontrust.com/media/39220/ctv013\\_hospitality.pdf](http://www.carbontrust.com/media/39220/ctv013_hospitality.pdf)
- [18] <http://www.unicom.rs/zip/energetska-efikasnost-hoteli.pdf>
- [19] [http://dtxqtq4w60xqpw.cloudfront.net/sites/all/files/pdf/unwto\\_highlights14\\_en\\_hr\\_0.pdf](http://dtxqtq4w60xqpw.cloudfront.net/sites/all/files/pdf/unwto_highlights14_en_hr_0.pdf)
- [20] <http://www2.unwto.org/content/why-tourism>

# Fluidized bed drying of granules

T. Poós\* and V. Szabó\*

\*Department of Building Services and Process Engineering, Faculty of Mechanical Engineering,  
Budapest University of Technology and Economics, Budapest, Hungary  
poos@mail.bme.hu, szabo1viktor1@gmail.com

**Abstract** – *A pilot plant fluidized bed dryer was developed, which is suitable to dry particles fast and effective. The instrumentation of equipment ensures the measurement of the parameters of drying gas, and the surface temperature of the particles. We performed experiments on batch mode, thereby the simultaneous heat- and mass transfer can be examined during the fluidized drying. Experiments performed on batch mode.*

**Keywords:** *fluidized bed dryer, heat- and mass transfer, instrumentation, batch process, granules*

## I. INTRODUCTION

Heat transfer is widely used to remove moisture from a wet solid by diffusing the liquid into the vapor state. In most drying operations, water is the liquid that is evaporated, air is the normally employed purge gas.

During convectional drying simultaneous heat- and mass transfer occurs between the wet material and the drying gas. Heat transfers from the drying gas to the material and at the same time, the moisture diffuses from the material to the drying gas. Fluidized bed dryers are used for particles with small and unique geometry.

There are several types of fluidized bed dryers for industrial purposes. The most common classification is based on the mode of heat input. The heat is needed for drying the material at least with one of the following methods:

- radiation drying;
- convective drying (using drying gas);
- contact drying (by conduction from a surface that is in direct contact with the material to be dried) [1].

Fixed bed is if a fluid is passed upward through a bed of fine particles, the fluid merely percolates through the void spaces between stationary particles. In gas-solid systems, increasing the flow rate of the air beyond minimum fluidization velocity, large instabilities with bubbling and channeling of gas are observed. At higher flow rates, agitation becomes more violent and the movement of solids becomes more intensive, like a vigorously boiling liquid. The upper surface of the bed disappears, entrainment becomes appreciable, turbulent motion of solids clusters and voids of gas of various sizes and shapes are observable. With a further increase of gas velocity, solids are carried out from the tube with the gas [2]. Scaling of fluidized bed dryers as compared to other form dryers are more complex due to intense mixing of phases and the heterogeneous behavior of the bed. The heterogeneity is due to the presence of different phases such as emulsion phase, bubble phase and cloud phase with the exchange simultaneous of heat- and mass transfer between these phases [3].

## II. MODEL

### A. Bubbling bed model

Early investigators [4] identified that the fluidized bed has to be treated as a two-phase system contains an emulsion phase and bubble phase (often called as dense and lean phases). The bubbles contain very small amounts of solids. They have an approximately hemispherical geometry on the top and a pushed-in bottom. Each bubble of gas has a wake which contains a significant amount of solids. The gas within a particular bubble remains largely within that bubble, penetrating only a short distance into the surrounding emulsion phase. This region penetrated by gas from a rising bubble called as cloud [5]. The schematic illustration of these phases are shown on Fig. 1.

The three-phase back-mixing (bubbling bed) model was developed by Kunii et al. [2]. The bubbling bed consists of three distinct phases such as bubble phase, cloud-wake phase and emulsion of dense solid phase. There are some assumptions and limitations of the model:

- In the bubble phase, gas moves upward as a plug flow.
- In the cloud-wake phase, gas moves upward along with bubbles.
- In the emulsion or dense phase, solids move downward.
- The moisture and temperature distributions of the emulsion and solids phase are uniform over the bed, but have distribution for bubble phase.
- Solids do not tend to agglomerate.
- All particle interaction is ignored, implying that any heat- and mass transfer between individual particles and the emulsion phase.
- No attempt is made to allow for particle size distribution.
- The wall of the bed is insulated and there is no heat transfer between the wall and the interstitial gas and solids phases [6].

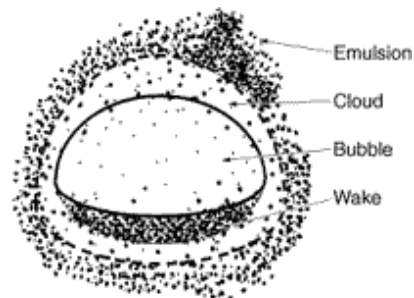


Figure 1. Schematic illustration of phases near the bubble [5]

TABLE I.  
SOME NU-RE CORRELATIONS FROM THE LITERATURE

Ref.	Equation	Range
Kunii [2]	$Nu = 2 + 1.8Re^{0.5}Pr^{0.33}$	$100 < Re$
Yang [9]	$Nu = 1.01Re^{0.48}Pr^{0.33}$	$50 < Re < 10^4$
Molerus [10]	$Nu = 0.02469Ar^{0.4304}Pr^{0.33}$	$10^5 < Ar < 10^9$
Roy [11]	$Nu = 0.0205Re^{1.3876}Pr^{0.33}$	$1 \leq Re \leq 10^3$
Kumaresan [12]	$Nu = 0.00000565Re^{1.997}$	$30 < Re < 70$ $0.0106 < Nu < 0.298$
Alvarez [13]	$Nu = 0.000241Re^{1.753}$	$80 < Re < 250$
Alvarez [13]	$Nu = 0.000824Re^{1.655}$	$80 < Re < 250$
Ciesielczyk [14]	$Nu = 0.106ReAr^{0.0437} \left( \frac{L_{sta}}{d_{1P}} \right)^{-0.803} \Phi^{1.12}$	$3.61 < Re < 125.9$ $1.24 \cdot 10^3 < Ar < 1.14 \cdot 10^5$ $121 < \frac{L_{sta}}{d_{1P}} < 705$ $1.14 < \Phi < 1.81$

Some authors [7], [8] uses the theory of bubbling bed model for the completion of numerical simulations, where the heat transfer characteristics are well examinable. There are heat- and mass transfer between the phases, as:

- transfer from gas in the bubble to solids in the bubble phase,
- transfer from bubble phase to cloud phase,
- transfer from gas in cloud to solid phase,
- transfer from cloud phase to emulsion phase,
- transfer from gas in emulsion phase to solid [1].

The practical use of bubbling bed model is fairly difficult to evaluate laboratory measurements due the hard measureable parameters e.g. diameter of bubbles. Hereafter we will treat the fluidized bed as two-phase model contains solid- and gas phases, assumed flow around sphere.

#### B. Nu-Re relationship

This approach relates transfer coefficients to the dimensionless numbers, which are evaluated using a wide range of experimental data. In the literature there are several  $Nu=f(Re)$  equations using the characterization to heat transfer between solids and drying gas. These are necessary to scale up fluidized bed dryers using for a process. A summary of the correlations proposed by the authors is included in Table I. Our goal is to make a widely applicable correlation with well measurable parameters.

### III. INSTRUMENTATION AND EXPERIMENTS

#### A. Experimental apparatus

Fig. 2 shows the instrumental flow diagram of the fluidized bed dryer apparatus. This equipment is suitable to examine the phenomenon of fluidization and to evaluate the transfer coefficient that are used for the equations of simultaneous heat- and mass transfer. The central section of this apparatus is a vertical positioned dryer (D-102-01). The air is blown by a fan (P-101-01) through an electric heater (H-101-03) and the orifice flow meter (O-101-04) for the volumetric flow rate. The flow rate of air can be modified by a knife gate valve (L-101-02). The wet particles are fed to the fluidized bed dryer from a vessel signed V-102-03 by a conveyer screw (CS-102-04). The process of fluidized bed drying starts from the feed entrance. At the end of the drying, when the final moisture content of particles is reached, the particles are carried out from the tube to the cyclone (C-103-01), where the particles are separated from the gas. The wet air leaves the apparatus to the ambient. The dried particles are collected in a vessel (V-103-03) through a rotary valve (RV-103-02).

Before the measurements the particles are submitted to some preparations. First, the dust and other contaminants have to be separated. This process is made using a wind classification equipment. After that, the particles are wetted with a given amount of water. The mass of the particles is measured with a scale before and after the measurement.

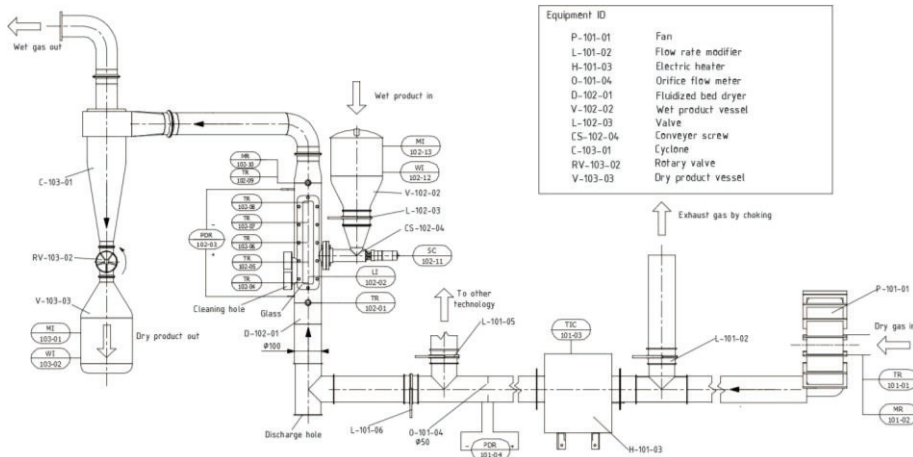


Figure 2. Instrumental flow diagram of the apparatus



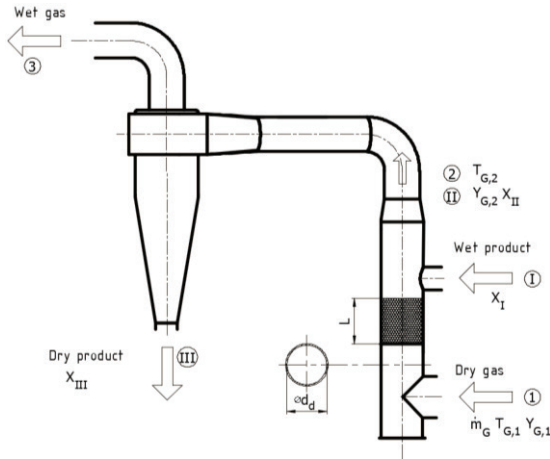


Figure 3. Instrumental flow diagram of the apparatus

With a small sample experiment the moisture content of particles is evaluated to check the equilibrium moisture content.

During the measurement the flow rate of drying air is modified by a valve (L-101-02) and measured by the orifice flow meter (O-101-04). The temperature of drying gas is controlled by the electric heater (H-101-03). The temperature (TR-101-01) and the absolute humidity (MR-101-02) of ambient air, furthermore the inlet (TR-102-01) and outlet (TR-102-09) temperature and absolute humidity (MR-102-10), and at five points through the height of dryer (TR-102-04, TR-102-05, TR-102-06, TR-102-07, TR-102-08) are measured. The height of the static bed is measured by a measuring scale with stopping the air flow in an arbitrary moment. The pressure difference of the fluidized bed is measured by a differential pressure transmitter (PDR-102-03). The measurement can only be performed at the reaching of static stage – until the measured values of the instruments are stabilized. The measured values is registered by data logger and PC in 10 seconds intervals. The feed and the removal of particles are in batch mode during the measurement. Reaching the required moisture content of particles, they are discharged from the tube closing valve L-101-02.

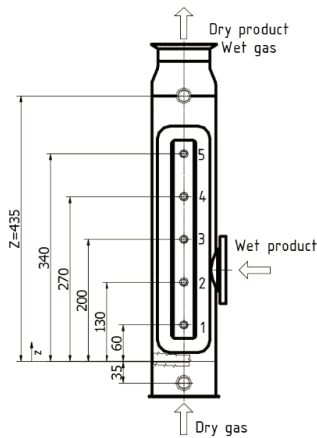


Figure 4. The sketch of the dryer represented the position of thermometers

## B. Methods

The measurements are done in batch mode. The wet materials were fed into the tube, and dried without discharging them. After the drying process the particles were carried out from the tube above maximal fluidization velocity.

Fig. 3 shows the sketch of the dryer and cyclone which represented the measuring points and the stream of airflow and materials. In the subscripts of the nominations the Arabic numerals (1,2,3) refer to the drying gas, Roman numerals (I,II,III) refer to the material. I and I mark the inlet point of drying gas and materials. At this point the initial moisture content of materials ( $X_I$ ), the mass flow ( $\dot{m}_G$ ), temperature ( $T_{G,1}$ ) and absolute humidity ( $Y_{G,1}$ ) are measured. At stage 2 the outlet temperature ( $T_{G,2}$ ) and absolute humidity ( $Y_{G,2}$ ) are recorded. At the end of drying process the final moisture content ( $X_{III}$ ) of materials is measured at point III. There are 5 thermocouples are placed vertical along the tube, being continuous contact with the fluidized bed. The temperatures measured by thermometers are equivalent with the surface temperature of materials. The position of thermometers along the dryer are shown in Fig. 4.

In case of constant drying rate period the drying rate can be expressed by the following equation:

$$N_{const} = \frac{\dot{m}_G}{A_{con}} (Y_{G,2} - Y_{G,1}) = \frac{m_s}{A_{con} t_{const}} (X_I - X_{III}) = \sigma (Y_P - Y_{G,12}), \quad (1)$$

where  $\dot{m}_G$  is the mass flow of drying gas,  $A_{con}$  represents the contact surface between the gas and particles,  $Y_P$  is the absolute humidity of gas near the surface of particles,  $Y_G$  is the absolute humidity of gas,  $m_s$  is the mass of dry material and  $t_{const}$  is the time interval of constant drying rate period,  $X$  is the moisture content of particles,  $\sigma$  is the evaporation coefficient.

The heat transfer coefficient between the surface of particles and drying gas during the constant drying rate period:

$$\alpha = \frac{N_{const} r_P}{T_{G,12} - T_{P,const}}, \quad (2)$$

where  $r_P$  is the heat of vaporization  $T_{P,const}$  is the temperature of the surface of particles during the constant drying rate period. In case of an air-water system, the Lewis-number is  $Le^z \cong 1$ , the following correlation exists between the heat transfer and the mass transfer coefficients [15]:

$$\frac{\alpha}{\sigma} = c_G Le^z, \quad (3)$$

where  $c_G$  is the specific heat of humid gas.

For further researches we would like to incorporate the latest researches in the field of heat transfer studies [16], [17]. Sánta et al. developed a new equation describing the heat transfer in the field of evaporation, which can be used to describe the mechanisms of evaporating water from the particles [18]. Using the measurement experiences of Kassai et al. [19] can help to improve our measurement technique of measuring the humidity of air.

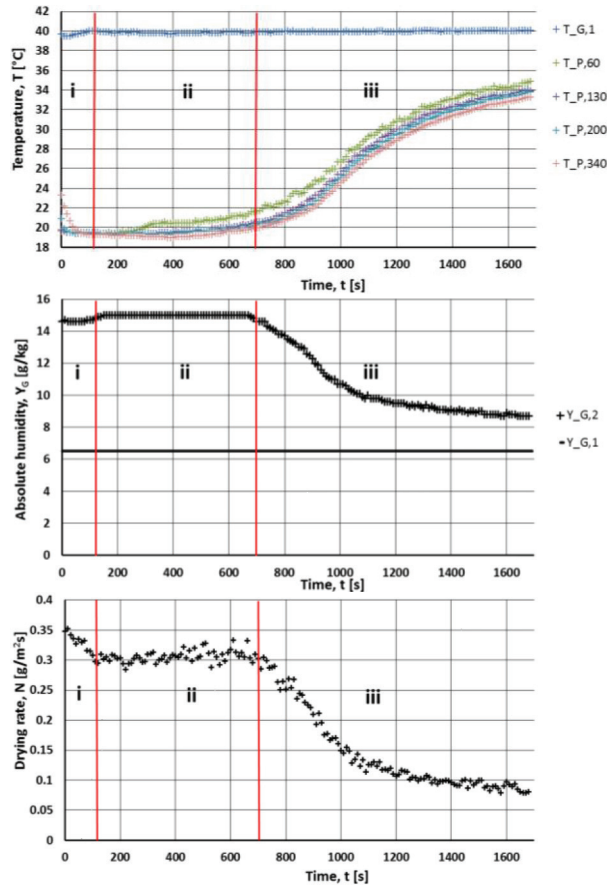


Figure 5. Drying curves (upper: temperature of drying gas and particles in function of time, middle: absolute humidity of drying gas in the function of time, lower: drying rate in the function of time)

#### IV. RESULTS

During the measurements, the temperature, absolute humidity and velocity of inlet air were constant. The temperature and moisture content of particles varies in function of the time. The drying curves of fluidized bed are shown in Fig 5.

The time interval of starting period (*i* period) is negligible compared to the total drying time. This section lasts until the surface temperature of the material will be constant. During the constant drying rate period (*ii* period) the surface humidity evaporates to the drying gas, the temperature of the material is constant, and it is equal to the wet-bulb temperature. The moisture content of particles decreases, the drying gas deemed to be saturated. During the falling drying rate period (*iii* period) dry spots can be observed on the surface of the material, and the moisture exhausts from the pores and capillaries. The moisture content of the wet particles decreases, the surface temperature increases. The humidity of drying gas begins to decrease due to the falling drying rate [20]. We performed drying measurements of barley and millet. In Table II. we summarized the results from the measurements evaluated heat transfer and evaporation coefficients.

The last column of Table II shows, that the analogy of heat- and mass transfer based on equation (3) is valid within an acceptable margin of error, therefore this measurement method is suitable to carry out further experiments.

TABLE II.  
SUMMARY OF MEASUREMENT RESULTS

Measurements	$\alpha$	$\sigma$	$\frac{\alpha}{\sigma}$
	$\left[ \frac{W}{m^2 K} \right]$	$\left[ \frac{kg}{m^2 s} \right]$	$\left[ \frac{J}{kg K} \right]$
Barley #1	53.7	$4.9 \cdot 10^{-2}$	1095.9
Barley #2	41.9	$4.2 \cdot 10^{-2}$	997.6
Barley #3	47.3	$4.4 \cdot 10^{-2}$	1075
Barley #4	36.1	$3.3 \cdot 10^{-2}$	1093.9
Barley #5	38.7	$3.7 \cdot 10^{-2}$	1042.2
Millet #1	29.2	$3.0 \cdot 10^{-2}$	973.3

#### V. CONCLUSION

Measurement technique was developed to observe the drying characteristics and typical drying periods of fluidized bed drying in batch mode. The evaluation method makes possible to calculate the heat transfer- and evaporation coefficient from measured values. The aim of our further investigation will be to create widely applicable  $Nu=f(Re)$  correlation.

#### ACKNOWLEDGMENT

Special thanks for Mária Örvös PhD for her helps in this study, and for "Richter Gedeon Talentum Foundation (H-1103 Budapest, Gyömrői str. 19-21, Hungary)" for financial supporting this research.

#### REFERENCES

- [1] S. Syahrul, F. Hamdullahpur, I. Dincer, *Exergy analysis of fluidized bed drying of moist particles*, Exergy, an International Journal, vol. 2. n. 2. pp. 87-98, 2002.
- [2] D. Kunii and O. Levenspiel, *Fluidization Engineering*, 2nd edition, Butterworth-Heinemann, New York, (1991).
- [3] C. Srinivasakannan, A.A. Shoibi, N. Balasubramanian, *Combined resistance bubbling bed model for drying of solids in fluidized beds*, Heat and Mass Transfer, Vol. 48. n. 4. pp. 621-625, 2012.
- [4] J. F. Davidson, D. Harrison, *Fluidized Particles*, New York: Cambridge University Press, 1963.
- [5] Diffusion and Reaction in Porous Catalysts, 10.02.2015. <http://www.umich.edu/~elements/12chap/html/12prof2a.htm>
- [6] H. G. Wang, T. Dyakowski, P. Senior, R. S. Raghavan, W. Q. Yang, *Modelling of batch fluidised bed drying of pharmaceutical granules*, Chemical Engineering Science, Vol. 62. n. 5. pp. 1524-1535, 2007.
- [7] J. Khorshidi, H. Davari, F. Dehbozorgi, *Model Making for Heat Transfer in a Fluidized Bed Dryer*, Journal of Basic and Applied Scientific Research, 1(10), pp. 1732-1738, 2011.
- [8] A. C. Rizzi Jr., M. L. Passos, J. T. Freire, *Modeling and simulating the drying of grass seeds (Brachiaria brizantha) in fluidized beds: evaluation of heat transfer coefficients*, Brazilian Journal of Chemical Engineering, Vol. 26. n. 3. pp. 545-554, 2009.
- [9] W. C. Yang, *Handbook of fluidization and fluid-particle systems*, Siemens Westinghouse Power Corporation, Pittsburgh, Pennsylvania, USA, 2003.
- [10] O. Molerus, *Heat transfer in gas fluidized beds Part I.*, Powder Technology, Vol. 70. pp. 1-14, 1992.
- [11] P. Roy, M. Vashishtha, R. Khanna, D. Subbarao, *Heat and mass transfer study in fluidized bed granulation—Prediction of entry length*, Particology, Vol. 7. n. 3. pp. 215-219, 2009.
- [12] R. Kumaresan, T. Viruthagiri, *Simultaneous heat and mass transfer studies in drying ammonium chloride in a batch-fluidized bed dryer*, Indian Journal of Chemical Technology, Vol. 13. n. 5. pp. 440-447, 2006.

- [13] P. Alvarez, C. Shene, *Experimental study of the heat and mass transfer during drying in a fluidized bed dryer*, Drying Technology, Vol. 14. n. 3-4, pp. 701-718, 1996.
- [14] W. Ciesielczyk, M. Mrowiec, *The method of decreasing the number of experiments needed to design a fluidized bed drying*, Inz. Chem. I Proc. Vol. 4. n. 12. pp. 551-567.
- [15] R. E. Treybal, *Mass-transfer operations* (3rd edition, McGraw-Hill Company, New York, 1981)
- [16] J. Nyers, Z. Pek, *Mathematical Model of Heat Pumps' Coaxial Evaporator with Distributed Parameters*, International J. Acta Polytechnica Hungarica, Vol.11. n.10. pp.41-57, 2014.
- [17] J. Nyers, S. Tomic, A. Nyers, *Economic Optimum of Thermal Insulating Layer for External Wall of Brick*, International J. Acta Polytechnica Hungarica. Vol. 11. n. 7. pp. 209-222, 2014.
- [18] R. Sánta, L. Garbai. *Measurement testing of heat transfer coefficient in the evaporator and condenser heat pumps*, Journal of Thermal Analysis and Calorimetry, Vol. 119. n. 3. pp. 2099-2106, 2015.
- [19] M. Kassai, C.J. Simonson, *Dehumidification performance investigation of run-around membrane energy exchanger system*, Thermal Science, OnLine-First (00):129-129 Details Full text (399 KB) DOI:10.2298/TSCI140816129K, Accepted article (2014).
- [20] S. Szentgyörgyi, K. Molnár, M. Parti, *Transzportfolyamatok*, Tankönyvkiadó, Budapest, 1986.

# The status and history of the Hungarian district heating

László Garbai Dr.\*, Gergely Pacza

\*Budapest University of Technology and Economics, Hungary

garbai.laszlo@gmail.com

paczagergely@gmail.com

**Abstract** – This paper demonstrates the development in the past and the status in the present of district heating services. Furthermore the article presents the change in consumers and in consumption, and the reasons of reduction.

In Hungary the district heating services have a long history, as it is a sign sector of the energetic. In Hungary the industrial district heating services began in the early 1950s. The residential district heating services started in 1960s with the national social housing program. Between the 1960s and 1990s economic requirements of district heating services were not formulated. In the socialism it operated as a flat-rate service and furthermore it had high levels of national support. Within the framework of the above mentioned housing program till 1990 890 thousand flats were built, overwhelming part of it prepared with industrialized technology. [1][2]

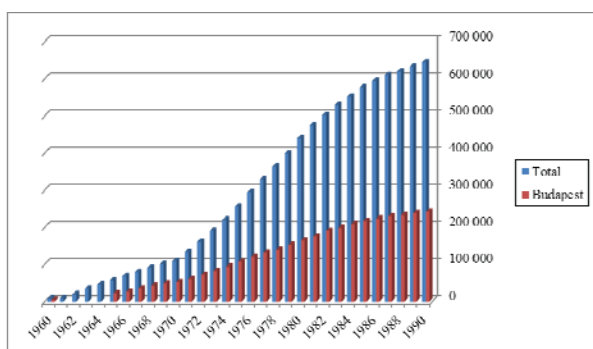


Figure 1. Alteration of number for district heated flats between 1960 and 1990

After the change of regime the assets of state ownership got to the council property, based on the 1991. XXXIII. law, in pursuance of it the district heating systems got to the council property, too. Therefore the normative support of the recipient costumers ceased and the structure of the service and circumstances of the operation were changed radically. Thereby the district heating service set foot into the competitive market of the utility service.

Only a little part of the councils could achieved that heat energy providing power plant for the newly come into existence district heating service come into council's own. The price of purchased heat energy, and price of primary energy source were increased substantially, furthermore the operating costs were raised, too. In pursuance of the above mentioned reasons the charge of the district heating service was increased too.

In the Hungarian district heating the next huge change was brought by the 1998 year, when standardized legislative environment and legislation came into effect with creating the 1998 XVIII law. Actually, the legal framework of the district heating contains the 2005 XVIII law.

After the change of regime between energy policy guidelines came into view again the increase of the combined heat and power production. The latter's image was specified by the presence and explosive growth of gas engine plants at the end of the 1990s and at the beginning of the 2000s. But nowadays combined cycle power plants represent a significant capacity, primarily in each bigger system of Budapest and for example in Miskolc, Debrecen and Nyíregyháza. Unfortunately the major scale ideas for improvements of combined heat and power production took place later. Actually the benefits of it appear in degree of financial integration in the European market management processes in the absence of national electricity companies and investment companies. Exception is Miskolc, where trading profit of combined heat and power produce can be enjoyed by MIHŐ, furthermore the gas engine plants, which were realized by the provider's own investments, such as Győr, Kecskemét and Salgótarján. [1][2]

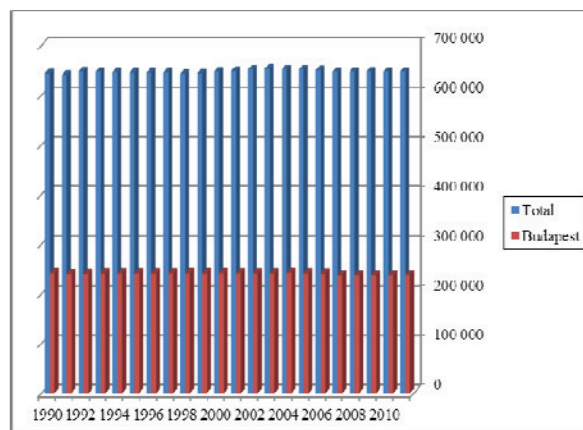


Figure 2. Changes of district heating-used apartment's number between 1990 and 2011

At the beginning of the 1990s the effect of the outage for the housing program the number of retail costumers related district heating was increased slightly; consumer apartment number of 2013 compared to the values of 1990 grew less than 0.6 percent. Figure 2 presents the changes of district heating used apartment's number between 1990 and 2011.



In Hungary opposite the residential district heating the industrial district heating had the heyday in the middle of the 1980s, next from 2000s decreased below the value of the end of the 1960s. Figure 3 shows the industrial and the total district heating usage.

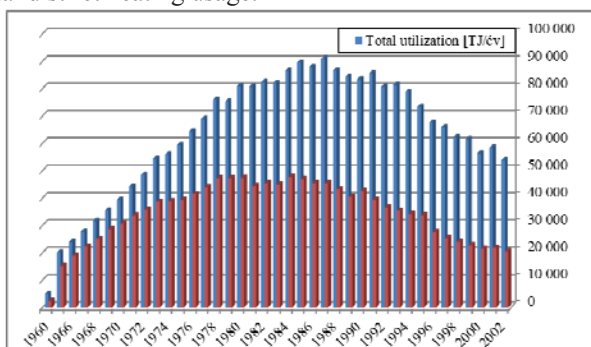


Figure 3. Utilization of district heating

The residential district heating consumption reached the peak point at the beginning of the 1990s. In 1991 the utilized heat in district heating was 85.7 PJ. From it 46 PJ was communal value. In 2009 the heat demand of industrial and residential consumers was 40.4 PJ. It means 50 % reduction. The district heating service's share of the annual national primary energy consumption decreased by 50 % in 2009 compared to 1990s.

This drastic reduction has a number of reasons.

- Stereotypes
- Energy prices rise
- Energy awareness
- Developments

The biggest problem is people forecast a high cost of service, because the unregulated systems which was used in the old times. After the change of regime and the spread of energy-aware lifestyle people appreciate less the disposing of the heat out of the window in mild winter days. The above mentioned stereotype lives still in the majority of the consumers, which is correct only in the non-modernized buildings. Due to this influential factor the district heating service neglected in cases of building of new apartment houses. Although the new built systems are made with appropriate expectations of today's technical content. It contains adjustable and energy saving solutions.

In parallel with the growth of energy prices the energy awareness gained ground in the range of consumers. The cause of it is the increase of the energy prices. Users try to decrease their energy consumption with different solutions. These two factors implicated in the reduction of district heating' consumption.

Connection with the district heating service several development model could be separated:

- Service improvements
- Panel program
- European Union aid applications

The services develop their systems continuously using state and European Union supports. The vast majority of the thermal centre is in the service own. The services modified the formerly used constant mass flow thermal

centre to variable mass flow, furthermore the replacement of old lines is prepared continuously with the best use of sources. These developments repair the controllability and decrease the pressure- and heat losses in the pipelines.



Figure 4. After renovation statement of institution (in KEOP-5.4.0/12 construction framework)

The “support of modernization for industrialized technology built residential buildings which result energy savings” application system has become known as the Block program begins in 2001. Initially, replacement of external fenestrations, insulation of frontage and roof was supported, which later supplemented with modernization of engineering systems. The program later went on other names. In the framework of the development till 2007 approximately 190 000 flats were modernized. The energy consumption of these flats could not be specified uniformly because the different technical content. The savings approximately 8-50 % compared to the consumption data of the previous year. Compared development concepts the monitored consumption data are weaker than the expected. It due to for the consumption habits, too.



Figure 5. Renovated building in the framework of Bloc program

Currently can be competed for energy efficient renovation of 4-60 flats of apartment buildings in „Support of modernization for apartment house which result energy savings” project of „Warm of the Home” called program. Only a part of these buildings use district heating. In the immediate future probably a project of the “Warm of the Home” program will be appeared, in which

the more flats and district heating used, industrialized technology built apartment buildings can compete.

Several of the realized tender construction supported by the European Union aided full or partial energy efficient improvements. Technical content of the modernization within the framework of the projects the following elements could be realized:

- Insulation of the external frontage
- Insulation of flat roof or attic floor
- Replacement or renovation of external fenestrations
- Heating system converted into regulable
- Modernization of thermal center or boiler house
- Modernization of lighting
- Renewable energy usage

In the bigger part of the published and mostly carried out projects the following criterion is included: "Detachment from the district heating system is not eligible in this construction, the gas medium district heating is except". Moreover in the tenders which striving for energy efficiency "Preparing the conditions of accession to the district heating system" appears as supported project type. These criterions can be found in the „Warm of the Home” project.

Institutions or owner, conservator of it can be applied for the bigger part of the tenders. Consequently educational institutions, hospitals, offices and other public institutions received from these financial resources of the tenders.



Figure 6. Before renovation statement of institution (in KEOP-5.5.0/B construction framework)



Figure 7. After renovation statement of institution (in KEOP-5.5.0/B construction framework)

Technical content of the development is diversified, however it can be determined that, after the implementation the heat energy of these institutions decreased drastically. In case of each institution the forecasted heat energy savings are 40 % compared to the heat energy consumption data from the previous year. This is due to both the controllability of the heating system, both the replacement of the fenestrations and both the covering of complete volume with insulation.

These developments protect the district heating service with the competition criteria and help the market penetration, but similarly to the previous mentioned the consumption of heating energy is decreased.

The modernization of the district heating of residential districts and reduction of consumer charges can be fitted to the implementation of Hungarian national energy policy objectives, which is the following:

- Improvement efficiency of the production and transportation,
- Improvement of the composition of energy sources,
- Increase the proportion of renewable energy sources,
- increase the energy use of waste,
- Reduction of consumption, increase of sparing, modernization of consumer systems, forming the application of measurement and controlling fully comprehensive.

The loss of transportation is significant. In the heating season is 10-13 %, in the summer DHW service is 20-30 %. The consumer sparing, the posterior insulation worsen the efficiency of transportation. With the panel program expands, because the heating demand due to the permanent loss the specific transportation loss can reach 20 % in the heating season. [1][2]

The specific costs of the service grow proportionately reducing consumption.

In the unit price of the provided heat the standard rate is approximately 40-50 % and the charge of heat is 50-60 %. The district heating is not competitive with neither the individual gas supply nor the individual gas-based central heating, because the district heating is more expensive than these approximately with 20-30 %. The VAT reduction helps on it, the well-functioning district heating services became nearly competitive. [1][2]

The district heating systems give place and opportunity the most modern, the most effective and the fastest way of electricity production, which is the combined heat and power production, inside of it energy production with combined cycle furthermore gas engine. The materialized district heating is valuable component of energetic and environmental protection. In addition, it is an important device of the future energy policy, the local urban policy and the environmental policy. Actually and maybe in the future the district heating service – if it based on the combined energy plants- is the most effective energetic way, and the most beneficial environmental protection way, and it cannot be replaced with other heat supply method in national economy way. It is effective energetically, because the heat which generated from the

production of combined electricity is utilized in the district heating systems. Nowadays, the co-generation reached 18 % of the total national electricity production, and more than 80 % of it is realized on base district heating. The expansion and development of the co-generation cannot be achieved without the heat of utilized in district heating systems. The environmental protection's significance of district heating supply is beyond dispute, because the pollution is less than all other supply mode, better the opportunity of pollutant deposition and the less emission get to atmosphere, furthermore scattered away from inhabited areas. The most important function of the district heating based combined heat and power production is in reduction of greenhouse gas emissions. In the short and in the medium term the district heating exceeds each other devices and methods (utilization of renewable energy sources, insulation of building, efficiency repairing of consumer side) as regards both the available reduction and economic efficiency. The district heating systems ensure the flexibility of energy source structure, the opportunity of utilization of alternative energy sources and the opportunity of change of energy sources, furthermore the large-scale utilization of renewable energy sources. Only the district heating services and this heat production technology can ensure combustion of household municipal waste and biomass, furthermore the large-scale utilization of renewable energy sources and thermal water. The consumer group and the status of district heating is "historical category", in case of panel buildings the district heating has not alternative, the replacement of it technically is unrealistic. Not only in economic level but in the light of environmental requirements the replacement of the district heating system is anti-common sense. In urban environment the gratification of new consumer's heat demand is not direct economic issue but solely district heating supply based on the combined heat and power production or utilization of renewable energy sources, in line with international obligations. [3]

The large scale secession from the district heating systems would lead to the collapse of the district heating service and heat generating systems. As a result of it the power supply of the country would be disastrous situation.

As we mentioned, nowadays the 18-20 % of electricity production of the country is combined with heat supply. The residential gas consumption of the country would not be reduced, the emission of CO<sub>2</sub> and the seasonality of gas consumption would be increased, and the cost of winter needs would be increased, too. In possible degradation of the district heating gas service companies have not got economically interest, because they don't achieve a substantial economic advantage, if the gas service companies gratify the develops into individual gas users instead of district heating's thermal source.

Furthermore because of the reduction of combined power generation the gas consumption can be reduced (if the electricity is prepared in an other place or is not prepared from natural gas). The cable systems of the district heating services form a natural monopoly. Real market and competition cannot be achieved. In the heat production limited-scale competition can be formed, only with two or three members. However the service not only natural, but also entered into a legal monopoly license. [3]

From 2011 the support of electricity selling of the combined heat and power is ceased. Their situation is bad, because the produced power have to be cheaper compared to the charge of before 2011, but the price of gas which used for power generation is expensive. In 2013 in Hungary, as the coal was cheaper, operated a coal power plant was more profitable than a combined heat and power plant. [3]

## CONCLUSIONS

Recently, a new type of the district heating service is started its development, which is based on renewable energy sources. The feasibility studies and design documentation of systems which based on renewable energy sources are in progress in several cities. The district heating service is a very important part of the Hungarian energetic. It is significant in aspect of environmental and image of towns, so it is important to get more state support and reach the rightful place at consumers. Between 2014 and 2020 several development can be waited both of service and consumer sight, too.

## REFERENCES

- [1] Dr. Garbai L.: District heating in Hungary I. (in hungarian), Hungarian Energy, Issue 17, Volume 2, 2010, pp. 22-25
- [2] Dr. Garbai L.: District heating in Hungary II. (in hungarian), Hungarian Energy, Issue 17, Volume 3, 2010, pp. 22-25
- [3] Dr. Garbai L.: The action plan of sustainment and development for the Hungarian district heating services (in hungarian), Hungarian Energy, Issue 19, Volume 6, 2012, pp. 35-37
- [4] Garbai, L.: District heating (in hungarian), 2012. ISBN: 978-963-279-739-7
- [5] National Energy Strategy 2030, Ministry of National Development, 2012
- [6] Database of Hungarian Central Statistic Office, <http://www.ksh.hu/>
- [7] Association of Hungarian District Heating Enterprises, <http://www.mataszsz.hu/>
- [8] Széchenyi 2020, <http://palyazat.gov.hu/>
- [9] „Warm of the Home” project , <http://www.kormany.hu/download/d/a6/30000/P%C3%A1ly%C3%A1zati%20Felt%C3%A9telrendszer.pdf>
- [10] Environment and Energy Operational Programme, <http://palyazat.gov.hu/doc/359>
- [11] District Heating Enterprise of Debrecen., <http://www.dhrt.hu/>



# Approach to the Concurrent Programming in the Microsystems

Anita Sabo\*, Bojan Kuljić\*\*, Tibor Szakáll\*\*\*, Andor Sagi\*\*\*\*

Subotica Tech, Subotica, Serbia

\* saboanita@gmail.com \*\* bojan.kuljic@gmail.com \*\*\* szakall.tibor@gmail.com \*\*\*\* peva@vts.su.ac.rs

**Abstract** — Today processors with multiple cores are commonplace, not only in the personal computers and the servers, but also in the embedded systems. On the other hand, implementation of the algorithms for parallel instruction execution is a very complex task. The methods of concurrent programming are very complicated and unfortunately their performance depends on the system parameters so the vast majority of the applications on the market are still developed using the classical sequential programming. In the case of the embedded systems concurrent programming is even less available. This means that the problem of easy concurrency is an important problem for embedded systems as well. There are numerous solutions for the problem of concurrency, but not with embedded systems in mind. Due to the constraints of embedded hardware and use cases of embedded systems, specific concurrency solutions are required. In this paper we present a solution which is targeted for embedded systems and builds on existing concurrency algorithms and solutions. The presented method emphasizes on the development and design of concurrent software.

*Keywords* – concurrent programming, embedded systems, parallel algorithms

## I. INTRODUCTION

Concurrent computing is the concurrent (simultaneous) execution of multiple interacting computational tasks. These tasks may be implemented as separate programs, or as a set of processes or threads created by a single program. The tasks may also be executing on a single processor, several processors in close proximity, or distributed across a network. Concurrent computing is related to parallel computing, but focuses more on the interactions between tasks. Correct sequencing of the interactions or communications between different tasks, and the coordination of access to resources that are shared between tasks, are key concerns during the design of concurrent computing systems. In some concurrent computing systems communication between the concurrent components is hidden from the programmer, while in others it must be handled explicitly. Explicit communication can be divided into two classes:

### A. Shared memory communication

Concurrent components communicate by altering the contents of shared memory location. This style of concurrent programming usually requires the application of some form of locking (e.g., mutexes (meaning(s) mutual exclusion), semaphores, or monitors) to coordinate between threads. Shared memory communication can be achieved with the use of Software Transactional Memory (STM) [1][2][3]. Software Transactional Memory (STM) is an abstraction for concurrent communication mechanism analogous to database transactions for controlling access to shared memory. The main benefits of STM are composability and modularity. That is, by using STM one can write concurrent abstractions that can be easily composed with any other abstraction built using STM, without exposing the details of how the abstraction ensures safety.

### B. Message Passing Communication

Concurrent components communicate by exchanging messages. The exchange of messages may be carried out asynchronously (sometimes referred to as "send and pray"), or one may use a rendezvous style in which the sender blocks until the message is received. Message-passing concurrency tends to be far easier to reason about than shared-memory concurrency, and is typically considered a more robust, although slower, form of concurrent programming. The most basic feature of concurrent programming is illustrated in Figure 1. The numbered nodes present instructions that need to be performed and as seen in the figure certain nodes must be executed simultaneously. Since most of the time intermediate results from the node operations are part of the same calculus this presents great challenge for practical systems. A wide variety of mathematical theories for understanding and analyzing message-passing systems are available, including the Actor model [4]. In computer science, the Actor model is a mathematical model of concurrent computation that treats "actors" as the universal primitives of concurrent digital computation: in response to a message that it receives, an actor can make local decisions, create more actors, send more messages,



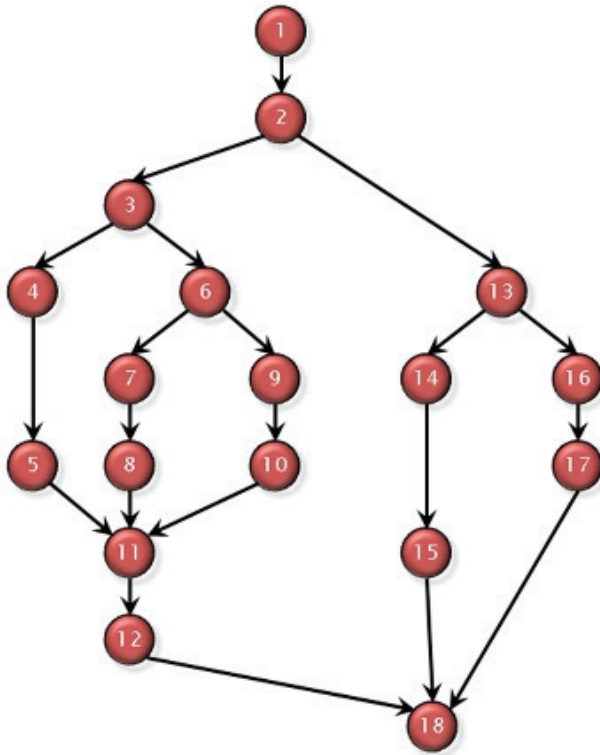


Figure 1. The data flow of a software

and determine how to respond to the next message received. Figure 1 demonstrates the most basic but essential problem in the concurrent programming. Each number represents one process or one operation to be performed. The main goal is not to find the resource for parallel computing but to find the way to pass intermediate results between the numbered nodes.

### C. Advantages

Increased application throughput - the number of tasks done in certain time period will increase. High responsiveness for input/output - input/output intensive applications mostly wait for input or output operations to complete. Concurrent programming allows the time that would be spent waiting to be used for another task. It can be stated that there are more appropriate program structures - some problems and problem domains are well-suited to representation as concurrent tasks or processes.

## II. COMMUNICATION

In case of distributed systems the performance of parallelization largely depends on the performance of the communication between the peers of the system. Two peers communicate by sending data to each other, therefore the performance of the peers depends on the processing of the data sent and received. The communication data contains the application data as well as the transfer layer data. It is important for the transfer layer to operate with small overhead and provide fast processing. Embedded systems have specific requirements. It is important that the communication meets these requirements.

The design of the presented method is focused around the possibility to support and execute high level optimizations and abstractions on the whole program. The graph-based software layout of the method provides the

possibility to execute graph algorithms on the software architecture itself. The graph algorithms operate on the software's logical graph not the execution graph. This provides the possibility for higher level optimizations (super optimization). The architecture is designed to be easily modelable with a domain specific language. This domain specific language eases the development of the software, but its primary purpose is to provide information for higher level optimizations. It can be viewed as the logical description, documentation of the software. Based on the description language it is possible to generate the low level execution of the software, this means that it is not necessary to work at a low level during the development of the software. The development is concentrated around the logic of the application. It focuses on what is to be achieved instead of the small steps that need to be taken in order to get there.

## III. REALIZATION IN EMBEDDED SYSTEMS

The architecture of modern embedded systems is based on multi-core or multi-processor setups. This makes concurrent computing an important problem in the case of these systems, as well. The existing algorithms and solutions for concurrency were not designed for embedded systems with resource constraints. In the case of real-time embedded systems it is necessary to meet time and resource constraints. It is important to create algorithms which prioritize these requirements. Also, it is vital to take human factor into consideration and simplify the development of concurrent applications as much as possible and help the transition from the sequential world to the parallel world. It is also important to have the possibility to trace and verify the created concurrent applications. The traditional methods used for parallel programming are not suitable for embedded systems because of the possibility of dead-locks. Dead-locks pose a serious problem for embedded systems [5], because they can cause huge losses. The methods presented in [6] (Actor model and STM), which do not have dead-locks, have increased memory and processing requirements, this also means that achieving real-time execution becomes harder due to the use of garbage collection. Using these methods and taking into account the requirements of embedded systems one can create a method which is easier to use than low-level threading and the resource requirements are negligible. In the development of concurrent software the primary affecting factor is not the method used for parallelization, but the possibility to parallelize the algorithms and the software itself. To create an efficient method for parallel programming, it is important to ease the process of parallelizing software and algorithms. To achieve this, the used method must force the user to a correct, concurrent approach of developing software. This has its drawbacks as well, since the user has to follow the rules set by the method. The presented method has a steep learning curve, due to its requirements toward its usage (software architecture, algorithm implementations, data structures, resource management). On the other hand, these strict rules provide advantages to the users as well, both in correctness of the application and the speed of development. The created applications can be checked by verification algorithms and the integration of parts, created by other users is provided by the method itself. The requirements of the method provide a solid base for the users. In the case of sequential

applications the development, optimization and management is easier than in the case of concurrent applications. Imperative applications when executed have a state. This state can be viewed as the context of the application. The results produced by imperative applications are context-dependent. Imperative applications can produce different results for the same input because of different contexts. Sequential applications execute one action at a given moment with a given context. In the case of concurrent applications, at a given moment, one or more actions are executed with in one or more contexts, where the contexts may affect each other. Concurrent applications can be decomposed into sequential applications which communicate with each other through their input, but their contexts are independent. This is the simplest and cleanest form of concurrent programming.

#### IV. MAIN PROBLEMS

Embedded systems are designed to execute specific tasks in a specific field. The tasks can range from processing to peripheral control. In the case of peripheral control, concurrent execution is not as important, in most cases the use of event-driven asynchronous execution or collective IO is a better solution [7]. In the case of data- and signal processing systems the parallelization of processing tasks and algorithms is important. It provides a significant advantage in scaling and increasing processing capabilities of the system. The importance of peripheral and resource management is present in data processing systems as well. The processing of the data and peripheral management needs to be synchronized. If we fail to synchronize the data acquisition with data processing the processing will be blocked until the necessary data are acquired, this means that the available resources are not being used effectively. The idea of the presented method is to separate the execution, data management and resource handling parts of the application. The presented method emphasizes on data processing and is made up of separate modules. Every module has a specific task and can only communicate with one other module. These modules are peripheral/resource management module, data management module and the execution module. The execution module is a light weight thread, it does not have its own stack or heap. This is a requirement due to the resource constraints of embedded systems. If required, the stack or heap can be added into the components of the execution thread with to the possibility of extending the components of the execution thread with user-defined data structures. The main advantage of light weight threads is that they have small resource requirements and fast task switching capabilities [8][9]. The execution module interacts with the data manager module which converts raw data to a specific data type and provides input for the execution module. The connection between the data manager and the execution module is based on the Actor model [10] which can be optimally implemented in this case, due to the restrictions put on the execution module which can only read and create new data (types) and cannot modify it. The execution module can be monolithic or modular. The modular composition is required for complex threads where processing is coupled with actions (IO). The execution threads can be built up from two kinds of components, processing and execution/action components. The component used in the execution

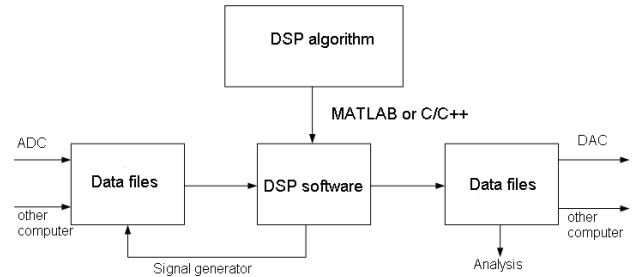


Figure 2. The software development process

module is a type which for a given input type 'a' creates a given type 'b'. This operation will always give the same result for the same input.

The processing component is referentially transparent, meaning it does not support destructive actions [11]. The type variables 'a' and 'b' can have the same types. The action component is similar to the processing component, it is usable in case where one needs to support destructive actions. These components request the execution of specific actions which are received and executed by a transactional unit. The design of the transactional mechanism is based on transactions, just as in software transactional memory. The threads in the execution module are not connected to each other. It is possible to achieve interaction between the threads. One or more execution threads can be joined with the use of the reduce component. The reduce component iterates through the values of the given threads, merging them into one component or value. The merging algorithm is specified by the user, as well as the order of the merging. The joining of the threads follows the MapReduce model, where the map functions correspond to the threads and the reduce function corresponds to the merging algorithm provided by the user [12]. The method introduced in this paper is usable for concurrent programming in real-time embedded systems as well. The complexities of the algorithms used in the method are linear in the worst case. The priority of threads can be specified, this means that the order of execution can be predetermined. It is possible to calculate the amount of time required to execute a specific action. This way the created systems can be deterministic.

Threads can be separated into two parts. The two parts create a client server architecture, where the server is the data manager and the client is the actions/steps of the thread. The job of the server (producer) is to provide the client (consumer) with data. The server part sends the data to the client part. The server part protects the system from possible collisions due to concurrent access or request to resources. The client part has a simple design it is made up of processing steps and actions.

The job of the asynchronous resource manager is to provide safe access to resources for the server part of the threads. The resource manager does not check the integrity of data, its only job is to provide the execution threads server part with raw data. Parallelization of software is not trivial in most cases. The method presented in the paper takes this fact into consideration. It is important that the parallelizable and sequential parts of the software can be easily synchronizable. The presented view of software (as seen in Figure 2) is easily implementable into the model of the presented method. Based on the data

flow of the software, it is possible to implement it into the model of the presented method for concurrency.

## V. USED HARDWARE PLATFORM (DSK5510)

Modern hardware and software products must meet strict criteria dictated by the current standards. However, the development of the complex systems is very difficult using current means and methods. Development of algorithms is hindered by the fact that it is very difficult to develop them on a real-time hardware system, and so most algorithms get developed only in simulations. The simulations do not contain the characteristic boundaries of the real system. This often leads to repeated changes in the algorithms when the simulation environment is not faithful

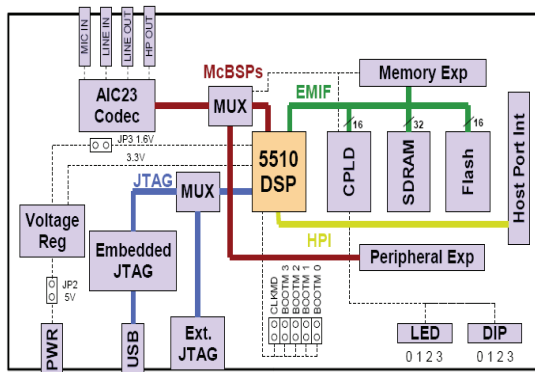


Figure 3. The block diagram of DSK development environment - DSK5510

enough to the real hardware system.

DSK (DSP Starter Kit) is the primary development environment for the DSP processors. This is a fully rounded solution for testing the software and hardware development. This board was used for the realization of the topics described in this paper. Figure 3 shows the block diagram of DSK development environment. This development board has the following characteristics:

- TI 5510 DSP processor, which runs at 200 MHz
- AIC23 stereo audio codec
- 8 MB DRAM memory
- 512 KB of flash memory
- 4 LEDs and DIP switches that can be used to manage and control processes
- Configuration settings panel can be modified by writing special software for CPLD chip that controls the board settings

Figure 4 shows the physical layout of DSK development board. DSK (DSP Starter Kit) is a complete development tool that allows the developers to become familiar with the processor and the programming process and in addition can serve as a good basis for writing and testing the concurrent algorithms. Together with the development board comes the software environment (Code Composer Studio), but the version of the program

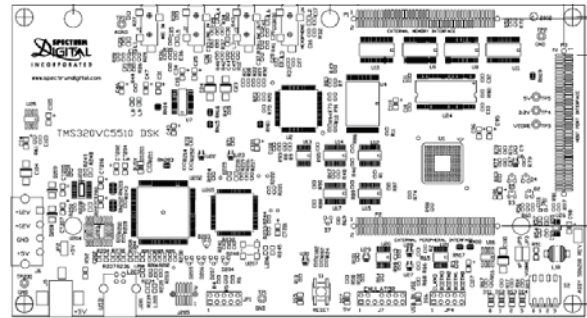


Figure 4. The physical layout of DSK development board - DSK5510

that is supplied only works with DSK boards and will not work with custom designed boards.

## VI. CONCLUSION

Concurrent programming is complex and hard to achieve. In most cases the parallelization of software is not a straightforward and easy task. The realized concurrent programs usually have safety and performance issues. For embedded systems the existing parallelization algorithms and solutions are not optimal due to resource requirements and safety issues. The goal is to realize such a solution for concurrent programming, which is optimal for embedded systems and helps and simplifies the development of concurrent programs. The key to successful development of parallel programs is in the realization of tools which take into consideration the human factors and aspects of parallel development.

The model presented in this paper builds on the advantages of existing parallelization algorithms with human factor as its primary deciding factor. In the development of a concurrent applications, the used parallelization algorithms and solutions are important, but the most important factor is the developer/user itself. To achieve the best possible results, to achieve efficient software, we must concentrate on the most important factor of development, the human (developer).

The presented parallelization model is best applicable if the problem we would like to solve is not trivially parallelizable, which is true for the great number of algorithms and software.

## REFERENCES

- [1] Tim Harris, Simon Marlow, Simon Peyton Jones, Maurice Herlihy, "Composable memory transactions," Proceedings of the tenth ACM SIGPLAN symposium on Principles and practice of parallel programming, pp. 48–60, 2005.
- [2] Anthony Discolo, Tim Harris, Simon Marlow, Simon Peyton Jones, Satnam Singh, "Lock -Free Data Structures using STMs in Haskell," Functional and Logic Programming, pp. 65–80, 2006.
- [3] Tim Harris and Simon Peyton Jones, "Transactional memory with data invariants," ACM SIGPLAN Workshop on Transactional Computing, 2006.
- [4] Paul Baran, "On Distributed Communications Networks," IEEE Transactions on Communications Systems, vol. 12, issue 1., pp 1-9, 1964.
- [5] César Sanchez, "Deadlock Avoidance for Distributed Real-Time and Embedded", Dissertation, Department of Computer Science of Stanford University, 2007 May.

- [6] Y. Yorozu, M. Hirano, K. Oka, and Y. Tagawa, "MTIO. A multithreaded parallel I/O system," Parallel Processing Symposium, Proceedings, 11th International, pp. 368-373, 1997.
- [7] Girija J. Narlikar, Guy E. Blelloch, "Space-efficient scheduling of nested parallelism," ACM Transactions on Programming Languages and Systems, pp. 138-173, 1999.
- [8] Girija J. Narlikar, Guy E. Blelloch, "Space-efficient implementation of nested parallelism," Proceedings of the Sixth ACM SIGPLAN Symposium on Principles and Practice of Parallel Programming, 1997.
- [9] Bondavalli, A.; Simoncini, L., "Functional paradigm for designing dependable large-scale parallel computing systems," Autonomous Decentralized Systems, 1993. Proceedings. ISADS 93, International Symposium on Volume, Issue, 1993, pp. 108 – 114.
- [10] Jeffrey Dean and Sanjay Ghemawat, "MapReduce: Simplified Data Processing on Large Clusters," OSDI'04: Sixth Symposium on Operating System Design and Implementation, 2004.
- [11] Gene Amdahl, "Validity of the Single Processor Approach to Achieving Large-Scale Computing Capabilities," AFIPS Conference Proceedings, (30), pp. 483-485, 1967.
- [12] Rodgers, David P., "Improvements in multiprocessor system design," ACM SIGARCH Computer Architecture News archive Volume 13, Issue 3, pp. 225-231, 1985



# Energy sources for heating/cooling and low-exergy systems

**Dušan Petráš**

Department of Building Services, Faculty of Civil Engineering,  
Slovak University of Technology in Bratislava, Slovakia  
Radlinského 11, 813 68 Bratislava, Slovak Republic  
e-mail: [dusan.petras@stuba.sk](mailto:dusan.petras@stuba.sk)

**Abstract** — Low-exergy systems, e.g. low-temperature heating and high temperature cooling, are beneficial regarding distribution losses and efficiency of boilers, especially modern condensing boilers, and also heat pumps or solar collectors. The paper is focused on energy sources for heating/cooling used as low exergy systems.

## I. INTRODUCTION

The main purpose of increased insulation of the building envelope is to reduce the annually energy usage. In addition, the supply, distribution, and emission of the heating/cooling systems must be optimized. The differences in heat losses/gains by heat/cool emission of different types of systems (radiators, convectors, warm air, floor and ceiling heating) are small in well-insulated houses.

## I. ENERGY SOURCES

### *A/ Energy source for heating*

Available sources for low temperature heating (Babiak, Olesen, Petráš, 2007):

- boiler
- low temperature boiler
- condensing boiler
- geothermal energy / ground coupling
- ground water during a direct ground heat exchanger
- lake water
- waste heat
- heat pumps
- solar energy / solar collectors with absorption heat pump

### *B/ Energy source for cooling*

The floor, ceiling and wall system as a high-temperature cooling system enables a higher efficiency for a reversible heat pump or chiller. As the ground temperature is often around 10°C, it also is possible to cool a radiant surface directly from a ground heat exchanger (pipes embedded in the ground or foundation) without the use of a heat pump.

A radiant surface cooling system can be used in combination with an air system. The radiant surface system takes care of most of the sensible load, while the air system takes care of the latent load. At the same time, the dew point in the space will be lowered resulting in a higher cooling capacity for the radiant surface system. Also, the high return water temperature (18°C to 20°C) of the system increases the efficiency of a chiller or heat pump.

Available sources for high temperature cooling (Babiak, Olesen, Petráš, 2007):

- reversible heat pump
- ground coupling
- ambient air / free cooling
- refrigerant machine

### *C/ Heat pumps*

Heat pumps transfer the heat from one place to another. Heat pumps convert the renewable energy of the environment and electricity directly into heat, which can be added to or extracted from the conditioned places. In the winter, it transfers heat from outdoors to indoors in order to heat the occupied space, and in the summer, it removes heat in the opposite direction from the occupied space to the heat sink. The heat pumps principle operates by following the Carnot Cycle.

The use of a heat pump as heat source or heat sink with a integrated heating / cooling system that operates with the temperature of the heat carrier close to the room operative temperature is very efficiency.

The heat pump will perform with a high COP (Coefficient of Performance), which express the energy efficiency of the heat pump. The COP of the heat pump for heating means the ratio of heat delivered to energy input (electricity).

General classification (heat source / sink):

Heat Pumps :

- Water-water (Ground-water)
- Air-water
- Air-air

Ground-water:

The ground system links the heat pump to the underground and allows or extraction of heat from the ground or injection of heat into the ground. These systems can be classified generally as open or closed systems:

- Open systems: Groundwater is used as the heat carrier, and is brought directly to the heat pump. Return ground water can be directly routed back into the ground or.
- Closed systems: Heat exchangers are located underground (either in a horizontal, vertical or oblique fashion), and a heat carrier medium is circulated within the heat exchangers, transporting heat from the ground to the heat pump (or vice versa).

The system cannot always be attributed exactly to one of the above categories; standing column wells, mine water or tunnel water are examples.

## II. HEATING AND COOLING SYSTEMS FOR LOW ENERGY BUILDINGS

From the above mentioned it is clear that there is a need to adapt the HVAC systems in such a way that they optimise energy consumption of the buildings, but at the same time, the systems must be able to provide healthy and comfortable indoor environment.

### A/ Radiant low temperature heating and high temperature cooling systems

Based on the technique of the heat exchange between the pipe and the emitting surface, the following systems can work either with emitting elements thermally coupled or thermally insulated from the building structure (EN 15733-1).

#### B/ Radiant ceiling suspended under the ceiling

Radiant ceiling panels suspended under the ceiling have heat carrier temperature relatively close to room temperature. Radiant ceilings can be installed by means of hangers in order to fix the pipes, which are usually made of steel or copper. The ceiling is composed by insulation, hanger, pipes, wire net and plaster. Ceiling heating and cooling panels are primarily used for large spaces such as open plan offices or storage halls (EN 15733-1).

#### C/ Embedded systems insulated from the main building structure

These systems are used in all types of buildings and work with heat carriers at relatively low temperatures for heating and high temperatures for cooling. The standard EN 15377 (2008) defines six system types insulated from the main building structure:

- System with pipes embedded in the screed or concrete (Type A).
- System with pipes embedded outside the screed (Type B).

- Systems with pipes embedded in the screed (Type C).
- Plane section systems (Type D).
- System with pipes embedded in a wooden construction (Type G).

#### D/ Systems with pipes embedded in the building structure

These systems are operated at heat carrier temperatures very close to room temperature and take advantage of the thermal storage capacity of the building structure. The main feature of this type of radiant surface system is the thermal coupling of the emitting element with the main building structure. The standard EN 15377 (2008) defines two system types with pipes embedded in the building structure:

- System with pipes embedded in the massive concrete slabs (Type E).
- Capillary pipes embedded in a layer at the inner surface (Type F).

## III. HEAT EXCHANGE COEFFICIENT BETWEEN SURFACE AND SPACE

The relationship between heat flow density and mean differential surface temperature so called Characteristic Curve depend on the type of heat emitting surface (floor, wall, ceiling) and if the temperature of the surface is lower (cooling) or higher (heating) than the space temperature. Heat exchange coefficient is the parameter that affects the amount of heat transferred between surface and the space (Babiak, Olesen, Petráš, 2007).

Floor Heating and Ceiling Cooling

$$q = 8,92 (\theta_i - \theta_{s,m})^{1,1} \quad (1)$$

For other types of situations the following equations should be used:

Wall heating and Wall cooling

$$q = 8 (\theta_i - \theta_{s,m}) \quad (2)$$

Ceiling Heating

$$q = 6 (\theta_i - \theta_{s,m}) \quad (3)$$

Floor Cooling

$$q = 7 (\theta_i - \theta_{s,m}) \quad (4)$$

The heat exchange coefficient depends on the position of the surface and the surface temperature in relation to the room temperature (heating or cooling). While the radiant heat exchange coefficient is for all cases in the temperature range 15-35 °C approximately 5,5 W/m<sup>2</sup>.K, the convective heat exchange coefficient will change and depending on type of the surface, air velocity (forced convection) and temperature difference between surface and air (natural convection).

The heating - cooling capacity depends on the heat exchange coefficient and the temperature difference between surface and space. Acceptable surface temperature is determined based on comfort considerations and the risk for condensation. For sensible cooling the ceiling has a capacity up to 100 W/m<sup>2</sup> and for heating 40 to 50 W/m<sup>2</sup>. A floor has the highest capacity for heating, up to 100 W/m<sup>2</sup>, and 40 W/m<sup>2</sup> for sensible cooling.

A special case for floor cooling is when there is direct sun radiation on the floor. In this case the sensible cooling capacity of the floor may exceed 100 W/m<sup>2</sup>. This is also why floor cooling is increasingly used in spaces with large fenestration like airports, atriums and entrance halls. The heat transfer between the embedded pipes and the surface of wall, ceiling or floor will as long as there is no airspace in the construction, follow the same physics for heat conduction. It is then possible for all three type of surfaces to use the standard for floor heating as the basis for design and calculation of the direct heating and sensible cooling capacity depending on the spacing between pipes, thickness above (below) pipes, surface material and water temperature.

#### IV. CONCLUSION

The Low-exergy systems, e.g. low-temperature heating and high temperature cooling, using the renewable energy sources for heating/cooling represent the new trends for low-energy buildings (Petráš, 2013)

#### REFERENCES

- [1] Babiak, J., Olesen, B.W. and Petráš, D. (2007) *Low temperature heating and high temperature cooling*, Rehva Guidebook No 7, Brussels, Rehva
- [2] Petráš, D. (2013) *New trends in combined HVAC-R systems*. E-NOVA Kongres. Pinkafeld 193 – 198 pp
- [3] EN 15251(2007) *Indoor environmental input parameters for design and assessment of energy performance of buildings addressing indoor air quality, thermal environment, lighting and acoustics*, Brussels, European Committee for Standardization
- [4] EN 15377 (2008) *Heating systems in buildings - Design of embedded water based surface heating and cooling systems*, Brussels, European Committee for Standardization
- [5] EN 15733-1: *Design of embedded water based surface heating and cooling systems: - Part 1: Determination of the design heating and cooling capacity*

# The present state of district heating in Hungary

György 'Sigmond

MaTáSzSz (Association of Hungarian District Heating Enterprises)

## I. HISTORY OF DISTRICT HEATING IN HUNGARY

After some local projects district heating started to develop in the 60s of the 20<sup>th</sup> century, when some older power condensing steam plants were redeveloped for heat supply. Close laying industrial plants, settlements and institutions were connected.

In the 70s and 80s the government carried out a housing building programme with prefabricated buildings, which represented a better quality of life for many people at that time. Most of those buildings were supplied with district heating, they do the majority of district heated buildings till now. In some cities the city centres with high dwelling density and public institutions were connected, too. The number of district heated dwellings increased up to 640 thousand in the early 90s (Fig 1).

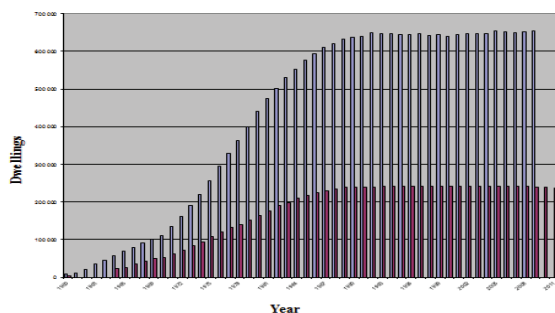


Fig. 1

Dwellings with district heating in Hungary and in Budapest 1960-2011

Because of the cheap fuels and the cheap technology, at the beginning oil fired and later mostly natural gas fired heat only boilers were erected for heat production. In the same time many industrial plants would be provided with heat from the neighbour power plants. They used generally steam, at some systems with quite high pressures up to 70 bars.

Before 1990 the annual district heat supply was near 90 PJ. Industrial district heating amounted to approximately the half of total (Fig 2).

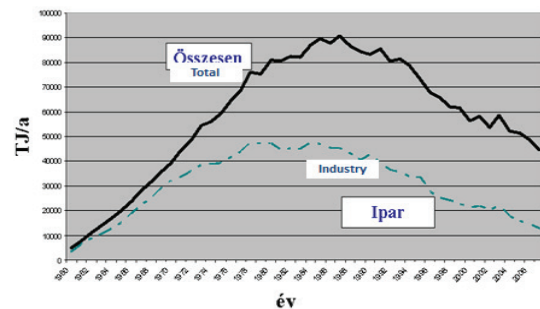


Fig. 2 District heat consumption in Hungary 1960-2009

Because of increasing fuel prices, the district heating for residential and public goals demanded more and more price subvention; in 1992 it reached 60 % already.

After the political and economic system changing in 1990, the housing building programme was stopped. In 1992 also the price subvention was ceased. Since that there is a stagnation at the residential district heating market.

Because of privatization of natural gas supply after 1995 a strong competitor appeared at the heat market. In the next decade the natural gas network reached all cities and the majority of other settlements. Today the number of natural gas heated dwellings is 2,7 Million, which amounts 63 % of all dwellings.

After 1990 many district heated industrial plants were stopped because of economic reasons. Other ones would be privatized and they started to modernize their energy systems. They disconnected of steam networks with high heat losses and erected own energy plants. Because of this, the annual industrial district heating demand decreased below 10 % of the previous highest peak and it amounted merely 3,9 PJ in 2013 (Fig. 2 and Table 1).

		1990	2009	2013
Heated dwellings (thousand)		639	655	648
Rate of heated dwellings	%	16,6	15,2	15,1
Heat consumption				
Residential	PJ/a	34,7	22,5	22,3
Services and others	PJ/a	6,1	7,6	4,9
Industrial	PJ/a	42,7	10,2	3,7
Total	PJ/a	83,5	40,4	30,9
DH related CHP electricity	TWh/a	2,2	5,4	3,9



District heating from CHP	%	46,2	62,0	39,6
---------------------------	---	------	------	------

Table 1  
Development of heat market for district heating and of DH-related cogeneration after 1990

## II. ACTORS AND FIGURES IN THE DISTRICT HEATING MARKET

In Hungary there is district heating with a few exception in all large and medium size and in many smaller cities. As a single case also a small village with only 400 inhabitants has district heating with biomass firing. The share of heated dwellings is different, in some so cold socialist industry cities with many prefab buildings even up to 80 %. In Budapest 240.000 dwellings are connected to the district heating, which is 30% of the total stock (Fig 1). In the most cities there is only one district heating system, but in some other ones there are many island-systems, in Budapest 9 pieces, in the city Szeged more than 20. There are many small systems with less than 10 MW installed capacity. All large and medium size and many smaller systems are equipped with cogeneration or they purchase heat from cogeneration plants.

In Hungary there were erected some district cooling systems, practically adsorption or absorption type base load equipment, which would be heated with cheap heat from CHP plants in the summer time. However, after disadvantageous modifying of CHP subvention system more of them have been disconnected from district heating because of increased heat prices and only two remained in operation.

Table 2 shows the actors and figures of the Hungarian district heating market.

Number of district heating systems		214
Number of systems less than 10 MW		148
Number of district heating related CHP plants		114
Route length of pipe networks	km	2158
Installed heating capacity	MW <sub>th</sub>	8 377
District Cooling		
Number of systems in operation		2
Route length of pipe networks	km	2
Installed cooling capacity	MW <sub>th</sub>	10

Table 2  
Actors and figures in the district heating market

## III. DEVELOPMENT OF HEAT MARKET FOR DISTRICT HEATING AND OF DH-RELATED COGENERATION AFTER 1990

After 2000 the number of heated dwellings fluctuated between 640 and 655 thousand, because of some new connections and some disconnections, which is app. 15 % of the total stock of dwellings in Hungary.

During the last five years period there was no significant changing in the residential district heating market. In 2010-2012 there was a slowly growing of the number of heated dwellings (from 647 to 648 thousand). Since that there were only a few new connections, mainly together with the connection of commercial or institutional customers. The former fluctuation of connections and disconnections has been stopped thanks to decreasing of VAT for DH from 27 to 5 % in 2010 and because of decreasing of heating tariffs since 2013.

In the 90s many heating power plants and heating plants have been privatized. In some of them the new owners modernized the plants with the erection of combined cycle power plants (Fig 3).

District heating		
Number of cities with district heating		95
Village with district heating		1
Number of district heating utilities		110

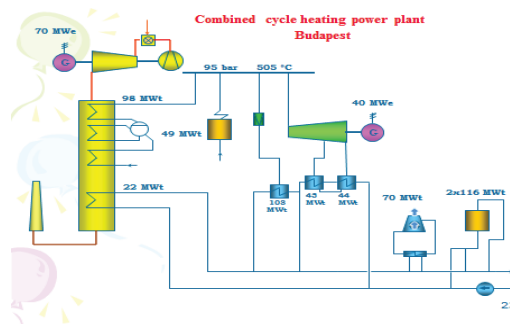


Fig. 3

From 2002 feed in tariffs were introduced for cogenerated electricity with mandatory purchase until 20 MW. Thanks to this a lot of local CHP units – mainly gas engines (Fig 4) – were erected, 75 % of their capacities were used for district heating. Later feed in tariffs were extended for all CHP units, which served heat for district heating.

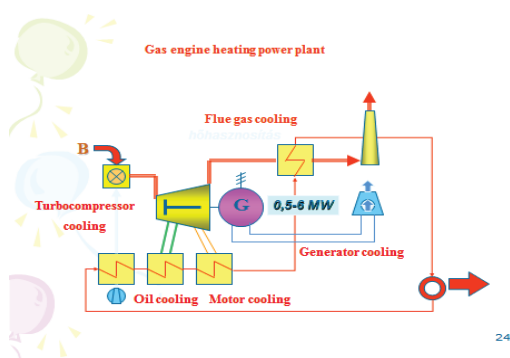


Fig. 4

Gas engine heating power plant

Thanks to these actions the CHP power capacity increased above 2000 MW. (See Fig. 5.) With more than 20 % of share of total domestic power production Hungary belonged to the six largest CHP producers within the European Union. More than 60 % of heat for district heating was produced by CHP units, similarly more than 50 % of residential heat was CHP heat. In the best year 2007 Hungary realized 50 PJ/a primary energy saving with CHP production (that was almost 5 % of national consumption), from which 37 PJ/a was DH related. In the same time the avoided CO<sub>2</sub>-emission was 3,15 Mt/a, from which 2,33 Mt/a was DH related. During the period 1990-2007 no other sector could realize similar energy saving and climate protection outcome in Hungary.

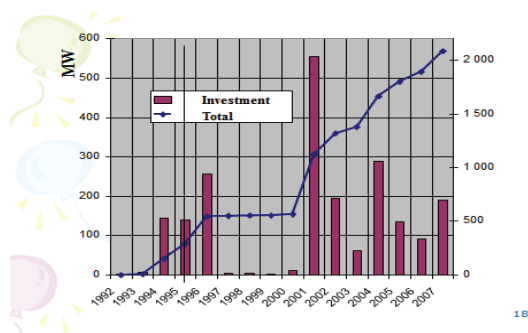


Fig. 5

After the former rapid expansion, CHP decreases now, because official CHP feed-in tariffs were cancelled in 2011 (except electricity production from renewable sources). CHP producers have to sell the produced electricity on the free market, and natural gas prices for district heating and CHP electricity prices became market-driven. Because of low market prices of electricity in the previous years and high prices of natural gas many CHP producers have decreased or suspended their production. (See Table 1 and Fig 6.)

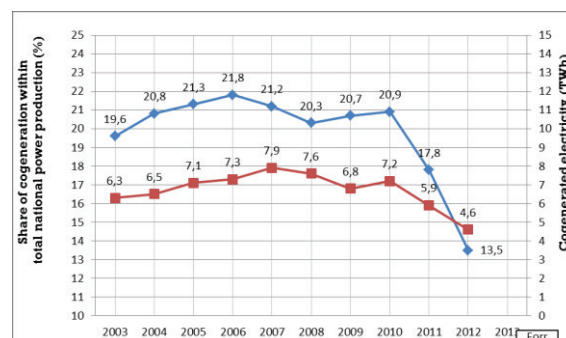


Fig. 6

CHP electricity production and share within the total domestic production

Other reason of decreasing of CHP electricity production is the decreasing of heat demands because of the increasing of building insulation (See Fig 7) and heating system modernisation, the introduction of mandatory metering of heat consumption and the spreading of cost allocators (See Fig 8).

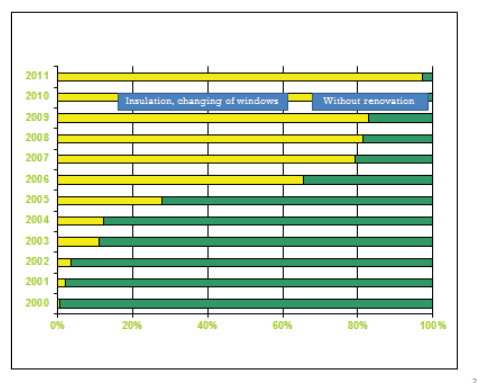


Fig. 7

Showcase building insulation in the city Kaposvár



For renewable CHP projects there are still valid favourable feed in tariffs.

In the city Komló a wood chips fired biomass heating plant has been installed in 2010. Now, 75 % of heat is produced from biomass (Fig 10). District heating related CO<sub>2</sub>-emission decreased below 25 % of former one.

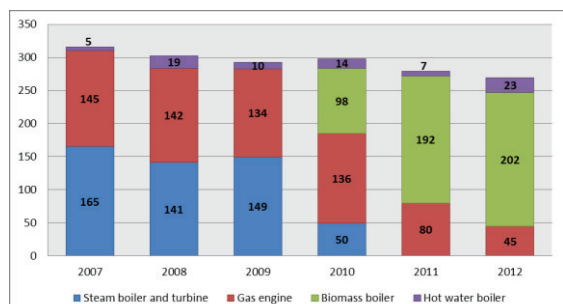


Fig. 10. Biomass heating in the district heating system of the city Komló (TJ/a)

In the year 2013, a geothermal plant has been installed in the city Miskolc. It has provided 530 TJ heat for the DH system in its first heating season, which is almost 40 % of total demand.

In 2004, in the city Pécs a wood chips fired CHP plant with 300 TJ heat output was put into operation. In 2013 also a straw and maize stalk fired large CHP plant was put into operation in the same city, with 1000 TJ heat output (Fig 11). Thanks to these two projects, Pécs is provided with district heating based on nearly 100 % by renewable energy (except renovation time of biomass equipment).

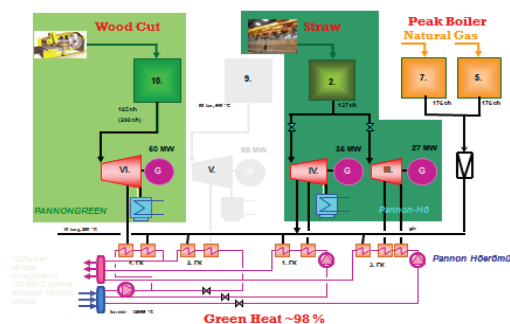


Fig. 11. Biomass district heating power plant in the city Pécs

In Budapest there is a waste incineration power plant, which supplies 500 TJ heat into the Northern Pest district heating system. This is the cheapest heat source, but its heating capacity is not exploited well. Budapest District Heating Co. builds a new connection pipeline, which will be completed in 2015. It is partly financed from business profit and 10 % subvention from KEOP fund. The new pipeline connects a separate network with the Northern Pest system, which results in doubling of heat production, in replacing of 16-26 Mm<sup>3</sup>/a surplus natural gas, and in the avoiding 31-49 thousand t/a surplus CO<sub>2</sub>-Emission.

## VI. NATIONAL ENERGY STRATEGY OF HUNGARY TILL 2030

The National Energy Strategy 2030, with an outlook until 2050, was issued by the Hungarian Parliament in 2011. It estimates a constant level of District Heating until 2030. It foresees only a limited increase in the share of residential District Heating above the current 15%, even with expected connection of heat islands and the construction of local district heating plants. On the other hand, it projects a decrease of the share of district heating in the residential and tertiary heat market from the actual 12 % down to 10 % until 2020 due to building and heating modernisation.

The goal emphasised in the strategy is increased use of renewable energy and energy from waste incineration. According to the opinion of MaTáSzSz it will be possible only with an increased role of district heating. Main available renewable sources in Hungary are biomass, geothermal energy and communal waste. Latter ones can be utilized only in large heating systems, in the first place for district heating. Also the majority of biomass selection (wood cut, straw) can be used only in large boilers on an effective and environment friendly way, small heating equipment need expansive high quality or processed biomass. Lately also government communiqués have forecasted new district heating objectives, which promise an increased role of district heating in the Hungarian energy policy. They project the connection of all accessible dwellings in cities with existing district heating systems.

The Strategy forecasts a continuous determinant role of natural gas even in the planning cycle until 2030. Its present share in the electricity production would be increase from the present 30 % up to 40% according the different alternatives. At the same time, the present share of natural gas in space heating would be decrease from the present 72 % down to 55 %, which is still a high amount. Well-known, Hungary imports approximately 80 % of the natural gas consumption. This share may increase in the future. According to the opinion of MaTáSzSz it would be an unpardonable squandering not to use the possibility of the saving of import energy through cogeneration, in the first place for district heating. This opinion of MaTáSzSz is in harmony also with the energy efficiency directive of the European Union, which promotes the exploitation of the energy saving possibilities through district heating based cogeneration.

## VII. LEGISLATION

District heating is regulated by a separate law in Hungary. It regulates the legal relation between the district heating supplier (utility) and the customer and between the heat producer and the district heating utility. District heating is considered a public service. Because of this, municipalities must provide for licensees (i.e. district



heating utilities, which have supply license) in order to ensure heat supply for the consumers.

The law authorises local municipalities to designate preference districts for district heating within the city for environmental protection reasons, however this does not mean compulsory connection. Municipalities must be the majority owner of the district heating utility by force of law. They may privatise maximum 49% of the shares or they can privatise the district heating operation in the framework of a concession tender. Most district heating utilities are owned up to 100% by local municipalities, with only a few exceptions. Heat sources may be owned by the district heating utility but also by private owners. Currently, the government plans to establish state-owned national energy holding companies in the natural gas, electricity and later in the district heating sector for fostering competition within each market.

In 2011, the official CHP feed-in tariffs were cancelled, but they are still valid for electricity production from renewable sources. Since that, district heating utilities get subvention. Heat prices from CHP plants, heat price for the residential and public utility customers and the subventions are regulated by the minister in decrees and they are different for each utility. Natural gas prices and heat prices for the residential and public sector are also regulated, while natural gas prices for district heating and CHP electricity prices are market-driven.

The legal framework limits the profit of heat supply from renewable heat sources and from efficient CHP plants for district heating utilities at highest 4.5 % and at 2% for other district heating producers and utilities. The eventual surplus profit has to be given to the end user, but it can be used for investments in energy efficiency, carbon emission savings or environmental protection if approved by the energy authority.

In 2013, the government passed a law on the reduction of residential overhead costs, including natural gas supply, electricity supply, district heating, water supply, etc. The price of natural gas has been reduced by 25.2%, the electricity supply price by 24.6% and the price of district heating by 22.6%. The biggest part of district heating price reduction is covered by subventions. Utilities must find budget sources to cover the remaining part.

CHP made viable district heating for a ten-year period until 2011. Since that plants can sell their electricity production only on the free marketer they can sell it for system operation goals (e.g. peak load services), sometimes without heat output.

CHP plants and district heating utilities have to buy natural gas on the free market. Because of high actual natural gas prices and low market prices for electricity CHP production including heat production for district heating has decreased almost by 40% (Fig 6).

## VIII. MATÁSZSZ (ASSOCIATION OF HUNGARIAN DISTRICT HEATING ENTERPRISES)

MaTáSzsZ was founded in 1993. It is the representative of the Hungarian district heating branch. It has 64 ordinary members (district heating utilities, heating power plant companies, partner associations) and 36 associated members (suppliers, energy contracting and marketing companies, within them foreign companies or their representatives). 60 % of district heating utilities are members of MaTáSzsZ, which represent 85 % of heated dwelling stock.

MaTáSzsZ is a lobby and advocacy association. It represents the interests of its membership at the authorities. It participates in the preparation of laws and decrees in connection with district heating and in the wider energetic in the frame of cooperation agreements with more ministries and authorities. It organizes professional conferences and it is present with presentations at events about energetic, climate and environment protection and customer protection, too.

MaTáSzsZ is supporting member of Euro heat& Power. It organizes technical trips for their members in countries with advanced district heating and it establishes contacts with other foreign organizations and experts.

---

## **EXPRES 2015**

### **7<sup>th</sup> International Symposium on Exploitation of Renewable Energy Sources and Efficiency**

<http://conf.uni-obuda.hu/expres2015>

---

---

#### **In technical co-operation with**

---

- **V3ME, Subotica**
  -  **Government of Subotica**
  -  **Subotica Tech, Subotica**
  -  **Óbuda University, Hungary**
  - **Tera Term doo, Subotica**
- 

#### **In technical co-sponsors**

---

- **Faculty of Economics, Subotica**
- **Faculty of Civil Engineering, Subotica**
- **Annus Auto Saloon and Service, Subotica**
- **Cim-Gas, Subotica**
- **ELZETT, Subotica**
- **Mini Pani, Subotica**